KU Leuven
Biomedical Sciences Group
Faculty of Medicine
Department of Cardiovascular Sciences

KU LEUVEN

DOCTORAL SCHOOL
BIOMEDICAL SCIENCES

TOWARDS IMPROVED THROMBOLYSIS IN ISCHEMIC STROKE EXPLORING NOVEL THERAPEUTIC TARGETS

Sarah VANDELANOTTE

Jury:

Supervisor:	Prof. Dr. Simon F. De Meyer
Co-supervisors:	Prof. Dr. Karen Vanhoorelbeke
	Prof. Dr. Claudia Tersteeg
Chair examining committee:	Prof. Dr. Jan Verbakel
Chair public defense:	Prof. Dr. Lieven Thorrez
Jury members:	Prof. Dr. Robin Lemmens
	Prof. Dr. Peter Verhamme
	Prof. Dr. Benoit Ho Tin-Noé
	Prof. Dr. Annelies Bronckaers

Dissertation presented in partial fulfilment of the requirements for the degree of Doctor in Biomedical Sciences

December 2024

© 2024 KU Leuven, Faculty of Medicine, Biomedical Sciences Group
Uitgegeven in eigen beheer, Sarah Vandelanotte, Kortrijk, België

Alle rechten voorbehouden. Niets uit deze uitgave mag worden vermenigvuldigd en/of openbaar gemaakt worden, hetzij elektronisch, mechanisch, door print-outs, kopieën, of op welke andere manier dan ook, zonder voorafgaande schriftelijke toestemming van de uitgever.

All rights reserved. No part of this publication may be reproduced, distributed, or transmitted in any form or by any means, including photocopying, recording, or other electronic or mechanical methods, without the prior written permission of the publisher.

DANKWOORD / ACKNOWLEDGEMENTS

Na vier intensieve jaren van onderzoek, ontdekkingen en persoonlijke groei, is het moment aangebroken om mijn doctoraat af te ronden. De afgelopen vier jaar hebben me letterlijk veel bloed, het nodige zweet en toch ook heel wat tranen gekost, maar het was een fantastische ervaring. Het voltooien van mijn doctoraat zou dan ook niet mogelijk geweest zijn zonder de steun, aanmoediging en begeleiding van heel wat mensen aan wie ik mijn dankbaarheid wil uiten.

Het zou onmogelijk geweest zijn om mijn doctoraat te behalen zonder de fantastische begeleiding van mijn promotor Simon De Meyer. Een welgemeende dank je wel. Niet alleen om mij de kans te geven een doctoraat te starten maar ook voor alle begeleiding tijdens het traject. Je gaf me de kans om te groeien als onderzoeker en als mens. Je zorgde ervoor dat ik mijn grenzen verlegde en bleef me motiveren om door te gaan als de resultaten even tegenvielen. Waar ik begonnen ben als een onzeker iemand die het een helemaal niet leuk vond om voor een groep te spreken, leerde je me vol zelfvertrouwen spreken op congressen. Jouw deur stond altijd open om een vraag te beantwoorden, nieuwe resultaten te bespreken of wetenschappelijke vragen te bediscussiëren. Jouw kritische blik op mijn experimenten en resultaten zorgde ervoor dat ik mezelf telkens moest uitdagen om zelf kritisch naar mijn werk te kijken. Bedankt om mij ook de kans te geven mijn interesse voor organisatie en management te kunnen ontplooien door mij te steunen als ABAP-vertegenwoordiger in verschillend beleidsorganen en raden. Naast alle werk-gerelateerde steun, vroeg je altijd hoe met mij ging en had je begrip indien het door omstandigheden soms even niet goed ging. Dat heb ik gedurende mijn ganse doctoraat enorm geapprecieerd. Dank je wel!

Daarnaast wil ik graag mijn copromotoren Karen en Claudia bedanken. Karen, bedankt voor jouw kritische blik en jouw constructieve feedback op mijn experimenten en resultaten. Claudia, de leuke en interessante gesprekken op de trein van en naar Brugge zullen me altijd bij blijven. Bedankt voor jouw eerlijke feedback en input op mijn resultaten.

I would also like to thank all the members of the examination committee. Prof. Dr. Robin Lemmens en Prof. Dr. Peter Verhamme, bedankt voor de interessante en kritische vragen en feedback tijdens de verschillende evaluatiemomenten gedurende mijn PhD traject. Prof. Dr. Benoit Ho Tin-Noé and Prof. Dr. Annelies Bronckaers, thank you for taking the time to critically revise my thesis manuscript. Graag bedankt ik ook Prof. Dr. Jan Verbakel als voorzitter van het evaluatiecomité. Ten slotte zou ik graag Prof. Dr. Lieven Thorrez bedanken om mijn publieke verdediging in goede banen te leiden.

I would also like to thank my many colleagues and former colleagues who made the past four years fly by. Hierbij begin ik graag met Senna. Jouw enorme kennis over de klonterwereld is indrukwekkend en inspirerend. Bedankt dat je me met geduld en toewijding alle kneepjes van het vak hebt bijgebracht en me in de eerste maanden van mijn doctoraat hebt begeleid. Het was een eer om jouw project te mogen voortzetten en daar mijn eigen bijdrage aan te leveren. Daarnaast ook bedankt voor de vele leuke gesprekken en weetjes over de kulak die je vertelde! Shannen, ik heb zoveel bewondering voor jouw gedrevenheid, passie en behulpzaamheid waarmee jij naar het werk komt. Ik zal het moment op het ECTH-congres toen ik je in de wc's vertelde dat ik zwanger was en jij reageerde met 'ik ook!' nooit vergeten. Charlotte, bedankt om altijd een vrolijke en enthousiaste sfeer in de schrijfruimte te brengen. Wim, bedankt voor jouw kritische insteek en vragen tijdens mijn labmeetings. Jouw kennis en ervaring zijn een grote meerwaarde voor mij en voor het labo. Laure, op congres of op een labo feestje kon ik altijd op jou rekenen om samen de dansvloer te betreden. Ik kijk dan ook met veel plezier terug naar al deze mooie momenten. Maaike, dat we Google maps niet altijd mogen vertrouwen hebben we in Lyon duidelijk mogen ondervinden. Samen op congres was je dan ook vaak mijn vast kamergenootje. Bedankt voor alle mooie gesprekken, roddel momentjes of peptalks. Bas, vanaf het eerste moment was ik verbaasd van jouw enorme kennis. Niet enkel over trombose en hemostase maar ook jouw enorme kennis over de kulak. Ik ging dan ook met plezier af en toe mee voor een korte wandeling op de campus. Jens, mijn overbuur. Je hielp me over mijn angst voor muizen heen en zorgde ervoor dat ik zonder roepen de muisjes kon vastnemen. Alleen al daarvoor, dank je wel! Daarnaast zorgde je altijd voor de nodige sfeer en stond altijd klaar voor een feestje en voor wat plezier! Quintijn, samen starten aan een doctoraat schept toch wel een band. Dat we beide graag

ondernemend zijn en vooruit willen, zorgde ervoor dat je me uitdaagde een betere onderzoeker te worden. Of het altijd de meest tijdsefficiënte keuze was om naast elkaar te zitten in de schrijfruimte, dat durf ik te betwijfelen. Maar wat ben ik blij dat je er altijd was om even een pauze te nemen, mijn hart te luchten of even te klagen over alles. Dit zorgde ervoor dat ik telkens verder kon. Bedankt voor de vele leuke herinneringen die mee mijn doctoraat vorm gegeven hebben. Lisa, wat een fantastische onderzoeker ben jij! Jouw gedrevenheid en groei tijdens jouw doctoraat zijn nu al bewonderenswaardig. Ik kijk al uit naar jouw verdediging. Sara, as the only international in the lab, it was nice to hear your stories about Spain. I loved sitting next to you and help you with small practical question! I already look forward to your defense. Emile, nu al vol gedrevenheid gestart aan jouw doctoraat. Ik kijk er alvast naar uit om het gentherapie project samen verder te zetten.

Naast de vele (post-)doctoraatsstudenten telt ons laboratorium ook enkele vaste krachten zonder wie het labo niet zou functioneren zoals het hoort. Inge, bedankt om altijd vol enthousiasme klaar te staan om mij te helpen, een vraag te beantwoorden of voor een babbeltje. Ik kan jou niet genoeg bedanken voor alles wat je mij hebt geleerd en voor jouw vele hulp. Anne-Sophie, als nieuwe laborante heb je je meteen goed ingewerkt in het labo en was je een grote hulp bij experimenten. Dat ik in jou een danspartner gevonden heb is zeker! Ik kijk er alvast naar uit om samen nog eens een stapje te zetten en ooit raken we op de Sinkse-feesten. Katleen, jouw enthousiasme en zorgzaamheid zullen me altijd bijblijven. Ik vond het dan ook heel aangenaam om op het einde van mijn doctoraat wat vaker samen te kunnen werken. Bedankt om mij wegwijs te maken in de wondere wereld van de muisjes en voor jouw vele bemoedigende woorden en berichtjes. Aline, bedankt voor alle hulp tijdens experimenten en om mijn vele vragen te beantwoorden. En last but not least, Linda, bedankt voor jouw uren snij en kleurwerk van de klonters. Ik vond het heel aangenaam om samen te werken en moest toch even wennen toen jij op pensioen ging. During my PhD-project, many international colleagues joined our lab. I would like to thank Kazuya, Wattie and Gonzalo, for the interesting talks and discussions during your stay in the lab. I wish you all the best!

Graag bedank ik het volledige stroke team van het AZ Groeninge ziekenhuis in Kortrijk zonder wie mijn doctoraat niet mogelijk was. Prof. Dr. Tommy Andersson, Dr.

Fréderick Van Gool and Prof. Dr. Peter Vanacker, I would like to thank all of you for the fruitful collaboration and proving me with the patient thrombi and clinical data. Thank you for your valuable feedback and suggestions on abstracts and papers. In het bijzonder bedank ik graag Dr. Olivier François, voor de fijne samenwerking. Bedankt om altijd klaar te staan om het klinische aspect van de klonters te bespreken en zo mijn doctoraat tot een mooi geheel te brengen. Vervolgens wil ik ook mijn dank uiten aan alle verpleegkundigen van het Stroke Team om mij telkens te verwittigen wanneer er een klonter klaar stond, mij altijd hartelijk te ontvangen en de leuke korte babbels.

Graag wil ik ook alle collega's van het IRF bedanken voor de fijne werksfeer. De vele jaarlijkse activiteiten waren telkens een leuke afwisseling tussen het werk door. In het bijzonder wil ik graag Sigrid bedanken voor alle administratieve hulp bij het plannen van lokalen, congressen naar het buitenland, het verzenden van pakketjes en nog zoveel meer. Bedankt! Naast het IRF wil ik graag ook alle collega's van de faculteit geneeskunde bedanken voor de vele toffe personeelsactiviteiten en voor de hulp bij het plannen van lessen of het beantwoorden van vragen. In het bijzonder dank ik graag de (post)doctoraatsstudenten van het Tissue Engineering Lab voor de fijne samenwerkingen en babbels. Het was altijd aangenaam om iemand van jullie tegen te komen in het histologie labo of aan de microscopen. Veel succes met jullie onderzoek.

Na al het harde werk was er afgelopen 4 jaar ook tijd voor heel wat plezier omringd door mijn liefste vrienden. Ik wil dan ook graag iedereen, zonder specifieke namen te noemen, bedanken om mij de afgelopen 4 jaar op een af andere manier te steunen. Bedankt voor de vele succes berichtjes, de luisterende oren, de peptalks en wijze raad! Maar vooral ook bedankt voor alle fantastische momenten die ik afgelopen 4 (en meer) jaren samen met jullie beleefd heb. Van spontane apero'tjes tot gezellige etentjes, tot late dansavondjes; van wandelingen tot intensieve sportsessie tot languit in de zetel babbelen; van daguitstapjes tot memorabele weekendjes en reizen; van mijn vrijgezellen tot mijn trouw tot de liefde voor Ralph. Kortom bedankt om mijn leven de voorbije 4 jaar zoveel mooier te maken.

Naast mijn fantastische vrienden, kan ik mij gelukkig prijzen omringd te zijn door een liefdevolle (schoon)familie. Jullie onvoorwaardelijke steun en vertrouwen in mij zorgen ervoor dat ik mij telkens verder kan ontwikkelen als persoon en als onderzoeker. Bedankt om aan de zijlijn van mijn doctoraat en eigenlijk mijn ganse leven mee te supporteren. Bedankt dat ik bij ieder van jullie altijd terecht kan. In het bijzonder wil ik toch even mijn mama, papa, broer en zus bedanken. Mama en Papa, bedankt om mij alle kansen te geven om het leven te ontdekken en om uit te groeien tot wie ik vandaag ben. Ik zou hier vandaag letterlijk, maar vooral ook figuurlijk niet staan zonder jullie. Maar ook Thomas en Nele kan ik niet vergeten. Bedank om altijd naar het geratel over mijn doctoraat en experimenten te luisteren, bedankt om mij altijd te steunen in wat ik doe. Ik ben zo trots op hoe jullie door het leven gaan en wie jullie geworden zijn!

Ik kan mijn dankwoord niet eindigen zonder Sven te bedanken. Al meer dan 11 jaar sta jij aan mijn zijde waarin je een ongelofelijke steun voor me bent geweest. Afgelopen 4 jaar waren 4 intense jaren waarin we samen een huis kochten en verbouwden, waarin we tijdens corona gingen samenwonen, waarin we na een moeilijke periode afscheid moesten nemen van jouw mama, waarin we getrouwd zijn en een fantastische huwelijksreis maakten en waarin we na een niet zo eenvoudige periode de gelukkigste ouders werden van onze kleine Ralph. Meer dan ooit hebben we afgelopen vier jaar als een fantastisch team beleefd. Waarin je mij telkens het duwtje in de rug gaf wanneer dat nodig was. Ook al leek mijn onderzoek in het begin zo ingewikkeld, je stond altijd open om naar mijn resultaten, mislukte experimenten en presentaties te luisteren. Bedankt!

TABLE OF CONTENTS

DANKWOORD / ACKNOWLEDGEMENTS I
TABLE OF CONTENTS VI
LIST OF ABBREVIATIONS VIII
CHAPTER 1 - GENERAL INTRODUCTION 1
1 Hemostasis and thrombosis 2
1.1 Hemostasis 2
1.2 Pathological thrombus formation 10
2 Ischemic stroke 16
2.1 Epidemiology of stroke 16
2.2 Etiology 18
3 Diagnosis of ischemic stroke 21
3.1 Symptoms of ischemic stroke 21
3.2 Diagnostic imaging of ischemic stroke 21
3.3 Stroke severity 23
4 Recanalization strategies 23
4.1 Pharmacological thrombolysis 25
4.2 Mechanical thrombectomy 28
5 Composition of ischemic stroke thrombi 31
CHAPTER 2 - ACUTE ISCHEMIC STROKE THROMBUS COMPOSITION 43
CHAPTER 3 - AIMS OF THE RESEARCH 55
CHAPTER 4 – MODEL FOR HUMAN ACUTE ISCHEMIC STROKE CLOT ANALOGS WITH DIFFERENT RT-PA RESPONSIVENESS 59
CHAPTER 5 - RT-PA RESISTANCE IS SPECIFIC FOR PLATELET-RICH STROKE THROMBI AND CAN BE OVERCOME BY TARGETING NON-FIBRIN COMPONENTS 82
CHAPTER 6 - ASSOCIATION BETWEEN THROMBUS COMPOSITION AND FIRST PASS RECANALIZATION AFTER THROMBECTOMY IN ACUTE ISCHEMIC STROKE 99
CHAPTER 7 - ULTRASTRUCTURE OF ACUTE ISCHEMIC STROKE THROMBI VIA SCANNING ELECTRON MICROSCOPY: AN OBSERVATIONAL STUDY 111
CHAPTER 8 - DISCUSSION AND FUTURE PERSPECTIVES 135
SUMMARY – SAMENVATTING 151
ACKNOWLEDGEMENTS, PERSONAL CONTRIBUTION AND CONFLICT OF INTEREST 157
CURRICULUM VITAE 159

LIST OF ABBREVIATIONS

ACA	Anterior cerebral artery
AIS	Acute ischemic stroke
(r)ADAMTS13	(Recombinant) a disintegrin and metalloprotease with thrombospondin type 1 repeats, member 13
(r)t-PA	(Recombinant) tissue plasminogen activator
3D	Three dimensional
BA	Basilar artery
BSA	Bovine serum albumin
$CaCl_2$	Calcium chloride
CD42b	Cluster of differentiation 42 b
CD45	Cluster of differentiation 45
CE	Cardioembolic
CLEM	Correlative light and electron microscopy
CT	Computed tomography
DALYs	Disability-adjusted life-years lost
diNAC	N,N'-Diacetyl-L-cystine
DVT	Deep vein thrombosis
ESUS	Embolic stroke of undetermined source
eTICI	Expanded thrombolysis in cerebral infarction score
EVT	Endovascular thrombectomy
exDNA	Extracellular DNA
FDA	US Food and Drug Administration
Fp	Fibrinopeptides
FPR	First pass recanalization
GP	Glycoprotein
H&E	Hematoxylin and eosin
H3Cit	Citrullinated histone 3
HAS	Hyperdense artery sign
HMGB1	High mobility group box 1

HU	Hounsfield units
ICA(-T)	(terminal end) Internal carotid artery
IHC	Immunohistochemical
IQR	Inter quartile range
IV	Intravenous
LAA	Large-artery atherosclerotic
LVO	Large vessel occlusion
MCA	Middle cerebral artery
MED	Magnetically enhanced diffusion
MPO	Myeloperoxidase
MRI	Magnetic resonance imaging
mRS	Modified Ranking score
MSB	Martius scarlet blue
MT	Mechanical thrombectomy
mTICI	Modified thrombolysis in cerebral infarction score
NAC	N,N'-acetyl-L-cystine
NCCT	Non-contrast computed tomography
NE	Neutrophil elastase
NET	Neutrophil extracellular trap
NFPR	Non-first pass recanalization
NHP	Normal human plasma
NIHSS	National Institute of Health Stroke Scale
PAD4	Peptidylarginine deiminase 4
PAI-1	Plasminogen activator inhibitor 1
PBS	Phosphate-buffered saline
PCA	Posterior cerebral artery
PRP	Platelet-rich plasma
RBC	Red blood cell
RPM	Revolutions per minute
RT	Room temperature

$RW_{timepoint}$	Residual thrombus weight
SD	Standard deviation
SEM	Scanning electron microscopy
SVS	Susceptibility vessel sign
TAFI	Thrombin-activatable fibrinolysis inhibitor
TBS	Tris buffered saline
TF	Tissue factor
TIA	Transient ischemic attack
TNK	Tenecteplase
TOAST	Trial of Org 10172 in Acute Stroke Treatment
u-PA	Urokinase-type plasminogen activator
VWD	Von Willebrand disease
VWF	Von Willebrand factor
WPB	Weibel-Palade bodies

CHAPTER 1 - GENERAL INTRODUCTION

1 Hemostasis and thrombosis

1.1 Hemostasis

Hemostasis is a crucial, dynamic physiological process responsible for the cessation of bleeding while maintaining normal blood flow within the body. The term hemostasis originates from the ancient Greek words “haeme” meaning blood and “stasis” meaning to stop. Through a series of coordinated steps, hemostasis allows the body to form a blood clot to seal off damaged blood vessels, maintain the fluid state of the blood and dissolve the blood clot once vascular integrity is restored.[1] The process of hemostasis can be divided into three distinct processes. Initially, platelets will adhere to the damaged vessel wall, forming an initial plug to seal the injury (**primary hemostasis**). Subsequently, a series of coagulation factors will be activated leading to the formation of fibrin to further stabilize the initial platelet plug (**secondary hemostasis**). Finally the clot is dissolved once the risk of bleeding has been restored (**fibrinolysis)**.[2] Tight regulation of hemostasis is crucial and any disruption may lead to pathological hemorrhage or thrombosis.

1.1.1 Primary hemostasis

Following damage to a blood vessel, the primary objective of the hemostatic system is to restore the rupture in the damaged vessel wall. Figure 1A provides a simplified overview of the primary hemostasis. Local vasoconstriction mediated by the smooth muscle cells in the vessel wall result in an initial reduction of the blood flow through the damaged vessel to immediately limit blood loss. Upon damage to the vessel wall, the underlying subendothelial extracellular matrix containing the highly thrombogenic collagen becomes exposed. At low shear rates such as in the venous circulation, platelets can bind directly to collagen via their collagen receptors glycoprotein (GP) VI and integrin α2β1.[3] Under high shear rates, deceleration of the rapidly flowing platelets is mediated by the interaction of platelets with von Willebrand factor (VWF). VWF, found in the Weibel-Palade bodies (WPB) of endothelial cells, α-granules and blood plasma, circulates in a compact, folded structure.[4,5] It is composed of different structural domains as illustrated in Figure 1B. Upon damage of the vessel wall, the VWF A3 domain can bind to the exposed collagen resulting in unfolding of the VWF protein revealing the GPIbα platelet binding site within the A1 domain. This allows initial transient binding of the platelet GPIbα of the GPIb-V-IX receptor complex and

the VWF A1 domain, resulting in the deceleration of platelets allowing firm adhesion of platelets through binding of GPVI and α2β1 to collagen.[3] The final step in the formation of the initial platelet plug is aggregation of platelets following platelet activation. Platelet activation is mediated through several platelet signaling pathways including activation of the GPVI collagen receptor and downstream signaling of the GPIb-V-IX complex.[6] Upon activation, platelets will undergo conformational shape changes into a more spherical shape with filopodia and release agonists from their dense and α-storage granules such as adenosine diphosphate, thromboxane A2, VWF and fibrinogen, further enhancing platelet adhesion, activation and aggregation. Simultaneously, platelet integrin $\alpha_{IIb}\beta_3$, which is normally present in an inactive form on the platelet surface, undergoes a conformational transition to an open conformation. This results in platelet aggregation trough firm VWF, fibronectin and fibrinogen binding.

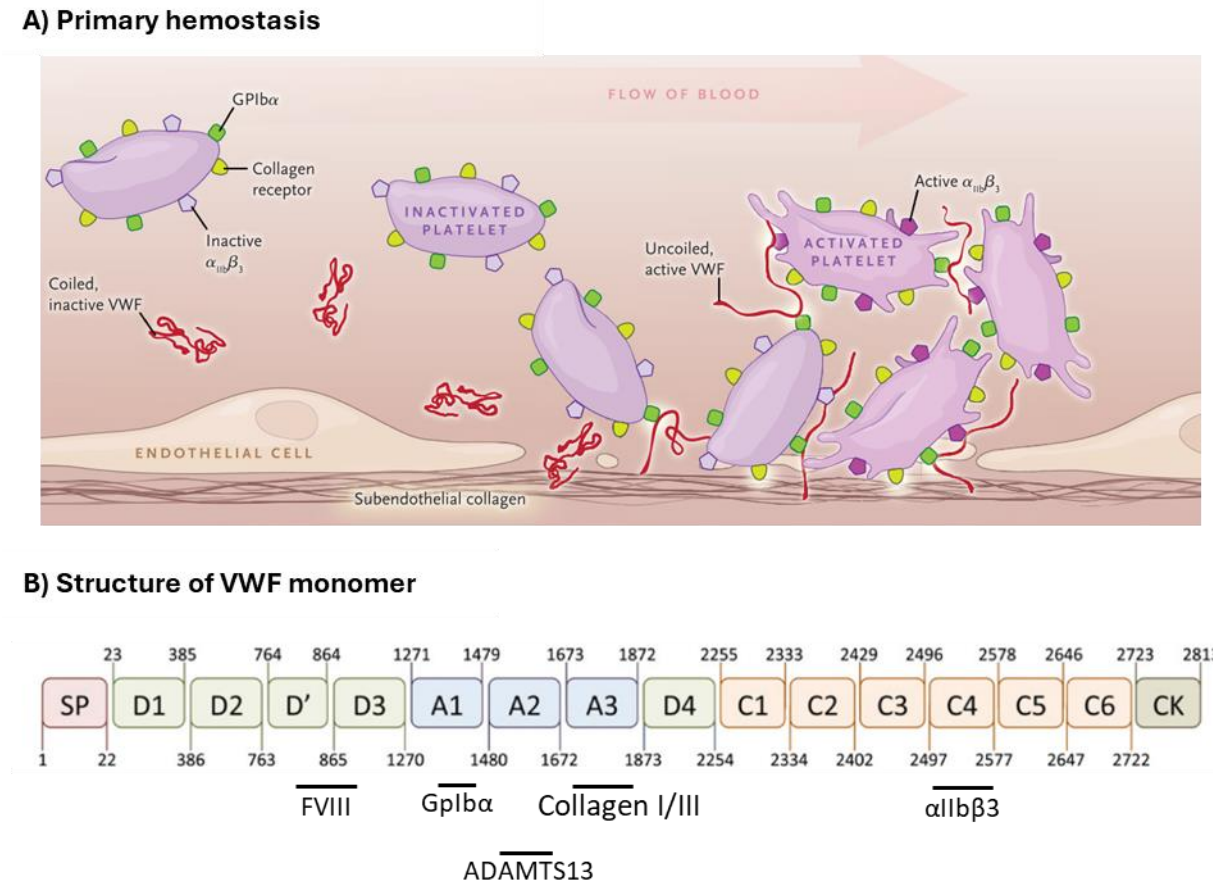

Figure 1: Simplified model of primary hemostasis. (A) Overview of primary hemostasis. Von Willebrand factor (VWF) circulates as a coiled, inactive molecule. Upon vascular damage the VWF A3 domain can bind to the exposed subendothelial collagen resulting in uncoiling of the VWF protein revealing the platelet binding site within the A1 domain. The binding of platelet GPIbα to the VWF A1 domain slows down platelets, facilitating their adhesion to collagen through their collagen receptors

GPVI and α2β1. This leads to firm adhesion and aggregation of platelets, driven by platelet activation. Activated platelets undergo shape changes, release agonists like adenosine diphosphate, thromboxane A2, VWF, and fibrinogen, and express platelet integrin $\alpha_{IIb}\beta_3$ on the surface of platelets intensifying platelet adhesion, activation, and aggregation. (B) Schematic representation of VWF monomer and different domains. The main binding sites are indicated. Figure adapted from Leebeek et al. and Lenting et al. [7,8]

1.1.2 Secondary hemostasis

Primary hemostasis leads to an initial platelet plug, which is further stabilized by fibrin formed as the result of the secondary hemostasis. The formation of fibrin involves a cascade of stepwise activation of multiple coagulation factors to generate thrombin, which converts fibrinogen into fibrin. The coagulation cascade involves two cascades, the extrinsic and the intrinsic pathway, as depicted in Figure 2. The extrinsic pathway is triggered by damage to the vascular endothelium, which exposes tissue factor (TF) and allows factor VII (FVII) to bind, forming the TF/FVIIa complex. This enzyme complex can activate factor X and factor IX. Activated factor X will bind to its cofactor V in the presence of calcium ions to form the prothrombinase complex on the negatively charged surface of platelets. This complex converts the proenzyme prothrombin to the active thrombin. The intrinsic pathway or contact activation pathway is initiated when factor XII is activated upon contact with negatively charged surfaces, such as glass or the negatively charged phosphates on the membrane of activated platelets. Initially, factor XII activation is limited in speed. However, as a small quantity of activated factor XIIa accumulates, it results in the conversion of prekallikrein to kallikrein which in turn, accelerates the conversion of factor XII to factor XIIa. Subsequently, factor XIIa leads to formation of factor XIa that activates factor IX. When factor IXa binds with its cofactor VIIIa, it creates the tenase complex, leading to the conversion of factor X into factor Xa and to the common step of thrombin generation.[9,10]

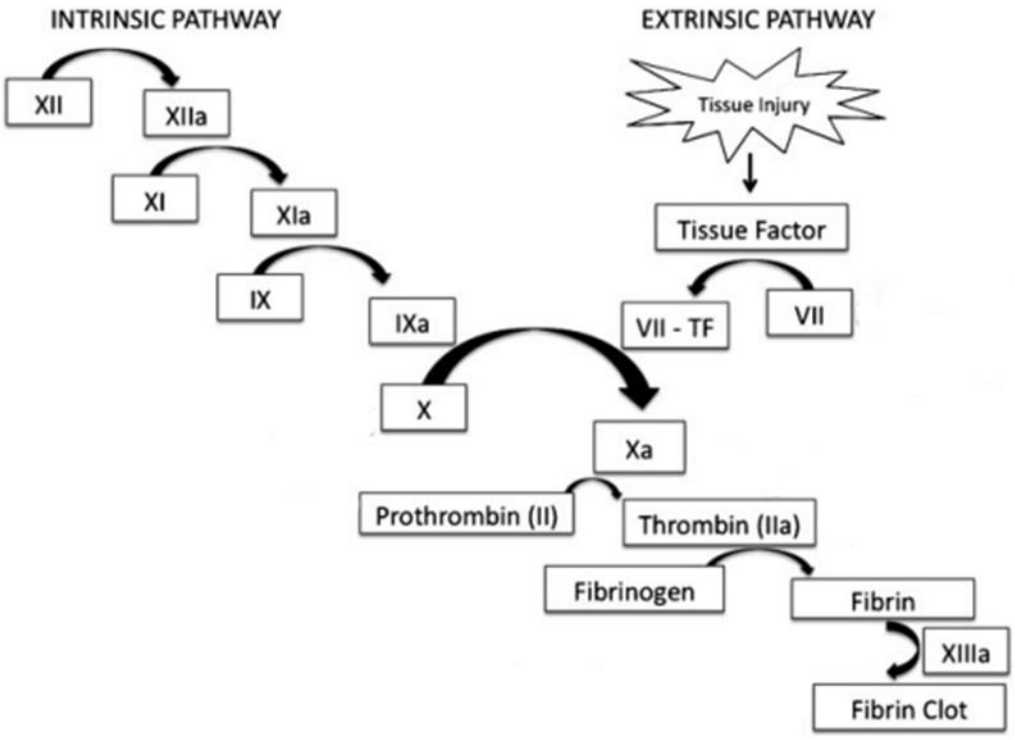

Figure 2: Overview of the coagulation system. Upon vascular injury, the extrinsic pathway initiates coagulation via tissue factor (TF) exposure in the subendothelial matrix resulting in the formation of the TF/ factor VIIa complex. The TF/ factor VIIa complex activates factor X. The intrinsic pathway is initiated by contact with negatively charged surfaces leading to the activation of factor XII. Subsequently, factor XIIa leads to formation of factor XIa which activates factor IX. When factor IXa binds with its cofactor factor VIIIa, it creates the tenase complex, leading to the conversion of factor X into factor Xa. The intrinsic and extrinsic pathway come together into the common pathway, leading to thrombin generation. Thrombin initiates fibrin formation and crosslinking by activated factor XIII, resulting in the stabilization of the fibrin clot. Figure adapted from Lazzaro et. al.[11]

The primary outcome of thrombin formation is the conversion of fibrinogen into fibrin. Fibrinogen is a homo-dimeric glycoprotein circulating in the plasma at concentrations of 1.5-4 mg/ml and has a half-life of three to five days.[12] Before secretion into the blood, fibrinogen undergoes several assembly steps in the hepatocytes. Fibrinogen consists of 2Aα, 2Bβ, and 2γ polypeptide chains. These chains are assembled with their N termini located in a central E nodule and extend outward in a coiled-coil arrangement forming two distal D-regions (Figure 3A).[12] The final fibrinogen circulate in the blood until thrombin cleaves fibrinopeptides from the Aα and Bβ chains (FpA and FpB, respectively) to form fibrin monomers (Figure 3B).[12,13] Subsequently, fibrin monomer molecules undergo spontaneous assembly into two-stranded, half-staggered oligomers in which knob ‘A’ of one monomer binds hole ‘a’ of another monomer, and

two ‘A-a’ knob-hole interactions holding the two monomers together. Lateral interactions between two strands of fibrin oligomers are mediated by the central E region of one fibrin molecule and two lateral D regions of two other fibrin molecules forming a D-E-D complex. This complex is held together by the ‘A-a’ knob-hole bonds and by additional interactions at the D:E and D:D interfaces. Additional fibrin monomers can add longitudinally to form larger oligomers, which lengthen further to make protofibrils, a critically important intermediate product of fibrin polymerization. The formed protofibrils associate with each other laterally to create thick fibrin fibers.[12,13] As they further develop, the formed network starts branching to create a three dimensional (3D) network. Branching can originate from two protofibrils that undergo incomplete lateral aggregation but diverge into two separate protofibrils, each of them giving rise to a new fiber forming a bilateral junction or originates when a fibrin monomer attached to the end of a protofibril via only one ‘A-a’ bond so that both the monomeric molecule and the protofibril can grow independently, forming two strands each (trimolecular junction). In order to stabilize the formed clot against proteolytic and mechanical disruption, the fibrin is covalently crosslinked by Factor XIIIa that is activated by thrombin in the presence of calcium ions.[12] Increased thrombin concentrations result in the formation dense networks of thin and highly branched fibrin fibers that are relatively resistant to fibrinolysis.[14]

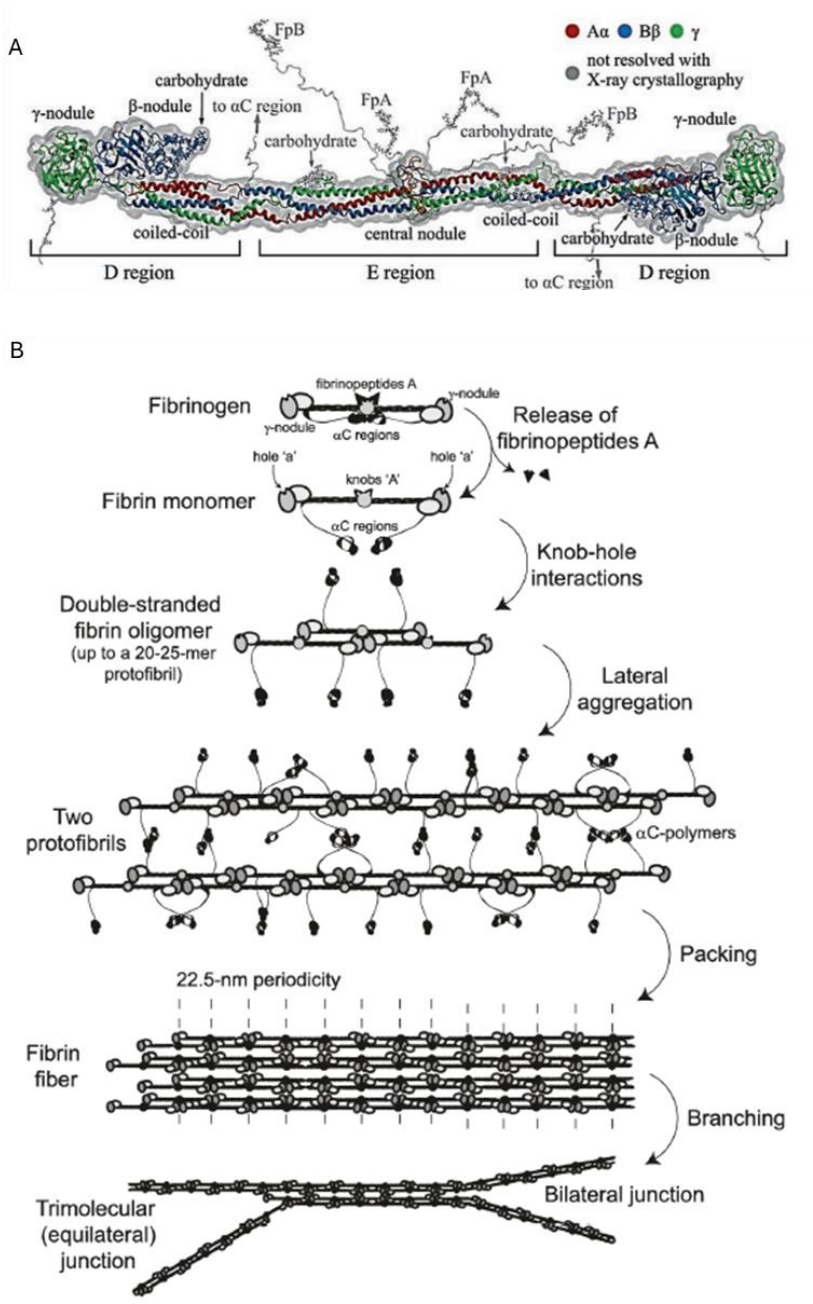

Figure 3: Schematic representation fibrin polymerization. (A) Schematic structure of a fibrinogen molecule showing 2Aα, 2Bβ, and 2γ polypeptide chains, with their N termini located in the central E nodule, extending outward in a coiled-coil arrangement to form two distal D-regions. (B) Overview of fibrin polymerization. Enzymatic release of fibrinopeptides from fibrinogen mediated by thrombin results in the formation of fibrin monomers. These monomers self-assemble via knob-hole interactions into half-staggered, double-stranded oligomers, which then associate longitudinally to form protofibrils. Protofibrils aggregate longitudinally and laterally into fibrin fibers. Branching results in the formation of a three-dimensional network. Figure adapted from Weisel et al.[12,13]

1.1.3 Fibrinolysis

The fibrinolysis process prevents excessive fibrin formation and dissolves the formed blood clot once it has fulfilled its purpose. It thereby avoids unnecessary obstruction in blood vessels and supports maintenance of the vascular health. The process of fibrinolysis occurs in two consecutive phases: the conversion of plasminogen to plasmin, followed by the cleavage of fibrin by plasmin. Plasminogen, synthesized in the liver, circulates in the plasma at a concentration of 1-5 µmol/l. It is composed of 791 amino acids that are crosslinked to form five homologous triple-loop structures known as kringles.[15] In the first phase of fibrinolysis, plasminogen is cleaved at the arginine-alanine peptide bond by the serine proteases tissue-type plasminogen activator (t-PA) or urokinase-type plasminogen activator (u-PA), resulting in the formation of the active protease plasmin.[16] Under normal physiological conditions, t-PA is present in the blood at low concentration (5 ng/ml). Upon activation of endothelial cell, following tissue damage, t-PA is secreted at the site of the clot formation.[17] Figure 4 provides an overview of the structure of t-PA, illustrating its heavy and light chain. The heavy chain contains four domains, including the fibrin binding domain (the finger domain) and the plasminogen binding domain (Kringle 2 domain). The light chain is composed of one large domain containing the catalytic activity of t-PA.[18]

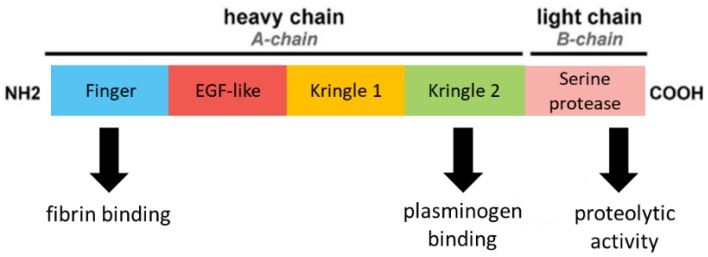

Figure 4: Schematic overview of the structure of t-PA. t-PA is composed of two chains. The heavy chain containing the 'Finger', 'EGF-like', 'Kringle 1' and 'Kringle 2' domains. The Finger domain contains the fibrin binding site and the Kringle 2 domain contains the plasminogen binding site. The light chain contains the 'serine protease' domain that has a proteolytic activity. Figure adapted from Hébert, M et al.[18]

u-PA is generated by monocytes, macrophages, and urinary epithelium. In contrast to t-PA, u-PA demonstrates lower affinity for plasminogen, doesn't necessitate fibrin as a cofactor, and, under typical circumstances, primarily functions in extravascular sites.[19] In the absence of fibrin, t-PA exhibits weak activation of plasminogen, but its

catalytic efficiency for plasminogen activation is significantly boosted by at least two orders of magnitude in the presence of fibrin. Binding of plasminogen via its kringle 1 domain to fibrin results in a conformational change of the relatively closed spiral structure of plasminogen, in which the cleavage site at arginine 561 is inaccessible, to a semi-open conformation.[20] Similarly, binding of the finger domain and kringle 2 domain of t-PA to free lysing residues on fibrin results in a 10^2 to 10^3 fold increase in its activity. Activation of plasmin results in a positive feedback mechanism of its own activation via the generation of additional C-terminal lysine residues on fibrin. In the second phase of fibrinolysis, the activated plasmin cleaves fibrin in the αC-domains followed by removal of an N-terminal peptide of the β-chain and cleavage the of coiled-coil connector in the E- and D-domains of fibrin.[20] The breakdown of fibrin initially results in large fibrin degradation products that are subsequently cleaved to smaller soluble fragments. The smaller fragments including fibrinopeptide B and D-dimers, are released in the circulation (Figure 5).[19] Of note, when excessive fibrinogen is present in the circulation, plasmin can cleave small fragments from the fibrinogen polypeptide chain resulting in fragment X and other small fragments that inhibit polymerization of fibrinogen.[16]

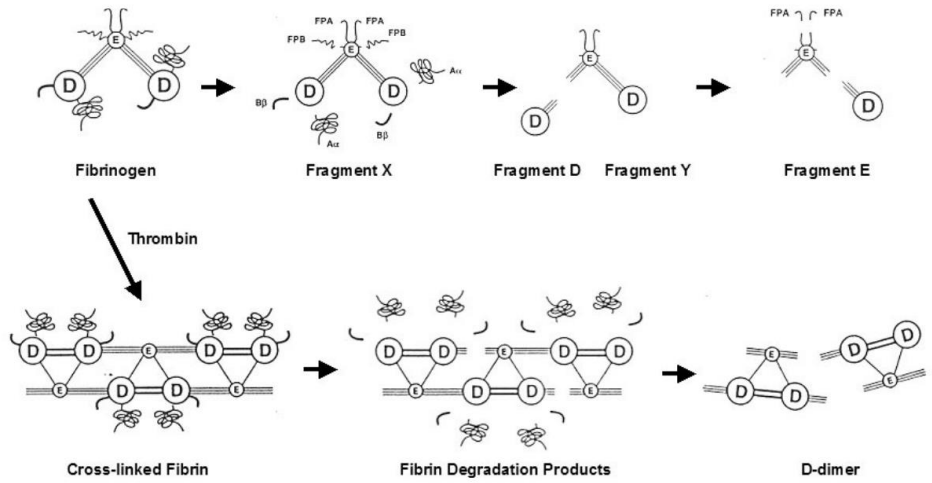

Figure 5: Degradation of fibrinogen and cross-linked fibrin by plasmin. Fibrinogen is cleaved by plasmin resulting in fragment X and other small fragments that inhibit polymerization of fibrinogen. After polymerization of fibrinogen to fibrin by thrombin, degradation of fibrin results in large fibrin degradation products and eventually in D-dimers. Figure taken from Cesarman-Maus et al.[16]

As depicted in Figure 6, the process of fibrinolysis is closely regulated through endogenous inhibitory proteins. Regulation of fibrinolysis occurs via (i) inhibition of plasminogen activators (plasminogen activator inhibitor (PAI)-1,-2,-3, neuroserpin and

protease nexin-1), (ii) modulation of the fibrin surface (Thrombin-activatable fibrinolysis inhibitor (TAFI)) or (iii) direct inhibition of plasmin (α2-antiplasmin and α2-macroglobulin).[16] PAI-I and TAFI are two key regulators of fibrinolysis, closely associated with adverse cardiovascular events, making them important targets for drug development. PAI-I is released by endothelial cells, monocytes, macrophages, hepatocytes, adipocytes and platelets. It is part of the serpins family that forms covalent complexes with their unique target enzymes resulting in rapid clearance from the circulation (resulting in the short half-lives of 4 to 8 minutes of t-PA and u-PA, respectively). However, when plasminogen and its activator bind to the C-terminal lysine residues on fibrin, they are protected from inhibition, allowing fibrinolysis to occur localized to the injury site.[21] Removal of these C-terminal lysine residues on fibrin by TAFI after its activation by thrombin and thrombomodulin further reduces fibrinolysis.[22]

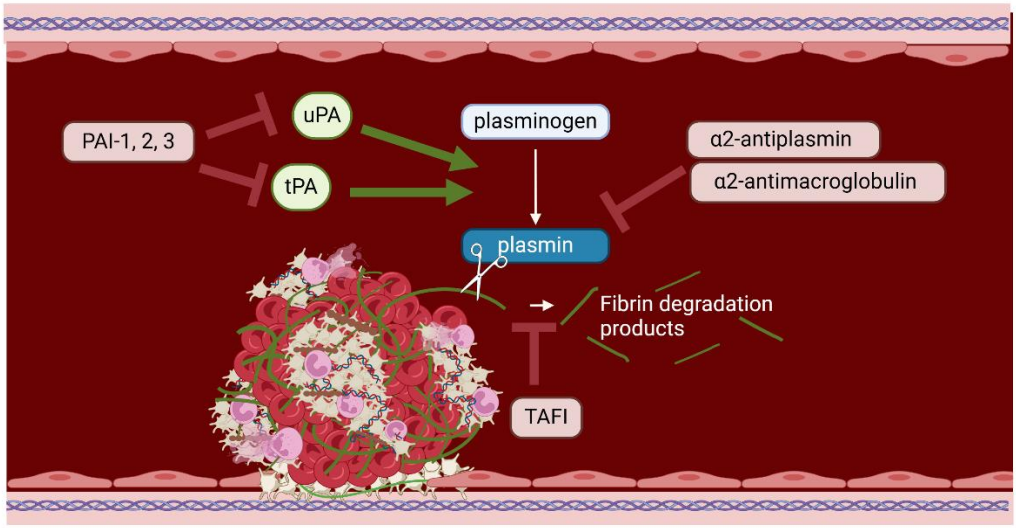

Figure 6: Regulation of fibrinolysis. Fibrinolysis is regulated through endogenous inhibitory proteins that can inhibit plasminogen activators (plasminogen activator inhibitor (PAI)-1 or by direct inhibition of plasmin (α2-antiplasmin and α2-macroglobulin). Thrombin activable fibrinolysis inhibitor (TAFI) impedes fibrinolysis by removing C-terminal residues from fibrin, these lysine residues are vital for plasminogen binding to fibrin. Figure made with Biorender.

1.2 Pathological thrombus formation

When the tight balance of thrombus formation to stop bleeding and fibrinolysis is disrupted, it can lead to pathological hemorrhaging or thrombosis. Disorders affecting proteins of the primary and secondary hemostasis can cause bleeding, as seen in hemophilia A (FVIII deficiency) and von Willebrand disease (VWD) (VWF deficiency).

Conversely, excessive thrombus formation can lead to partial or complete blockage of arteries or veins, resulting in conditions such as ischemic stroke, myocardial infarction, and deep vein thrombosis. Epidemiological studies as well as histopathological analysis of stroke thrombi revealed various structural components that are abundantly present and appear to play an important role in thrombus formation. Recently, VWF and neutrophil extracellular traps (NET) gained much attention as potential therapeutic targets due to their crucial involvement in thrombus formation and stroke pathology. In this part of the introduction the role of these structural components in (pathological) thrombus formation will be highlighted since they play an important role in this PhD project.

1.2.1 VWF in pathological thrombus formation

As described earlier, VWF has an essential role in the formation of the platelet-plug via its interaction with collagen and platelets. The importance of VWF becomes apparent in patients with either quantitative or qualitative abnormalities, as these conditions contribute to the intensified bleeding phenotype observed in patients with VWD. VWF is synthesized in endothelial cells and megakaryocytes as a single pre-pro-polypeptide. After cleavage of the signal peptide, two pro-VWF subunits form a covalent dimer trough the formation of 3 interchain cysteine pairs in the cysteine knot domains in the endoplasmic reticulum. Thereafter, VWF dimers translocate to the Golgi in which the low pH and high Ca^{2+} level stimulate the formation of VWF multimers through disulfide bridges between D3 domains.[4,7,24] The VWF pro-peptide is cleaved but remains noncovalently associated with VWF, facilitating multimerization. Furthermore the VWF pro-peptide is essential for targeting VWF to storage granules.[25] As the VWF multimer grows, it arranges into a right-handed helix, shaping itself into a tubular form for storage within the WPBs in endothelial cells or it is stored in α-granules of megakaryocytes.[24] VWF is released from α-granules primarily upon platelet activation, while it is released from endothelial cells both constitutively and in a regulated manner through the release of WPBs.[4] After secretion of the ultra large VWF multimers, the cryptic A2-domain unfolds due to normal shear within the blood resulting in proteolytic cleavage by ADAMTS13 (a disintegrin and metalloproteinase with a thrombospondin type 1 motif, member 13) into smaller multimers that circulate in plasma.[26] These smaller high molecular weight VWF multimers circulate in a

globular conformation, with the bindings sites for ADAMTS13 in the A2 domain and the binding sites for platelets in the A1 domain hidden.[27] The collagen binding A3 domain is however constitutively exposed and acts as a molecular sensor of damage to the vessel wall. Upon binding to collagen, VWF will unfold exposing the platelet binding A1 and ADAMTS13 binding A3 domains. This conformational regulation ensures localized and restricted thrombogenicity of VWF.

The importance of VWF in thrombus formation and stroke pathology becomes evident when examining the plasma VWF levels in patients. Patients with elevated plasma VWF levels have an increased risk for acute ischemic stroke (AIS).[28–30] Moreover, increased plasma VWF levels are associated with disease severity and poor outcome following AIS.[31] Due to the close regulation of VWF by ADAMTS13, irregularities in ADAMTS13 levels were also observed in various thrombotic disorders. For example in thrombotic thrombocytopenic purpura, deficiency or absence of ADAMTS13 results in systemic platelet clumping of the microcirculation and organ ischemia due to insufficient VWF cleavage.[32] Furthermore, reduced plasma ADAMTS13 levels are observed in AIS patients, and lower ADAMTS13 activity is linked to increased risk, severity, and all-cause mortality associated with ischemic stroke.[30,31,33–35] Logically, irregularities in the VWF/ADAMTS13 ratio can result in increased thrombus formation. An increased VWF/ADAMTS13 ratio is associated with an increased stroke severity.[36] This was also indicated by the predictive value of the VWF/ADAMTS13 ratio for AIS mortality and outcome.[33]

1.2.2 Neutrophils and extracellular DNA in pathological thrombus formation

The traditional view of the hemostatic system based on the interplay between platelet activation and the coagulation factor cascade has evolved in accepting the important influence of the immune system in the development of pathological thrombus formation.[37] Leukocytes are recruited to the damaged blood vessels. Leukocytes contribute to thrombus formation by the expression and release of coagulation factors, by the release of cytokines, which modulate the expression of procoagulant and adhesive molecules on vascular endothelial cells and promote the activation and aggregation of platelets.[38,39] The important role of leukocytes in pathological thrombus formation is further supported by clinical evidence that higher leukocyte and especially

high neutrophil levels predict unfavorable outcomes in different thrombotic diseases, including coronary artery disease and AIS.[40–43] Leukocytes activate platelets by forming platelet-leukocyte aggregates. This is facilitated by the binding of leukocyte P-selectin glycoprotein ligand-1 to platelet P-selectin, which in turn further promotes primary thrombus formation.[44] Among all leukocytes, neutrophils are the most abundant leukocyte present in the blood and play an important role in promoting thrombus formation. One of the most fascinating characteristics of neutrophils is their capability to release NETs.

NETs were initially identified as a novel defense mechanism to pathogens by disarming bacteria and removing them from the circulation.[45] NETs are composed of decondensed chromatin decorated with granular proteins such as neutrophil elastase (NE), cathepsin G and myeloperoxidase (MPO), forming a fibrous network (Figure 7).[46] The formation of NETs, called NETosis, is an active process during which neutrophils undergo changes in there morphology after stimulation with a variety of agonists including pathogens, microbial wall components, platelets, several cytokines or thrombin.[47,48] NETs formation can be classified into two types: suicidal NETosis and survival NETosis (Figure 7). Following the activation of neutrophils, nicotinamide-adenine-dinucleotide-phosphate oxidase and intracellular granular proteases are activated. This leads to an increase in reactive oxygen species and activation of peptidyl arginine deiminase 4 (PAD4). PAD4 modifies arginine residues of histones H3 and H4 by citrullination leading to removal of the positive charge from the histones. This results in a weakening of the interaction between the histones and DNA allowing decondensation of chromatin and swelling of the nucleus. The increase in reactive oxygen species can also promote the release of MPO and NE, and the NE can enter the nucleus to assist in the cleavage of histones and chromatin condensation.[49] As a result of the swelling of the nucleus, the nuclear envelope breaks and the decondensed chromatin is mixed with cytoplasmic and granular components such as NE and MPO.[46] In the final step, the cytoplasmic membrane is disrupted, resulting in the release of the NETs.[48,50] In survival NETosis, PAD4 is activated in a non-reactive-oxygen-species-activated manner and the neutrophils themselves do not die upon release of their nuclear DNA.[49] Although NETs are currently the most studied form of extracellular traps, many other types of immune cells have been demonstrated to be

able to form extracellular DNA networks including, macrophages, monocytes, mast cells and eosinophils.[51–53]

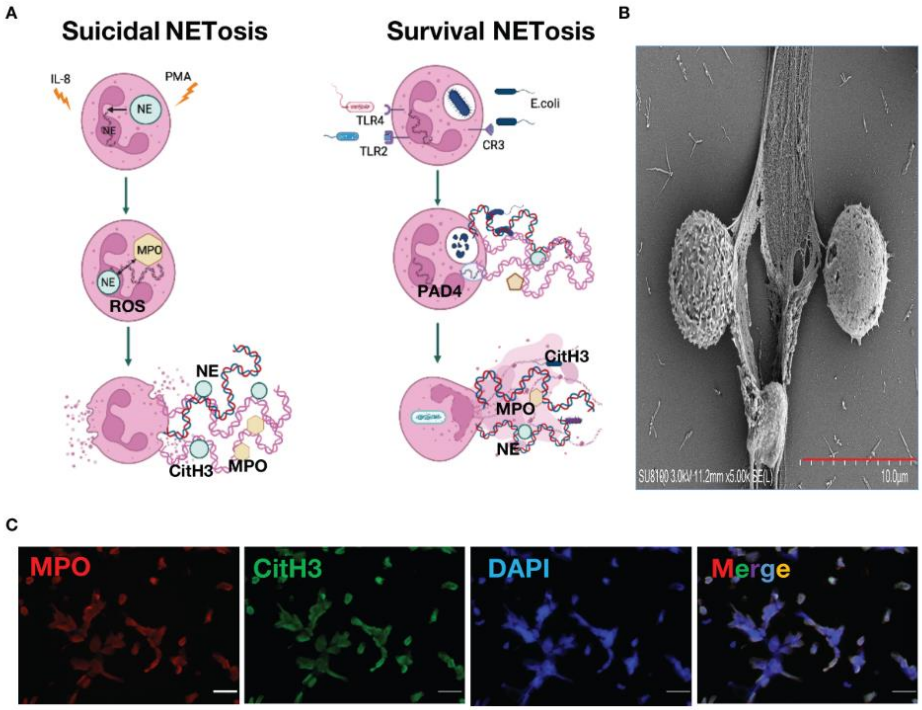

Figure 7: Neutrophil extracellular traps. (A) overview of the different mechanisms of neutrophil extracellular traps formation (B) Neutrophil extracellular traps structure under scanning electron microscope (C). Neutrophil extracellular traps stained with immunofluorescence, green, citrullinated histone H3; red, myeloperoxidase; blue, DAPI. Cit.: citrullinated; PAD4: peptidyl arginine deiminase 4; NE: neutrophil elastase; MPO: myeloperoxidase; PMA: phorbol myristate acetate. Figure taken from Zhou Y et al.[49]

The presence NET components such as DNA, histones and neutrophil elastase contribute to pathological thrombus formation through different processes. The web-like structure of NETs provides a physical scaffold for the deposition of platelets, RBCs, fibrinogen and VWF.[54] Additionally, NETs and their components, like histones and cathepsin G, can activate platelet adhesion and aggregation through the interaction of fibrinogen and Toll-like receptor 2 and 4.[49,54,55] Furthermore, extracellular DNA and citrullinated histones from NETs can bind and activate coagulation factors, thereby enhancing thrombin generation.[49,54,56,57] This effect is further potentiated by the impairment of coagulation inhibitors due to the presence of histones.[49] Moreover, NETs can bind plasma proteins such as VWF and fibrinogen enhancing the stability of the thrombus.[54] As illustrated in Figure 8, the interaction between NETs and VWF

play an important role in the formation of thrombi.[58,59] Neutrophil granular components, including neutrophil elastase and cathepsin G, released during NET formation, also promote thrombosis by inhibiting tissue factor pathway inhibitor, promoting endothelial activation and promoting prothrombin production.[49,60]

The presence of extracellular DNA and other NET components were shown to stabilize the thrombus via different mechanisms. DNA and histones can alter the structure of fibrin, leading to the formation of thicker fibrin fibers that exhibit increased resistance to fibrinolysis.[61,62] Fibrinolysis is further limited by the released NE during NET formation that can reduce plasminogen into small fragments decreasing its binding to fibrin and the formation of plasmin.[63] Moreover, under high-shear conditions, NETs can bind to VWF and PAI-I, again enhancing thrombus stability and counteracting fibrinolysis.[58,64] Recent findings demonstrate that NET components can inhibit ADAMTS13 activity through various mechanisms, including oxidation, citrullination, proteolysis or competitively binding to VWF A2 substrate. This inhibition leads to increased concentrations of VWF antigen, promoting the formation of ultra large VWF multimers, which enhance prothrombotic effects at sites of vascular injury.[59]

Clinical evidence supports the detrimental role of NETs in thrombosis-related conditions, such as AIS, myocardial infarction and venous thromboembolism.[65–67] Various NET biomarkers, including H3Cit, cell-free DNA, nucleosomes, neutrophil elastase and myeloperoxidase, have been investigated.[65,68–70] These biomarkers are increased in ischemic stroke patients.[67,68] Higher levels of H3Cit, myeloperoxidase and cell-free DNA levels are associated with worse outcome and increased mortality risk.[65,68,69]

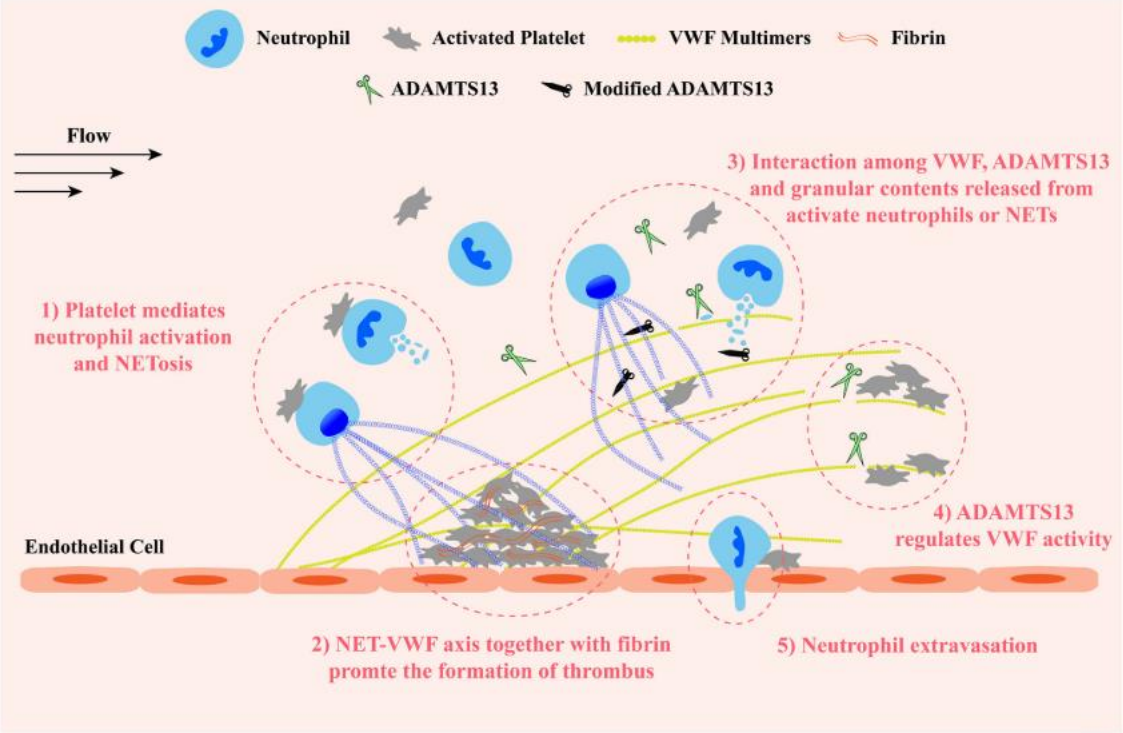

Figure 8: schematic overview of the VWF-NET axis in thrombus formation. 1) The interaction between platelets, VWF and neutrophils forms a vicious cycle promoting thrombosis. Platelets mediate neutrophil activation, and NET can interact with VWF and exert prothrombotic and proinflammatory effects, inducing the release of VWF multimers and promoting platelet adhesion in turn. 2) Both NETs and VWF alter fibrin networks enhancing their procoagulant activity and increasing resistance to fibrinolysis. 3) Granular components released during neutrophil activation and NETosis not only inactivate ADAMTS13 via chemical modification or competitive combination but also cleave VWF. Figure taken from Yang J et al. [59]

2 Ischemic stroke

2.1 Epidemiology of stroke

A well-functioning hemostatic system is essential for the proper functioning of the human body, as blood serves as the primary carrier of oxygen and energy to all organs. Disruption of blood supply to a region can result in cell death and impaired function in the affected area. In stroke, the blood supply to a specific region of the brain is interrupted, leading to severe neurological deficits with devastating consequences.[71] Stroke can be broadly classified into AIS and hemorrhagic stroke. AIS accounts for the majority of strokes (62%) and generally results from an arterial occlusion caused by a thrombus blocking the blood flow.[72] The remaining part of stroke presentations are intracerebral (28%) or subarachnoid (16%) hemorrhagic and result from the

rupture of cerebral arteries.[72] The subsequent sections of this thesis manuscript will focus predominantly on AIS.

Stroke is considered the second leading cause of death globally and the third leading cause of both death and disability when considering disability-adjusted life-years lost (DALYs).[73] Annually, over 12.2 million new stroke cases are reported worldwide.[72] Notably, one out of every four individuals aged 25 or above will experience a stroke at least once in their lifetime.[72] Significant variations between countries were observed in age-standardized stroke incidence rates (Figure 9A) mortality and DALY rates (Figure 9B).[73]

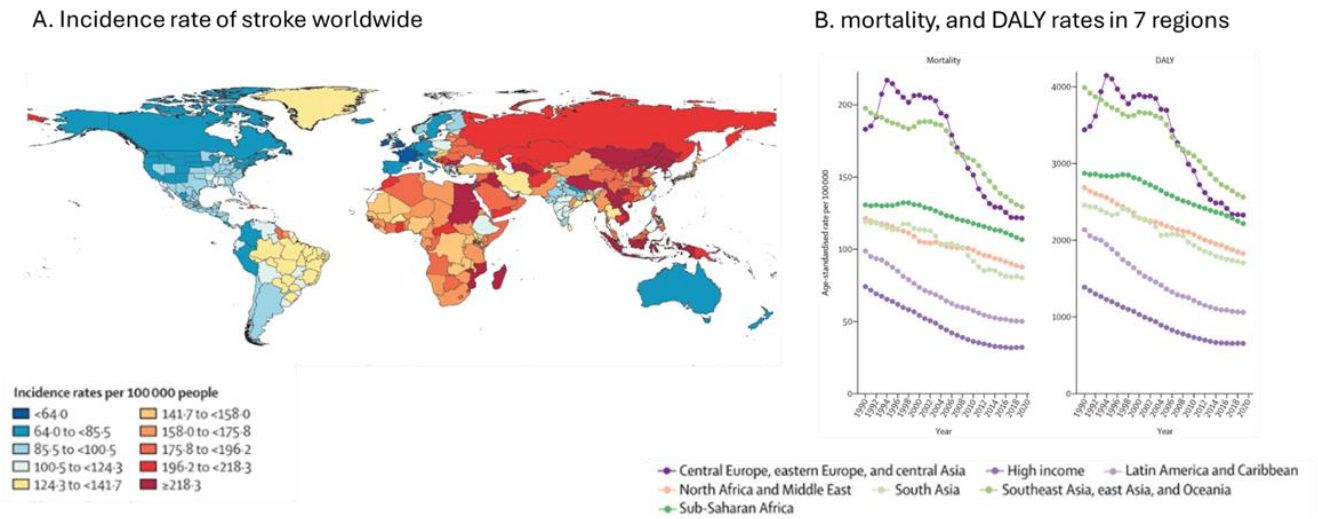

Figure 9: Age-standardized stroke incidence rates, mortality and DALYs per 100 000 people. (A) overview of age-standardized stroke incidence rates per 100,000 individuals, for all stroke types, encompassing both genders in the year 2019. (B) overview of age-standardized stroke mortality and DALY rates per 100,000 individuals, for all stroke types in seven Global Burden of Diseases regions. Figure adapted from GBD 2019 Stroke Collaborators.[73]

While strokes are more commonly associated with older age groups, they can occur at any age, with a significant portion (62%) happening before the age of 70.[72] This prevalence is exacerbated by various behavioral and metabolic risk factors, including high systolic blood pressure (accounting for 55.5% of total stroke DALYs), high body mass-index (24.3%), elevated fasting plasma glucose (20.2%), ambient particulate matter pollution (20.1%), and smoking (17.6%).[72,74] These risk factors are influenced by dynamic factors such as rapid economic development, shifting social ideologies, and population aging. Besides its profound effect on the patient's life, stroke also carries a substantial socioeconomic burden.[75,76] It is estimated that approximately 34%

of the global total healthcare expenditure is spent on stroke.[76] Stroke related cost can be attributed to direct health related costs such as medical care expenditures for diagnosis, treatment, and rehabilitation, direct non-health related costs such as transportation, household expenses, relocation, property loss, and informal care of any kind, and to indirect cost as a result of the social welfare loss due to diseases.[75,77]

2.2 Etiology

The majority of AIS originate from thromboembolic events, stemming from various sources of embolism (Figure 10). Understanding the underlying cause of AIS is crucial as it informs therapeutic approaches aimed at preventing recurrent strokes. Among the various systems used for categorizing stroke, the "Trial of ORG 10172 in Acute Stroke Treatment" (TOAST) classification stands out as the most widely employed worldwide.[78] This classification system categorizes ischemic strokes based on the pathophysiological mechanisms underlying stroke onset. It is based on comprehensive clinical and diagnostic assessment, including neurological examination, brain imaging, electrocardiography, echocardiography, ultrasound of intra- and extracranial arteries, and laboratory assessments for prothrombotic states. Using the TOAST classification system, five stroke categories can be defined: large artery atherosclerosis (LAA), cardioembolic stroke (CE), small vessel occlusion, stroke of other determined origin, and embolic stroke of undetermined source (ESUS). Each subtype is further elaborated upon in subsequent sections.

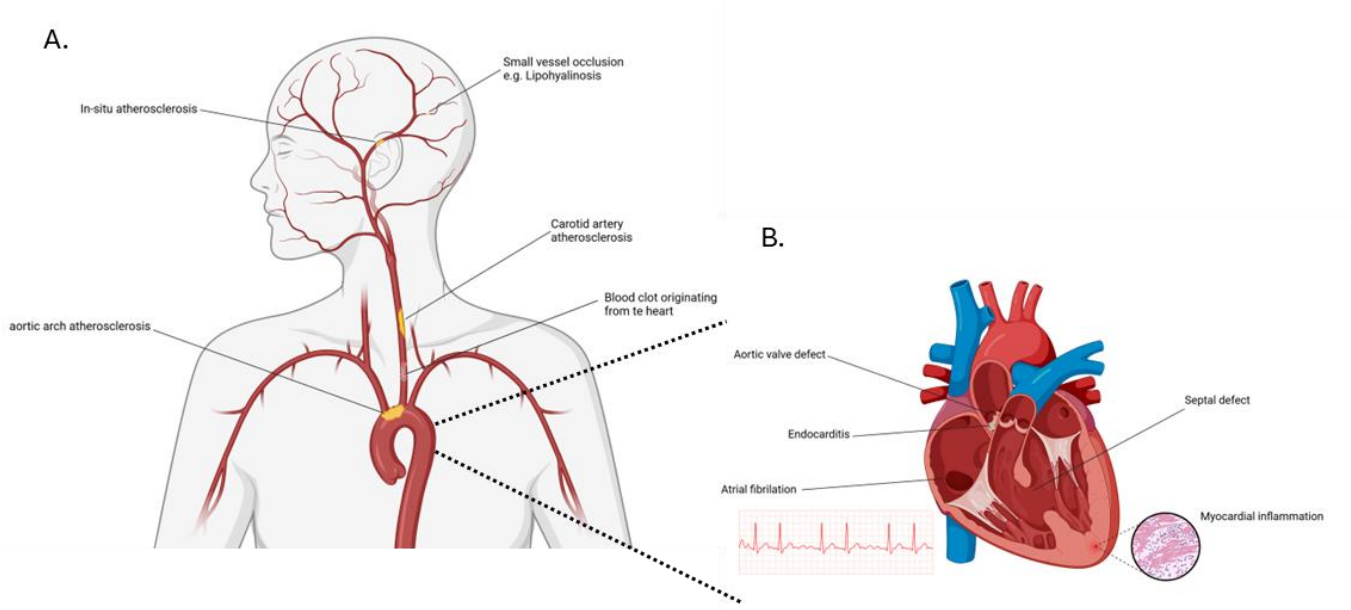

Figure 10: Acute ischemic stroke mechanisms: A. Overview of the common mechanisms resulting in an acute ischemic stroke including aortic arch atherosclerosis, carotid artery atherosclerosis, in-situ atherosclerosis, cardioembolic and small vessel disease due to lipohyalinosis. B. Common heart-related causes of stroke: atrial fibrillation, endocarditis, aortic valve defects, septal defects, myocardial inflammation. Figure made with biorender.

2.2.1 Large artery atherosclerosis

LAA can originate from an ulcerated and usually stenotic atherosclerotic plaque located in the aortic arch, neck or intra-cranial vessels.[78] The progression of atherosclerosis in these large arteries can lead to ischemic events through various mechanisms. When the lipid core of atherosclerotic plaques is exposed to the bloodstream, which can be caused by inflammation and ulceration of the fibrous cap of plaques, thrombi can develop. These thrombi block the atherosclerotic vessel directly (called in situ thrombosis) or can embolize distally (called artery-to-artery embolism).[79] The latter is known as the primary cause of LAA strokes. Among Western populations, the internal carotid artery, situated immediately after its bifurcation from the common carotid artery, emerges as the most common site for atherosclerotic plaques that can precipitate ischemic stroke.[79]

2.2.2 Cardioembolic stroke

CE stroke etiology encompasses patients with arterial occlusions originating from an embolus in the heart.[78] Various underlying pathologies including, atrial fibrillation, recent myocardial infarction, dilated cardiomyopathy, valvular heart disease, cardiac

tumors and (non-)infectious endocarditis can contribute to the formation of a thrombus that can embolize. The proportion of AIS associated with atrial fibrillation increases with age from 6.7% to 36.2%.[80] One of the suggested mechanisms involved in the development of thrombi in the heart in patients with atrial fibrillation or myocardial infarction is stasis of the blood in the left atrium or left ventricle, respectively, due to insufficient pumping of the heart.[81]

2.2.3 Small vessel occlusion

Small vessel occlusions, also known as lacunar strokes, primarily affect the small cerebral penetrating arteries that supply blood to deeper brain structures like the basal ganglia, thalamus, and brainstem. It is often caused by small vessel diseases that includes any pathologic process that damages small end arteries, arterioles, venules, and brain capillaries.[82] Small vessel disease accounts for approximately 25% of AIS and plays an important role in vascular dementias.[83] The most common pathologies leading to small vessel occlusions include arteriolosclerosis, often caused by aging, hypertension, and other conventional vascular risk factors; cerebral amyloid angiopathy, resulting from the vascular accumulation of β-amyloid; and lipohyalinosis, caused by thickening of the vessel wall due to fibrin deposits.[82]

2.2.4 Stroke of other determined origin

This category includes patients with rare causes of stroke and accounts for approximately 2% to 9% of all strokes.[78,84] The most common causes of stroke of other determined origin are atrial dissection (39.1%), cancer-related stroke (17.3%), intrinsic diseases if the arterial wall (16.7%), primary hemostatic diseases (7.9%), infectious and inflammatory diseases (4.6%), hypoperfusion syndromes (4.6%), hereditary syndromes (4.3%), iatrogenic (3.8%) or related to migraine and drugs (0.4%).[84]

2.2.5 Embolic stroke of undetermined origin

The last subtype of AIS encompasses patients with cryptogenic strokes and consists of three distinct groups. The first group includes patients with incomplete diagnostic evaluations, impeding the identification of the underlying pathology.[78,85] This category often includes individuals who passed away shortly after hospital admission, leaving insufficient time for diagnostic investigations, as well as patients with terminal illnesses that diminish the importance of diagnostic evaluations and therapeutic decisions. The

second group comprises patients diagnosed with two or more concurrent potential causes of stroke. Approximately 5% of patients with AIS have multiple obvious stroke etiologies.[78,86] The final group contains patients in which all diagnostic tests were completed but no cause of stroke was identified.[78] In 2014, this group was called ESUS and accounts for about 18% (with a range of 8-28%) of all AIS cases.[85,87]

3 Diagnosis of ischemic stroke

3.1 Symptoms of ischemic stroke

AIS clinically presents with a sudden onset of focal deficits attributed to a specific location within the central nervous system. Symptoms can include hemiparesis, hemianesthesia (numbness on one side of the body), aphasia (language disorder), homonymous hemianopia (loss of the same half of the visual field in each eye) and hemispatial inattention.[79] The American Heart Association/American Stroke Association has introduced the "FAST" acronym to improve awareness of stroke symptoms in the prehospital setting.[88] The acronym stands for Facial drop, Arm weakness, Speech difficulty and Time of onset/time to call the emergency department as depicted in Figure 11 and is able to identify 69 to 90% of strokes.[89–91] However some stroke patients, especially patients with posterior circulation events tend to be missed using the FAST acronym. Recent studies suggest to change the acronym to "BE FAST" to include balance and eyes as this increased the number of strokes identified.[91,92]



Figure 11: FAST acronym to improve awareness of stroke symptoms. Acronym implemented by the American Heart association to improve the general awareness of stroke symptoms in the pre-hospital setting. The acronym stands for Facial drop, Arm weakness, Speech difficulty and Time to call the emergency department. Figure taken from American Heart Association.

3.2 Diagnostic imaging of ischemic stroke

Upon arrival at the emergency room, all patients with a suspected stroke will undergo a non-contrast computed tomography (NCCT) scan to differentiate AIS from intracerebral hemorrhage.[79] NCCT is readily accessible, cost-effective, rapidly

obtained, and can be utilized in mobile stroke units.[93] Acute hemorrhages are characterized by hyperdense appearances (Figure 12A) on NCCT, whereas AIS manifest as hypodense regions (Figure 12B). Once intracerebral hemorrhage is ruled out, advanced diagnostic imaging will further focus on visualizing the occluded vessel and vascular anatomy using computed tomography (CT) angiography (Figure 12C), and on assessing cerebral blood flow to determine the ischemic core region and ischemic penumbra using CT perfusion (Figure 12D).[94–96]

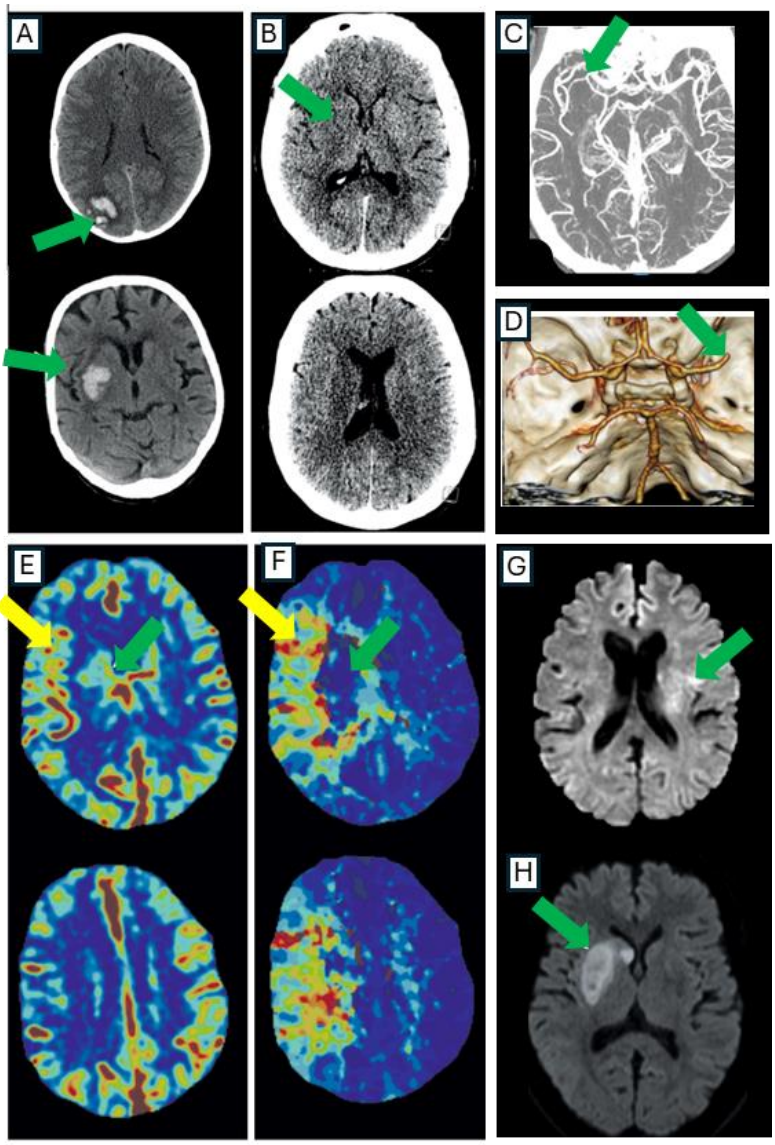

Figure 12: Brain imaging for ischemic stroke diagnosis: Non-contrast computed tomography (NCCT) imaging of (A) intracerebral hemorrhage as hyperdense areas (green arrows) and (B) ischemic changes appearing as a hypodense zone indicating occlusion at the proximal right middle cerebral artery (green arrow). (C and D) CT angiography used to visualize the occluded vessel (green arrows) and vascular anatomy of the patients. (E and F) CT-perfusion imaging used to assess cerebral

blood flow demonstrates regions with increased cerebral blood-flow (green arrow) that could likely indicate salvageable penumbra and regions with delayed arrival of contrast agent (yellow arrow) indicating tissue that is critically hypo-perfused indicating a middle cerebral artery occlusion (G) MRI diffusion imaging 11 minutes after the onset of ischemic stroke already shows hyperintense regions (green arrow). (H) MRI diffusion of the following day shows the expected infarct in the basal ganglia (green arrow) with salvage of the cortical regions. Figure adapted from Puig J. et al, Hjort N. et al and Campbell B. et al 2019 and 2020.[79,97–99]

In addition to CT, certain hospitals utilize magnetic resonance imaging (MRI) as the primary imaging method. Although MRI is superior to NCCT in identifying ischemia at earlier stages and smaller or posterior fossa lesions, it is not always available, comes with a higher cost and is contra-indicated for certain patients with metallic foreign bodies or older generation implantable devices.[93] Diffusion MRI evaluates the movement of water molecules and stands as the most sensitive imaging technique for detecting acute ischemia. In regions with cytotoxic oedema, characterized by a redistribution of water from extracellular to intracellular spaces, the diffusion is restricted.[79] Abnormal diffusion MRI findings typically manifest within minutes after the onset of ischemic stroke (Figure 12G).[99] Diffusion MRI imaging is often used post treatment to evaluate the infarct region (Figure 12H).[79]

3.3 Stroke severity

Stroke severity is generally assessed using a 15-item assessment tool called National Institutes of Health Stroke Scale (NIHSS).[100] It is based on various clinical assessments including consciousness level, eye movements, visual field integrity, facial movements, muscle strength in arms and legs, sensation, coordination, language, speech, and neglect.[101] Each impairment within these domains is assessed on a scale ranging from 0 to 2, 0 to 3, or 0 to 4. The individual item scores are then added together to generate a total score between 0 and 42, with higher scores indicating greater stroke severity.[101] The NIHSS can also serve a strong predictor of post-stroke outcomes.[102]

4 Recanalization strategies

The general aim of AIS treatment is fast and rapid recanalization of the occluded artery. Upon occlusion of a cerebral artery, the downstream regions of the brain are at risk of permanent infarction due to the lack of oxygen (Figure 13). This region at risk

is called the ischemic penumbra and will progress into irreversible infarction if no reperfusion occurs. The ischemic core region, however already experienced irreversible damage and cannot be salvaged by reperfusion.[103] Over time and if no reperfusion occurs, the ischemic penumbra will gradually progress into ischemic core.[104,105] The rate at which this occurs depends on multiple factors including the amount of collaterals. It is estimated that approximately 1.9 million neurons and 14 billion synapses will be lost every minute during an acute ischemic event.[106]

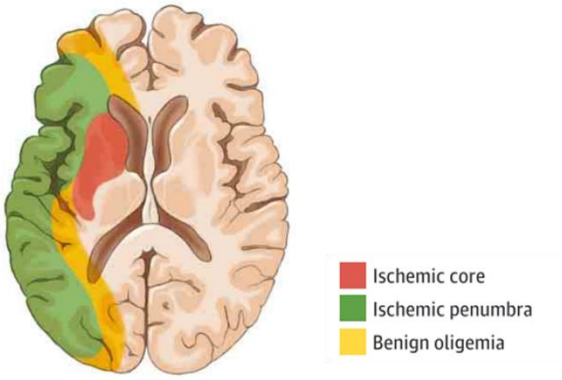

Figure 13: Progression of brain damage after acute ischemic stroke. Brain tissue impacted by a blockage in a blood vessel can be categorized into distinct regions: the ischemic core, comprising irreversibly damaged tissue; the ischemic penumbra, comprising salvageable brain tissue; and the benign oligemia comprising a region with reduced perfusion but not at risk of irreversible damage. Over time, the penumbra may transition into the ischemic core. Figure taken from Prabhakaran S. et al[103]

Treatment success is in clinical practice often assessed and divided into recanalization success and functional outcome. Recanalization success is scored using the modified Thrombolysis In Cerebral Infarction (mTICI) score, which ranges from 0 (indicating no reperfusion) to 3 (representing complete reperfusion).[107,108] The functional outcome of patients following a stroke is assessed at different timepoints post-stroke using the modified Rankin Scale (mRS), which spans from 0 (indicating no symptoms) to 6 (indicating death).[109,110] Further details on both scoring systems are provided in Table 1.

mTICI		mRS	
0	No perfusion or anterograde flow beyond site of occlusion	0	No symptoms at all
1	Penetration but not perfusion. Contrast penetration exists past the initial obstruction but with minimal filling of the normal territory	1	No significant disability: despite symptoms, able to carry out all usual duties and activities
2a	Some perfusion with distal branch filling of <50% of territory visualized	2	Slight disability: unable to perform all previous activities (e.g. performing basic household chores) but able to look after own affairs without assistance
2b	Substantial perfusion with distal branch filling of ≥50% of territory visualized	3	Moderate disability: Requiring some help but able to walk without assistance
2c	Near-complete perfusion except for slow flow in a few distal cortical vessels or presence of small distal cortical emboli	4	Moderate severe disability: unable to walk unassisted and unable to attend to own bodily needs
3	Complete perfusion with normal filling of all distal branches	5	Severe disability: bedridden, incontinent and requiring constant nursing care and attention
		6	Death

Table 1: explanation of modified Thrombolysis In Cerebral Infarction (mTICI) score and modified Rankin Scale (mRS)

4.1 Pharmacological thrombolysis

Pharmacological thrombolysis of AIS thrombi is based on the endogenous fibrinolytic system. As described in section 1.1.3, the process of fibrinolysis can eliminate the formed blood clot when the risk of bleeding is restored. This process is based upon the activation of plasminogen by t-PA or u-PA to form plasmin. Subsequently, plasmin can degrade fibrin fibers leading to the lysis of the blood clot. In 1995, a groundbreaking clinical trial by National Institute of Neurological Disorders and Stroke was published using alteplase, a recombinant (r)t-PA, for the treatment of AIS patients.[111] Although an increased incidence of intracerebral hemorrhage was observed, this trial for the first time showed an improved clinical outcome if treatment was initiated within three hours after symptom onset.[111] Following this trial, alteplase treatment for AIS was approved by the food and drug administration (FDA) in 1996 and to this day, remains the only pharmacological drug to have received FDA approval for the treatment of AIS. Alteplase treatment should be administered to a final rt-PA dose of 0.9 mg/kg of which 10% is administered as a one-minute bolus and the remaining 90% as an infusion over 60 minutes. The main limitation and a major logistic issue was the limited time-window of three hours after symptom onset mainly due to the increased risk of hemorrhage if treatment was initiated later.[111] In 2008 the time-window for alteplase treatment was expanded to 4.5 hours post symptom onset after

the positive results of the European Cooperative Acute Stroke III (ECASS III) study.[112] Recent evidence shows that in some patients with specific features identified by advanced imaging such as diffusion-weighted MRI or CT prefusion, alteplase treatment can be beneficial even 9 hours after symptom onset.[113] The latest European Stroke Organisation guidelines published in 2021, strongly recommend the use of alteplase in patients not eligible for mechanical thrombectomy presenting within 4.5-9 hours of symptom onset and who show a CT or MRI core/ perfusion mismatch.[114]

Due to multiple contra-indications and the limited time-window, alteplase treatment is still only available to around 15% of the patients.[115] Contra-indications for alteplase treatment include acute intracranial hemorrhage, history of hemorrhage, severe uncontrolled hypertension, thrombocytopenia and coagulopathy, anti-coagulant medication (low-molecular-weight heparin, factor Xa inhibitors, direct thrombin inhibitors), advanced age and recent major surgery.[116] Strikingly, of the patients who receive alteplase treatment, it leads to successful recanalization in only 30% of the patients.[117,118] Multiple factors are associated with a reduced efficacy of alteplase treatment including longer time for treatment initiation, proximal thrombi, increased clot length and low residual clot permeability.[119] Indeed, it was observed that the number of patients needed to be treated to achieve a favorable outcome for one additional patient increases significantly over time, rising from about 4.5 patients within the first 90 minutes to around 15 patients between 3 and 4.5 hours.[120] This trend correlates to the reduced amount of salvageable penumbral tissue over time. Furthermore several patients clinical risk-factors including hyperglycemia, diabetes mellitus and atrial fibrillation are linked with poor outcome after alteplase treatment.[118] The exact mechanisms underlying resistance to rt-PA treatment, however remains not fully understood but it is believed that also thrombus composition has a major impact on treatment efficacy. The link between thrombus composition and thrombolysis resistance is discussed in detail in chapter 2.

Although not included in the official drug labelling indications, research into the use of tenecteplase for the treatment of AIS is rising. Tenecteplase is a genetically altered version of alteplase possessing several pharmacological and practical advantages over alteplase (Figure 14).[119] These advantages arise from different mutations of t-PA

resulting in its increased affinity to fibrin (lysine 296, histidine 297, arginine 298, and arginine 299 to alanine, alanine, alanine, and alanine), faster onset of action, longer half-life (threonine 103 to asparagine and asparagine 117 to glutamine), reduced inhibition of PAI-I (lysine 296, histidine 297, arginine 298, and arginine 299 to alanine-alanine-alanine-alanine) and the possibility of a single-bolus injection.[121,122] Multiple phase 2 and 3 clinical trials have investigated the efficacy and safety of different dosages of tenecteplase compared to alteplase. The Tenecteplase versus Alteplase Before Endovascular Therapy for Ischemic Stroke trial (EXTEND-IA TNK) showed that patients treated with tenecteplase showed better functional outcomes after three months without differences in intracranial hemorrhage.[123] A meta-analysis including 5 large clinical trials showed the non-inferiority of tenecteplase compared with alteplase when investigating functional outcomes and safety.[124] The latest European Stroke Organisation guidelines do not recommend the use of tenecteplase over alteplase in patients within the 4.5 hour time-frame and who are not eligible for mechanical thrombectomy.[114] Given all current and upcoming data on the use of tenecteplase, new indications could emerge changing the standard treatment of care.

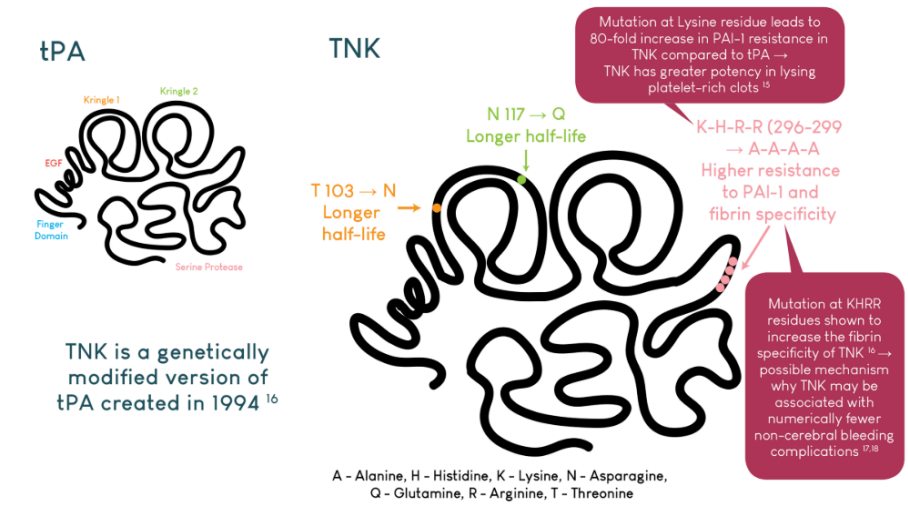

Figure 14: Structural differences between standard rt-PA and Tenecteplase (TNK). Structural representation of the genetical modifications of t-PA to obtain tenecteplase. A point mutation in de Kringle 1 domain (threonine 103 to asparagine) and in the Kringle 2 domain (asparagine 117 to glutamine) results in a longer half-life of tenecteplase. Four-point mutations in the serine protease domain (lysine 296, histidine 297, arginine 298, and arginine 299 to alanine-alanine-alanine-alanine) result in a higher resistance to PAI-I and increased specificity to fibrin. Figure taken from Zhu A et al.[119]

4.1.1 Towards improved thrombolysis in ischemic stroke

Since tenecteplase has a similar mechanism of action to alteplase, it is likely to encounter similar difficulties in lysing thrombi that are resistant to alteplase. New thrombolytic strategies focusing on targeting other structural components of stroke thrombi besides fibrin are increasingly investigated. Recent findings on the structure of stroke thrombi have uncovered their complex composition, which includes an interplay between RBCs, fibrin, platelets and VWF, alongside inflammatory components such as leukocytes and NETs.[125–127] The presence of these non-fibrin components could play a role in currently observed rt-PA resistance. Recently, novel strategies targeting these non-fibrin components such as VWF or NETs have attracted much interest as potential ways to improve thrombolysis success in patients. Several experimental stroke models in mice targeting VWF either via administration of supraphysiological ADAMTS13, a gain-of-function ADAMTS13 variant or the reducing agent N-acetylcysteine (NAC), have been shown to promote the lysis of arterial thrombi and reduce infarct size.[128–130] In an in vitro arterial stenosis model, the dimerized form of NAC, diNAC, was shown to be superior to NAC in the lysis of VWF-platelet–rich clots.[131] An alternative approach recently tested in mice is microlyse, a single polypeptide that combines a VWF-targeting nanobody with the catalytic domain of urokinase plasminogen activator.[132] Following VWF binding, microlyse locally activates plasminogen, resulting in a reduction in cerebral lesion volume compared to standard rt-PA treatment.[133] In addition to targeting VWF in stroke thrombi, NETs and extracellular DNA (exDNA) in general can create an additional network stabilizing the thrombus. Targeting exDNA using the DNA degrading enzyme DNase-1 has been shown to improve lysis of stroke thrombi.[134–136] Furthermore, in a mouse stroke model, addition of DNase-1 significantly improved stroke outcome.[137]

4.2 Mechanical thrombectomy

Besides the pharmacological lysis of the thrombus, mechanical removal of the occluding thrombus is currently increasingly being used. Mechanical thrombectomy (MT) involves a minimally invasive procedure in which a neuro-interventional radiologist employs a specialized thrombectomy device, inserted through a guiding catheter, to extract the thrombus from the circulation. The first MT device, the MERCI (Mechanical Embolus Removal in Cerebral Ischemia), was already FDA approved in

2004 but although favorable clinical outcomes tended to be higher, recanalization rates were lower than expected.[138] The MERCI device is a type coil retriever and consists of a long wire with a helical coil at the distal end. This coil reforms at the site of the thrombus, wrapping around the thrombus allowing its removal, as shown in Figure 16.[138] Later a second first-generation device, the Penumbra Clot Aspiration system that uses proximal suction to remove the thrombus was FDA approved.[139] Nevertheless, despite achieving higher rates of revascularization, only 27.7% of patients demonstrated clinical independence at 90 days.[139] In 2012 the second-generation MT devices namely the stent retrievers were FDA approved. As illustrated in Figure 15, the stent retrievers can deploy within the thrombus allowing quick restoration of the blood flow.

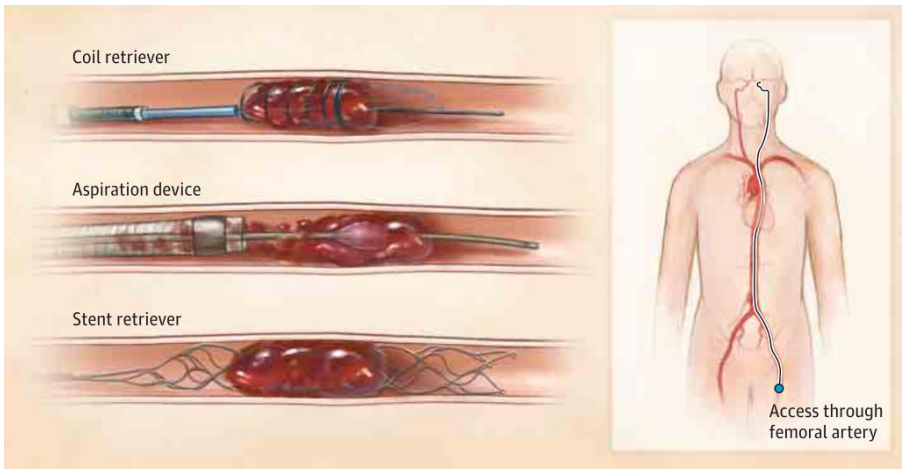

Figure 15: Mechanical thrombectomy: (A) Schematic representation of three types of mechanical thrombectomy devices. The first approved device, a coil retriever, consists of a long wire with a helical coil at the distal end that reforms at the site of the thrombus, wrapping around the thrombus allowing its removal. Aspiration devices use proximal suction to remove the thrombus. Stent retriever devices of second-generation devices deploy within the thrombus. (B) Vascular access to the cerebral vasculature is generally via the femoral artery. Figure taken from Prabhakaran S. et. al.[103]

The use of MT for the treatment of AIS was however not widely accepted due to the lack of effectiveness compared to pharmacological thrombolysis in many of the trails. These trials however, had several limitations, including treatment delays, unstructured workflow, minimal use of stent retrievers, and lack of imaging-based selection to prove large vessel occlusion, as well as exclusion of patients with large areas of irreversible brain damage.[105] After the publication of the five positive thrombectomy trials in 2015, employing second-generation devices, which demonstrated significantly enhanced reperfusion and functional outcomes in patients with anterior AIS and who presented

within 6 hours of onset of symptoms in comparison to pharmacological thrombolysis, the use of MT was boosted and found its way into general AIS treatment.[140–144] After publication of the DAWN and DEFUSE 3 trials, the treatment window was expanded from 6 to 24 hours.[145,146] This is especially important for patients with a wake-up stroke in which it is often difficult to determine the exact time of symptom onset. New trials are constantly looking into the effect of further expanding the treatment window. Recently, a meta-analysis including 569 patients showed the safety and beneficial effect of MT performed after 24 hours since symptom onset.[147]

When patients are eligible for both intravenous thrombolysis and MT, the question arises how to treat these patients especially in patients with large proximal thrombi in which the efficacy of alteplase is low. Possible risks of alteplase treatment before the use of MT include the possibility of fragmentation of the thrombus resulting in distal embolization complicating MT treatment. Multiple trials have been conducted to investigate the efficacy of bridging therapy, which consists of alteplase treatment before MT versus direct MT.[148–150] Although conflicting results have been reported, the main trials report a small increase in the percentage of patients achieving functional independence and small decrease in mortality in patients treated with alteplase followed by MT.[149] The current guidelines support the use of alteplase treatment before MT in patients with large vessel AIS within 4.5 hours after symptom onset.[151,152] Of note, successful recanalization does not always lead to good clinical outcomes. Indeed, data from a meta-analysis including 1287 patients indicated successful recanalization in 71% of patients, however only 27% of the treated patients were disability free at 90 days.[153] A possible mechanism related to this phenomenon could be impaired reperfusion of the microcirculation. Recently, the preliminary results of the Chemical Optimization of Cerebral Embolectomy (CHOICE) trial showed the beneficial effects of intra-arterial alteplase treatment after successful MT.[154]

Complications following MT are rare when investigated at individual level, but globally, they occur in about 10 to 20% of the patients.[155] Commonly reported complications are thrombus embolization, symptomatic intracerebral hemorrhage, subarachnoid hemorrhage/arterial perforation and dissection.[155] Therefore, it is important to identify possible risk factors for complications such as ongoing antiplatelet therapy, diabetes, and longer groin-to-reperfusion time to limit the risk of complications.[155] Although

complications are rare and MT resulted in a substantial improvement in patient outcome, several factors limit its application in clinical practice. These include patient-related factors such as distal occlusion, low NIHSS score and large ischemic core, as well as logistic factors including the need for specialized neurointerventional radiologist. As a result, only a small portion of patients are eligible for MT.[156] Another challenge in MT is the occurrence of unsuccessful reperfusion, with approximately 20-30% of thrombi proving difficult to retrieve efficiently.[157]

Recent reports indicate that obtaining recanalization in the first pass, known as first pass recanalization (FPR), is strongly associated with improved patient outcome. This improved patient outcome may possible be linked to decreased time to reperfusion, reduction of vessel wall injury, and lower risk of clot fragments.[158–161] Currently, FPR is achieved in only 25-35% of the patients[162], illustrating the need for better insights to increase FPR rates. Various factors influencing FPR have been identified, including age, sex, occlusion site, anesthesia type and choice of technique.[163]

5 Composition of ischemic stroke thrombi

Recanalization strategies as described above target the occluding thrombus present in the brain. Although there use significantly improved patient outcomes, some thrombi tend to be more resistant to rt-PA mediated lysis or seem to be more challenging to be removed via MT. Since the thrombus itself is the central target, it most likely plays a key factor in recanalization success. The availability of stroke thrombi after MT opened a new field in stroke research studying the composition of stroke thrombi.[125,164,165] Emerging evidence points towards a complex and highly variable structure of stroke thrombi involving not only RBCs but also thrombotic factors like platelets, VWF, and fibrin, alongside inflammatory components such as leukocytes and NETs.[125–127] Good understanding of the structural organization of stroke thrombi is important to better understand pathophysiological mechanisms underlying thrombus formation in AIS patients and to refine recanalization therapies. Additionally, knowledge on thrombus composition may enable the customization of secondary prevention strategies to mitigate the risk of recurrent strokes. Given that the composition of the occluding thrombus is a fundamental and central topic of this PhD thesis, a dedicated and comprehensive summary of the current state-of-the-art on the

composition of stroke thrombi is given in Chapter 2 (a published review entitled “Acute Ischemic Stroke Thrombus Composition”).

References

1. Versteeg HH, Heemskerk JWM, Levi M, Reitsma PH. New Fundamentals in hemostasis. Physiological Reviews. 2013 Jan 1;93(1):327–58.
2. Palta S, Saroa R, Palta A. Overview of the coagulation system. Indian Journal of Anaesthesia. 2014;58(5):515–23.
3. Broos K, Feys HB, De Meyer SF, Vanhoorelbeke K, Deckmyn H. Platelets at work in primary hemostasis. Blood Reviews. 2011;25(4):155–67.
4. Lenting PJ, Christophe OD, Denis C V. Von Willebrand factor biosynthesis, secretion, and clearance: Connecting the far ends. Blood. 2015;125(13):2019–28.
5. Bryckaert M, Rosa JP, Denis C V., Lenting PJ. Review of von Willebrand factor and platelets. Cellular and Molecular Life Sciences. 2015;72(2):307–26.
6. Tomaiuolo M, Brass LF, Stalker TJ. Regulation of Platelet Activation and Coagulation and Its Role in Vascular Injury and Arterial Thrombosis. Interventional Cardiology Clinics. 2017;6(1):1–12.
7. Leebeek FWG, Eikenboom JCJ. Von Willebrand's Disease. The new engl and journal of medicine. 2016;375(21):2067–80.
8. Lenting PJ, Christophe OD, Denis C V. Von Willebrand factor biosynthesis, secretion, and clearance: Connecting the far ends. Blood. 2015;125(13):2019–28.
9. Riddel JP, Aouizerat BE, Miaskowski C, Lillicrap DP. Theories of blood coagulation. Journal of Pediatric Oncology Nursing. 2007 May;24(3):123–31.
10. Madhusudhan T, Kerlin BA, Isermann B. The emerging role of coagulation proteases in kidney disease. Nature Reviews Nephrology. 2016 Nov 23;12(2):94–109.
11. Lazzaro MA, Malhotra K, Mohammad YM. The Role of Antithrombotics in Secondary Stroke Prevention. SEMINARS IN NEUROLOGY. 2010;30(5):492–500.
12. Weisel JW, Litvinov RI. Fibrin formation, structure and properties. Sub-Cellular Biochemistry. 2017;82:405–56.
13. Weisel JW, Litvinov RI. Mechanisms of fibrin polymerization and clinical implications. Blood. 2013;121(10):1712–9.
14. Alisa S. Wolberg, Campbell RA. Thrombin Generation, Fibrin Clot Formation and Hemostasis. Transfus Apher Sci. 2008;38(1):15_23.
15. Storti R V., Szwast AE. Molecular cloning and characterization of a full-length cDNA clone for human plasminogen. FEBS Letters. 1987;213(2):254–60.
16. Cesarman-Maus G, Hajjar KA. Molecular mechanisms of fibrinolysis. British Journal of Haematology. 2005;129(3):307–21.
17. Levin EG, Santell L, Osborn KG. The expression of endothelial tissue plasminogen activator in vivo: A function defined by vessel size and anatomic location. Journal of Cell Science. 1997;110(2):139–48.
18. Hébert M, Lesept F, Vivien D, Macrez R. The story of an exceptional serine protease, tissue-type plasminogen activator (tPA). Revue Neurologique. 2016;172(3):186–97.
19. Chapin JC, Hajjar KA. Fibrinolysis and the control of blood coagulation. Blood Reviews. 2015;29(1):17–24.
20. Longstaff C, Kolev K. Basic mechanisms and regulation of fibrinolysis. Journal of Thrombosis and Haemostasis. 2015;13(S1):S98–105.
21. Thelwell C, Longstaff C. The regulation by fibrinogen and fibrin of tissue plasminogen activator kinetics and inhibition by plasminogen activator inhibitor 1. Journal of Thrombosis and Haemostasis. 2007;5(4):804–11.
22. Foley JH, Kim PY, Mutch NJ, Gils A. Insights into thrombin activatable fibrinolysis inhibitor function and regulation. Journal of Thrombosis and Haemostasis. 2013;11(SUPPL.1):306–15.

23. Mutch NJ, Medcalf RL. The fibrinolysis renaissance. Journal of Thrombosis and Haemostasis. 2023;21(12):3304–16.
24. Springer TA. Von Willebrand factor, Jedi knight of the bloodstream. Blood. 2014;124(9):1412–25.
25. Haberichter SL, Fahs SA, Montgomery RR. Von Willebrand factor storage and multimerization: 2 independent intracellular processes. Blood. 2000;96(5):1808–15.
26. Zhang Q, Zhou YF, Zhang CZ, Zhang X, Lu C, Springer TA. Structural specializations of A2, a force-sensing domain in the ultralarge vascular protein von Willebrand factor. Proceedings of the National Academy of Sciences of the United States of America. 2009;106(23):9226–31.
27. Deng W, Wang Y, Druzak SA, Healey JF, Syed AK, Lollar P, et al. A discontinuous autoinhibitory module masks the A1 domain of von Willebrand factor. Journal of Thrombosis and Haemostasis. 2017;15(9):1867–77.
28. Bongers TN, De Maat MPM, Van Goor MLPJ, Bhagwanbali V, Van Vliet HHDM, García EBG, et al. High von Willebrand factor levels increase the risk of first ischemic stroke: Influence of ADAMTS13, inflammation, and genetic variability. Stroke. 2006 Nov;37(11):2672–7.
29. Wieberdink RG, Van Schie MC, Koudstaal PJ, Hofman A, Witteman JCM, De Maat MPM, et al. High von Willebrand factor levels increase the risk of stroke: The Rotterdam study. Stroke. 2010 Oct;41(10):2151–6.
30. Sonneveld MAH, De Maat MPM, Leebeek FWG. Von Willebrand factor and ADAMTS13 in arterial thrombosis: A systematic review and meta-analysis. Blood Reviews. 2014;28(4):167–78.
31. Sonneveld MAH, Franco OH, Ikram MA, Hofman A, Kavousi M, De Maat MPM, et al. Von Willebrand Factor, ADAMTS13, and the Risk of Mortality: The Rotterdam Study. Arteriosclerosis, Thrombosis, and Vascular Biology. 2016 Dec 1;36(12):2446–51.
32. Kremer Hovinga JA, Coppo P, Lämmle B, Moake JL, Miyata T, Vanhoorelbeke K. Thrombotic thrombocytopenic purpura. Nature Reviews Disease Primers. 2017;3:1–17.
33. Taylor A, Vendramin C, Singh D, Brown MM, Scully M. Von Willebrand factor/ADAMTS13 ratio at presentation of acute ischemic brain injury is predictive of outcome. Blood Advances. 2020;4(2):398–407.
34. Sonneveld MAH, De Maat MPM, Portegies MLP, Kavousi M, Hofman A, Turecek PL, et al. Low ADAMTS13 activity is associated with an increased risk of ischemic stroke. Blood. 2015;126(25):2739–46.
35. Denorme F, Kraft P, Pareyn I, Drechsler C, Deckmyn H, Vanhoorelbeke K, et al. Reduced ADAMTS13 levels in patients with acute and chronic cerebrovascular disease. PLoS ONE. 2017;12(6).
36. Prochazka V, Jonszta T, Czerny D, Krajca J, Roubec M, Macak J, et al. The role of von willebrand factor, ADAMTS13, and cerebral artery thrombus composition in patient outcome following mechanical thrombectomy for acute ischemic stroke. Medical Science Monitor. 2018;24:3929–45.
37. Swystun LL, Liaw PC. The role of leukocytes in thrombosis. Blood. 2016;128(6):753–62.
38. Bi R, Chen S, Chen S, Peng Q, Jin H, Hu B. The role of leukocytes in acute ischemic stroke-related thrombosis: a notable but neglected topic. Cellular and Molecular Life Sciences 2021. 2021 Aug 16;1:1–14.
39. Mandel J, Casari M, Stepanyan M, Martyanov A, Deppermann C. Beyond Hemostasis: Platelet Innate Immune Interactions and Thromboinflammation. International Journal of Molecular Sciences. 2022;23(7):1–30.

40. Xie J, Pang C, Yu H, Zhang W, Ren C, Deng B. Leukocyte indicators and variations predict worse outcomes after intravenous thrombolysis in patients with acute ischemic stroke. Journal of Cerebral Blood Flow and Metabolism. 2023;43(3):393–403.
41. Wang C, Zhang Q, Ji M, Mang J, Xu Z. Prognostic value of the neutrophil-to-lymphocyte ratio in acute ischemic stroke patients treated with intravenous thrombolysis: a systematic review and meta-analysis. BMC Neurology. 2021;21(1):1–9.
42. Sadeghi F, Sarkady F, Zsóri KS, Szegedi I, Orbán-Kálmándi R, Székely EG, et al. High Neutrophil–Lymphocyte Ratio and Low Lymphocyte–Monocyte Ratio Combination after Thrombolysis Is a Potential Predictor of Poor Functional Outcome of Acute Ischemic Stroke. Journal of Personalized Medicine. 2022;12(8).
43. Borissoff JI, Joosen IA, Versteylen MO, Brill A, Fuchs TA, Savchenko AS, et al. Elevated Levels of Circulating DNA and Chromatin Are Independently Associated with Severe Coronary Atherosclerosis and a Prothrombotic State. Arterioscler Thromb Vasc Biol. 2013;33(8):2032–40.
44. Schrottmaier WC, Mussbacher M, Salzmann M, Assinger A. Platelet-leukocyte interplay during vascular disease. Atherosclerosis. 2020;307:109–20.
45. De Bont CM, Boelens WC, Pruijn GJM. NETosis, complement, and coagulation: a triangular relationship. Cellular and Molecular Immunology. 2019 Jan;16(1):19–27.
46. Brinkmann V, Reichard U, Goosmann C, Fauler B, Uhlemann Y, Weiss DS, et al. Neutrophil Extracellular Traps Kill Bacteria. Science. 2004;303(5663):1532–5.
47. Martinod K, Wagner DD. Thrombosis: tangled up in NETs. Blood. 2014;123(18):2768–76.
48. Laridan E, Martinod K, De Meyer SF. Neutrophil Extracellular Traps in Arterial and Venous Thrombosis. Seminars in Thrombosis and Hemostasis. 2019;45(1):86–93.
49. Zhou Y, Xu Z, Liu Z. Impact of Neutrophil Extracellular Traps on Thrombosis Formation: New Findings and Future Perspective. Frontiers in Cellular and Infection Microbiology. 2022;12(May):1–10.
50. Demkow U. Molecular Mechanisms of Neutrophil Extracellular Trap (NETs) Degradation. International Journal of Molecular Sciences. 2023;24(5).
51. Pertiwi KR, de Boer OJ, Mackaaij C, Pabittei DR, de Winter RJ, Li X, et al. Extracellular traps derived from macrophages, mast cells, eosinophils and neutrophils are generated in a time-dependent manner during atherothrombosis. Journal of Pathology. 2019 Apr 1;247(4):505–12.
52. Echevarría LU, Leimgruber C, González JG, Nevado A, Álvarez R, García LN, et al. Evidence of eosinophil extracellular trap cell death in copd: Does it represent the trigger that switches on the disease? International Journal of COPD. 2017;12:885–96.
53. Granger V, Faille D, Marani V, Noël B, Gallais Y, Szely N, et al. Human blood monocytes are able to form extracellular traps. Journal of Leukocyte Biology. 2017;102(3):775–81.
54. Fuchs TA, Brill A, Duerschmied D, Schatzberg D, Monestier M, Myers DD, et al. Extracellular DNA traps promote thrombosis. Proceedings of the National Academy of Sciences of the United States of America. 2010;107(36):15880–5.
55. Elaskalani O, Abdol Razak NB, Metharom P. Neutrophil extracellular traps induce aggregation of washed human platelets independently of extracellular DNA and histones. Cell Communication and Signaling. 2018 May 29;16(1):24.
56. Wang Y, Luo L, Braun O, Westman J, Madhi R, Herwald H, et al. Neutrophil extracellular trap-microparticle complexes enhance thrombin generation via the

intrinsic pathway of coagulation in mice. Scientific Reports 2018 8:1. 2018 Mar 5;8(1):1–14.
57. Zhou P, Li T, Jin J, Liu Y, Li B, Sun Q, et al. Interactions between neutrophil extracellular traps and activated platelets enhance procoagulant activity in acute stroke patients with ICA occlusion. EBioMedicine. 2020;53:102671.
58. Grässle S, Huck V, Pappelbaum KI, Gorzelanny C, Aponte-Santamaría C, Baldauf C, et al. Von willebrand factor directly interacts with DNA from neutrophil extracellular traps. Arteriosclerosis, Thrombosis, and Vascular Biology. 2014;34(7):1382–9.
59. Yang J, Wu Z, Long Q, Huang J, Hong T, Liu W, et al. Insights Into Immunothrombosis: The Interplay Among Neutrophil Extracellular Trap, von Willebrand Factor, and ADAMTS13. Frontiers in Immunology. 2020;11(December):1–16.
60. Han T, Tang H, Lin C, Shen Y, Yan D, Tang X, et al. Extracellular traps and the role in thrombosis. Frontiers in Cardiovascular Medicine. 2022;9(August):1–14.
61. Longstaff C, Varjú I, Sótonyi P, Szabó L, Krumrey M, Hoell A, et al. Mechanical stability and fibrinolytic resistance of clots containing fibrin, DNA, and histones. Journal of Biological Chemistry. 2013 Mar;288(10):6946–56.
62. Varjú I, Longstaff C, Szabó L, Farkas ÁZ, Varga-Szabó VJ, Tanka-Salamon A, et al. DNA, histones and neutrophil extracellular traps exert anti-fibrinolytic effects in a plasma environment. Thrombosis and Haemostasis. 2015;113(6):1289–99.
63. Cruz DB da, Helms J, Aquino LR, Stiel L, Cougourdan L, Broussard C, et al. DNA-bound elastase of neutrophil extracellular traps degrades plasminogen, reduces plasmin formation, and decreases fibrinolysis: proof of concept in septic shock plasma. FASEB Journal. 2019 Dec 1;33(12):14270–80.
64. Zhang S, Cao Y, Du J, Liu H, Chen X, Li M, et al. Neutrophil extracellular traps contribute to tissue plasminogen activator resistance in acute ischemic stroke. The FASEB Journal. 2021;35(9):1–22.
65. Vallés J, Lago A, Santos MT, Latorre AM, Tembl JI, Salom JB, et al. Neutrophil extracellular traps are increased in patients with acute ischemic stroke: Prognostic significance. Thrombosis and Haemostasis. 2017;117(10):1919–29.
66. Mauracher LM, Posch F, Martinod K, Grilz E, Däullary T, Hell L, et al. Citrullinated histone H3, a biomarker of neutrophil extracellular trap formation, predicts the risk of venous thromboembolism in cancer patients. Journal of Thrombosis and Haemostasis. 2018;16(3):508–18.
67. Gao X, Zhao X, Li J, Liu C, Li W, Zhao J, et al. Neutrophil extracellular traps mediated by platelet microvesicles promote thrombosis and brain injury in acute ischemic stroke. Cell Communication and Signaling. 2024;22(1):1–12.
68. Denorme F, Portier I, Rustad JL, Cody MJ, de Araujo C V., Hoki C, et al. Neutrophil extracellular traps regulate ischemic stroke brain injury. Journal of Clinical Investigation. 2022 May 16;132(10):e154225.
69. Rainer TH, Wong LKS, Lam W, Yuen E, Lam NYL, Metreweli C, et al. Prognostic use of circulating plasma nucleic acid concentrations in patients with acute stroke. Clinical Chemistry. 2003 Apr;49(4):562–9.
70. Lim HH, Jeong IH, An GD, Woo KS, Kim KH, Kim JM, et al. Evaluation of neutrophil extracellular traps as the circulating marker for patients with acute coronary syndrome and acute ischemic stroke. Journal of Clinical Laboratory Analysis. 2020 May;34(5).
71. Sacco RL, Kasner SE, Broderick JP, Caplan LR, Connors JJ, Culebras A, et al. An updated definition of stroke for the 21st century: A statement for healthcare

professionals from the American heart association/American stroke association. Stroke. 2013;44(7):2064–89.
72. Feigin VL, Brainin M, Norrving B, Martins S, Sacco RL, Hacke W, et al. World Stroke Organization (WSO): Global Stroke Fact Sheet 2022. International Journal of Stroke. 2022;17(1):18–29.
73. GBD 2019 Stroke Collaborators. Global, regional, and national burden of stroke and its risk factors, 1990-2019: A systematic analysis for the Global Burden of Disease Study 2019. Lancet Neurol. 2021;20(10):1–26.
74. Fan J, Li X, Yu X, Liu Z, Jiang Y, Fang Y, et al. Global Burden, Risk Factor Analysis, and Prediction Study of Ischemic Stroke, 1990-2030. Neurology. 2023;101(2):E137–50.
75. Rochmah TN, Rahmawati IT, Dahlui M, Budiarto W, Bilqis N. Economic burden of stroke disease: A systematic review. International Journal of Environmental Research and Public Health. 2021;18(14).
76. Katan M, Luft A. Global Burden of Stroke. Seminars in Neurology. 2018;38(2):208–11.
77. Di Carlo A. Human and economic burden of stroke. Age and Ageing. 2009;38(1):4–5.
78. Love BB, Bendixen BH. Classification of subtype of acute ischemic stroke definitions for use in a multicenter clinical trial. Stroke. 1993;24(1):35–41.
79. Campbell BCV, De Silva DA, Macleod MR, Coutts SB, Schwamm LH, Davis SM, et al. Ischaemic stroke. Nature Reviews Disease Primers. 2019;5(1).
80. Essa H, Hill AM, Lip GYH. Atrial Fibrillation and Stroke. Cardiac Electrophysiology Clinics. 2021;13(1):243–55.
81. Kamel H, Okin PM, Elkind MSV, Iadecola C. Atrial Fibrillation and Mechanisms of Stroke: Time for a New Model. Stroke. 2016 Mar 1;47(3):895–900.
82. Markus HS, Erik de Leeuw F. Cerebral small vessel disease: Recent advances and future directions. International Journal of Stroke. 2023;18(1):4–14.
83. Miceli G, Basso MG, Rizzo G, Pintus C, Cocciola E, Pennacchio AR, et al. Artificial Intelligence in Acute Ischemic Stroke Subtypes According to Toast Classification: A Comprehensive Narrative Review. Biomedicines. 2023;11(4).
84. Hyunsoo K, Joon Tae K, Ji Sung L, Beom Joon K, Jihoon K, Keon Joo L, et al. Stroke of Other Determined Etiology: Results from the Nationwide Multicenter Stroke Registry. Stroke. 2022 Aug 1;53(8):2597–606.
85. Diener HC, Easton JD, Hart RG, Kasner S, Kamel H, Ntaios G. Review and update of the concept of embolic stroke of undetermined source. Nature Reviews Neurology. 2022;18(8):455–65.
86. Michel P, Odier C, Rutgers M, Reichhart M, Maeder P, Meuli R, et al. The acute stroke registry and analysis of Lausanne (ASTRAL): Design and baseline analysis of an ischemic stroke registry including acute multimodal imaging. Stroke. 2010 Nov;41(11):2491–8.
87. Gratz PP, Gralla J, Mattle HP, Schroth G. Embolic strokes of undetermined source: Support for a new clinical construct. The Lancet Neurology. 2014;13(10):967.
88. Chugh C. Acute ischemic stroke: Management approach. Indian Journal of Critical Care Medicine. 2019;23:S140–6.
89. Kothari RU, Pancioli A, Liu T, Brott T, Broderick J. Cincinnati prehospital stroke scale: Reproducibility and validity. Annals of Emergency Medicine. 1999;33(4):373–8.

90. Kleindorfer DO, Miller R, Moomaw CJ, Alwell K, Broderick JP, Khoury J, et al. Designing a message for public education regarding stroke: Does FAST capture enough stroke? Stroke. 2007;38(10):2864–8.
91. Aroor S, Singh R, Goldstein LB. BE-FAST (Balance, Eyes, Face, Arm, Speech, Time): Reducing the Proportion of Strokes Missed Using the FAST Mnemonic. Stroke. 2017 Feb 1;48(2):479–81.
92. Toral L. BE FAST to recognize stroke. Nursing. 2021 Feb 1;51(2):51–4.
93. Czap AL, Sheth SA. Overview of Imaging Modalities in Stroke. Neurology. 2021;97(20):S42–51.
94. Herpich F, Rincon F. Management of Acute Ischemic Stroke. Critical Care Medicine. 2020;48(11):1654–63.
95. Donahue J, Wintermark M. Perfusion CT and acute stroke imaging: Foundations, applications, and literature review. Journal of Neuroradiology. 2015;42:21–9.
96. Vaclavik D, Volny O, Cimflova P, Svub K, Dvornikova K, Bar M. The importance of CT perfusion for diagnosis and treatment of ischemic stroke in anterior circulation. Journal of Integrative Neuroscience. 2022;21(3).
97. Campbell BCV, Khatri P. Stroke. The Lancet. 2020;396(10244):129–42.
98. Puig J, Shankar J, Liebeskind D, Terceño M, Nael K, Demchuk AM, et al. From “Time is Brain” to “Imaging is Brain”: A Paradigm Shift in the Management of Acute Ischemic Stroke. Journal of Neuroimaging. 2020;30(5):562–71.
99. Hjort N, Christensen S, Sølling C, Ashkanian M, Wu O, Røhl L, et al. Ischemic injury detected by diffusion imaging 11 minutes after stroke. Annals of Neurology. 2005 Sep 1;58(3):462–5.
100. Brott T, Adams HP, Olinger CP, Marle JR, Barsan WG, Biller J, et al. Measurements of acute cerebral infarction: A clinical examination scale. Stroke. 1989;20(7):864–70.
101. Kwah LK, Diong J. National Institutes of Health Stroke Scale (NIHSS). Journal of Physiotherapy. 2014;60(1):61.
102. Du J, Wang Y, Che B, Miao M, Bao A, Peng Y, et al. The relationship between neurological function trajectory, assessed by repeated NIHSS measurement, and long-term cardiovascular events, recurrent stroke, and mortality after ischemic stroke. International Journal of Stroke. 2023 Oct 1;18(8):1005–14.
103. Prabhakaran S, Ruff I, Bernstein RA. Acute stroke intervention: A systematic review. JAMA - Journal of the American Medical Association. 2015;313(14):1451–62.
104. Fisher M, Bastan B. Identifying and utilizing the ischemic penumbra. Neurology. 2012 Sep 25;79(13 SUPPL. 1).
105. Catanese L, Tarsia J, Fisher M. Acute Ischemic Stroke Therapy Overview. Circulation Research. 2017 Feb;120(3):541–58.
106. Saver JL. Time is brain - Quantified. Stroke. 2006;37(1):263–6.
107. Goyal M, Fargen KM, Turk AS, Mocco J, Liebeskind DS, Frei D, et al. 2C or not 2C: Defining an improved revascularization grading scale and the need for standardization of angiography outcomes in stroke trials. Journal of NeuroInterventional Surgery. 2014;6(2):83–6.
108. Khatri P, Hill MD, Palesch YY, Spilker J, Jauch EC, Carrozzella JA, et al. Methodology of the Interventional Management of Stroke III trial. International Journal of Stroke. 2008 May;3(2):130–7.
109. Bamford JM, Sandercock PAG, Wariow CP, Slattery J. Interobserver agreement for the assessment of handicap in stroke patients: To the editor. Stroke. 1989;20(6):828.
110. Banks JL, Marotta CA. Outcomes validity and reliability of the modified rankin scale: Implications for stroke clinical trials - A literature review and synthesis. Stroke. 2007 Mar;38(3):1091–6.

111. The national institute of neurological disorders and stroke rt-pa stroke study group. tissue plasminogen activator for acute ischemic stroke. NEJM. 1995;333(24):1581–7.
112. Hacke W, Kaste M, Bluhmki E, Brozman M, Dávalos A, Guidetti D, et al. Thrombolysis with Alteplase 3 to 4.5 Hours after Acute Ischemic Stroke. N Engl J Med. 2008 Sep;359(13):1317–29.
113. Ma H, Campbell BCV, Parsons MW, Churilov L, Levi CR, Hsu C, et al. Thrombolysis Guided by Perfusion Imaging up to 9 Hours after Onset of Stroke. New England Journal of Medicine. 2019;380(19):1795–803.
114. Berge E, Whiteley W, Audebert H, Marchis GM De, Fonseca AC, Padiglioni C, et al. European Stroke Organisation (ESO) guidelines on intravenous thrombolysis for acute ischaemic stroke. European Stroke Journal. 2021;6(1):I–LXII.
115. Aguiar de Sousa D, von Martial R, Abilleira S, Gattringer T, Kobayashi A, Gallofré M, et al. Access to and delivery of acute ischaemic stroke treatments: A survey of national scientific societies and stroke experts in 44 European countries. Eur Stroke J. 2019;4(1):13–28.
116. Fugate JE, Rabinstein AA. Absolute and Relative Contraindications to IV rt-PA for Acute Ischemic Stroke. The Neurohospitalist. 2015;5(3):110–21.
117. Menon BK, Al-Ajlan FS, Najm M, Puig J, Castellanos M, Dowlatshahi D, et al. Association of clinical, imaging, and thrombus characteristics with recanalization of visible intracranial occlusion in patients with acute ischemic stroke. JAMA - Journal of the American Medical Association. 2018;320(10):1017–26.
118. Zeinhom MG, Khalil MFE, Kamel IFM, Kohail AM, Ahmed SR, Elbassiouny A, et al. Predictors of the unfavorable outcomes in acute ischemic stroke patients treated with alteplase, a multi-center randomized trial. Sci Rep. 2024;14(1):1–9.
119. Zhu A, Rajendram P, Tseng E, Coutts SB, Yu AYX. Alteplase or tenecteplase for thrombolysis in ischemic stroke: An illustrated review. Research and Practice in Thrombosis and Haemostasis. 2022;6(6):1–13.
120. Lees KR, Bluhmki E, von Kummer R, Brott TG, Toni D, Grotta JC, et al. Time to treatment with intravenous alteplase and outcome in stroke: an updated pooled analysis of ECASS, ATLANTIS, NINDS, and EPITHET trials. The Lancet. 2010;375(9727):1695–703.
121. Paoni N, Chow A, Peña L, Keyt B, Zoller M, Bennett W. Making tissue- type plasminogen activator more fibrin specific. Protein Eng. 1993;6(5):529–34.
122. Keyt BA, Paoni NF, Refino CJ, Berleau L, Nguyen H, Chow A, et al. A faster-acting and more potent form of tissue plasminogen activator. Proceedings of the National Academy of Sciences of the United States of America. 1994;91(9):3670–4.
123. Campbell BCV, Mitchell PJ, Churilov L, Yassi N, Kleinig TJ, Dowling RJ, et al. Effect of Intravenous Tenecteplase Dose on Cerebral Reperfusion before Thrombectomy in Patients with Large Vessel Occlusion Ischemic Stroke: The EXTEND-IA TNK Part 2 Randomized Clinical Trial. JAMA - Journal of the American Medical Association. 2020;323(13):1257–65.
124. Burgos AM, Saver JL. Evidence that Tenecteplase Is Noninferior to Alteplase for Acute Ischemic Stroke: Meta-Analysis of 5 Randomized Trials. Stroke. 2019 Aug 1;50(8):2156–62.
125. Staessens S, Denorme F, François O, Desender L, Dewaele T, Vanacker P, et al. Structural analysis of ischemic stroke thrombi: Histological indications for therapy resistance. Haematologica. 2020;105(2):498–507.
126. Staessens S, De Meyer SF. Thrombus heterogeneity in ischemic stroke. Platelets. 2020;32(3):331–9.

127. Ho-Tin-Noé B, Desilles JP, Mazighi M. Thrombus composition and thrombolysis resistance in stroke. Res Pract Thromb Haemost. 2023;7(4):100178.
128. Denorme F, Langhauser F, Desender L, Vandenbulcke A, Rottensteiner H, Plaimauer B, et al. ADAMTS13-mediated thrombolysis of t-PA–resistant occlusions in ischemic stroke in mice. Blood. 2016 May;127(19):2337–45.
129. De Lizarrondo SM, Gakuba C, Herbig BA, Repessé Y, Ali C, Denis C V., et al. Potent thrombolytic effect of N-acetylcysteine on arterial thrombi. Circulation. 2017;136(7):646–60.
130. South K, Saleh O, Lemarchand E, Coutts G, Smith CJ, Schiessl I, et al. Robust thrombolytic and anti-inflammatory action of a constitutively active ADAMTS13 variant in murine stroke models. Blood. 2022;139(10):1575–87.
131. Kim D, Shea SM, Ku DN. Lysis of arterial thrombi by perfusion of N,N'- Diacetyl-L-cystine (DiNAC). PLoS One. 2021;16(2 February):1–16.
132. de Maat S, Clark CC, Barendrecht AD, Smits S, van Kleef ND, El Otmani H, et al. Microlyse: a thrombolytic agent that targets VWF for clearance of microvascular thrombosis. Blood. 2022;139(4):597–607.
133. van Moorsel MVA, de Maat S, Vercruysse K, van Leeuwen EM, Jacqmarcq C, Bonnard T, et al. VWF-targeted thrombolysis to overcome rh-tPA resistance in experimental murine ischemic stroke models. Blood. 2022 Dec 29;140(26):2844–8.
134. Ducroux C, Meglio L Di, Loyau S, Delbosc S, Boisseau W, Deschildre C, et al. Thrombus Neutrophil Extracellular Traps Content Impair tPA-Induced Thrombolysis in Acute Ischemic Stroke. Stroke. 2018;49(3):754–7.
135. Laridan E, Denorme F, Desender L, François O, Andersson T, Deckmyn H, et al. Neutrophil extracellular traps in ischemic stroke thrombi. Ann Neurol. 2017;82(2):223–32.
136. Peña-Martínez, Carolina Durán-Laforet, Violeta García-Culebras, Alicia Ostos, Fernando Hernández-Jiménez M. Pharmacological Modulation of Neutrophil Extracellular Traps Reverses Thrombotic Stroke tPA (Tissue-Type Plasminogen Activator) Resistance. Stroke. 2019;50(11):3228–37.
137. De Meyer SF, Suidan GL, Fuchs TA, Monestier M, Wagner DD. Extracellular chromatin is an important mediator of ischemic stroke in mice. Arteriosclerosis, Thrombosis, and Vascular Biology. 2012;32(8):1884–91.
138. Smith WS, Sung G, Saver J, Budzik R, Duckwiler G, Liebeskind DS, et al. Mechanical thrombectomy for acute ischemic stroke: Final results of the multi MERCI trial. Stroke. 2008;39(4):1205–12.
139. Po Sit S. The penumbra pivotal stroke trial: Safety and effectiveness of a new generation of mechanical devices for clot removal in intracranial large vessel occlusive disease. Stroke. 2009 Aug;40(8):2761–8.
140. Campbell BCV, Mitchell PJ, Kleinig TJ, Dewey HM, Churilov L, Yassi N, et al. Endovascular Therapy for Ischemic Stroke with Perfusion-Imaging Selection. New England Journal of Medicine. 2015;372(11):1009–18.
141. Goyal M, Demchuk AM, Menon BK, Eesa M, Rempel JL, Thornton J, et al. Randomized Assessment of Rapid Endovascular Treatment of Ischemic Stroke. New England Journal of Medicine. 2015;372(11):1019–30.
142. Jovin TG, Chamorro A, Cobo E, de Miquel MA, Molina CA, Rovira A, et al. Thrombectomy within 8 Hours after Symptom Onset in Ischemic Stroke. New England Journal of Medicine. 2015;372(24):2296–306.
143. Berkhemer OA, Fransen PSS, Beumer D, van den Berg LA, Lingsma HF, Yoo AJ, et al. A Randomized Trial of Intraarterial Treatment for Acute Ischemic Stroke. New England Journal of Medicine. 2015;372(1):11–20.

144. Saver JL, Goyal M, Bonafe A, Diener HC, Levy EI, Pereira VM, et al. Stent-Retriever Thrombectomy after Intravenous t-PA vs. t-PA Alone in Stroke. New England Journal of Medicine. 2015;372(24):2285–95.
145. Nogueira RG, Jadhav AP, Haussen DC, Bonafe A, Budzik RF, Bhuva P, et al. Thrombectomy 6 to 24 Hours after Stroke with a Mismatch between Deficit and Infarct. New England Journal of Medicine. 2018 Jan 4;378(1):11–21.
146. Albers GW, Marks MP, Kemp S, Christensen S, Tsai JP, Ortega-Gutierrez S, et al. Thrombectomy for Stroke at 6 to 16 Hours with Selection by Perfusion Imaging. New England Journal of Medicine. 2018 Feb 22;378(8):708–18.
147. Kobeissi H, Ghozy S, Adusumilli G, Kadirvel R, Brinjikji W, Rabinstein AA, et al. Endovascular Therapy for Stroke Presenting beyond 24 Hours: A Systematic Review and Meta-analysis. JAMA Network Open. 2023;6(5):E2311768.
148. Zhang J, Chen S, Shi S, Zhang Y, Kong D, Xie Y, et al. Direct endovascular treatment versus bridging therapy in patients with acute ischemic stroke eligible for intravenous thrombolysis: Systematic review and meta-analysis. Journal of NeuroInterventional Surgery. 2022;14(4):321–5.
149. Wang X, Ye Z, Busse JW, Hill MD, Smith EE, Guyatt GH, et al. Endovascular thrombectomy with or without intravenous alteplase for acute ischemic stroke due to large vessel occlusion: A systematic review and meta-analysis of randomized trials. Stroke and Vascular Neurology. 2022;7(6):510–7.
150. Wang R, Li S, Hao L, Wang Z, Ge Z, Yang S. A meta-analysis of intravenous thrombolysis versus bridging therapy for ischemic stroke. Medicine. 2022;101(39):e30879.
151. Powers WJ, Rabinstein AA, Ackerson T, Adeoye OM, Bambakidis NC, Becker K, et al. Guidelines for the early management of patients with acute ischemic stroke: 2019 update to the 2018 guidelines for the early management of acute ischemic stroke a guideline for healthcare professionals from the American Heart Association/American Stroke A. Vol. 50, Stroke. 2019. 344–418 p.
152. Turc G, Bhogal P, Fischer U, Khatri P, Lobotesis K, Mazighi M, et al. European Stroke Organisation (ESO) - European Society for Minimally Invasive Neurological Therapy (ESMINT) Guidelines on Mechanical Thrombectomy in Acute Ischemic Stroke. Journal of NeuroInterventional Surgery. 2023;15(8):1–30.
153. Goyal M, Menon BK, Van Zwam WH, Dippel DWJ, Mitchell PJ, Demchuk AM, et al. Endovascular thrombectomy after large-vessel ischaemic stroke: A meta-analysis of individual patient data from five randomised trials. The Lancet. 2016;387(10029):1723–31.
154. Renu A, Millan M, San Roman L, Blasco J, Marti-Fàbregas J, Terceño M, et al. Effect of Intra-arterial Alteplase vs Placebo Following Successful Thrombectomy on Functional Outcomes in Patients With Large Vessel Occlusion Acute Ischemic Stroke: The CHOICE Randomized Clinical Trial. Jama. 2022 Mar;327(9):826–35.
155. Salsano G, Pracucci G, Mavilio N, Saia V, di Poggio MB, Malfatto L, et al. Complications of mechanical thrombectomy for acute ischemic stroke: Incidence, risk factors, and clinical relevance in the Italian Registry of Endovascular Treatment in acute stroke. International Journal of Stroke. 2020;0(0):1–10.
156. Jadhav AP, Desai SM, Jovin TG. Indications for Mechanical Thrombectomy for Acute Ischemic Stroke: Current Guidelines and Beyond. Neurology. 2021;97(20):S126–36.
157. Yoo AJ, Andersson T. Thrombectomy in acute ischemic stroke: Challenges to procedural success. J Stroke. 2017;19(2):121–30.

158. Remollo S, Werner M, Blasco J, López-Rueda A, San Roman L, Jimenez-Gomez E, et al. First-Pass Effect in M1-Occlusion Stroke Patients Treated with Combined Stent-Retriever/Large-Bore Distal Aspiration Catheter Thrombectomy. Clinical Neuroradiology. 2023 Mar 1;33(3):701–8.
159. Jadhav AP, Desai SM, Zaidat OO, Nogueira RG, Jovin TG, Haussen DC, et al. First Pass Effect with Neurothrombectomy for Acute Ischemic Stroke: Analysis of the Systematic Evaluation of Patients Treated with Stroke Devices for Acute Ischemic Stroke Registry. Stroke. 2022 Feb 1;53(2):E30–2.
160. Zaidat OO, Castonguay AC, Linfante I, Gupta R, Martin CO, Holloway WE, et al. First pass effect: A new measure for stroke thrombectomy devices. Stroke. 2018;49(3):660–6.
161. Bai X, Zhang X, Wang J, Zhang Y, Dmytriw AA, Wang T, et al. Factors Influencing Recanalization After Mechanical Thrombectomy With First-Pass Effect for Acute Ischemic Stroke: A Systematic Review and Meta-Analysis. Frontiers in Neurology. 2021;12(April):1–10.
162. Abbasi M, Liu Y, Fitzgerald S, Mereuta OM, Arturo Larco JL, Rizvi A, et al. Systematic review and meta-analysis of current rates of first pass effect by thrombectomy technique and associations with clinical outcomes. J Neurointerv Surg. 2021;13(3):212–6.
163. Den Hartog SJ, Zaidat O, Roozenbeek B, Adriaan ;, Van Es CGM, Bruggeman AAE, et al. Effect of First-Pass Reperfusion on Outcome After Endovascular Treatment for Ischemic Stroke the MR CLEAN (Multicenter Randomized Clinical Trial of Endovascular Treatment for Acute Ischemic Stroke in the Netherlands) Registry Investigators*. Journal of the American Heart Association J Am Heart Assoc. 2021;10:19988.
164. Staessens S, François O, Brinjikji W, Doyle KM, Vanacker P, Andersson T, et al. Stroke Studying Stroke Thrombus Composition After Thrombectomy What Can We Learn? Stroke. 2021 Nov 1;52(11):3718–27.
165. De Meyer SF, Andersson T, Baxter B, Bendszus M, Brouwer P, Brinjikji W, et al. Analyses of thrombi in acute ischemic stroke: A consensus statement on current knowledge and future directions. International Journal of Stroke. 2017;12(6):606–14.

CHAPTER 2 - ACUTE ISCHEMIC STROKE THROMBUS COMPOSITION

Sarah Vandelanotte and Simon F. De Meyer

Laboratory for Thrombosis Research, KU Leuven Kulak, Kortrijk, Belgium

Published article: *Neuroscience* IBRO; 2024; 550: 11–20.

Neuroscience 550 (2024) 11–20

Contents lists available at ScienceDirect

Neuroscience

journal homepage: www.elsevier.com/locate/nsc

Review

Acute Ischemic Stroke Thrombus Composition

Sarah Vandelanotte, Simon F. De Meyer *

Laboratory for Thrombosis Research, KU Leuven Kulak, Kortrijk, Belgium

ARTICLE INFO

Key words:
ischemic stroke
thrombus composition
thrombolysis
thrombectomy

ABSTRACT

Ischemic stroke is caused by a thrombus blocking one or multiple arteries in the brain, resulting in irreversible damage in the associated brain tissue. The aim of therapy is to restore the blood flow as fast as possible. Two recanalization strategies are currently available: pharmacological thrombolysis using recombinant tissue plasminogen activator (rt-PA) and mechanical removal of the thrombus. Despite recent advancements, achieving efficient recanalization remains a challenge. The precise causes of therapy failure are not fully understood but thrombus composition is likely a key factor in successful recanalization. This review explores acute ischemic stroke thrombus composition, its recently identified components, and how it affects stroke treatment. It also discusses how new insights could enhance current recanalization strategies for ischemic stroke patients.

Introduction

Ischemic stroke is primarily caused by a thrombus that obstructs one or multiple arteries in the brain. Consequently, this disruption of cerebral blood flow leads to irreversible damage in the associated brain tissue. The central focus of primary care is aimed at restoring the blood flow to the brain as fast as possible by recanalizing the occluded blood vessel. Currently, only two US Food and Drug Administration (FDA)-approved treatment regimens are available to remove the thrombus and thus recanalize the occluded blood vessel in stroke patients: (i) pharmacological thrombolysis using recombinant tissue plasminogen activator (rt-PA), which promotes degradation of fibrin in the thrombus; and (ii) endovascular thrombectomy (EVT), which mechanically removes the thrombus from the occluded artery.

Despite recent advances, efficient recanalization remains a challenge. The administration of rt-PA is limited to a window of 4.5 hours from the initiation of stroke symptoms, rendering this treatment accessible to less than 15% of patients (Hacke et al., 2008; Aguiar de Sousa et al., 2019). Additionally, the efficacy of rt-PA-induced thrombolysis remains suboptimal since rt-PA fails to establish recanalization in more than half of patients who receive it (Rha and Saver, 2007; Berkhemer et al., 2015).

Mechanical thrombectomy has become frequently used after randomized trials have confirmed its efficacy and benefit for neurological outcome in patients with ischemic stroke (Attenello and Mack, 2016). EVT can be used in selected patients with imaging-proven proximal large artery occlusion, regardless of whether they receive intravenous (IV) rt-PA. A significant challenge in endovascular therapy lies in the variability of thrombus consistency and ease of removal, resulting in the inability to retrieve the thrombus in as many as 20% of patients undergoing treatment (Yoo and Andersson, 2017).

The reasons why certain thrombi are more resistant to rt-PA or prove more challenging to remove through thrombectomy remain unclear. As the central target in recanalization therapy, the thrombus itself is most likely a key factor dictating recanalization success rates. Not surprisingly, there has been a growing interest in studying the composition of thrombi associated with ischemic strokes. This interest has been sparked by the integration of EVT into standard stroke treatments, which in addition to enhancing clinical care, has created the opportunity to provide thrombus material for research purposes. This access to patient-derived thrombi has catalyzed the emergence of a prominent subfield in stroke research, studying the composition and structure of actute ischemic stroke (AIS) thrombi (De Meyer et al., 2017; Staessens et al., 2021a; Ospel et al., 2023). Better understanding of thrombus organization and structure is, not only to enhance our understanding of the pathophysiological processes that lead to formation of thrombi in stroke patients, but also to refine recanalization therapies that target these thrombi and potentially to tailor secondary

Abbreviations: rt-PA, recombinant tissue plasminogen activator; FDA, Food and Drug Administration; EVT, endovascular thrombectomy; IV, intravenous; RBC, red blood cells; AIS, acute ischemic stroke; VWF, von Willebrand factor; NETs, Neutrophil extracellular traps; GP, glycoprotein; DVP, deep vein thrombosis; PAI-1, plasminogen activator inhibitor 1; FPR, first pass recanalization; mTICI, modified thrombolysis in cerebral infarction scale; CT, computed tomography; MRI, magnetic resonance imaging; HAS, hyperdense artery sign; SVS, susceptibility vessel sign.

* Corresponding author. Address: Laboratory for Thrombosis Research, KU Leuven Kulak, E. Sabbelaan 53, 8500 Kortrijk Belgium.
E-mail address: simon.demeyer@kuleuven.be (S.F. De Meyer).

https://doi.org/10.1016/j.neuroscience.2023.12.010
Received 27 October 2023; Accepted 20 December 2023
Available online 5 January 2024
0306-4522/© 2024 IBRO. Published by Elsevier Ltd. All rights reserved.

prevention measures to reduce the risk of a recurrent stroke. Accumulating evidence points toward a complex and variable structure of ischemic stroke thrombi, with, besides red blood cells (RBC), showing the involvement of thrombotic factors such as platelets, von Willebrand factor (VWF) and fibrin, as well as inflammatory components such as leukocytes and neutrophil extracellular traps (Staessens and De Meyer, 2020; Staessens et al., 2021a; Ho-Tin-Noé et al., 2023).

In this review, we discuss thrombus composition and the main components that have been recently characterized in ischemic stroke thrombi. We also consider how thrombus composition can impact stroke treatment and how novel insights can lead to improvement of current recanalization strategies in patients with ischemic stroke.

Composition of stroke thrombi

Conventional histopathological evaluation has become the standard approach to study thrombus composition. Early studies on the composition of AIS thrombi relied on the general hematoxylin and eosin staining to identify RBC, white blood cells and fibrin (Marder et al., 2006; Liebeskind et al., 2011). During the last decade, more specific protocols, including immunohistochemical staining techniques have been introduced to study various structural components of AIS thrombi such as platelets, VWF, leukocytes, DNA, and neutrophil extracellular traps (NETs). Although these structural elements are found in the majority of AIS thrombi, each individual thrombus possesses a distinct appearance characterized by varying quantities and arrangements of these components. Staessens et al. identified two distinct categories of thrombus organization, referred to as 'RBC-rich' and 'platelet-rich', based on the molecular and cellular structures (Staessens et al., 2020). As illustrated in Fig. 1, most thrombi removed from patients exhibit a combination of RBC-rich and platelet-rich materials, spanning a broad range of relative proportions. The internal structure of RBC-rich material significantly contrasts with that of platelet-rich material. RBC-rich areas have a rather simple organization of densely packed RBCs intertwined within a network of thin fibrin, with a small number of leukocytes that are uniformly distributed throughout the RBC-rich area (Staessens et al., 2020). In contrast, platelet-rich areas have a more complex organization and typically contain besides platelets and dense fibrin fibers also VWF and extracellular DNA. These dense fibrin structures align with VWF and are packed with platelet-aggregates. In addition, leukocytes and extracellular DNA tend to accumulate within the platelet-rich areas and on the interface between platelet- and RBC-rich areas (Staessens et al., 2020). These differences between RBC-rich and platelet-rich material are illustrated in Fig. 2. Interestingly, Di Meglio et al. reported that AIS have a thick compact outer shell that primarily comprises a platelet-rich region with varying thickness, overlaid by a dense fibrin crust (Di Meglio et al., 2018, 2019). The precise mechanisms underlying these organizational aspects or explaining the observed compositional heterogeneity among thrombi are still not totally understood. Most likely, variations in the local conditions in which thrombus formation occurred, along with differences in thrombus age, thrombus maturation and thrombus contraction contribute to the observed differences in thrombus organization within AIS thrombi. Thrombus aging and maturation can result in dynamic changes after thrombus formation. For instance, crosslinking of fibrin can enhance both the elasticity and thrombus stiffness over time (Helms et al., 2012). Thrombus contraction can lead to internal rearrangements and changes in thrombus size and permeability (Litvinov and Weisel, 2023). The impact of thrombus aging and maturation in acute ischemic stroke however remains an area open for exploration in the future.

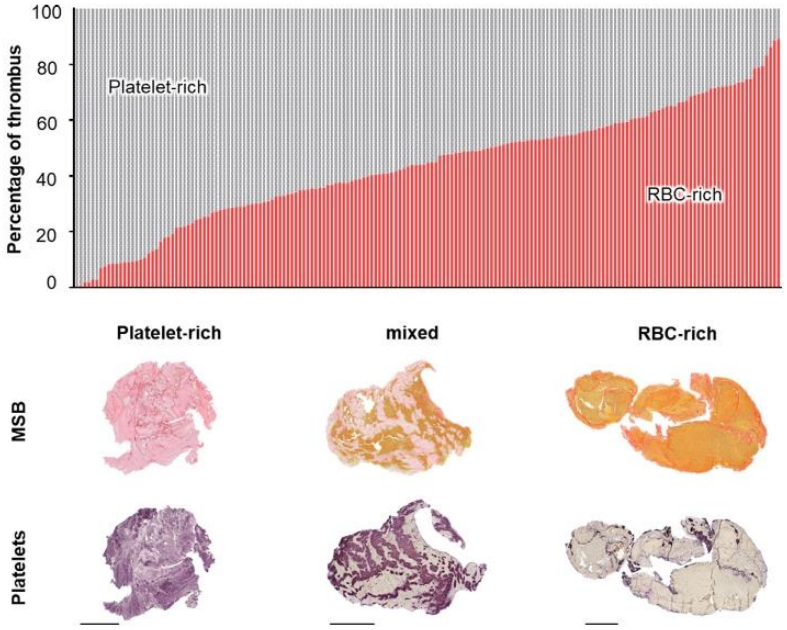

Fig. 1. Heterogeneity of acute ischemic stroke thrombi. Thrombi retrieved from acute ischemic stroke patients (n = 177, shown as vertical bars) were analyzed via histological staining and the relative proportions of platelet-rich (grey) and RBC-rich (red) material was determined. The thrombus composition spectrum ranged from thrombi that are predominantly platelet-rich (left), over thrombi with mixed composition (middle) to thrombi that mainly contain RBC-rich thrombus material (right). Representative images of a platelet-rich thrombus (left), mixed thrombus (middle) and RBC-rich thrombus (right) are shown below the graph, stained using MSB (top) or using an immunohistochemical staining to identify platelets (CD42b) (bottom). MSB stains RBCs yellow, fibrin dark pink/red and collagen blue (not present in these examples). Immunohistochemical staining for CD42b results in a purple color for platelets. Scale bar = 1 mm. RBC, red blood cell; H&E, Haematoxylin and Eosin; MSB, Martius Scarlet Blue. Figure adapted from Staessens et al. Structural analysis of ischemic stroke thrombi: histological indications for therapy resistance. Haematologica. 2019 May 2: haematol.2019.219881, with permission.

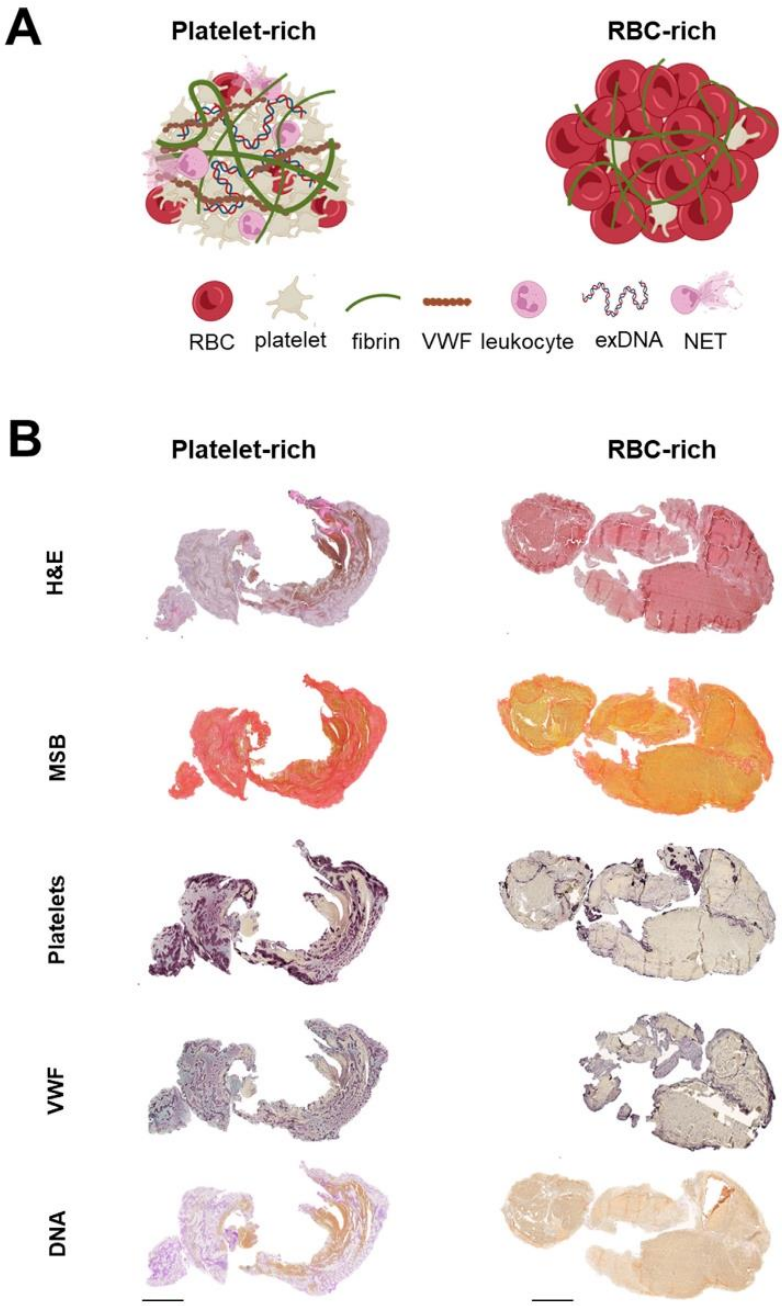

Fig. 2. Composition of platelet-rich and RBC-rich acute ischemic stroke thrombi. (A) Schematic representation of a platelet-rich and an RBC-rich thrombus. RBC-rich thrombi have a relatively simple structure of RBCs and fibrin fibers. Platelet-rich thrombi contain besides platelets and fibrin also VWF, leukocytes, exDNA and NETs. (B) Representative images of different stainings of a typical platelet-rich (left) and RBC-rich (right) thrombus. Sections were stained with Haematoxylin and eosin staining for a general overview and an MSB staining was used to identify RBCs (yellow), fibrin (dark pink/red) and collagen (blue, not present in these examples). Immunohistochemical stainings were used to identify platelets (CD42b; purple) and VWF (purple). Feulgen's reaction was used to visualize both intra-(nuclei) and extracellular DNA (smears), staining DNA in pink. Scale bar = 1 mm. RBC, red blood cell; H&E, Haematoxylin and Eosin; MSB, Martius Scarlet Blue; VWF, von Willebrand factor; exDNA, extracellular DNA; NET, neutrophil extracellular trap.

The following section will provide descriptions of the main components that have been described in AIS thrombi. While this review focuses on the composition of AIS thrombi, it is interesting to note that various compositional aspects of AIS thrombi show similarities with thrombi from other pathologies such as deep vein thrombosis (DVT) and coronary artery disease. For example, distinct RBC-rich and platelet-rich areas, as

well as the presence of VWF, leukocytes and NETs have been shown to be present in both coronary artery and DVT thrombi (Hoshiba et al., 2006; Savchenko et al., 2014). More in-depth research is needed to further elucidate the specific differences and similarities between thrombi from originating from different pathologies.

Fibrin

Conversion of circulating fibrinogen into insoluble fibrin is the final step of the coagulation cascade. As a result of the activated coagulation cascade, thrombin cleaves fibrinogen into fibrin, which then undergoes polymerization, resulting in the creation of an interconnected fibrin network, consolidating the growing thrombus. Fibrin is also important for the conversion of plasminogen into plasmin by rt-PA since binding of both plasminogen and rt-PA on the fibrin surface significantly improves the efficiency of rt-PA to convert plasminogen into plasmin. Given its important role in blood coagulation, it is not surprising that fibrin constitutes a major structural component of AIS thrombi (Staessens et al., 2020). Yet, the abundance and structure of fibrin can vary significantly between AIS thrombi. The organization of fibrin was described to be different between RBC-rich and platelet-rich regions, with fibrin appearing as a thin, branched network in RBC-rich regions whereas, denser fibrin bundles that delineate platelet clusters are observed in platelet-rich regions (Staessens et al., 2020). Further investigation is needed to clarify how differences in fibrin structure and organization impact fibrinolysis as well as mechanical removal. Recently, scanning electron microscopy and immunofluorescence microscopy revealed that fibrin molecules can form a continuous, dense layer around the thrombus forming a protective shell (Di Meglio et al., 2019). The structure of the outer shell was found to be highly similar between different AIS thrombi and contains besides tightly packed fibrin also VWF, aggregated platelets and antifibrinolytic components such as plasminogen activator inhibitor (PAI-1), rendering the thrombus less susceptible to rt-PA mediated fibrinolysis (Di Meglio et al., 2019).

Red blood cells

As the most common cell type in blood, RBCs are found in nearly all AIS thrombi. However, as illustrated in Fig. 1, the overall RBC content in AIS can exhibit considerable variation, spanning from highly RBC-rich thrombi to thrombi completely devoid of RBCs. RBC in AIS thrombi are typically packed within thin fibrin strands and RBC-rich thrombus structures can be interspersed with platelet-rich regions, as shown in Fig. 2 (Staessens et al., 2020). One explanation of the segregation of these areas could be thrombus contraction. Contraction of thrombi is mediated by contractile forces of platelets on fibrin and can result in the separation of RBC and platelet aggregates in the thrombus (Cines et al., 2014). This contraction also leads to the deformation of typically biconcave RBCs into a polyhedral structure known as polyhedrocytes (Cines et al., 2014; Tutwiler et al., 2018). Polyhedrocytes have been observed in AIS thrombi, forming a densely packed core of RBCs that enhance thrombus rigidity and reduce susceptibility to fibrinolysis (Tutwiler et al., 2017, 2019; Mereuta et al., 2021; Lagrange et al., 2022; Saghamanesh et al., 2022).

Platelets

Platelets play a pivotal role in coagulation and thrombus formation. Upon vessel wall damage, platelets can directly interact with subendothelial collagen via the platelet collagen receptors glycoprotein (GP) VI and integrin α2β1 or indirect via binding to VWF via the GPIb-V-IX receptor complex (Lippi et al., 2011). Upon platelet activation, integrin αIIbβ3 undergoes a transition from a low to a high affinity binding state, allowing subsequent binding with fibrinogen and VWF, leading to firm adhesion and platelet aggregation. The release of storage granules from platelets such as VWF, fibrinogen, adenosine diphosphate and thromboxane A2 further reinforces adhesion, activation, coagulant activity, and aggregation of platelets (Lippi et al., 2011). As expected, platelets have been shown to be important components of AIS thrombi (Staessens et al., 2020). Platelet-rich zones are demarcated by dense fibrin and VWF structures that interact with each other forming platelet islands in the thrombus (Staessens et al., 2020).

von Willebrand factor

Besides RBCs, platelets and fibrin, VWF is another major component of AIS thrombi. VWF is a large multimeric protein that plays a crucial role in platelet adhesion and thrombus formation. It is constitutively released in the circulation by endothelial cells, but also stored in platelet α-granules and endothelial Weibel-Palade bodies from which it is released during injury, inflammation or ischemia (Lenting et al., 2015). Rapid immobilization of VWF to the exposed subendothelial collagen or exposure to high shear reveals the binding site for platelet GPIbα in the VWF A1 domain (Fu et al., 2017). Following this initial reversible binding, platelets undergo deceleration, enabling the firm adhesion of platelets through integrin αIIbβ3 and collagen receptors. Together with fibrinogen, VWF acts as a molecular bridge that links activated platelets, resulting in steady platelet-platelet interactions and the stabilization of the developing platelet thrombus. In addition to its role in thrombus formation, VWF has also been observed to facilitate inflammatory processes via promotion of leukocyte adhesion by functioning as a ligand for the leukocyte receptors P-selectin GP ligand 1 and β2 integrin (Pendu et al., 2006). Given the important role of VWF in thrombus formation, it is not surprising that various studies demonstrated the presence of VWF in AIS thrombi via immunohistochemical VWF staining (Denorme et al., 2016; Prochazka et al., 2018; Di Meglio et al., 2019; Douglas et al., 2020; Staessens et al., 2020). As illustrated in Fig. 2, VWF is typically found in platelet-rich areas and the amount ranges from as little as 1% to more than 90% (Douglas et al., 2020; Staessens et al., 2020). It has become evident that VWF, much like fibrin, can serve as a substantial framework extending across the thrombus, presumably playing a crucial role in enhancing the overall stability of the thrombus. Detailed analysis revealed colocalization of VWF and fibrin as dense structures that align platelet-rich areas (Staessens et al., 2020). This close interaction of VWF and fibrin could be the result of covalent binding of VWF to fibrin via FXIII, potentially playing a crucial role in thrombus stabilization (Hada et al., 1986).

Leukocytes

Recent research challenges the traditional view of the hemostatic system by highlighting the significant impact of the immune system on blood coagulation and thrombus formation. This new evidence reveals that immune activation can stimulate leukocytes to produce tissue factor and release molecules with proinflammatory and procoagulant properties, including enzymes, cytokines, and damage-associated molecular patterns. Consequently, leukocytes have been shown to promote both venous and arterial thrombosis by initiating blood coagulation cascades (e.g. tissue factor and factor XII), releasing proteases/cytokines, interacting with platelets and releasing NETs (Swystun and Liaw, 2016). Leukocytes are present in all types of AIS thrombi but mainly accumulate in platelet-rich areas or at the border between RBC-rich and platelet-rich areas (Boeckh-Behrens et al., 2016b; Laridan et al., 2017; Sporns et al., 2017b; Staessens et al., 2020). The majority of leukocytes in AIS thrombi are neutrophils followed by macrophages, T-cells and to a limited extend also B-cells have been found in AIS thrombi (Laridan et al., 2017; Sporns et al., 2017b). It is currently unclear whether the presence of leukocytes in AIS thrombi is a result of them being passively trapped during thrombus formation or if it indicates their active involvement in the process of thrombogenesis.

Neutrophil extracellular traps and extracellular DNA

An intriguing constituent of AIS are NETs. First described as a novel immune defense mechanism of neutrophils, NETs are generated by neutrophils that release decondensed chromatin that is decorated with anti-microbial granular proteins, forming a network of extracellular DNA fibers (Brinkmann et al., 2004). NETs are also known to promote thrombosis and serve as a scaffold for thrombus formation in both arterial and venous settings (Fuchs et al., 2010; Laridan et al., 2019). Various studies have shown the presence of NETs in AIS using immunostaining of neutrophil markers (such as CD66b, neutrophil elastase and myeloperoxidase) together with markers for NETs (citrullinated histones and extracellular DNA) (Laridan et al., 2017; Ducroux et al., 2018; Farkas et al., 2019; Essig et al., 2020; Novotny et al., 2020; Staessens et al., 2020; Chen et al., 2021; Genchi et al., 2021; Denorme et al., 2022). Together, these findings have substantiated the notion that NETs constitute a common structural feature of AIS thrombi. The colocalization of NETs with HMGB-1 and inflammasome proteins supports the link between thrombus formation and inflammation (Denorme et al., 2022). Remarkably, NETs tend to accumulate within platelet-rich areas and in the interface between platelet-rich and RBC-rich regions (Staessens et al., 2020). The presence of increased NETs and extracellular DNA in older thrombi and those originating from the heart, as opposed to other causes, suggests a potential involvement of NETs in thrombus formation under static conditions (Laridan et al., 2017; Essig et al., 2020; Novotny et al., 2020; Genchi et al., 2021; Kitano et al., 2022). This is in line with the accumulation of NETs in human venous thrombi where NETs are localized during the static organization phase (Savchenko et al., 2014). Utilizing Feulgen's staining, a method highly sensitive to all DNA, and thus not limited to NETs, we have recently reported the presence of extensive extracellular DNA networks in AIS thrombi (Staessens et al., 2020). These extracellular DNA networks exhibit a pronounced presence in platelet-rich regions and at the interface where platelet-rich regions meet areas rich in RBCs (Fig. 2). The exact origin of these vast extracellular DNA networks remains uncertain but possible origins could include NETs, circulating DNA or DNA derived from necrotic cells.

Other components

Besides the main constituents described above, there are also less commonly encountered components reported in AIS thrombi. These include cholesterol, adipocyte-like patterns, collagen and other vascular wall components, calcifications, myxomatous material (Staessens et al., 2021b; Aspegren et al., 2022). The circumstances under which these elements manifest in AIS thrombi and their impact on mechanical thrombectomy and clinical outcomes remain largely unknown. Notably, infections have been identified as a risk factor for ischemic stroke (Grau and Urbanek, 2010). Interestingly, Gram staining revealed the presence of Gram-positive bacteria, particularly Staphylococcus species, in patients suffering from infectious endocarditis (-Hernández-Fernández et al., 2017; Bhaskar et al., 2019; Mak et al., 2021).

Thrombus composition and etiology

The factors contributing to the formation of thromboemboli in ischemic strokes are varied, frequently stemming from underlying vascular and cardiac conditions that elevate the likelihood of thrombus formation of embolism. Several studies have sought to explore possible relationships between the primary site of thrombus formation and thrombus composition. Early studies, mostly using smaller samples cohorts, yielded inconclusive outcomes, but larger cohort studies uniformly found that cardioembolic thrombi are less RBC-rich than large artery atherosclerotic thrombi (Boeckh-Behrens et al., 2016a; Sporns et al., 2017b; Hund et al., 2023). Furthermore, thrombi from undetermined origin closely resemble cardioembolic thrombi, indicated a potential cardioembolic cause (Boeckh-Behrens et al., 2016a; Sporns et al., 2017b; Hund et al., 2023). The link between stroke etiology and VWF levels remains underexplored with just one study to date directly examining this relationship and reporting no correlation (Denorme et al., 2016). A definitive connection between the presence of leukocytes or their subtypes and stroke etiology has not been conclusively established (Dargazanli et al., 2016; Schuhmann et al., 2016; Sporns et al., 2017b). However, one study did note a higher overall count of leukocytes in AIS thrombi of cardioembolic origin (Boeckh-Behrens et al., 2016b). The general trend observed between thrombus composition and stroke etiology is illustrated in Fig. 3.

Thrombus composition and thrombolysis

Currently, rt-PA is the only FDA-approved thrombolytic medication that is available for the treatment of AIS. The application of rt-PA is restricted to a narrow time frame of 4.5 hours following the onset of a stroke, primarily due to the heightened risk of hemorrhagic complications outweighing the benefits when used beyond this therapeutic win-

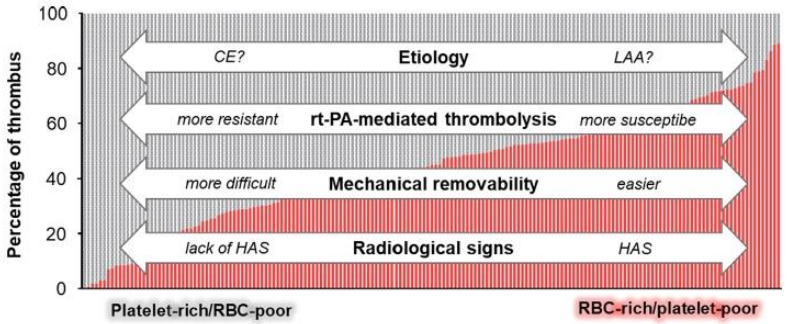

Fig. 3. Impact of thrombus composition on treatment parameters. Acute ischemic stroke thrombus composition ranges from platelet-rich (left) to RBC-rich (right). The largest studies show that thrombi originating from cardioembolic sources generally are more platelet-rich, whereas large artery atherosclerotic thrombi are typically more RBC-rich. Emerging evidence shows that platelet-rich thrombi tend to be more resistant to rt-PA mediated thrombolysis, in contrast to RBC-thrombi which are believed to be more susceptible to fibrinolysis. Platelet-rich thrombi are more difficult to retrieve via thrombectomy and typically require more passes, while RBC-rich thrombi are more prone to lead to a first pass recanalization procedure. RBC-rich thrombi typically give a hyperdense artery sign on CT-imaging, which is absent in platelet-rich thrombi. CE, cardioembolic; LAA, large artery atherosclerosis; HAS, hyperdense artery sign; RBC, red blood cell; rt-PA, recombinant tissue plasminogen activator.

dow. Importantly, in over half of patients receiving rt-PA, successful recanalization cannot be achieved (Lee et al., 2007; Bhatia et al., 2010; Prabhakaran et al., 2015). The exact causes of this phenomenon, often termed "rt-PA resistance", remain poorly understood, but it is likely that thrombus composition plays an essential role besides thrombus size, thrombus location and collateral status. The mechanism of action for rt-PA involves the conversion of plasminogen into plasmin, which degrades fibrin within the thrombus. As previously mentioned, stroke patients exhibit a diverse array of thrombus compositions, of which fibrin constitutes just one, yet major, component (Figs. 1 and 2). The effectiveness of rt-PA in degrading the thrombus may vary depending on the composition of the culprit thrombus. Increasing evidence indicates that thrombi that are RBC-rich are more susceptible to dissolution by rt-PA than those that are platelet-rich (Fig. 3) (Jang et al., 1989; Nam et al., 2012; Puig et al., 2012; Moftakhar et al., 2013; Niesten et al., 2014; Tomkins et al., 2015; Denorme et al., 2016; Choi et al., 2018; Shin et al., 2018). As described above, RBC-rich thrombi tend to have a relatively simple internal architecture in which fibrin serves as the primary extracellular scaffold. Plasmin-mediated fibrinolysis may thus suffice for adequate degradation of RBC-rich thrombi. In contrast, platelet-rich thrombi are more complex, with a denser internal structure that also contains other non-fibrin components such as VWF, extracellular DNA, or NETs (Staessens et al., 2020). These non-fibrin components most likely contribute to rt-PA resistance in several ways. First, they create a structural scaffold that is not degradable via fibrinolysis, resulting in sustained mechanical thrombus stability. Second, multiple components within platelet-rich thrombi can modify the fibrin structure, making them less susceptible to fibrinolysis. NET components like DNA and histones can modify the structure of fibrin, resulting in thicker fibrin fibers that are more resistant to fibrinolysis (Longstaff et al., 2013; Varjú et al., 2015). Additionally, under shear conditions, NETs can bind to VWF and PAI-1 further enhancing thrombus stability and reversing fibrinolysis (Grässle et al., 2014; Zhang et al., 2021). Third, non-fibrin components, together with platelet-mediated thrombus contraction may decrease the overall permeability, rendering the internal structures less accessible (Cines et al., 2014; Khismatullin et al., 2020). It was indeed shown that a rise in RBC fraction leads to larger pores within the fibrin networks, allowing for an increased penetration of thrombolytic agents into the thrombi (Carr and Hardin, 1987). Furthermore, platelets in platelet-rich thrombi promote thrombus contraction, rendering the thrombus less permeable. In addition, platelets also store and release the direct inhibitors of t-PA, such as (PAI-1, which was identified in significant quantities within platelet-rich, rt-PA-resistant areas of AIS thrombi (Di Meglio et al., 2019).

Recent insights on the heterogeneity and composition of stroke thrombi have raised the notion that relying solely on fibrinolysis alone may not be adequate to dissolve platelet-rich thrombi. Therefore, exploring alternative approaches that target non-fibrin components could present promising avenues for improving the thrombolysis success rates in patients. Such novel strategies aim at the breakdown of VWF or extracellular DNA, which are particularly present in platelet-rich thrombi. Several studies using drugs that target VWF, including the metalloprotease ADAMTS13 and N-acetylcysteine, have been proven to successfully degrade platelet-rich or rt-PA resistant thrombi (Denorme et al., 2016; De Lizarrondo et al., 2017; Kim et al., 2021; van Moorsel et al., 2022). Additionally, the DNA-cleaving enzyme DNase-1 targets DNA and ex vivo thrombolysis experiments using human AIS thrombi demonstrated improved thrombolysis of rt-PA in combination with DNase-1 compared to rt-PA alone (Laridan et al., 2017; Ducroux et al., 2018). Desilles et al. showed that the thrombolytic benefits of degrading extracellular DNA in human AIS thrombi may be the result of enhancement of rt-PA–mediated fibrinolysis (Desilles et al., 2022), indeed suggesting that NETs in AIS thrombi are antifibrinolytic. NETs can directly impede fibrinolysis via degradation of plasminogen by NETs-associated neutrophil elastase (Cruz et al., 2019) and via the sequestration of PAI-1 within the thrombus (Zhang et al., 2021). The clinical variant of DNase-1, known as Dornase alfa (Pulmozyme), has entered Phase 2 trials (EXTEND-IA DNase, NCT05203224 and NETS-target, NCT04785066) with the objective of assessing its effectiveness in patients who have experienced an AIS, received intravenous thrombolysis, and are eligible for EVT.

Upcoming strategies designed to combat direct inhibitors of fibrinolysis, such as PAI-1 and TAFI (Wyseure et al., 2015), or using VWF-targeted plasminogen activators (van Moorsel et al., 2022) could further enhance the efficacy in overcoming rt-PA resistance in platelet-rich thrombi.

Thrombus composition and thrombectomy

Since 2015, EVT has become the standard of care for AIS patients who have large vessel occlusion. Continuous progress in EVT technology and methodologies has resulted in significant enhancements in recanalization rates. However, EVT also has limitations that restrict its broad adoption as a universal recanalization treatment for AIS. EVT is suitable exclusively for patients with AIS resulting from large vessel occlusion in the anterior circulation, which constitutes a minority (20–30%) of all AIS cases. Furthermore, it necessitates access to specialized stroke centers staffed with neuro-interventionalists trained in the procedure. A significant challenge in endovascular therapy remains the variability in the consistency and ease of removal of thrombi, and a deeper understanding of the 'challenging' cases is crucial for advancing the field and further enhancing the success rates of EVT (Ospel et al., 2023). It has become evident that striving for "first pass recanalization" (FPR) is crucial, as it is linked to improved neurological outcomes and reduced mortality rates (Jindal et al., 2019; Kang et al., 2020; Mokin et al., 2020; Abbasi et al., 2021; Abdullayev et al., 2021; Akpinar et al., 2021; Hassan et al., 2021). FPR is defined as achieving complete or near-complete recanalization (modified thrombolysis in cerebral infarction scale (mTICI) 2c-3) in the first pass (Zaidat et al., 2018). The composition of the thrombus can significantly influence its mechanical properties such as such as stiffness, stickiness, deformability, and friction, all of which can influence the ease of thrombus removal through EVT. There is growing evidence indicating that RBC-rich thrombi are easier to retrieve through endovascular procedures when compared to platelet-rich thrombi (Fig. 3) (Maekawa et al., 2018; Duffy et al., 2019). Increased quantities of RBCs have been shown to reduce thrombus stiffness (Gersh et al., 2009) and to increase retriever strut indentation (Gunning et al., 2018; Duffy et al., 2019; Weafer et al., 2019). Thrombi rich in RBCs also exhibit a reduced coefficient of friction, potentially reducing the occurrence of static friction between the thrombus and the vessel or catheter wall, factors that may contribute to the challenges associated with thrombus removal (Gunning et al., 2018). On the other hand, these properties may increase the risk for pre-interventional thrombus migration, which is correlated with reduced technical success of subsequent endovascular procedures (Kaesmacher et al., 2017). Maegerlein et al. indeed showed that RBC-rich thrombi are more prone to migrate (Maegerlein et al., 2018). On the other hand, it has been proposed that RBC-rich thrombi are less likely to produce secondary emboli, which is an undesirable aspect of thrombectomy procedures (Sporns et al., 2017a). The observation that RBC-rich thrombi require fewer passes to achieve recanalisation and contribute to higher procedural success during EVT is reinforced by their association with better reperfusion outcomes, as indicated by the mTICI scale (Hashimoto et al., 2016; Maekawa et al., 2018; Shin et al., 2018; Duffy et al., 2019; Funatsu et al., 2019; Douglas et al., 2020). Besides the characteristics of RBCs, other thrombus components could also influence thrombectomy resistance. Thrombi with higher levels of leukocytes were shown to require more passes for successful removal (Boeckh-Behrens et al., 2016b). This observation aligns with the finding that the presence of neutrophil-derived NETs also leads to a greater number of thrombectomy attempts

and longer times for thrombus removal (Ducroux et al., 2018; Novotny et al., 2020; Arturo Larco et al., 2021; Staessens et al., 2021b; Abbasi et al., 2022; Kitano et al., 2022). The constituents of NETs, like DNA and histones, can alter the structure of fibrin, making it resilient against mechanical deformation, which could explain the resistance observed during thrombectomy (Longstaff et al., 2013). Likewise, bacteria can enhance thrombus rigidity by modifying the microstructure of fibrin (Maria Ma et al., 2017). This could be the reason why the presence of bacteria has an adverse impact on the ease of septic thrombus removal (Hernández-Fernández et al., 2017). In addition to the specific presence of distinct thrombus components, the relative distribution of these components within the thrombus most likely plays an important yet underexplored role. Liu et al. hypothesized that a heterogeneous structure of a thrombus could contribute to fragmentation during the thrombectomy procedure due to lack of homogeneity in the structures binding the thrombus together (Liu et al., 2022). Using a self-developed algorithm to objectively determine the internal thrombus heterogeneity, heterogeneous clots were indeed found to have lower first pass recanalisation rates (Liu et al., 2022).

Prediction of thrombus composition

Prior to administering treatment to a patient with a potential AIS, diagnostic imaging tests such as computed tomography (CT) and magnetic resonance imaging (MRI) are conducted. These tests aim to rule out cerebral haemorrhage, evaluate the extent of infarction and the at-risk penumbra, determine collateral circulation quality, and pinpoint the site of arterial occlusion. Interestingly, diagnostic imaging may hold the promise of enabling the early assessment of thrombus composition and permeability. This, in turn, could influence procedural choices, including the selection of specific thrombus retrieval techniques or device technologies. The presence of a hyperdense artery sign (HAS), measured in Hounsfield units, on CT at the site of the occlusion is associated with RBC-rich thrombi (Fig. 3) and serves as a predictor for successful recanalization via mechanical thrombectomy (Liebeskind et al., 2011; Puig et al., 2012; Moftakhar et al., 2013; Simons et al., 2015; Brinjikji et al., 2017; Maekawa et al., 2018; Hund et al., 2022; Patel et al., 2023). Conversely, low clot density measurements are linked with fibrin- or platelet-rich thrombi which exhibit more resistance to IV thrombolysis (Puig et al., 2012; Moftakhar et al., 2013; Brinjikji et al., 2017). On MRI, the presence of a susceptibility vessel sign (SVS) shows a strong correlation with the HAS on CT and was linked with RBC-rich thrombi (Kim et al., 2015; Shin et al., 2018; Tang et al., 2021). A study by Mahmoud et al. suggested that HAS might guide device selection in mechanical thrombectomy, with patients showing a better response to stent retrievers than contact aspiration for achieving FPR (Mohammaden et al., 2021). However, the technique's sensitivity is limited due to the heterogeneous nature of AIS clots, emphasizing that such radiological signs as sole predictors for successful thrombus retrieval is cautioned. Emerging technologies, like electrochemical impedance spectroscopy, when integrated with machine learning, have the potential to enhance the accuracy and reliability of thrombus composition prediction in EVT procedures. This advancement could aid in making more informed decisions regarding the selection of thrombectomy devices, ultimately leading to improved recanalization rates (Patil et al., 2022; Darcourt et al., 2023; Messina et al., 2023).

Futures perspectives

The accessibility of AIS thrombi for research purposes, facilitated by EVT, has led to a rapid expansion of a novel research field that investigates AIS thrombus composition. Future studies, preferably using large, multi-centric cohorts will help to further establish relationships between thrombus histopathology, baseline characteristics, imaging findings, revascularization rates, and clinical outcomes of stroke patients (Siddiqui et al., 2022). Besides conventional histological analysis, novel, innovative imaging techniques for studying thrombus composition have emerged, which can further elucidate thrombus organisation in its impact on treatment. These include, for example, mass spectrometry-based proteomic profiling coupled to artificial intelligence to examine protein signatures (Muñoz et al., 2018; Dargazanli et al., 2020), microarray analyses to unravel microRNA expression patterns (Kim et al., 2022), electron microscopic approaches to investigate the ultrastructural composition of different thrombus components and their 3D arrangements (Mereuta et al., 2021; Lagrange et al., 2022; Saghamanesh et al., 2022), or tools such as optical diffraction tomography combined with deep learning to automate and accelerate the histological quantification process (Chung et al., 2023).

Future developments to better identify and remove occlusive thrombi through, innovative imaging, novel approaches to determine thrombus composition, new device technologies and adjuvant thrombolytic strategies are likely to be key for future improvements in AIS treatment and patient outcomes.

Acknowledgement

This work was supported by the Fonds voor Wetenschappelijk Onderzoek – Vlaanderen (research grants G.0A86.13, G.0785.17, and 1509216N to S.F.D.M), by research grants from KU Leuven (OT/14/099 and ISP/14/02L2 to S.F.D.M), and by a research grant from the Queen Elisabeth Medical Foundation (to S.F.D.M).

Conflict of interest

The authors declare no competing financial interests.

References

Abbasi, M., Arturo Larco, J., Mereuta, M.O., Liu, Y., Fitzgerald, S., Dai, D., Kadirvel, R., Savastano, L., Kallmes, D.F., Brinjikji, W., 2022. Diverse thrombus composition in thrombectomy stroke patients with longer time to recanalization. Thromb Res 209, 99–104.

Abbasi, M., Liu, Y., Fitzgerald, S., Mereuta, O.M., Arturo Larco, J.L., Rizvi, A., Kadirvel, R., Savastano, L., Brinjikji, W., Kallmes, D.F., 2021. Systematic review and meta-analysis of current rates of first pass effect by thrombectomy technique and associations with clinical outcomes. J Neurointerv Surg 13, 212–216.

Abdullayev, N., Maus, V., Behme, D., Barnikol, U.B., Kutschke, S., Stockero, A., Goertz, L., Celik, E., Zaeske, C., Borggrefe, J., Schlamann, M., Liebig, T., Kabbasch, C., Mpotsaris, A., 2021. True first-pass effect in basilar artery occlusions: First-pass complete reperfusion improves clinical outcome in stroke thrombectomy patients. J Clin Neurosci 89, 33–38.

Aguiar de Sousa, D., von Martial, R., Abilleira, S., Gattringer, T., Kobayashi, A., Gallofré, M., Fazekas, F., Szikora, I., Feigin, V., Caso, V., Fischer, U., 2019. Access to and delivery of acute ischaemic stroke treatments: A survey of national scientific societies and stroke experts in 44 European countries. Eur Stroke J 4, 13–28.

Akpinar, C.K., Ozdemir, A.O., Gurkas, E., Bilgic, A.B., Aykac, O., Inanc, Y., Giray, S., 2021. Favorable first-pass recanalization rates with NeVa™ thrombectomy device in acute stroke patients: Initial clinical experience. Interv Neuroradiol 27, 107–113.

Arturo Larco, J., Abbasi, M., Liu, Y., Madhani, S.I., Shahid, A.H., Kadirvel, R., Brinjikji, W., Savastano, L.E., 2021. Per-pass analysis of recanalization and good neurological outcome in thrombectomy for stroke: Systematic review and meta-analysis. Interv Neuroradiol 28, 358–363.

Aspegren, O., Staessens, S., Vandelanotte, S., Desender, L., Andersson, T., Arnberg, F., 2022. Unusual histopathological findings in mechanically removed stroke thrombi – a multicenter experience. Front Neurol 13, 1–16.

Attenello, B.Y.F.J., Mack, W.J., 2016. Thrombectomy trials in acute ischemic. Stroke 15, 13–16.

Berkhemer, O.A. et al, 2015. A randomized trial of intraarterial treatment for acute ischemic stroke. N Engl J Med 372, 11–20.

Bhaskar, S., Saab, J., Cappelen-Smith, C., Killingsworth, M., Wu, X.J., Cheung, A., Manning, N., Aouad, P., McDougall, A., Hodgkinson, S., Cordato, D., 2019. Clot histopathology in ischemic stroke with infective endocarditis. Can J Neurol Sci 46, 331–336.

Bhatia, R., Hill, M.D., Shobha, N., Menon, B., Bal, S., Kochar, P., Watson, T., Goyal, M., Demchuk, A.M., 2010. Low rates of acute recanalization with intravenous recombinant tissue plasminogen activator in ischemic stroke: Real-world experience and a call for action. Stroke 41, 2254–2258.

Boeckh-Behrens, T., Kleine, J.F., Zimmer, C., Neff, F., Scheipl, F., Pelisek, J., Schirmer, L., Nguyen, K., Karatas, D., Poppert, H., 2016a. Thrombus histology suggests cardioembolic cause in cryptogenic stroke. Stroke 47, 1864–1871.
Boeckh-Behrens, T., Schubert, M., Förschler, A., Prothmann, S., Kreiser, K., Zimmer, C., Riegger, J., Bauer, J., Neff, F., Kehl, V., Pelisek, J., Schirmer, L., Mehr, M., Poppert, H., 2016b. The impact of histological clot composition in embolic stroke. Clin Neuroradiol 26, 189–197.
Brinjikji, W., Duffy, S., Burrows, A., Hacke, W., Liebeskind, D., Majoie, C.B.L.M., Dippel, D.W.J., Siddiqui, A.H., Khatri, P., Baxter, B., Nogeuira, R., Gounis, M., Jovin, T., Kallmes, D.F., 2017. Correlation of imaging and histopathology of thrombi in acute ischemic stroke with etiology and outcome: A systematic review. J Neurointerv Surg 9, 529–534.
Brinkmann, V., Reichard, U., Goosmann, C., Fauler, B., Uhlemann, Y., Weiss, D.S., Weinrauch, Y., Zychlinsky, A., 2004. Neutrophil extracellular traps kill bacteria. Science 303, 1532–1536.
Carr, M.E., Hardin, C.L., 1987. Fibrin has larger pores when formed in the presence of erythrocytes. Am J Physiol – Hear Circ Physiol 253, 1069–1073.
Chen, S.H., Scott, X.O., Ferrer Marcelo, Y., Almeida, V.W., Blackwelder, P.L., Yavagal, D. R., Peterson, E.C., Starke, R.M., Dietrich, W.D., Keane, R.W., de Rivero Vaccari, J.P., 2021. Netosis and inflammasomes in large vessel occlusion thrombi. Front Pharmacol 11, 1–11.
Choi, M.H., Park, G.H., Lee, J.S., Lee, S.E., Lee, S.J., Kim, J.H., Hong, J.M., 2018. Erythrocyte fraction within retrieved thrombi contributes to thrombolytic response in acute ischemic stroke. Stroke 49, 652–659.
Chung, Y., Kim, G., Moon, A.R., Ryu, D.H., Hugonnet, H., Lee, M.J., Shin, D.S., Lee, S.J., Lee, E.S., Park, Y.K., 2023. Label-free histological analysis of retrieved thrombi in acute ischemic stroke using optical diffraction tomography and deep learning. J Biophotonics 16, 1–10.
Cines, D.B., Lebedeva, T., Nagaswami, C., Hayes, V., Massefski, W., Litvinov, R.I., Rauova, L., Lowery, T.J., Weisel, J.W., 2014. Clot contraction: Compression of erythrocytes into tightly packed polyhedra and redistribution of platelets and fibrin. Blood 123, 1596–1603.
Cruz, D.B. da, Helms, J., Aquino, L.R., Stiel, L., Cougourdan, L., Broussard, C., Chafey, P., Riès-Kautt, M., Meziani, F., Toti, F., Gaussem, P., Anglés-Cano, E., 2019. DNA-bound elastase of neutrophil extracellular traps degrades plasminogen, reduces plasmin formation, and decreases fibrinolysis: proof of concept in septic shock plasma. FASEB J 33, 14270–14280.
Darcourt, J. et al, 2023. Identifying ex vivo acute ischemic stroke thrombus composition using electrochemical impedance spectroscopy. Interv Neuroradiol.
Dargazanli, C., Rigau, V., Eker, O., Bareiro, C.R., Machi, P., Gascou, G., Arquizan, C., Ayrignac, X., Mourand, I., Corlobé, A., Lobotesis, K., Molinari, N., Costes, V., Bonafé, A., Costalat, V., 2016. High CD3+ cells in intracranial thrombi represent a biomarker of atherothrombotic stroke. PLoS One 11, 1–13.
Dargazanli, C., Zub, E., Deverdun, J., Decourcelle, M., de Bock, F., Labreuche, J., Lefèvre, P.H., Gascou, G., Derraz, I., Riquelme Bareiro, C., Cagnazzo, F., Bonafé, A., Marin, P., Costalat, V., Marchi, N., 2020. Machine learning analysis of the cerebrovascular thrombi proteome in human ischemic stroke: an exploratory study. Front Neurol 11.
De Lizarrondo, S.M., Gakuba, C., Herbig, B.A., Repessé, Y., Ali, C., Denis, C.V., Lenting, P.J., Touzé, E., Diamond, S.L., Vivien, D., Gauberti, M., 2017. Potent thrombolytic effect of N-acetylcysteine on arterial thrombi. Circulation 136, 646–660.
De Meyer, S.F. et al, 2017. Analyses of thrombi in acute ischemic stroke: A consensus statement on current knowledge and future directions. Int J Stroke 12, 606–614.
Denorme, F., Langhauser, F., Desender, L., Vandenbulcke, A., Rottensteiner, H., Plaimauer, B., François, O., Andersson, T., Deckmyn, H., Scheiflinger, F., Kleinschnitz, C., Vanhoorelbeke, K., De Meyer, S.F., 2016. ADAMTS13-mediated thrombolysis of t-PA-resistant occlusions in ischemic stroke in mice. Blood 127, 2337–2345.
Denorme, F., Portier, I., Rustad, J.L., Cody, M.J., de Araujo, C.V., Hoki, C., Alexander, M. D., Grandhi, R., Dyer, M.R., Neal, M.D., Majersik, J.J., Yost, C.C., Campbell, R.A., 2022. Neutrophil extracellular traps regulate ischemic stroke brain injury. J Clin Invest 132, e154225.
Desilles, J.P., Solo Nomenjanahary, M., Consoli, A., Ollivier, V., Faille, D., Bourrienne, M.C., Hamdani, M., Dupont, S., Di Meglio, L., Escalard, S., Maier, B., Blanc, R., Piotin, M., Lapergue, B., Ajzenberg, N., Vasse, M., Mazighi, M., Ho-Tin-Noé, B., 2022. Impact of COVID-19 on thrombus composition and response to thrombolysis: Insights from a monocentric cohort population of COVID-19 patients with acute ischemic stroke. J Thromb Haemost 20, 919–928.
Di Meglio, L., Desilles, J.P., Ollivier, V., Nomenjanahary, M.S., Di Meglio, S., Deschildre, C., Loyau, S., Olivot, J.M., Blanc, R., Piotin, M., Bouton, M.C., Michel, J.B., Jandrot-Perrus, M., Ho-Tin-Noé, B., Mazighi, M., 2019. Acute ischemic stroke thrombi have an outer shell that impairs fibrinolysis. Neurology 93, E1686–E1698.
Di Meglio, L., Philippe Desilles, J., Mazighi, M., Ho-Tin-Noé, B., 2018. Thrombolysis-resistant intracranial clot. Neurology 90, 1075.
Douglas, A. et al, 2020. Platelet-rich emboli are associated with von Willebrand factor levels and have poorer revascularization outcomes. J Neurointerv Surg 12, 557–562.
Ducroux, C., Di, M.L., Loyau, S., Delbosc, S., Boisseau, W., Deschildre, C., Ben, M.M., Blanc, R., Redjem, H., Ciccio, G., Smajda, S., Fahed, R., Michel, J., Piotin, M., 2018. Thrombus neutrophil extracellular traps content impair tPA-induced thrombolysis in acute ischemic stroke. Stroke 49, 754–757.
Duffy, S., Mccarthy, R., Farrell, M., Thomas, S., Brennan, P., Power, S., O'Hare, A., Morris, L., Rainsford, E., Maccarthy, E., Thornton, J., Gilvarry, M., 2019. Per-pass analysis of thrombus composition in patients with acute ischemic stroke undergoing mechanical thrombectomy. Stroke 50, 1156–1163.
Essig, F., Kollikowski, A.M., Pham, M., Solymosi, L., Stoll, G., Haeusler, K.G., Kraft, P., Schuhmann, M.K., 2020. Immunohistological analysis of neutrophils and neutrophil extracellular traps in human thrombemboli causing acute ischemic stroke. Int J Mol Sci 21, 1–13.
Farkas, Á.Z., Farkas, V.J., Gubucz, I., Szabó, L., Bálint, K., Tenekedjiev, K., Nagy, A.I., Sótonyi, P., Hidi, L., Nagy, Z., Szikora, I., Merkely, B., Kolev, K., 2019. Neutrophil extracellular traps in thrombi retrieved during interventional treatment of ischemic arterial diseases. Thromb Res 175, 46–52.
Fu, H., Jiang, Y., Yang, D., Scheiflinger, F., Wong, W.P., Springer, T.A., 2017. Flow-induced elongation of von Willebrand factor precedes tension-dependent activation. Nat Commun 8, 324.
Fuchs, T.A., Brill, A., Duerschmied, D., Schatzberg, D., Monestier, M., Myers, D.D., Wrobleski, S.K., Wakefield, T.W., Hartwig, J.H., Wagner, D.D., 2010. Extracellular DNA traps promote thrombosis. Proc Natl Acad Sci U S A 107, 15880–15885.
Funatsu, N., Hayakawa, M., Hashimoto, T., Yamagami, H., Satow, T., Takahashi, J.C., Koga, M., Nagatsuka, K., Ishibashi-Ueda, H., Iwama, T., Toyoda, K., 2019. Vascular wall components in thrombi obtained by acute stroke thrombectomy: clinical significance and related factors. J Neurointerv Surg 11, 232–236.
Genchi, A., Semerano, A., Gullotta, G.S., Strambo, D., Schwarz, G., Bergamaschi, A., Panni, P., Simionato, F., Scomazzoni, F., Michelozzi, C., Pozzato, M., Maugeri, N., Comi, G., Falini, A., Roveri, L., Filippi, M., Martino, G., Bacigaluppi, M., 2021. Cerebral thrombi of cardioembolic etiology have an increased content of neutrophil extracellular traps. J Neurol Sci 423, 117355.
Gersh, K.C., Nagaswami, C., Weisel, J.W., 2009. Fibrin network structure and clot mechanical properties are altered by incorporation of erythrocytes. Thromb Haemost 102, 1169–1175.
Grässle, S., Huck, V., Pappelbaum, K.I., Gorzelanny, C., Aponte-Santamaría, C., Baldauf, C., Gräter, F., Schneppenheim, R., Obser, T., Schneider, S.W., 2014. Von willebrand factor directly interacts with DNA from neutrophil extracellular traps. Arterioscler Thromb Vasc Biol 34, 1382–1389.
Grau, A.J., Urbanek, C., 2010. Palm F (2010) Common infections and the risk of stroke. Nat Rev Neurol 612 (6), 681–694.
Gunning, G.M., McArdle, K., Mirza, M., Duffy, S., Gilvarry, M., Brouwer, P.A., 2018. Clot friction variation with fibrin content; implications for resistance to thrombectomy. J Neurointerv Surg 10, 34–38.
Hacke, W., Kaste, M., Bluhmki, E., Bronzman, M., Davalos, A., Guidetti, D., Larrue, V., 2008. Thrombolysis with alteplase 3 to 4.5 hours after acute ischemic stroke. N Engl J Med 359, 1317–1329.
Hada, M., Kaminski, M., Bockenstedt, P., McDonagh, J., 1986. Covalent crosslinking of von Willebrand factor to fibrin. Blood 68, 95–101.
Hashimoto, T., Hayakawa, M., Funatsu, N., Yamagami, H., Satow, T., Takahashi, J.C., Nagatsuka, K., Ishibashi-Ueda, H., Kira, J.I., Toyoda, K., 2016. Histopathologic analysis of retrieved thrombi associated with successful reperfusion after acute stroke thrombectomy. Stroke 47, 3035–3037.
Hassan, A.E., Dibas, M., Sarraj, A., Ghozy, S., El-Qushayri, A.E., Dmytriw, A.A., Tekle, W. G., 2021. First pass effect vs multiple passes complete reperfusion: A retrospective study. Neuroradiol J, 1–7.
Helms, C.C., Arië, R.A.S., Uitte De Willige, S., Standeven, K.F., Guthold, M., 2012. α-α cross-links increase fibrin fiber elasticity and stiffness. Biophys J 102 (1), 168–175.
Hernández-Fernández, F., Rojas-Bartolomé, L., García-García, J., Ayo-Martín, Ó., Molina-Nuevo, J.D., Barbella-Aponte, R.A., Serrano-Heras, G., Juliá-Molla, E., Pedrosa-Jiménez, M.J., Segura, T., 2017. Histopathological and bacteriological analysis of thrombus material extracted during mechanical thrombectomy in acute stroke patients. Cardiovasc Intervent Radiol 40, 1851–1860.
Ho-Tin-Noé, B., Desilles, J.P., Mazighi, M., 2023. Thrombus composition and thrombolysis resistance in stroke. Res Pract Thromb Haemost 7, 100178.
Hoshiba, Y., Hatakeyama, K., Tanabe, T., Asada, Y., Goto, S., 2006. Co-localization of von Willebrand factor with platelet thrombi, tissue factor and platelets with fibrin, and consistent presence of inflammatory cells in coronary thrombi obtained by an aspiration device from patients with acute myocardial infarction. J Thromb Haemost 4, 114–120.
Hund, H., Boodt, N., Arrarte Terreros, N., Taha, A., Marquering, H.A., van Es, A.C.G.M., Bokkers, R.P.H., Lycklama à Nijeholt, G.J., Majoie, C.B.L.M., Dippel, D.W.J., Lingsma, H.F., van Beusekom, H.M.M., van der Lugt, A., 2022. Quantitative thrombus characteristics on thin-slice computed tomography improve prediction of thrombus histopathology: results of the MR CLEAN Registry. Eur Radiol 32, 7811–7823.
Hund, H.M. et al, 2023. Association between thrombus composition and stroke etiology in the MR CLEAN Registry biobank. Neuroradiology 65, 933–943.
Jang, I.K., Gold, H.K., Ziskind, A.A., Fallon, J.T., Holt, R.E., Leinbach, R.C., May, J.W., Collen, D., 1989. Differential sensitivity of erythrocyte-rich and platelet-rich arterial thrombi to lysis with recombinant tissue-type plasminogen activator. A possible explanation for resistance to coronary thrombolysis. Circulation 79, 920–928.
Jindal, G., Carvalho, H.D.P., Wessell, A., Le, E., Naragum, V., Miller, T.R., Wozniak, M., Shivashankar, R., Cronin, C.A., Schrier, C., Gandhi, D., 2019. Beyond the first pass: Revascularization remains critical in stroke thrombectomy. J Neurointerv Surg 11, 1095–1099.
Kaesmacher, J., Maegerlein, C., Kaesmacher, M., Zimmer, C., Poppert, H., Friedrich, B., Boeckh-Behrens, T., Kleine, J.F., 2017. Thrombus migration in the middle cerebral artery: Incidence, imaging signs, and impact on success of endovascular thrombectomy. J Am Heart Assoc 6, e005149.
Kang, D.H., Kim, B.M., Heo, J.H., Nam, H.S., Kim, Y.D., Hwang, Y.H., Kim, Y.W., Kim, D. J., Kim, J.W., Baek, J.H., Kim, Y.S., 2020. Effects of first pass recanalization on outcomes of contact aspiration thrombectomy. J Neurointerv Surg 12, 466–470.
Khismatullin, R.R., Nagaswami, C., Shakirova, A.Z., Vrtková, A., Procházka, V., Gumulec, J., Mačák, J., Litvinov, R.I., Weisel, J.W., 2020. Quantitative morphology of cerebral thrombi related to intravital contraction and clinical features of ischemic stroke. Stroke, 3640–3650.

Kim, D., Shea, S.M., Ku, D.N., 2021. Lysis of arterial thrombi by perfusion of N,N′-Diacetyl-L-cystine (DiNAC). PLoS One 16, 1–16.
Kim, J.M., Byun, J.S., Kim, J., Park, M.S., Hong, S.A., Nam, T.K., Choi, H.H., Hong, S., Han, S.H., Jeong, H.B., Park, K.Y., Kim, H.R., 2022. Analysis of microRNA signatures in ischemic stroke thrombus. J Neurointerv Surg 14, 469–474.
Kim, S.K., Yoon, W., Kim, T.S., Kim, H.S., Heo, T.W., Park, M.S., 2015. Histologic analysis of retrieved clots in acute ischemic stroke: Correlation with stroke etiology and gradient-echo MRI. Am J Neuroradiol 36, 1756–1762.
Kitano, T. et al, 2022. An older thrombus delays reperfusion after mechanical thrombectomy for ischemic stroke. Thromb Haemost 122, 415–426.
Lagrange, D.D., Bernava, G., Reymond, P., Wanke, I., Vargas, M.I., Machi, P., Lövblad, K. O., 2022. OPEN A high resolution scanning electron microscopy analysis of intracranial thrombi embedded along the stent retrievers. Sci Rep, 1–11.
Laridan, E., Denorme, F., Desender, L., François, O., Andersson, T., Deckmyn, H., Vanhoorelbeke, K., De Meyer, S.F., 2017. Neutrophil extracellular traps in ischemic stroke thrombi. Ann Neurol 82, 223–232.
Laridan, E., Martinod, K., De, M.SF., 2019. Neutrophil extracellular traps in arterial and venous. Thrombosis, 86–93.
Lee, K.Y., Han, S.W., Kim, S.H., Nam, H.S., Ahn, S.W., Kim, D.J., Seo, S.H., Kim, D.I., Heo, J.H., 2007. Early recanalization after intravenous administration of recombinant tissue plasminogen activator as assessed by pre- and post-thrombolytic angiography in acute ischemic stroke patients. Stroke 38, 192–193.
Lenting, P.J., Christophe, O.D., Denis, C.V., 2015. Von Willebrand factor biosynthesis, secretion, and clearance: Connecting the far ends. Blood 125, 2019–2028.
Liebeskind, D.S. et al, 2011. CT and MRI early vessel signs reflect clot composition in acute stroke. Stroke 42, 1237–1243.
Lippi, G., Franchini, M., Targher, G., 2011. Arterial thrombus formation in cardiovascular disease. Nat Rev Cardiol 8, 502–512.
Litvinov, R.I., Weisel, J.W., 2023. Blood clot contraction: Mechanisms, pathophysiology, and disease. Res Pract Thromb Haemost 7, 100023.
Liu, Y. et al, 2022. Quantification of clot spatial heterogeneity and its impact on thrombectomy Basic science. J NeuroIntervent Surg 14, 1248–1252.
Longstaff, C., Varjú, I., Sótonyi, P., Szabó, L., Krumrey, M., Hoell, A., Bóta, A., Varga, Z., Komorowicz, E., Kolev, K., 2013. Mechanical stability and fibrinolytic resistance of clots containing fibrin, DNA, and histones. J Biol Chem 288, 6946–6956.
Maegerlein, C., Friedrich, B., Berndt, M., Lucia, K.E., Schirmer, L., Poppert, H., Zimmer, C., Pelisek, J., Boeckh-Behrens, T., Kaesmacher, J., 2018. Impact of histological thrombus composition on preinterventional thrombus migration in patients with acute occlusions of the middle cerebral artery. Interv Neuroradiol 24, 70–75.
Maekawa, K., Shibata, M., Nakajima, H., Mizutani, A., Kitano, Y., Seguchi, M., Yamasaki, M., Kobayashi, K., Sano, T., Mori, G., Yabana, T., Naito, Y., Shimizu, S., Miya, F., 2018. Erythrocyte-rich thrombus is associated with reduced number of maneuvers and procedure time in patients with acute ischemic stroke undergoing mechanical thrombectomy. Cerebrovasc Dis Extra 8, 39–49.
Mak, G., Lu, J.Q., Perera, K., 2021. Histopathologic analysis of retrieved cerebral thrombi in acute ischemic stroke patients with proximal anterior circulation occlusions amenable to endovascular thrombectomy. J Neurol Sci 429, 6–8.
Marder, V.J., Chute, D.J., Starkman, S., Abolian, A.M., Kidwell, C., Liebeskind, D., Ovbiagele, B., Vinuela, F., Duckwiler, G., Jahan, R., Vespa, P.M., Selco, S., Rajajee, V., Kim, D., Sanossian, N., Saver, J.L., 2006. Analysis of thrombi retrieved from cerebral arteries of patients with acute ischemic stroke. Stroke 37, 2086–2093.
Maria Ma, T., Scott VanEpps, J., Solomon, M.J., 2017. Structure, mechanics, and instability of fibrin clot infected with staphylococcus epidermidis. Biophysj 113, 2100–2109.
Mereuta, O.M., Fitzgerald, S., Christensen, T.A., Jaspersen, A.L., Dai, D., Abbasi, M., Puttappa, T., Kadirvel, R., Kallmes, D.F., Doyle, K.M., Brinjikji, W., 2021. High-resolution scanning electron microscopy for the analysis of three-dimensional ultrastructure of clots in acute ischemic stroke. J Neurointerv Surg 13, 906–911.
Messina, P., Garcia, C., Rambeau, J., Darcourt, J., Balland, R., Carreel, B., Cottance, M., Gusarova, E., Lafaurie-Janvore, J., Lebedev, G., Bozsak, F., Barakat, A.I., Payrastre, B., Cognard, C., 2023. Impedance-based sensors discriminate among different types of blood thrombi with very high specificity and sensitivity. J Neurointerv Surg 15, 526–531.
Moftakhar, P., English, J.D., Cooke, D.L., Kim, W.T., Stout, C., Smith, W.S., Dowd, C.F., Higashida, R.T., Halbach, V.V., Hetts, S.W., 2013. Density of thrombus on admission CT predicts revascularization efficacy in large vessel occlusion acute ischemic stroke. Stroke 44, 243–245.
Mohammaden, M.H., Haussen, D.C., Da Camara, C.P., Pisani, L., Gadea, M.O., Al-Bayati, A.R., Liberato, B., Rangaraju, S., Frankel, M.R., Nogueira, R.G., 2021. Hyperdense vessel sign as a potential guide for the choice of stent retriever versus contact aspiration as first-line thrombectomy strategy. J Neurointerv Surg 13, 599–604.
Mokin, M. et al, 2020. First pass effect in patients treated with the trevo stent-retriever: a TRACK registry study analysis. Front Neurol 11, 1–6.
Muñoz, R., Santamaría, E., Rubio, I., Ausín, K., Ostolaza, A., Labarga, A., Roldán, M., Zandio, B., Mayor, S., Bermejo, R., Mendigaña, M., Herrera, M., Aymerich, N., Olier, J., Gállego, J., Mendioroz, M., Fernández-Irigoyen, J., 2018. Mass spectrometry-based proteomic profiling of thrombotic material obtained by endovascular thrombectomy in patients with ischemic stroke. Int J Mol Sci 19.
Nam, H.S., Kim, E.Y., Kim, S.H., Kim, Y.D., Kim, J., Lee, H.S., Nam, C.M., Heo, J.H., 2012. Prediction of thrombus resolution after intravenous thrombolysis assessed by CT-based thrombus imaging. Thromb Haemost 107, 786–794.
Niesten, J.M., Van Der Schaaf, I.C., Van Der Graaf, Y., Kappelle, L.J., Biessels, G.J., Horsch, A.D., Dankbaar, J.W., Luitse, M.J.A., Van Seeters, T., Smit, E.J., Mali, W.P.T. M., Velthuis, B.K., 2014. Predictive value of thrombus attenuation on thin-slice non-contrast CT for persistent occlusion after intravenous thrombolysis. Cerebrovasc Dis 37, 116–122.
Novotny, J., Oberdieck, P., Titova, A., Pelisek, J., Chandraratne, S., Nicol, P., Hapfelmeier, A., Joner, M., Maegdefessel, L., Poppert, H., Pircher, J., Massberg, S., Friedrich, B., Zimmer, C., Schulz, C., Boeckh-Behrens, T., 2020. Thrombus NET content is associated with clinical outcome in stroke and myocardial infarction. Neurology 94, e2346–e2360.
Ospel, J.M. et al, 2023. What is a challenging clot?: A DELPHI consensus statement from the CLOTS 7.0 summit. Clin Neuroradiol, 1–10.
Patel, T.R., Santo, B.A., Baig, A.A., Waqas, M., Monterio, A., Levy, E.I., Siddiqui, A.H., Tutino, V.M., 2023. Histologically interpretable clot radiomic features predict treatment outcomes of mechanical thrombectomy for ischemic stroke. Neuroradiology 65, 737–749.
Patil, S., Darcourt, J., Messina, P., Bozsak, F., Cognard, C., Doyle, K., 2022. Characterising acute ischaemic stroke thrombi: insights from histology, imaging and emerging impedance-based technologies. Stroke Vasc Neurol 7, 353–363.
Pendu, R., Terraube, V., Christophe, O.D., Gahmberg, C.G., De Groot, P.G., Lenting, P.J., Denis, C.V., 2006. P-selectin glycoprotein ligand 1 and β2-integrins cooperate in the adhesion of leukocytes to von Willebrand factor. Blood 108, 3746–3752.
Prabhakaran, S., Ruff, I., Bernstein, R.A., 2015. Acute stroke intervention: A systematic review. JAMA – J Am Med Assoc 313, 1451–1462.
Prochazka, V., Jonszta, T., Czerny, D., Krajca, J., Roubec, M., Macak, J., Kovar, P., Kovarova, P., Pulcer, M., Zoubkova, R., Lochman, I., Svachova, V., Pavliska, L., Vrtkova, A., Kasprak, D., Gumulec, J., Weisel, J.W., 2018. The role of von willebrand factor, ADAMTS13, and cerebral artery thrombus composition in patient outcome following mechanical thrombectomy for acute ischemic stroke. Med Sci Monit 24, 3929–3945.
Puig, J., Pedraza, S., Demchuk, A., Daunis-i-Estadella, J., Termes, H., Blasco, G., Soria, G., Boada, I., Remollo, S., Baños, J., Serena, J., Castellanos, M., 2012. Quantification of thrombus Hounsfield units on noncontrast CT predicts stroke subtype and early recanalization after intravenous recombinant tissue plasminogen activator. Am J Neuroradiol 33, 90–96.
Rha, J.H., Saver, J.L., 2007. The impact of recanalization on ischemic stroke outcome: A meta-analysis. Stroke 38, 967–973.
Saghamanesh, S., Dimitriu LaGrange, D., Reymond, P., Wanke, I., Lövblad, K.O., Neels, A., Zboray, R., 2022. Non contrast enhanced volumetric histology of blood clots through high resolution propagation-based X-ray microtomography. Sci Rep 12, 1–14.
Savchenko, A.S., Martinod, K., Seidman, M.A., Wong, S.L., Borissoff, J.I., Piazza, G., Libby, P., Goldhaber, S.Z., Mitchell, R.N., Wagner, D.D., 2014. Neutrophil extracellular traps form predominantly during the organizing stage of human venous thromboembolism development. J Thromb Haemost 12, 860–870.
Schuhmann, M.K., Gunreben, I., Kleinschnitz, C., Kraft, P., 2016. Immunohistochemical analysis of cerebral thrombi retrieved by mechanical thrombectomy from patients with acute ischemic stroke. Int J Mol Sci 17.
Shin, J.W., Jeong, H.S., Kwon, H.J., Song, K.S., Kim, J., 2018. High red blood cell composition in clots is associated with successful recanalization during intra-arterial thrombectomy. PLoS One 13, 1–13.
Siddiqui, A.H., Waqas, M., Brinjikji, W., De Meyer, S.F., Doyle, K., Fiehler, J., Hacke, W., Hanel, R.A., Jovin, T.G., Liebeskind, D.S., Yoo, A.J., Zaidat, O.O., Andersson, T., Nogueira, R.G., 2022. Embotrap Extraction & Clot Evaluation & Lesion Evaluation for NeuroThrombectomy (EXCELLENT) Registry design and methods. J Neurointerv Surg 14, 783–787.
Simons, N., Mitchell, P., Dowling, R., Gonzales, M., Yan, B., 2015. Thrombus composition in acute ischemic stroke: A histopathological study of thrombus extracted by endovascular retrieval. J Neuroradiol 42, 86–92.
Sporns, P.B., Hanning, U., Schwindt, W., Velasco, A., Buerke, B., Cnyrim, C., Minnerup, J., Heindel, W., Jeibmann, A., Niederstadt, T., 2017a. Ischemic stroke: Histological thrombus composition and pre-interventional CT attenuation are associated with intervention time and rate of secondary embolism. Cerebrovasc Dis 44, 344–350.
Sporns, P.B., Hanning, U., Schwindt, W., Velasco, A., Minnerup, J., Zoubi, T., Heindel, W., Jeibmann, A., Niederstadt, T.U., 2017b. Ischemic stroke: What does the histological composition tell us about the origin of the thrombus? Stroke 48, 2206–2210.
Staessens, S., De Meyer, S.F., 2020. Thrombus heterogeneity in ischemic stroke. Platelets 32, 331–339.
Staessens, S., Denorme, F., François, O., Desender, L., Dewaele, T., Vanacker, P., Deckmyn, H., Vanhoorelbeke, K., Andersson, T., De Meyer, S.F., 2020. Structural analysis of ischemic stroke thrombi: Histological indications for therapy resistance. Haematologica 105, 498–507.
Staessens, S., François, O., Brinjikji, W., Doyle, K.M., Vanacker, P., Andersson, T., De Meyer, S.F., 2021a. Studying stroke thrombus composition after thrombectomy: what can we learn? Stroke 52, 3718–3727.
Staessens, S., François, O., Desender, L., Vanacker, P., Dewaele, T., Sciot, R., Vanhoorelbeke, K., Andersson, T., De Meyer, S.F., 2021b. Detailed histological analysis of a thrombectomy-resistant ischemic stroke thrombus: a case report. Thromb J 19, 1–7.
Swystun, L.L., Liaw, P.C., 2016. The role of leukocytes in thrombosis. Blood 128, 753–762.
Tang, S.Z., Sen, J., Goh, Y.G., Anil, G., 2021. Susceptibility vessel sign as a predictor for recanalization and clinical outcome in acute ischaemic stroke: A systematic review and meta-analysis. J Clin Neurosci 94, 159–165.
Tomkins, A.J., Schleicher, N., Murtha, L., Kaps, M., Levi, C.R., Nedelmann, M., Spratt, N. J., 2015. Platelet rich clots are resistant to lysis by thrombolytic therapy in a rat model of embolic stroke. Exp Transl Stroke Med 7, 1–9.
Tutwiler, V., Mukhitov, A.R., Peshkova, A.D., Le Minh, G., Khismatullin, R.R., Vicksman, J., Nagaswami, C., Litvinov, R.I., Weisel, J.W., 2018. Shape changes of erythrocytes during blood clot contraction and the structure of polyhedrocytes. Sci Rep 8, 1–14.

Tutwiler, V., Peshkova, A.D., Andrianova, I.A., Khasanova, D.R., Weisel, J.W., Litvinov, R.I., 2017. Contraction of blood clots is impaired in acute ischemic stroke. Arterioscler Thromb Vasc Biol 37, 271–279.
Tutwiler, V., Peshkova, A.D., Le Minh, G., Zaitsev, S., Litvinov, R.I., Cines, D.B., Weisel, J.W., 2019. Blood clot contraction differentially modulates internal and external fibrinolysis. J Thromb Haemost 17, 361–370.
van Moorsel, M.V.A., de Maat, S., Vercruysse, K., van Leeuwen, E.M., Jacqmarcq, C., Bonnard, T., Vivien, D., van der Worp, H.B., Dijkhuizen, R.M., Maas, C., 2022. VWF-targeted thrombolysis to overcome rh-tPA resistance in experimental murine ischemic stroke models. Blood 140, 2844–2848.
Varjú, I., Longstaff, C., Szabó, L., Farkas, Á.Z., Varga-Szabó, V.J., Tanka-Salamon, A., Machovich, R., Kolev, K., 2015. DNA, histones and neutrophil extracellular traps exert anti-fibrinolytic effects in a plasma environment. Thromb Haemost 113, 1289–1299.
Weafer, F.M., Duffy, S., Machado, I., Gunning, G., Mordasini, P., Roche, E., McHugh, P. E., Gilvarry, M., 2019. Characterization of strut indentation during mechanical thrombectomy in acute ischemic stroke clot analogs. J Neurointerv Surg 11, 891–897.
Wyseure, T., Rubio, M., Denorme, F., De Lizarrondo, S.M., Peeters, M., Gils, A., De Meyer, S.F., Vivien, D., Declerck, P.J., 2015. Innovative thrombolytic strategy using a heterodimer diabody against TAFI and PAI-1 in mouse models of thrombosis and stroke. Blood 125, 1325–1332.
Yoo, A.J., Andersson, T., 2017. Thrombectomy in acute ischemic stroke: Challenges to procedural success. J Stroke 19, 121–130.
Zaidat, O.O. et al, 2018. First pass effect: A new measure for stroke thrombectomy devices. Stroke 49, 660–666.
Zhang, S., Cao, Y., Du, J., Liu, H., Chen, X., Li, M., Xiang, M., Wang, C., Wu, X., Liu, L., Wang, C., Wu, Y., Li, Z., Fang, S., Shi, J., Wang, L., 2021. Neutrophil extracellular traps contribute to tissue plasminogen activator resistance in acute ischemic stroke. FASEB J 35.

CHAPTER 3 - AIMS OF THE RESEARCH

In acute ischemic stroke (AIS), the main problem is a blood clot that blocks the blood flow to the brain. The mainstay of AIS therapy therefore is timely recanalization of the occluded artery by either mechanical removal of the occluding thrombus via mechanical thrombectomy (MT) or pharmacological thrombolysis using the fibrinolytic agent recombinant tissue plasminogen activator (rt-PA), or a combination of the two. However, recanalization is not always successful, which in most cases leads to poor patient outcomes. Indeed, the use of rt-PA leads to successful recanalization only in less than half of the patients that receive it. This so called rt-PA resistance is an important limitation of pharmacological recanalization. The implementation of MT has significantly improved patient outcome but still in approximately 30% of treated patients, the occluding thrombus is not retrieved efficiently leading to poor clinical outcome. Furthermore, various other factors, such as the time before recanalization and the number of passes needed to remove the thrombus highly influence patient outcome. Rapid recanalization of occluded blood vessels in all AIS patients continues to be a crucial unmet need in stroke management. The reasons why thrombolytic or mechanical removal of blood clot often fails remain poorly understood. Since the thrombus is the central target for both recanalization strategies, it is likely that the thrombus itself influences recanalization success. Previously our lab showed that AIS thrombi are highly variable in structure and composition. However, the precise involvement of individual thrombus components in both rt-PA resistance and MT success are not fully understood. The general aim of this thesis therefore was to gain better insights in how thrombus composition affects pharmacological and mechanical recanalization. More specifically, five sub-aims were defined:

Sub-aim 1: Development of ischemic stroke clot analogs

In recent years, the use of MT has become widespread, providing researchers access to the occluding thrombus as study material. Retrieved AIS clots have become very valuable to obtain new insights into the structure and composition of AIS clots. It has become clear that the composition of AIS is variable, ranging from clots that are RBC-rich to clots that are platelet-rich. Research on patient AIS clots is sometimes inconvenient as their use is frequently hindered by their unpredictable daily availability and highly variable composition. Our first sub-aim was therefore to generate AIS clot analogs from human blood, that would represent the range of clots typically found in

patients, but which can be prepared on-demand and under standardized conditions. The results of this research are covered in chapter 4.

Sub-aim 2: Exploring the relationship between AIS thrombus composition and the effectiveness of rt-PA-mediated thrombolysis.

In this part of the thesis, we aimed to determine whether thrombus composition is associated with successful lysis or resistance to rt-PA, based on the hypothesis that thrombus composition could be a crucial factor in the efficacy of rt-PA-mediated lysis. Using freshly collected thrombus material from patients with AIS, we tested their susceptibility to rt-PA-induced lysis and linked the degree of lysis to the composition of the thrombus, determined via histology. This work is addressed in chapter 5

Sub-aim 3: Developing novel thrombolytic strategies to successfully lyse AIS thrombi that are resistant to rt-PA

Since rt-PA fails to recanalize the occluded artery in more than half of the patients, novel thrombolytic strategies are needed to overcome this rt-PA resistance. In this part of the thesis, we therefore aimed to test several novel strategies to degrade blood clots that are not susceptible to rt-PA-mediated lysis. As discussed in Chapter 5, freshly collected thrombus material from patients with AIS were subjected to various thrombolytic strategies directed against DNA and von Willebrand factor instead of fibrin.

Sub-aim 4: Elucidation of the effect of thrombus composition on recanalization via mechanical thrombectomy

Since achieving first pass recanalization (FPR) is crucial for good patient outcome when performing MT, it is crucial to better understand factors that contribute to FPR failure. The aim of this study therefore was to explore the relationship between AIS thrombus composition and obtaining FPR. To this end, previously and newly obtained histological data from over 260 AIS thrombi were used to investigate the potential impact of thrombus composition on achieving FPR. This research is discussed in chapter 6.

Sub-aim 5: Ultrastructural analysis of AIS thrombi

Conventional histopathological investigation of AIS thrombi significantly improved our understanding of the composition of stroke thrombi. The existence of various staining techniques specific to different components provides an idea on how different elements are interconnected. However, the resolution of conventional histopathological analysis is limited. The aim of this section of the thesis, addressed in chapter 7, therefore was to utilize scanning electron microscopy to uncover various aspects of the ultrastructural organization of AIS thrombi, which could potentially impact recanalization strategies.

CHAPTER 4 – MODEL FOR HUMAN ACUTE ISCHEMIC STROKE CLOT ANALOGS WITH DIFFERENT RT-PA RESPONSIVENESS

Sarah Vandelanotte, MSc [1], Olivier François, MD[2], Linda Desender, BSc[1], Senna Staessens, PhD[1], Fréderick Van Gool, MD[2], Claudia Tersteeg, PhD[1], Karen Vanhoorelbeke, PhD[1], Peter Vanacker, MD[3,4,5], Tommy Andersson, MD[2,6] and Simon F. De Meyer, PhD[1]

[1]: Laboratory for Thrombosis Research, KU Leuven Kulak, Kortrijk, Belgium
[2]: Department of Medical Imaging, AZ Groeninge, Kortrijk, Belgium
[3]: Department of Neurology, AZ Groeninge, Kortrijk, Belgium
[4]: Department of Neurology, University Hospitals Antwerp, Antwerp, Belgium
[5]: Department of Translational Neuroscience, University of Antwerp, Antwerp, Belgium
[6]: Departments of Neuroradiology, Karolinska University Hospital, and Clinical Neuroscience Karolinska Institutet, Stockholm, Sweden

Manuscript in preparation for Scientific reports

Abstract

In acute ischemic stroke (AIS) treatment, removal of the obstructing blood clot is crucial. Thrombectomy has enabled research on patient clots, which is important to further improve recanalization. Studying clots from patients is challenging due to their unpredictable availability and variability. We therefore aimed to provide a standardized and readily available alternative by creating human blood clot analogs that reflect AIS patient clots. Additionally, we tested the susceptibility of these analogs to lysis by recombinant tissue plasminogen activator (rt-PA). Using a Chandler loop system, we developed three AIS clot analogs representing typical clot types found in AIS patients: Red blood cell (RBC)-rich clots, platelet-rich clots, and mixed composition clots. A comprehensive panel of histological stainings, including those for red blood cells, fibrin, platelets, von Willebrand factor, leukocytes, and DNA, as well as scanning electron microscopy, revealed high similarities between the generated AIS clot analogs and clots retrieved from AIS patients. Furthermore, the RBC-rich analogs showed enhanced rt-PA-mediated thrombolysis compared to the mixed and platelet-rich analogs. In conclusion, we developed a novel method to produce three AIS clot analogs that closely resemble patient clots and that respond differently to rt-PA-mediated thrombolysis. As an alternative for patient clots, such analogs could facilitate further AIS research.

Introduction

Acute ischemic stroke (AIS) is caused by a blood clot that obstructs an artery, impeding blood flow to the brain. The clot is the primary focus in initial treatment, as its removal is necessary to restore blood flow and supply the brain with oxygen and nutrients. Currently, three options are available to recanalize an occluded artery: recombinant tissue plasminogen activator (rt-PA) for pharmacological clot dissolution or mechanical removal through endovascular thrombectomy or a combination of both. While it is widely believed that various clot properties can influence the success of recanalization therapies, stroke clot research remains limited due to unavailability of stroke clots. However, the widespread adoption of thrombectomy has overcome this limitation, making clots more readily available for research.[1] Indeed, with the availability of AIS clots retrieved from patients, a new research field has emerged, studying various aspects such as the composition and structure of AIS stroke clots.[1–

[5] It has become evident that clots in AIS exhibit high variability on composition, ranging from those predominantly composed of red blood cells (RBCs) to those abundant in platelets with minimal presence of RBCs.[2,4] RBC-rich clots are characterized by a rather simple structure of RBCs embedded in a fibrin network whereas platelet-rich clots have more complex structures, containing platelets together with dense fibrin, high amounts of von Willebrand factor (VWF), leukocytes and extracellular DNA.[2,4] We and others have provided evidence indicating that the composition of clots can significantly influence their susceptibility to lysis or thrombectomy. Platelet-rich clots show higher resistance to both rt-PA-mediated lysis and mechanical removal compared to RBC-rich clots.[6–15] To improve recanalization rates in ischemic stroke patients, a better understanding of how clot composition affects clot lysis and thrombectomy is imperative. Clots obtained from patients are crucial for this research; however, their utilization is frequently hindered by their unpredictable daily availability and highly variable composition. AIS clot analogs that would represent the range of clots typically found in patients, but which can be prepared on-demand under standardized conditions, would greatly facilitate stroke clot research. Previous studies have shown that in vitro clot analogs generated by adding thrombin to animal whole blood under static conditions often produce homogeneous RBC-rich clots, failing to mimic the diversity of patient stroke clots.[16–19] In contrast, rotating systems like the Chandler loop system yielded more heterogeneous clots with varying compositions, better replicating real-world conditions due to dynamic flow.[20–22] The aim of this study was to develop three different AIS clot analogs from human blood that represent the primary types of clots found in patients: RBC-rich, platelet-rich and mixed. Additionally, the response of these clot analogs to rt-PA treatment was investigated.

Methods

Collection of clots from patients with acute ischemic stroke

Fresh clots retrieved from AIS patients by thrombectomy were obtained at the AZ Groeninge Hospital (Kortrijk, Belgium). Patients or their legal representative provided written consent under the approval of the AZ Groeninge Hospital ethical committee (AZGS2015065). The collection of patient material was performed in agreement with the principles outlined in the Declaration of Helsinki. Clots were retrieved using a stent-retriever or by contact aspiration depending on the preference of the treating physician. After retrieval, the clot was carefully separated from the thrombectomy

device and stored in saline at 4°C for a maximum of 48 hours before starting the experiment.

Collection of human whole blood

Fresh human whole blood was obtained from healthy donors in 3.2% sodium citrate tubes under approval of the Ethics Committee Research of University Hospitals Leuven (S66363) and written informed consent.

Generation of in vitro AIS clot analogs

Three different AIS clot analogs (RBC-rich, platelet-rich and mixed type) were generated, each by using a specific protocol. For all three types, a Chandler loop system was used, consisting of a circular loop made of silicon tubing (inner diameter of 7 mm and length of 30 cm) that was rotated in a 37°C water bath as schematically represented in Figure 1.[20] To create RBC-rich clots, the Chandler loop tubing was filled with 3 mL fresh human citrated whole blood, after which 10 mM calcium chloride ($CaCl_2$) (Merck Life Science B.V., Darmstadt, Germany) was added to initiate coagulation. Immediately after addition of $CaCl_2$ the loop was closed and rotated at 400 revolutions per minute (RPM) for 1 hour at 37°C. To create mixed AIS clot analogs, a similar approach was used but 2.5 U/mL thrombin (Stago BNL B.V., Leiden, The Netherlands) was added instead of $CaCl_2$ to the loop containing 3 mL citrated whole blood to initiate coagulation and platelet activation. Loops were rotated for 1 hour at 50 RPM at 37°C. To generate platelet-rich AIS clot analogs, platelet-rich plasma (PRP) was first prepared via centrifugation of whole blood at 173 g for 15 minutes without brake. Next, 3 ml PRP together with 2.5 U/mL thrombin was added to the loops, and loops were rotated for 1 hour at 50 RPM at 37°C. After 1 hour rotation, all clots were gently removed by pouring out the blood along with the clot from the tubing. If the clot remained inside the tubing, it was gently extracted using forceps. Following removal, the clot was rinsed with phosphate-buffered saline (PBS) for further use.

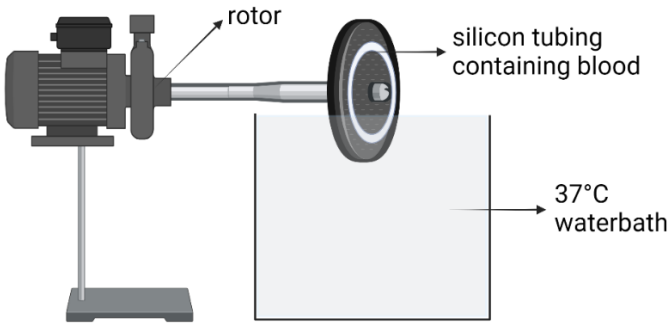

Figure 1: Schematic representation of the Chandler loop. A schematic overview is shown of the Chandler loop system used in this study. The system consists of a circular loop made of silicon tubing (inner diameter of 7 mm and length of 30 cm) that can be attached to a rotor in a 37°C water bath.

Histological analysis

To perform histological analysis of AIS clot analogs or collected patient clots, clot samples were placed in PBS and macroscopic images of the clots were taken with a Canon D70 digital camera. Next, clots were incubated in 4% paraformaldehyde for 24 hours at 4°C and then embedded in paraffin. Per clot, one 5 µm-thick section, exposing a large cross-sectional area of the entire clot, was selected for every staining. We previously demonstrated that one section per clot is a good representative for patient samples.[23] Clot processing and histological analysis of clot components was performed as described previously.[23] In brief, clot sections were stained with Martius Scarlet Blue (MSB) to identify RBCs (yellow), fibrin (dark pink/red) and collagen (blue). A Feulgen's reaction staining (1079070001, Merck Chemicals, MA, USA) was used to identify DNA. Immunohistochemical (IHC) stainings were performed to examine the presence of platelets (GPIbα, MA5-11642, Invitrogen, Waltham, MA, USA), VWF (A008202-2, Agilent Technologies, Santa Clara, CA, USA) and leukocytes (CD45, 304002, Biolegend, San Diego, CA). In the IHC stainings, nuclei were stained green using a Methyl Green solution (H-3402, Vector Laboratories, Peterborough, UK). Negative controls were obtained by omission of the primary antibody and were negative for all IHC procedures.

Quantitative determination of clot components

To quantify specific components of the clot, stained slides were digitized using a slide scanner (Nanozoomer SQ, Hamamatsu Photonics, Hamamatsu, Japan) and exported

in 5X resolution using NDP view2 Software (Hamamatsu, Japan). Background surrounding the clot section (e.g., dust particles, air bubbles) was removed using Adobe Photoshop CS5 (San José, CA, USA) to prevent false positive signal in the quantification. Histological stainings were examined by color segmentation and planimetric analysis to calculate the relative amount of each component using ImageJ software 1.49v (National Institutes of Health, Bethesda, MD, USA; http://imagej.nig.gov/ij/), as described previously.[23] MSB staining was used to quantify fibrin (dark pink/red) and RBCs (yellow). Quantification of platelets (purple), VWF (purple) and CD45 (purple) was performed on immunostainings for the respective component. The Feulgen staining (pink) was used to quantify the amount of total DNA in the clot section, which includes nuclear DNA and extracellular DNA (exDNA). All results are presented as percentage of positive signal relative to the total area of the examined clot section. Nine replicates of each clot type were made to quantify each component.

Scanning electron microscopy (SEM)

For SEM imaging, fresh AIS clot analogs were fixed in 2% glutaraldehyde, 0.1 M cacodylate buffer (pH = 7.4) (5169.1, Carl Roth, Karlsruhe, Germany) for 24 hours at 4°C. Following fixation, AIS clot analogs were halved using a surgical scalpel blade (Swann-Mortel Number 23, Sheffield, England). Next, samples were rinsed with 0.1 M cacodylate buffer and dehydrated in an increasing concentration of ethanol (50%, 70%, 85%, 96%, 100% ethanol) for 30 minutes each. Finally, samples were placed in hexamethyldisilazane (3840.2, Carl Roth, Karlsruhe, Germany) for 15 min and air dried overnight. Before imaging, samples were sputter-coated with platinum (3-5 nm). SEM analysis was conducted on the clot surface with a JSM-IT200 scanning electron microscope (JEOL, Akishima, Tokyo).

Thrombolysis experiments

Thrombolysis experiments were performed on fresh AIS clot analogs in 500 µl PBS, placed in a thermomixer at 37°C at 650 RPM. Clot lysis was assessed by measuring clot weight on a precision balance at baseline and every 10 minutes for a total of 60 minutes. To induce clot lysis by rt-PA, 1 µg/mL rt-PA (Actilyse; Boehringer-Ingelheim, Ingelheim am Rhein, Germany) was added to the sample at the beginning of the

experiment. As negative control, AIS clots analogs were placed in PBS without addition of rt-PA. At each timepoint, the degree of clot lysis was expressed as the percentage of residual clot weight (indicated as $RW_{timepoint}$) compared to its initial weight and results were normalized with negative control samples to correct for spontaneous degradation.

Statistical Analysis

Statistical analysis was performed using GraphPad Prism (Version 9.0.1; San Diego, CA, USA). The quantitative data of RBCs, fibrin, platelets, VWF, CD45 and total DNA are represented using the median and interquartile range and are based on clot analogs generated with blood from nine different donors. A Shapiro-Wilk test was used to analyze normal distribution. Differences between two groups were assessed using a student t-test or Mann-Whitney test based upon normality. When more than two groups were compared, a one-way ANOVA test or Kruskal–Wallis test (based upon normality) with Dunn multiple comparison was used. Two-tailed probability values ≤0.05 were regarded as significant.

Results

Generation and characterization of AIS clot analogs

In this study, our goal was to develop standardized human AIS clot analogs that closely resemble typical clots found in patients with AIS. Previously, we detailed the cellular and molecular makeup of clots in AIS patients and identified characteristic traits of their internal structure. Typically, two types of material compose AIS clots: material rich in red blood cells (RBC-rich) and material rich in platelets (platelet-rich).[2] Based on these findings, three main categories of clots can be delineated: those primarily comprised of RBC-material (RBC-rich), those predominantly composed of platelet-rich material (platelet-rich), and those containing significant amounts of both materials (mixed), as shown in Supplemental Figure 1. Using our Chandler loop system, the three main types of AIS clot analogs using fresh human blood can be produced. Each of these types is discussed below and depicted in Figures 2, 3, and 4, respectively. To allow easy comparison between the composition of the different clot analogs, all quantitative data is summarized in Figure 5.

RBC-rich AIS clot analogs

To generate RBC-rich clot analogs, citrated human whole blood was supplemented with $CaCl_2$ and subjected it to high-speed rotation. This protocol led to the generation of large and elongated red clots that were approximately 3 to 5 cm long and 0.5 cm wide. As shown in Figure 2A, the RBC-rich analogs are macroscopically similar to RBC-rich patient AIS clots. Detailed histological assessment showed that the composition and structure of the RBC-rich analogs closely resembled those found in thrombi from AIS patients (Figure 2B). MSB-staining highlighted RBCs as the predominant constituent (yellow color, Figure 2B), which are entangled in a thin fibrin network (pink color, Figure 2B). Dense fibrin structures (dark pink color) were absent. IHC staining for platelets showed that a near absence of platelets (purple color, Figure 2B). Similarly, IHC staining for VWF revealed only low amounts of VWF, primarily at the edge of the clots (purple color, Figure 2B). Staining for CD45, showed absence of leukocytes (not shown). Similarly, the highly specific Feulgen staining indicated the absence of nuclei and also revealed the absence of extracellular DNA within the clots (pink color, Figure 2B). Figure 5 shows the mean composition of RBC-rich AIS clot analogs (n=9), derived from blood samples obtained from nine different donors. To further characterize the AIS clot analogs, SEM imaging was conducted to gain better insights into the ultrastructural organization of the RBC-rich AIS clot analogs. As depicted in Figure 2C, SEM imaging revealed that RBC-rich AIS clot analogs predominantly consisted of loosely arranged RBCs mixed within a meshwork of thin fibrin fibers, occasionally alongside thicker fibrin bundles, as previously described by Johnson et al.[24]. Occasionally the presence of more densely packed deformed RBCs that assumed a polyhedrocytic form was noted (Figure 2C). The outer layer is characterized by a branched network of thin fibrin fibers with varying thickness, occasionally trapping loose RBCs within this structure (Figure 2C).

Taken together, similar to our previous observations of RBC-rich patient thrombi[2], our RBC-rich AIS clot analogs consisted mainly of RBCs with minimal presence of platelets, VWF, leukocytes and DNA.

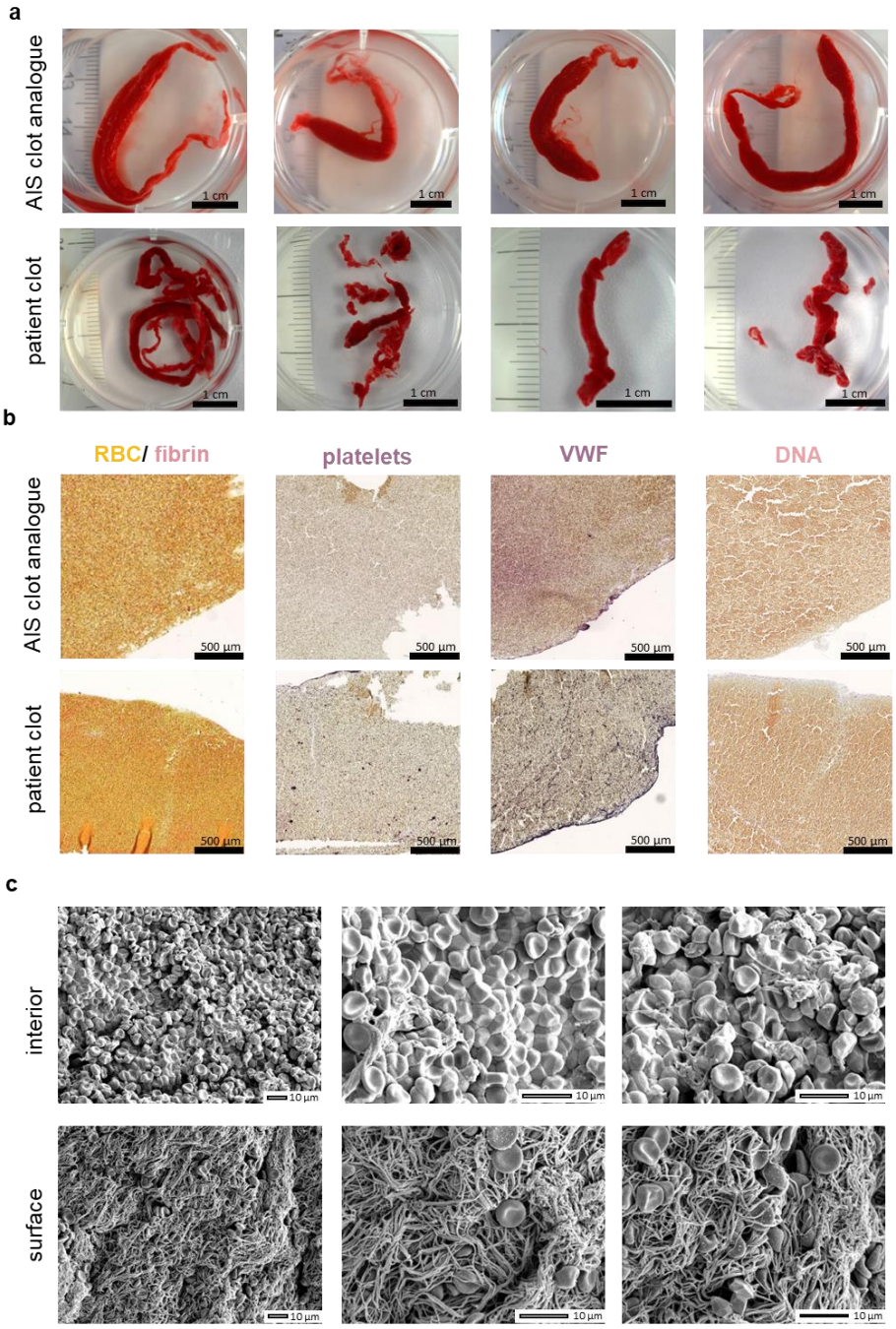

Figure 2: RBC-rich AIS clot analog: (A) Macroscopical images of four RBC-rich AIS clot analogs (upper panels, each clot is derived from a different blood donor) and RBC-rich AIS patient clots retrieved via thrombectomy (lower panels, each clot was retrieved from a different patient). Scale bar = 1 cm. (B) Representative histological images of an RBC-rich AIS clot analog (upper panels, n=9) and a RBC-rich AIS patient clot (lower panels). Sections were stained with Martius Scarlet Blue to identify RBCs (yellow) and fibrin (dark pink/red). Immunohistochemical stainings were used to identify platelets (CD42b; purple) and VWF (purple). A Feulgen's reaction was used to visualize DNA (pink). Scale bar = 500 µm. (C) Representative SEM images of the interior and surface of a RBC-rich clot analog (n=2) at different magnifications. Scale bar = 10 µm. RBC, red blood cell; VWF, von Willebrand factor.

Platelet-rich AIS clot analogs

In addition to patients with clots primarily containing RBC-rich material, a significant subset of patients presents with AIS clots that predominantly consist of platelet-rich material (Supplemental Figure 1). To generate AIS clot analogs that closely resemble platelet-rich patient clots, we used PRP instead of whole blood, combined with thrombin as an agonist in the rotating Chandler loop at low speed for 1 hour. As a result, platelet-rich clot analogs with a white appearance and a smaller size (0.5 cm – 1 cm in length) compared to RBC-rich clots were generated. Macroscopically, these platelet-rich AIS clot analogs show a high similarity to platelet-rich patient clots, as shown in Figure 3A. MSB-staining revealed the absence of RBCs (yellow color, Figure 3B), with significant amounts of dense fibrin (dark pink color, Figure 3B). Similar to patient clots that are platelet-rich, IHC platelet staining revealed that platelets are the dominant component of platelet-rich AIS clot analogs (purple color, Figure 3B). Additionally, substantial levels of VWF were detected through IHC VWF staining (purple color, Figure 3B). Only limited amounts of leukocytes (CD45, not shown), nuclei, and extracellular DNA (Feulgen staining, pink color, Figure 3B) were present. The quantification of the main components of platelet-rich AIS clot analogs is presented in Figure 5. Ultrastructural investigation of platelet-rich AIS clot analogs via SEM revealed a dense organization characterized by spongy platelet-rich structures along the fibrin fibers as described by Khismatullin et al (Figure 3C). [25] The density appeared to increase toward the periphery of the clot (Figure 3C). The outer layer of platelet-rich clot analogs formed a fully sealed layer where individual fibrin fibers were aligned into a dense network.[26]

Overall, consistent with our previous findings of platelet-rich patient thrombi[2], our platelet-rich AIS clot analogs showed high amounts of platelets, VWF and fibrin with an absence of RBCs.

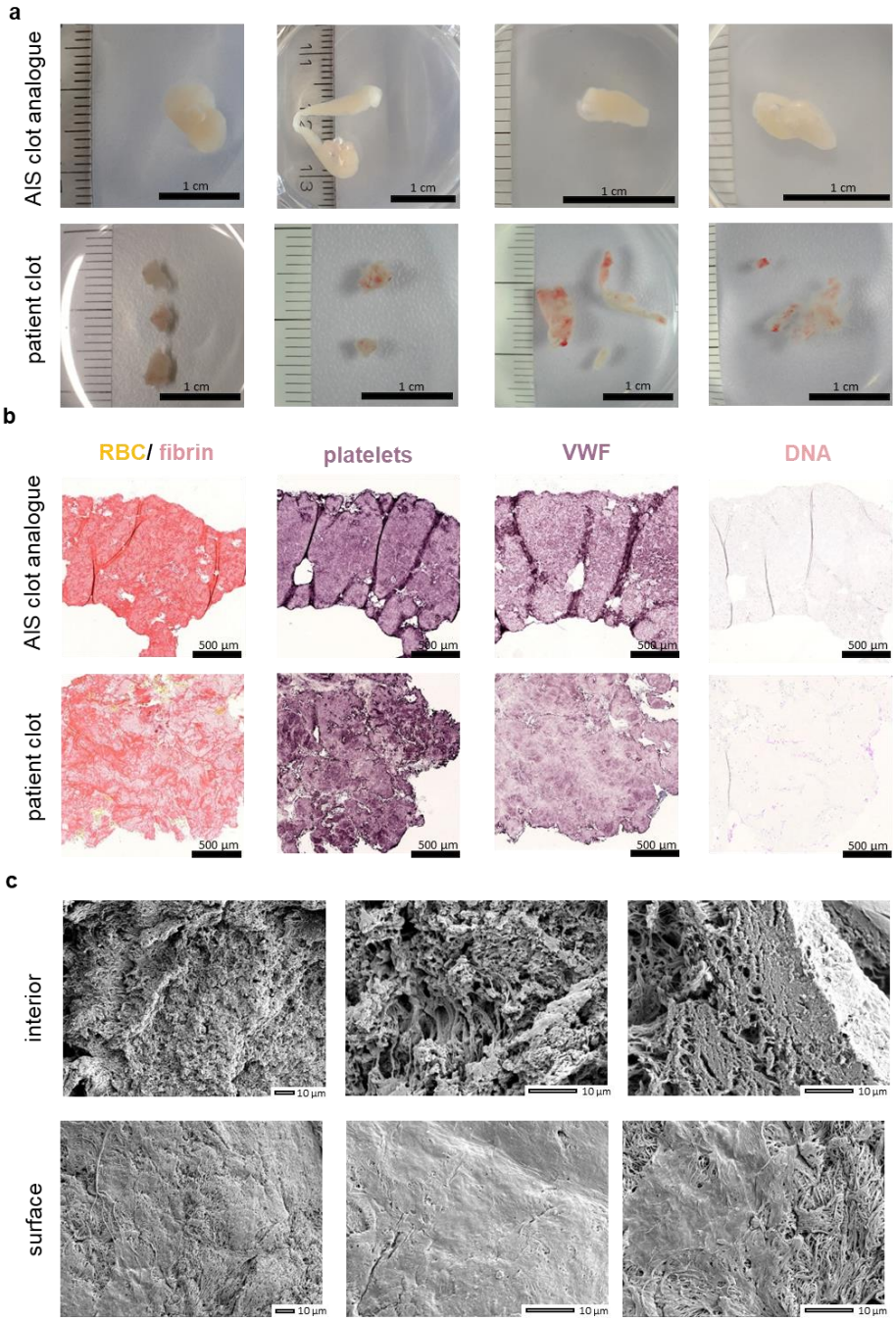

Figure 3: Platelet-rich AIS clot analog: (A) Macroscopical images of four platelet-rich AIS clot analogs (upper panels, each clot is derived from a different blood donor) and platelet-rich AIS patient clots retrieved via thrombectomy (lower panels, each clot was retrieved from a different patient). Scale bar = 1 cm. (B) Representative histological images of a platelet-rich AIS clot analog (upper panels, n=9) and a platelet-rich AIS patient clot (lower panels). Sections were stained with Martius Scarlet Blue to identify RBCs (yellow) and fibrin (dark pink/red). Immunohistochemical stainings were used to identify platelets (CD42b; purple) and VWF (purple). A Feulgen's reaction was used to visualize DNA (pink). Scale bar = 500 µm. (C) Representative SEM images of the interior and surface of an in vitro platelet-rich clot analog (n=2) at different magnifications. Scale bar = 10 µm. RBC, red blood cell; VWF, von Willebrand factor.

Mixed AIS clot analogs

In addition to RBC-rich and platelet-rich patient clots, many AIS patients have clots containing a mixture of RBC-rich and platelet-rich areas.[2,4] To mimic this class of AIS clots, a mixed AIS clot analog was created using whole blood that was supplemented with thrombin and rotated at low speed. This approach resulted in AIS clot analogs that are similar in size to platelet-rich AIS clot analogs but have a heterogeneous appearance with dark red and white regions. As depicted in Figure 4A, the microscopical appearance of the mixed clot analogs closely resembles patient mixed clots. Staining with MSB revealed a structured organization of RBC-rich areas (yellow color, Figure 4B), alternating with dense fibrin rich areas (dark pink color, Figure 4B). IHC platelet staining confirmed the alternating structure of platelet-rich and platelet-poor areas (purple color, Figure 4B). VWF staining showed the presence of high amounts of VWF colocalizing with the platelet positive areas (purple color, Figure 4B). Although not very abundant, slightly increased amounts of leukocytes (CD45 staining, not shown) and nuclei, along with extracellular DNA (pink color in Feulgen staining, Figure 4B), were detected in mixed AIS clot analogs compared to RBC-rich and platelet-rich AIS clot analogs. The quantification of the histological parameters is shown in Figure 5. SEM imaging revealed a combination of both loosely arranged RBC-rich regions and dense platelet/fibrin-rich areas inside the mixed clot analogs. Occasionally, compressed polyhedrocytic RBCs were observed in RBC-rich regions of the clot (Figure 4C). The outer layer of the mixed AIS clot analogs consisted of areas that were completely sealed, resembling the outer layer of platelet-rich clots, along with regions containing branched dense fibrin fibers (Figure 4C).[25,26]

In conclusion, mixed AIS clot analogs had a structured organization of RBC-rich regions alternating with platelet-rich regions, in line with our previous observations of mixed patient thrombi.[2,4,27]

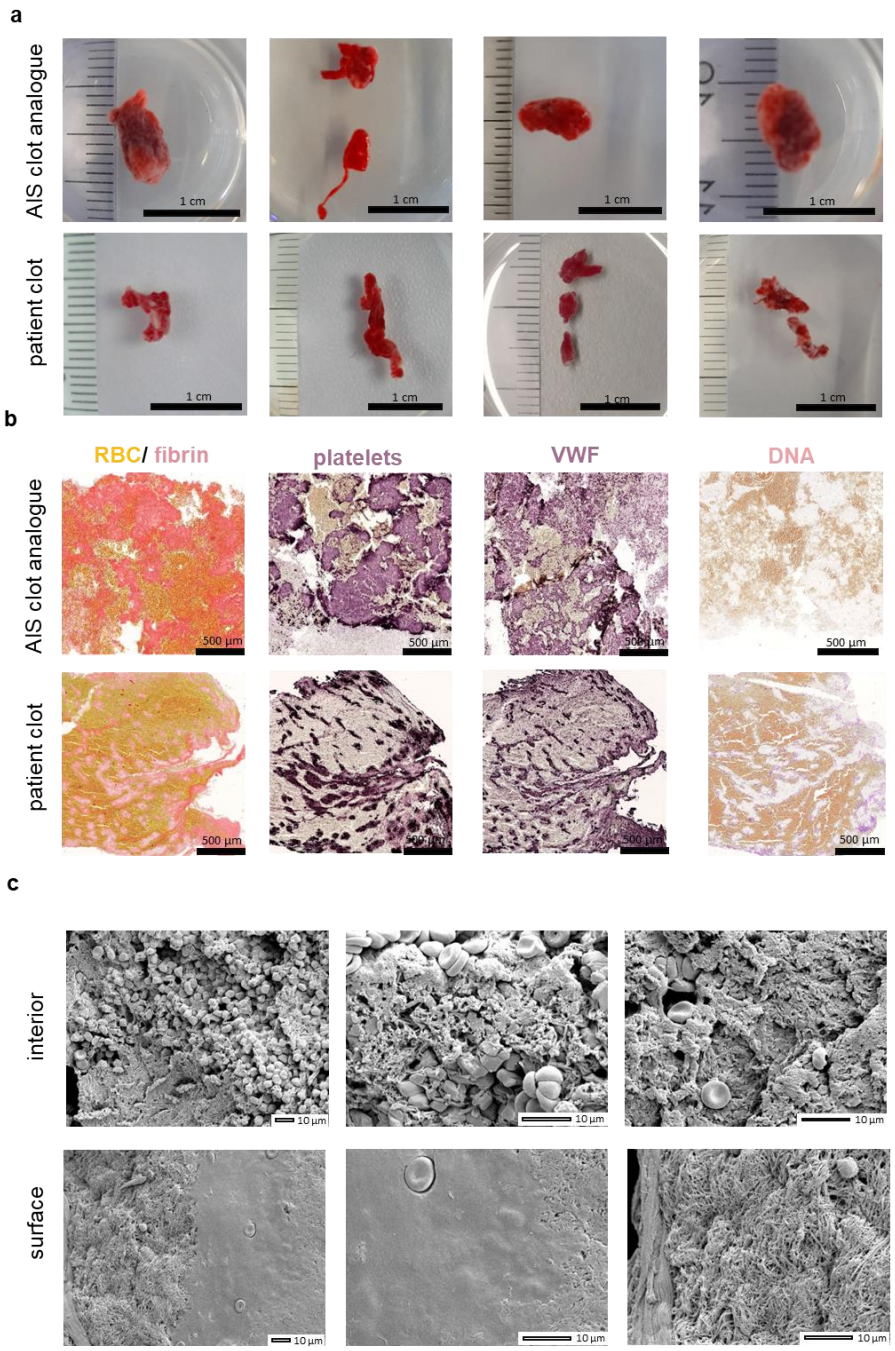

Figure 4: Mixed AIS clot analog: (A) Macroscopical images of four replicates from four mixed AIS clot analogs (upper panels, each clot is derived from a different blood donor) and mixed AIS patient clots retrieved via thrombectomy (lower panels, each clot was retrieved from a different patient). Scale bar = 1 cm. (B) Representative histological images of a mixed AIS clot analog (upper panels, n=9) and a mixed AIS patient clot (lower panels). Sections were stained with Martius Scarlet Blue to identify RBCs (yellow) and fibrin (dark pink/red). Immunohistochemical stainings were used to identify platelets (CD42b; purple) and VWF (purple). A Feulgen's reaction was used to visualize DNA (pink). Scale bar = 500 µm. (C) Representative SEM images of the interior and surface of an in vitro mixed clot analog (n=2) at different magnifications. Scale bar = 10 µm. RBC, red blood cell; VWF, von Willebrand factor.

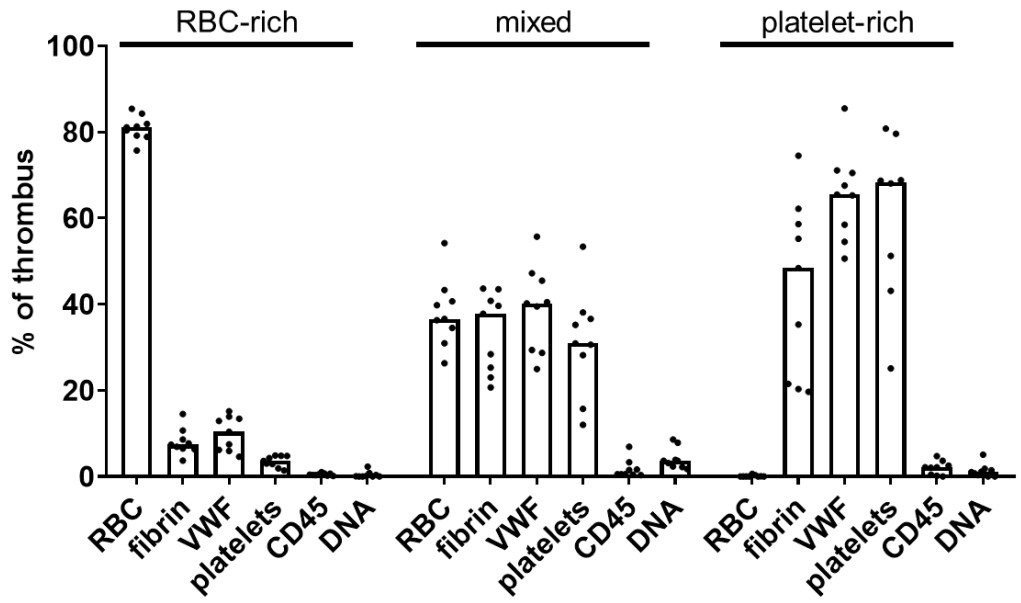

Figure 5: Overall composition of AIS clot analogs: AIS clot analogs of each of the three types were generated and clot sections were stained to quantify the number of RBCs, fibrin, VWF, platelets, leukocytes and DNA (n=9). Histological stainings were quantified by color segmentation and planimetric analysis to calculate the relative amount of each component. RBC, red blood cell; VWF, von Willebrand factor; CD45: cluster of differentiation 45. Bar plot represents the mean of the specific component.

Susceptibility of AIS clot analogs to rt-PA-mediated lysis

AIS clot analogs could serve as an easy source of standardized blood clots to assess the impact of clot composition on different aspects of recanalization therapy. Indeed, the structure and composition of AIS clots is known to influence the success rates of rt-PA-mediated thrombolysis.[6–8,10,13] In this study, we therefore used our three types of AIS clot analogs to examine their susceptibility to lysis by rt-PA. AIS clot analogs were incubated in PBS supplemented with rt-PA, for 60 min at 37°C and lysis was assessed by measuring the clot weight in function of time. Figure 6 shows the rt-PA specific lysis of each AIS clot analog. Interestingly, rt-PA induced significant thrombolysis in the RBC-rich clot analogs, resulting in approximately 50% reduction of the initial clot weight $RW_{60,\ RBC\text{-}rich}$ = 55.1% ± 8.3%). In contrast however, rt-PA was significantly less effective in lysing the mixed and platelet-rich clot analogs ($RW_{60,\ mixed}$ = 76.3% ± 10.9%; $RW_{60,\ platelet\text{-}rich}$ = 78.7% ± 0.9%, $p<0.01$). These results not only show how AIS clot analogs can be used to test important aspects of stroke management but also highlight the influence of clot composition on rt- PA resistance similar to patient clots.

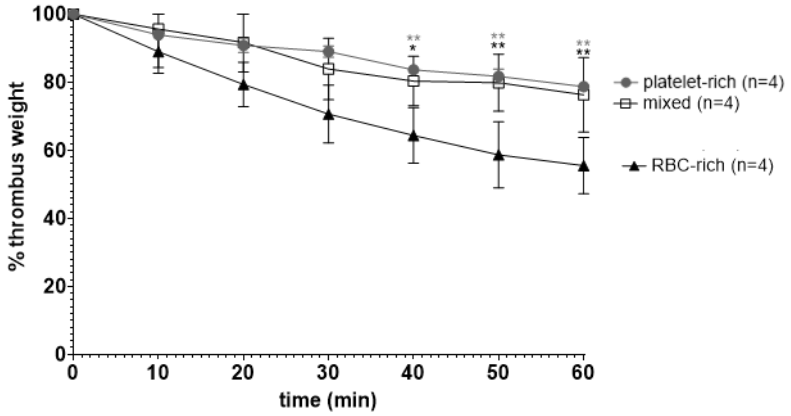

Figure 6: Thrombolysis of AIS clot analogs: AIS clot analogs made from human whole blood were generated. The three types of AIS clot analogs were generated, including RBC-rich clots, platelet-rich clots and clots with mixed composition (n=4). AIS clot analogs were incubated for 60 minutes at 37°C in the presence of recombinant tissue plasminogen activator (rt-PA, 1 µg/mL). Residual clot weight (percentage of initial weight) was measured at different time points and normalized for spontaneous degradation using a negative control lysis. Negative control lysis experiments were performed for each clot type and each donor on clots prepared from the same blood sample as used for the lysis experiment. Differences between different clot types at each time point were tested using a one-way ANOVA test with Dunn multiple comparison correction. Difference between RBC-rich and platelet-rich are indicated with grey asterisks whereas differences between RBC-rich and mixed clot analogs are indicated with black asterisks. Two-tailed probability values ≤0.05 were regarded as significant. All data are represented as mean with standard deviation. *p<0.05, **p<0.01

Discussion

Understanding clot behavior is crucial for improving the success rates of pharmacological and endovascular clot removal therapies in AIS patients. Patient clots retrieved via thrombectomy have become a valuable resource of study material, but their use is limited by their unpredictable availability and composition. In this study, we describe a and reproducible in vitro method for creating three different AIS clot analogs that replicate clots commonly found in AIS patients and can be prepared on demand.

The generation of in vitro AIS clot analogs has gained interest in recent years due to their importance and ease of use. To test thrombectomy devices, in vitro clot models based on animal whole blood stimulated by thrombin under static conditions have been used.[17–19,28] This method results in homogeneous RBC-rich clots that tend to be mechanically unstable, are prone to fragmentation during handling and do not

accurately replicate the diversity of clots found in AIS patients.[4,16–19,28] New protocols have been suggested to generate more diverse clots by employing different quantities of whole blood constituents, including platelet-rich plasma, platelet-poor plasma, and red blood cell fractions.[21,22] In particular, the use of flow models such as the Chandler loop system has been shown to increase the intra-thrombus heterogeneity of the formed clots.[21,22,29] Furthermore, due to significant variations in blood components among species, clot analogs derived from human blood are more likely to accurately represent clots formed within the human circulation. For example, clot analogs derived from animal blood, commonly bovine or porcine blood, exhibit different stiffness and elasticity profiles in comparison to their human counterparts.[16–18,21,29] Using dynamic flow conditions and human blood, Fitzgerald et al. produced diverse human clot analogs by combining thrombin and $CaCl_2$ with varying quantities of RBCs, plasma, and platelets in a flow model, yielding three main types: RBC-rich, fibrin-rich, and platelet-rich clots.[22] Building upon our previous findings of AIS clot composition (Supplementary Figure 1), our goal was to replicate three AIS clot analogs that mirror three common clot types observed in patients: RBC-rich, platelet-rich, or mixed composition clots. As shown in Figures 2, 3, and 4, the internal structure and composition of these three types of AIS clot analogs closely resembles those found in patients. When comparing the quantitative data of the AIS clot analogs with patient clots, we found that the RBC-rich and platelet-rich clot analogs both align with the fifth percentile of patient clots with the highest and lowest RBC content, respectively (data not shown).

SEM imaging of our in vitro clot analogs showed the presence of slightly deformed and polyhedrocytic RBCs in the mixed and RBC-rich clot analogs, a characteristic also observed in patient clots after clot contraction.[30,31] Further examination of the outer surface of the clot analogs uncovered the presence of a dense outer layer, resembling to some extent the outer shell that has been described in patient AIS clots. [26,32]

AIS clot analogs can be useful to test the response of different clot types to mechanical removal and pharmacological lysis. Interestingly thrombolysis of our AIS clot analogs revealed that the RBC-rich clot analogs were more susceptible to rt-PA compared to the mixed and platelet-rich AIS clot analogs. This is in line with previous studies indicating that the effectiveness of rt-PA is significantly influenced by the composition of the clot, with platelet-rich clots demonstrating greater resistance to rt-PA.[7,10,13,33–35] We recently demonstrated that rt-PA resistance of platelet-rich patient clots can be

overcome by targeting non-fibrin components in AIS patient clots.[7] The presence of non-fibrin components such as platelets, and to a lesser extent DNA, in the mixed and platelet-rich clot analogs could make them particularly suitable for studying rt-PA resistance and developing new strategies that target these components to improve thrombolysis. Previous studies have explored the mechanical properties of various AIS clot analogs, revealing various levels of stiffness that could influence the success rates of mechanical thrombectomy.[22,28,36] We did not test our AIS clot analogs in thrombectomy models; however, it would be interesting to further investigate their responses to thrombectomy to better understand the impact of clot composition on mechanical removal.

Our method of AIS clot analog generation has some limitations that need to be recognized. Firstly, due to intrinsic heterogeneity among clots from different stroke patients, classification to only three clot types may not fully encompass the complexity of clot variations seen in patients. However, by developing three clot types that span the spectrum from extremes to the middle of composition profiles, we aimed to capture the major differences between clot types. Additionally, the quantity of extracellular DNA and leukocytes in our clot analogs is relatively low and does not fully replicate the levels found in patient clots.[2,3] Despite exploring various methods, such as adding an isolated buffy coat, isolated leukocytes, in vitro generated neutrophil extracellular traps or purified DNA to our clot model (data not shown), none of these approaches successfully replicated the higher levels of extracellular DNA and NETs often observed in AIS patient clots.[3,37] The pathophysiology of AIS is complex, involving both thrombotic and inflammatory pathways that influence the formation and composition of the occluding clot.[38,39] This complexity, including thrombo-inflammation, clot maturation and aging during AIS, cannot be easily simulated in an in vitro flow model as used in this study, which may explain these discrepancies.

In conclusion, we describe a novel method to produce RBC-rich, platelet-rich and mixed AIS clot analogs that closely resemble the composition of the main clot types found in AIS patients. Furthermore, we demonstrate that compositional differences influence rt-PA mediated thrombolysis, with RBC-rich clots being more susceptible to lysis. The use of AIS clot analogs could serve as tools for developing and improving thrombectomy devices and assessing novel thrombolytic treatments.

Acknowledgements

We would like to thank the stroke team at the AZ Groeninge Hospital (Kortrijk, Belgium) for their support and collaboration in this research.

Author contributions statement

S.V. and S.F.D.M. designed the study. S.V. performed the experiments. O.F, L.D., S.S., F.V.G., P.V., T.A. contributed to data acquisition. SV analyzed data. S.V., S.F.D.M., C.T. and K.V. interpreted the results. S.V. and S.F.D.M. wrote the manuscript. All authors critically reviewed the manuscript.

Data availability statement:

All data are available upon reasonable request to the corresponding author.

Competing interest statement

The author(s) declared the following potential conflicts of interest with respect to the research, authorship, and/or publication to this article: S.V., L.D., S.S., F.V.G., C.T., K.V., S.F.D.M. have no relevant conflicts of interest to declare. O.F. is a consultant for iVascular. P.V. received speaker fees from Boehringer-Ingelheim, BMS, Pfizer, Daiichi-Sankyo, and Medtronic. T.A. holds equity for Cereflo Ltd and is a consultant for Anaconda, Cerenovus/Neuravi, Optimize Neurovascular and Rapid medical.

Sources of funding

This work was supported by the Fonds voor Wetenschappelijk Onderzoek – Vlaanderen (research grants G.0A86.13, G.0785.17, and 1509216N to S.F.D.M), by research grants from KU Leuven (OT/14/099 and ISP/14/02L2 to S.F.D.M), and by a research grant from the Queen Elisabeth Medical Foundation (to S.F.D.M).

References:

1. De Meyer SF, Andersson T, Baxter B, Bendszus M, Brouwer P, Brinjikji W, Campbell BCV, Costalat V, Dávalos A, Demchuk A, et al. Analyses of thrombi in acute ischemic stroke: A consensus statement on current knowledge and future directions. *Int. J. Stroke*. 2017;12:606–614.
2. Staessens S, Denorme F, François O, Desender L, Dewaele T, Vanacker P, Deckmyn H, Vanhoorelbeke K, Andersson T, De Meyer SF. Structural analysis of ischemic stroke thrombi: Histological indications for therapy resistance. *Haematologica*. 2020;105:498–507.
3. Laridan E, Denorme F, Desender L, François O, Andersson T, Deckmyn H, Vanhoorelbeke K, De Meyer SF. Neutrophil extracellular traps in ischemic stroke thrombi. *Ann. Neurol.* 2017;82:223–232.
4. Staessens S, De Meyer SF. Thrombus heterogeneity in ischemic stroke. *Platelets*. 2020;32:331–339.
5. Sporns PB, Hanning U, Schwindt W, Velasco A, Buerke B, Cnyrim C, Minnerup J, Heindel W, Jeibmann A, Niederstadt T. Ischemic Stroke: Histological Thrombus Composition and Pre-Interventional CT Attenuation Are Associated with Intervention Time and Rate of Secondary Embolism. *Cerebrovasc. Dis.* 2017;44:344–350.
6. Jang IK, Gold HK, Ziskind AA, Fallon JT, Holt RE, Leinbach RC, May JW, Collen D. Differential sensitivity of erythrocyte-rich and platelet-rich arterial thrombi to lysis with recombinant tissue-type plasminogen activator. A possible explanation for resistance to coronary thrombolysis. *Circulation*. 1989;79:920–928.
7. Vandelanotte S, François O, Desender L, Staessens S, Vanhoorne A, Van Gool F, Tersteeg C, Vanhoorelbeke K, Vanacker P, Andersson T, et al. Rt-PA resistance is specific for platelet-rich stroke thrombi and can be overcome by targeting non-fibrin components. *Stroke*. 2024;1–10.
8. Tomkins AJ, Schleicher N, Murtha L, Kaps M, Levi CR, Nedelmann M, Spratt NJ. Platelet rich clots are resistant to lysis by thrombolytic therapy in a rat model of embolic stroke. *Exp. Transl. Stroke Med.* 2015;7:1–9.
9. Shin JW, Jeong HS, Kwon HJ, Song KS, Kim J. High red blood cell composition in clots is associated with successful recanalization during intra-arterial thrombectomy. *PLoS One*. 2018;13:1–13.
10. Choi MH, Park GH, Lee JS, Lee SE, Lee SJ, Kim JH, Hong JM. Erythrocyte fraction within retrieved thrombi contributes to thrombolytic response in acute ischemic stroke. *Stroke*. 2018;49:652–659.
11. Maekawa K, Shibata M, Nakajima H, Mizutani A, Kitano Y, Seguchi M, Yamasaki M, Kobayashi K, Sano T, Mori G, et al. Erythrocyte-rich thrombus is associated with reduced number of maneuvers and procedure time in patients with acute ischemic stroke undergoing mechanical thrombectomy. *Cerebrovasc. Dis. Extra*. 2018;8:39–49.
12. Duffy S, Mccarthy R, Farrell M, Thomas S, Brennan P, Power S, O'Hare A, Morris L, Rainsford E, Maccarthy E, et al. Per-Pass Analysis of Thrombus Composition in Patients With Acute Ischemic Stroke Undergoing Mechanical Thrombectomy. *Stroke*. 2019;50:1156–1163.
13. Puig J, Pedraza S, Demchuk A, Daunis-i-Estadella J, Termes H, Blasco G, Soria G, Boada I, Remollo S, Baños J, et al. Quantification of thrombus

Hounsfield units on noncontrast CT predicts stroke subtype and early recanalization after intravenous recombinant tissue plasminogen activator. *Am. J. Neuroradiol.* 2012;33:90–96.
14. Liu Y, Brinjikji W, Abbasi M, Dai D, Arturo Larco JL, Madhani SI, Shahid AH, Mereuta OM, Nogueira RG, Kvamme P, et al. Quantification of clot spatial heterogeneity and its impact on thrombectomy. *J. Neurointerv. Surg.* 2021;14:neurintsurg-2021-018183.
15. Vandelanotte S, Staessens S, François O, De Wilde M, Desender L, De Sloovere AS, Dewaele T, Tersteeg C, Vanhoorelbeke K, Vanacker P, et al. Association between thrombus composition and first-pass recanalization after thrombectomy in acute ischemic stroke. *J. Thromb. Haemost.* 2024;1–7.
16. Chueh JY, Wakhloo AK, Hendricks GH, Silva CF, Weaver JP, Gounis MJ. Mechanical characterization of thromboemboli in acute ischemic stroke and laboratory embolus analogs. *Am. J. Neuroradiol.* 2011;32:1237–1244.
17. Gralla J, Schroth G, Remonda L, Fleischmann A, Fandino J, Slotboom J, Brekenfeld C. A dedicated animal model for mechanical thrombectomy in acute stroke. *Am. J. Neuroradiol.* 2006;27:1357–1361.
18. Kan I, Yuki I, Murayama Y, Viñuela FA, Kim RH, Vinters H V, Viñuela F. A novel method of thrombus preparation for use in a swine model for evaluation of thrombectomy devices. *Am. J. Neuroradiol.* 2010;31:1741–1743.
19. Roth C, Junk D, Papanagiotou P, Keuler A, Körner H, Schumacher M, Reith W. A comparison of 2 stroke devices: The new aperio clot-removal device and the solitaire AB/FR. *Am. J. Neuroradiol.* 2012;33:1317–1320.
20. Chandler AB. In vitro thrombotic coagulation of the blood; a method for producing a thrombus.” Laboratory investigation. *a J. Tech. methods Pathol.* 1958;7:110–4.
21. Duffy S, Farrell M, McArdle K, Thornton J, Vale D, Rainsford E, Morris L, Liebeskind DS, MacCarthy E, Gilvarry M. Novel methodology to replicate clot analogs with diverse composition in acute ischemic stroke. *J. Neurointerv. Surg.* 2017;9:486–491.
22. Fitzgerald STT, Liu Y, Dai D, Mereuta OMM, Abbasi M, Larco JLALA, Douglas ASS, Kallmes DFF, Savastano L, Doyle KMM, et al. Novel human acute ischemic stroke blood clot analogs for in vitro thrombectomy testing. *Am. J. Neuroradiol.* 2021;42:1250–1257.
23. Staessens S, Fitzgerald S, Andersson T, Clarençon F, Denorme F, Gounis MJ, Hacke W, Liebeskind DS, Szikora I, van Es ACGM, et al. Histological stroke clot analysis after thrombectomy: Technical aspects and recommendations. *Int. J. Stroke*. 2020;15:467–476.
24. Johnson S, McCarthy R, Gilvarry M, McHugh PE, McGarry JP. Investigating the Mechanical Behavior of Clot Analogues Through Experimental and Computational Analysis. *Ann. Biomed. Eng.* 2021;49:420–431.
25. Khismatullin RR, Nagaswami C, Shakirova AZ, Vrtková A, Procházka V, Gumulec J, MačÁk J, Litvinov RI, Weisel JW. Quantitative Morphology of Cerebral Thrombi Related to Intravital Contraction and Clinical Features of Ischemic Stroke. *Stroke*. 2020;51:3640–3650.
26. Di Meglio L, Desilles J-PP, Ollivier V, Nomenjanahary MS, Di Meglio S, Deschildre C, Loyau S, Olivot J-MM, Blanc R, Piotin M, et al. Acute ischemic stroke thrombi have an outer shell that impairs fibrinolysis. *Neurology*. 2019;93:E1686–E1698.
27. Vandelanotte S, De Meyer SF. Acute Ischemic Stroke Thrombus Composition.

Neuroscience. 2024;550:11–20.
28. Yuki I, Kan I, Vinters H V., Kim RH, Golshan A, Vinuela FA, Sayre JW, Murayama Y, Vinuela FA. The impact of thromboemboli histology on the performance of a mechanical thrombectomy device. *Am. J. Neuroradiol.* 2012;33:643–648.
29. Berndt M, Prothmann S, Maegerlein C, Oberdieck P, Zimmer C, Hegge B, Pelisek J, Schirmer L, Poppert H, Boeckh-Behrens T. Artificial Stroke Clots: How Wide is the Gap to the Real World? *World Neurosurg.* 2018;110:e90–e99.
30. Cines DB, Lebedeva T, Nagaswami C, Hayes V, Massefski W, Litvinov RI, Rauova L, Lowery TJ, Weisel JW. Clot contraction: Compression of erythrocytes into tightly packed polyhedra and redistribution of platelets and fibrin. *Blood*. 2014;123:1596–1603.
31. Tutwiler V, Mukhitov AR, Peshkova AD, Le Minh G, Khismatullin RR, Vicksman J, Nagaswami C, Litvinov RI, Weisel JW. Shape changes of erythrocytes during blood clot contraction and the structure of polyhedrocytes. *Sci. Rep.* 2018;8:1–14.
32. Mereuta OM, Agarwal T, Ghozy S, Dai D, Arul S, Brinjikji W, Kallmes DF, Kadirvel R. Shell Versus Core Architecture and Biology of Thrombi in Acute Ischemic Stroke: A Systematic Review. *Clin. Appl. Thromb.* 2023;29.
33. Ye G, Cao R, Lu J, Qi P, Hu S, Chen K, Tan T, Chen J, Wang D. Histological composition behind CT-based thrombus density and perviousness in acute ischemic stroke. *Clin. Neurol. Neurosurg.* 2021;207:106804.
34. Liebeskind DS, Sanossian N, Yong WH, Starkman S, Tsang MP, Moya AL, Zheng DD, Abolian AM, Kim D, Ali LK, et al. CT and MRI early vessel signs reflect clot composition in acute stroke. *Stroke*. 2011;42:1237–1243.
35. Simons N, Mitchell P, Dowling R, Gonzales M, Yan B. Thrombus composition in acute ischemic stroke: A histopathological study of thrombus extracted by endovascular retrieval. *J. Neuroradiol.* 2015;42:86–92.
36. Liu R, Lv B, Meng H, Zhang L, Ma W, He H, Wei R, Ma N, Fan Y, Wang J, et al. A novel method for preparing clot analogs under dynamic vortical flow for testing mechanical thrombectomy devices. *Interv. Neuroradiol.* 2023;1–8.
37. Ducroux C, Meglio L Di, Loyau S, Delbosc S, Boisseau W, Deschildre C, Maacha M Ben, Blanc R, Redjem H, Ciccio G, et al. Thrombus Neutrophil Extracellular Traps Content Impair tPA-Induced Thrombolysis in Acute Ischemic Stroke. *Stroke*. 2018;49:754–757.
38. Fuchs TA, Brill A, Wagner DD. Neutrophil extracellular trap (NET) impact on deep vein thrombosis. *Arterioscler. Thromb. Vasc. Biol.* 2012;32:1777–1783.
39. Fuchs TA, Brill A, Duerschmied D, Schatzberg D, Monestier M, Myers DD, Wrobleski SK, Wakefield TW, Hartwig JH, Wagner DD. Extracellular DNA traps promote thrombosis. *Proc. Natl. Acad. Sci. U. S. A.* 2010;107:15880–15885.

SUPPLEMENTAL MATERIAL

CHAPTER 4 – MODEL FOR HUMAN ACUTE ISCHEMIC STROKE CLOT ANALOGS WITH DIFFERENT RT-PA RESPONSIVENESS

Sarah Vandelanotte, MSc [1], Olivier François, MD[2], Linda Desender, BSc[1], Senna Staessens, PhD[1], Fréderick Van Gool, MD[2], Claudia Tersteeg, PhD[1], Karen Vanhoorelbeke, PhD[1], Peter Vanacker, MD[3,4,5], Tommy Andersson, MD[2,6] and Simon F. De Meyer, PhD[1]

Supplemental Figures:

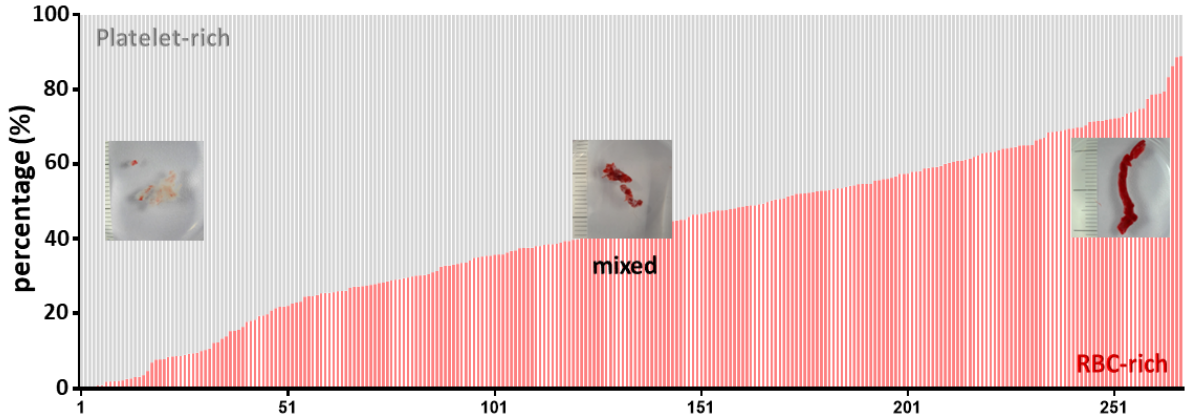

Supplemental Figure 1: Heterogeneity of acute ischemic stroke thrombi. Thrombi retrieved from acute ischemic stroke patients (n = 256, shown as vertical bars) were analyzed via Martius Scarlet Blue staining and the relative proportions of RBC-rich (red) and platelet-rich (grey) material was determined. The full range of composition profiles is represented, spanning from clots predominantly made up of platelet-rich material, through mixed compositions, to clots predominantly composed of RBC-rich material. Representative macroscopic images of patient AIS clots are shown. Figure adapted from Staessens S., Haematologica. 2019

CHAPTER 5 - RT-PA RESISTANCE IS SPECIFIC FOR PLATELET-RICH STROKE THROMBI AND CAN BE OVERCOME BY TARGETING NON-FIBRIN COMPONENTS

Short title: rt-PA resistance in ischemic stroke thrombi

Sarah Vandelanotte, MSc [1], Olivier François, MD[2], Linda Desender, BSc[1], Senna Staessens, PhD[1], Alexander Vanhoorne, MD[3], Fréderick Van Gool, MD[2], Claudia Tersteeg, PhD[1], Karen Vanhoorelbeke, PhD[1], Peter Vanacker, MD[3,4,5], Tommy Andersson, MD[2,6] and Simon F. De Meyer, PhD[1]

[1]: Laboratory for Thrombosis Research, KU Leuven Kulak, Kortrijk, Belgium
[2]: Department of Medical Imaging, AZ Groeninge, Kortrijk, Belgium
[3]: Department of Neurology, AZ Groeninge, Kortrijk, Belgium
[4]: Department of Neurology, University Hospitals Antwerp, Antwerp, Belgium
[5]: Department of Translational Neuroscience, University of Antwerp, Antwerp, Belgium
[6]: Departments of Neuroradiology, Karolinska University Hospital, and Clinical Neuroscience Karolinska Institutet, Stockholm, Sweden

Published article: Stroke. 2024 May;55(5):1181-1190.

Check for updates

Stroke

ORIGINAL CONTRIBUTION

R-tPA Resistance Is Specific for Platelet-Rich Stroke Thrombi and Can Be Overcome by Targeting Nonfibrin Components

Sarah Vandelanotte, MSc; Olivier François, MD; Linda Desender, BSc; Senna Staessens, PhD; Alexander Vanhoorne, MD; Fréderick Van Gool, MD; Claudia Tersteeg, PhD; Karen Vanhoorelbeke, PhD; Peter Vanacker, MD; Tommy Andersson, MD; Simon F. De Meyer, PhD

BACKGROUND: Resistance to r-tPA (recombinant tissue-type plasminogen activator) is a well-known but poorly understood phenomenon that hampers successful recanalization in patients with acute ischemic stroke. Using clinically relevant thrombi from patients with acute ischemic stroke, we investigated if and how thrombus composition impacts r-tPA-mediated lysis. In addition, we explored strategies to overcome r-tPA resistance.

METHODS: Thrombi were split into 2 parts, 1 of which was used for thrombolysis and the other for detailed histological analysis. Thrombolysis was performed in normal human plasma using r-tPA alone, using r-tPA in combination with DNase-1 or using r-tPA in combination with N,N′-diacetyl-L-cystine. Thrombus lysis was calculated as the percentage of residual thrombus weight compared with its initial weight and the degree of lysis was linked to thrombus composition determined via histology.

RESULTS: Interestingly, we found that the efficacy of r-tPA-mediated thrombolysis was strongly correlated with the composition of the thrombi. Thrombi containing high amounts of red blood cells and low amounts of DNA and von Willebrand Factor were efficiently degraded by r-tPA, whereas thrombi containing low amounts of red blood cells and higher amounts of DNA and von Willebrand Factor were resistant to r-tPA. Importantly, combination of r-tPA with DNase-1 or N,N′-diacetyl-L-cystine significantly and specifically improved the lysis of these r-tPA-resistant thrombi.

CONCLUSIONS: Using patient thrombus material, our results for the first time show that the composition of stroke thrombi largely determines their susceptibility to r-tPA-mediated thrombolysis. Red blood cell-poor thrombi have a specific resistance to r-tPA, which can be overcome by targeting nonfibrin components using DNase-1 or N,N′-diacetyl-L-cystine .

GRAPHIC ABSTRACT: A graphic abstract is available for this article.

Key Words: fibrinolysis ■ ischemic stroke ■ plasminogen ■ thrombolytic therapy ■ von Willebrand Factor

Downloaded from http://ahajournals.org by on March 26, 2024

Fast recanalization of the occluded artery is crucial in patients with acute ischemic stroke (AIS). Recanalization relies either on mechanical removal of the occluding thrombus via thrombectomy or on pharmacological thrombolysis using r-tPA (recombinant tissue-type plasminogen activator), or a combination of the 2. By converting plasminogen into plasmin, r-tPA promotes the degradation of fibrin, leading to thrombus dissolution. Successful use of r-tPA is however limited. Besides its narrow therapeutic time window,[1] r-tPA fails to establish recanalization in more than half of patients who receive it.[2,3] The precise mechanisms underlying this r-tPA resistance remain poorly understood but in addition to thrombus size, location, and collateral status, the thrombus composition likely plays an essential role. Despite its potential significance, there is limited research on how

Correspondence to: Simon F. De Meyer, PhD, Laboratory for Thrombosis Research, KU Leuven Kulak, E. Sabbelaan 53, 8500 Kortrijk, Belgium.
Email simon.demeyer@kuleuven.be
Supplemental Material is available at https://www.ahajournals.org/doi/suppl/10.1161/STROKEAHA.123.045880.
For Sources of Funding and Disclosures, see page xxx.
© 2024 American Heart Association, Inc.
Stroke is available at www.ahajournals.org/journal/str

ORIGINAL CONTRIBUTION

Nonstandard Abbreviations and Acronyms

AIS	acute ischemic stroke
diNAC	N,N′-diacetyl-l-cystine
NHP	normal human plasma
RBC	red blood cell
r-tPA	recombinant tissue-type plasminogen activator
$RW_{time\ point}$	percentage of residual thrombus weight
VWF	von Willebrand Factor

the thrombus composition affects the r-tPA response. We and others recently showed that the thrombus composition in patients is highly variable.[4–6] We previously described the presence of 2 distinct types of thrombus material, typically referred to as red blood cell (RBC)-rich and platelet-rich.[4] The 2 structures are present in variable quantities, resulting in a wide spectrum ranging from RBC-rich (and thus platelet-poor) thrombi to platelet-rich (RBC-poor) thrombi in patients with stroke.[4] RBC-rich thrombi have a relatively simple organization of densely packed RBCs within a network of thin fibrin.[4] In contrast, platelet-rich areas contain no RBCs and have a more complex organization of platelets, neutrophils, dense fibrin fibers, as well as von Willebrand Factor (VWF) and extracellular DNA.[4] In the present study, we hypothesized that the heterogeneity in thrombus composition is a major reason why the one-size fits all use of r-tPA is not always successful. We utilized freshly collected thrombus material from patients with AIS to test their susceptibility for r-tPA-induced lysis. Importantly, we linked efficacy of r-tPA lysis to the composition of the retrieved thrombi. In addition, we explored various approaches, targeting other structural components, to improve lysis of those thrombi that were resistant to r-tPA treatment.

METHODS

The data from this study are available from the corresponding author upon reasonable request.

Thrombus Collection

Fresh thrombi retrieved from patients with AIS via thrombectomy were obtained at the AZ Groeninge Hospital (Kortrijk, Belgium). Patients or their legal representative provided written consent under the approval of the AZ Groeninge Hospital ethical committee (AZGS2015065). The collection of patient material was performed in agreement with the principles outlined in the Declaration of Helsinki. Detailed description of clinical patient data can be found in the Supplemental Materials. Thrombi from consecutive patients were used per experimental condition. Each thrombus was divided in 2 parts, with 1 used for thrombolysis and the other for histological analysis. Our previous studies showed no large differences in composition within 1 thrombus retrieved from patients with stroke.[7] Nevertheless, careful attention was paid to avoid bias due to potential differences in composition between the 2 parts that were used either for thrombolysis and histology. Only thrombi that were sufficiently large for subdivision in 2 parts and exhibiting a macroscopically homogenous appearance were included.

Preparation of Pooled Normal Human Plasma

Whole blood was collected from 20 to 25 healthy volunteers into sodium citrate tubes (9:1 blood:sodium citrate, 3.2% vol/vol). Healthy volunteers provided written consent under the approval of the Medical Ethical Committee of KU/UZ Leuven (S66725). Whole blood was pooled and centrifuged at 2200*g* for 15 minutes without brake to generate normal human plasma (NHP), of which aliquots were stored at −80 °C until use.

Thrombolysis Experiment

The part of the thrombus used for the thrombolysis experiment was subjected to lysis. To standardize the reaction conditions, we performed all thrombolysis experiments in NHP (500 µL), which is the most relevant physiological medium containing a source of plasminogen. At the start of the experiment, the thrombus was placed in NHP, supplemented with the thrombolytic agent of interest, after which samples were placed in a thermomixer at 37 °C at 650 revolutions per minute. Thrombus weight was measured on a precision balance at baseline and after 10, 30, 60, 120, and 180 minutes. Lysis of the thrombus was expressed as the percentage of residual thrombus weight (indicated as $RW_{timepoint}$) compared with its initial weight. As a negative control, thrombi were incubated in NHP devoid of any supplemented thrombolytic agent. To resemble standard of care, 1 µg/mL r-tPA (Actilyse; Boehringer-Ingelheim, Ingelheim am Rhein, Germany) was added to NHP. To target nonfibrin components in addition to fibrin, 1 µg/mL r-tPA was combined with either 40 U/mL DNase-1 (dornase alfa, Pulmozyme; F.Hoffmann-La Roche, Basel, Switzerland) or with 2 mmol/L N,N'-diacetyl-L-cystine (diNAC; Cayman Chemical, Michigan).

D-Dimer ELISA

As a measure of fibrinolysis, D-dimers were determined in the supernatant after the thrombolysis experiment. Supernatant was stored at −20 °C and later used to measure D-dimers using the human D-dimer ELISA kit (EHDDIMER, Thermo Fisher Scientific, Waltham, MA, USA). NHP was used as control.

Histological Analysis

Histological analysis was conducted on the segment of the thrombus that remained unused for thrombolysis. Histological staining procedures were performed as described previously.[4] Detailed description of histological stainings and quantifications can be found in the Supplemental Materials.

Statistical Analysis

Statistical analysis was performed using GraphPad Prism (v9.01; GraphPad Software, San Diego, CA). Patient data are expressed as the absolute number and percentage, mean±SD for normally distributed variables, and median with interquartile range for non-normally distributed variables. Thrombolysis data are represented as mean±SD. Normality was tested using

Downloaded from http://ahajournals.org by on March 26, 2024

Stroke

a Shapiro-Wilk test. Group differences were assessed using a student *t* test or Mann-Whitney *U* test based upon normality. When >2 groups were compared a 1-way ANOVA test or Kruskal-Wallis test (based upon normality) with Dunn multiple comparison was used. Correlation between thrombus components and thrombolysis rate were assessed using Pearson or spearman correlation, based upon normality. Patient characteristics across groups were assessed with a χ^2 test. Two-tailed *P* values ≤0.05 were regarded as significant.

RESULTS

Efficacy of r-tPA-Mediated Lysis Is Linked With the Composition of the Thrombus

Fresh patient with AIS thrombi were collected after thrombectomy at AZ Groeninge Hospital. An overview of the patient characteristics and the composition of their thrombi is shown in Table 1. There were

Table 1. Clinical Characteristics of the Study Population and Histological Quantification of the Thrombus Cohort

	Negative control (n=22)	r-tPA (n=20)	r-tPA+DNase 1 (n=21)	r-tPA+diNAC (n=17)	*P* value
Patient characteristics, n (%)					
Age, y; mean (±SD)	73.8 (±11.1)	74.9 (±13.8)	70.5 (±14.3)	70.3 (±11.0)	0.3883
Sex, women	11 (50)	9 (45)	14 (66.7)	7 (41.2)	0.5023
Prior r-tPA treatment	15 (68.2)	15 (75)	12 (57.1)	13 (76.5)[1]	0.5408
Smoking	3 (15)[2]	1 (5.9)[4]	0 (0)[9]	3 (18.8)[1]	0.3095
Arterial hypertension	10 (45.5)	10 (50)	10 (52.6)[2]	9 (56.3)[1]	0.9604
Atrial fibrillation	6 (27.3)	3 (15.8)[1]	10 (52.6)[2]	5 (31.3)[1]	0.1353
Diabetes	4 (19.1)[1]	6 (31.6)[1]	2 (11.1)[3]	2 (12.5)[1]	0. 3719
Prior stroke/TIA	1 (4.7)[1]	3 (15.8)[1]	3 (20)[6]	2 (12.5)[1]	0.5556
Clinical outcome, median (IQR)					
NIHSS	18 (16 to 22)	22 (18 to 22.8)	18 (14 to 22)[2]	19 (10.0 to 25.5)	0.5492
NIHSS 24 h	15 (8 to 17)[4]	11 (5.5 to 20)[3]	10 (4 to 23)[14]	9.0 (1.5 to 21.5)[4]	0.9999
NIHSS difference	6 (1 to 9.8)[4]	8 (1–11.5)[3]	9 (−9 to 12)[14]	7.0 (1.5 to 11.0)[4]	0.9448
Etiology, n (%)					0.2323
Cardio embolic	13 (76.5)[5]	12 (60)	7 (58.3)[9]	7 (50)[2]	
LAA	3 (17.6)[5]	1 (5)	0 (0)[9]	2 (14.3)[2]	
Cryptogenic	1 (5.9)[5]	6 (30)	5 (41.7)[9]	5 (35.7)[2]	
Other	0 (0)[5]	0 (0)	0(0)[9]	1(7.1)[2]	
Thrombus location, n (%)					0.5213
MCA	7 (41.2)[5]	10 (58.8)[3]	13 (68.4)[2]	12 (70.6)	
Multi occlusion	7 (41.2)[5]	4 (23.5)[3]	4 (21.1)[2]	2 (11.8)	
Other	3 (17.6)[5]	3 (17.6)[3]	2 (10.5)[2]	3 (17.6)	
Thrombus composition, mean (±SD)					
RBC	45.1 (±19.5)	42.0 (±23.7)	38.4 (±18.7)	38.4 (±17.6)	0.5438
Fibrin	25.6 (±14.5)	21.1 (±11.9)	25.7 (±13.7)	27.3 (±13.4)	0.4765
Platelets	32.2 (±15.1)	41.6 (±24.7)	39.4 (±19.3)	26.9 (±12.2)	0.1952
VWF	42.1 (±15.2)	50.3 (±19.6)	44.9 (±17.4)	46.4 (±9.1)	0.4215
CD45	20.0 (±19.5)	15.0 (±11.0)	24.0 (±14.9)	11.6 (±7.8)	0.0387*
Total DNA	6.2 (±4.5)	5.4 (±3.8)	9.7 (±9.2)	7.3 (±4.4)	0.3668
nDNA	1.4 (±1.0)	1.8 (±1.4)	2.3 (±2.9)	1.6 (±1.6)	0.7327
exDNA	4.8 (±4.2)	3.6 (±2.9)	7.6 (±7.3)	5.5 (±4.0)	0.2861

Data are expressed as the absolute n (%), mean±SD for normally distributed variables, and median with interquartile range (IQR) for non-normally distributed variables. χ^2 test was used to evaluate the association between patient characteristics over different treatment groups. Differences between multiple groups were tested using a 1-way ANOVA test (normal distribution) or a Kruskal-Wallis test (not normal distribution) with Dunn multiple comparison correction. Two-tailed $P \leq 0.05$ were regarded as significant. Number of missing values indicated by superscript numbers. CD45 indicates cluster of differentiation 45; diNAC, N,N′-diacetyl-l-cystine; exDNA, extracellular DNA; LAA, large-artery atherosclerotic; MCA, middle cerebral artery; nDNA, nuclear DNA; and NIHSS, National Institutes of Health Stroke Scale; RBC, red blood cells; r-tPA, recombinant tissue-type plasminogen activator; TIA, transient ischemic attack; and VWF, von Willebrand Factor. Other including: Posterior cerebral artery, Basilar artery, T-segment of the internal carotid artery, anterior cerebral artery.

*$P \leq 0.05$.

Downloaded from http://ahajournals.org by on March 26, 2024

ORIGINAL CONTRIBUTION

no significant differences in patient characteristics and thrombus compositions across the different experimental groups except from the CD45+ signal (Table 1). To assess ex vivo thrombolysis, fresh thrombi were incubated in NHP for 180 minutes at 37 °C and their weight was measured in function of time. As negative control, we incubated a series of thrombi (n=22) without any thrombolytic agent. In these negative control experiments, minimal spontaneous thrombus degradation was observed (RW_{30}=87.9%±10.2%, RW_{60}=81.6%±13.6%, RW_{180}=72.2%±24.4%; Figure 1A). To confirm that no endogenous fibrinolysis occurs in these experiments, D-dimers were measured in a subset of samples (Figure S1). No increase in D-dimers could be detected in these negative controls, suggesting that mechanical degradation is most likely the cause of the small weight loss observed in the absence of a thrombolytic agent.

Next, we tested the efficacy of r-tPA (1 µg/mL) to degrade patient thrombi (n=20). As shown in Figure 1A, the use of r-tPA led to significant overall thrombus lysis, resulting in residual thrombus weights of RW_{30}=79.2%±17.1%, RW_{60}=64.6%±22.9%, and RW_{180}=44.0%±28.1%. Compared with the negative control group, these values are significantly lower, indicating a specific fibrinolytic effect of r-tPA (p_{RW30}=0.0494, p_{RW60}=0.005, and p_{RW180}=0.007). The specific fibrinolytic activity of r-tPA was further confirmed by a significant elevation of D-dimers in the supernatant of samples in which r-tPA was used as thrombolytic agent (*P*=0.0074; Figure S1).

When subjecting patient thrombi to r-tPA-mediated lysis, a striking variability in the degree of lysis was observed between different thrombi. Indeed, as shown in Figure 1B, r-tPA-mediated lysis ranged from complete lysis (RW_{180}=0.0%) to almost no degradation (RW_{180}=87.4%). To test our hypothesis that the extent of r-tPA-mediated lysis could be associated with thrombus composition, we correlated the degree of r-tPA-mediated lysis with various thrombus components quantified through histology. An overview of these correlations is given in Figure 2. Interestingly, a highly significant positive correlation was observed between lysis efficacy and the RBC content of the thrombi. Furthermore, a significant negative correlation was present between r-tPA efficacy and the VWF content at all-time points, as well as with the nDNA content at RW_{30} and RW_{60} and the extracellular DNA content at RW_{60}.

To better illustrate the composition-specific effect of r-tPA on thrombolysis, we chose the median RBC content of all thrombi as a cutoff to label each thrombus as either RBC-high or RBC-low depending on whether its RBC content was respectively higher or lower than the median RBC content (which was 41.6%). An overview of these 2 subcategories, including their mean compositions is shown in Figure 3A and Table 2. Besides a higher number of RBCs (*P*<0.0001), RBC-high thrombi contained significantly less platelets, fibrin, VWF, extracellular DNA, and nDNA compared with RBC-low thrombi (*P*<0.0001, *P*<0.0001, *P*=0.0032, *P*=0.0109, *P*=0.0004, respectively). When comparing the 2 groups in terms of r-tPA-mediated thrombus degradation, it is clear that RBC-high thrombi are particularly susceptible to r-tPA-mediated lysis with an RW_{30}=69.2%±16.3, RW_{60}=51.8%±22.0%, and RW_{180}=27.9%±19.9%, which are all significantly lower than the respective negative controls (*P*=0.0165, *P*=0.0043, *P*=0.0004). In contrast, r-tPA is not able to degrade RBC-low thrombi (RW_{30}=89.1%±11.2%, RW_{60}=77.3%±16.1%, RW_{180}=60.2%±26.4%), all of which were not significantly different from the negatives controls (*P*=0.9989, *P*=0.528, *P*=0.6308, respectively). Taken together, these results show that the success of

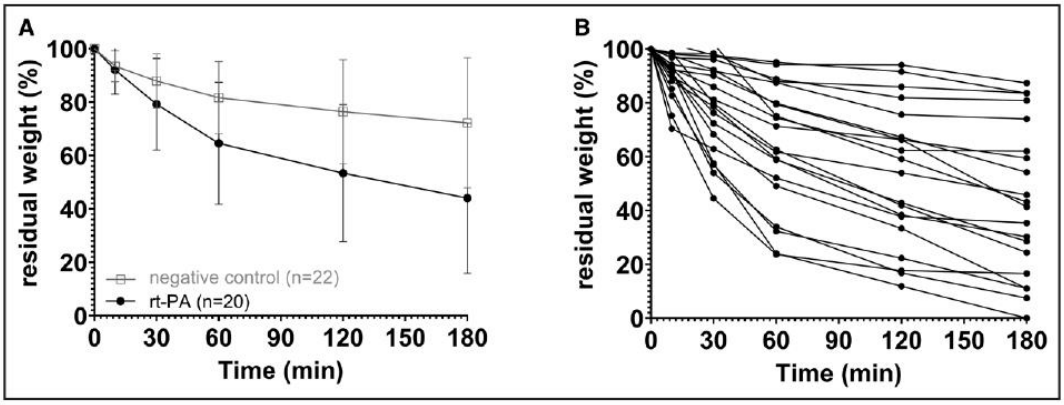

Figure 1. Thrombolysis of ischemic stroke thrombi.
A, Ex vivo lysis of acute ischemic stroke thrombi (n=20–22). One part of each thrombus was incubated for 180 min at 37 °C in the presence of either r-tPA (recombinant tissue-type plasminogen activator) or no thrombolytic agent (negative control). Residual thrombus weight (percentage of initial weight) was measured at time points 0, 10, 30, 60, 120, and 180 min. Data are represented as mean with SD (**B**) Individual r-tPA mediated thrombolysis curves of acute ischemic stroke thrombi. Each curve represents the lysis of the thrombus from a different patient.

Downloaded from http://ahajournals.org by on March 26, 2024

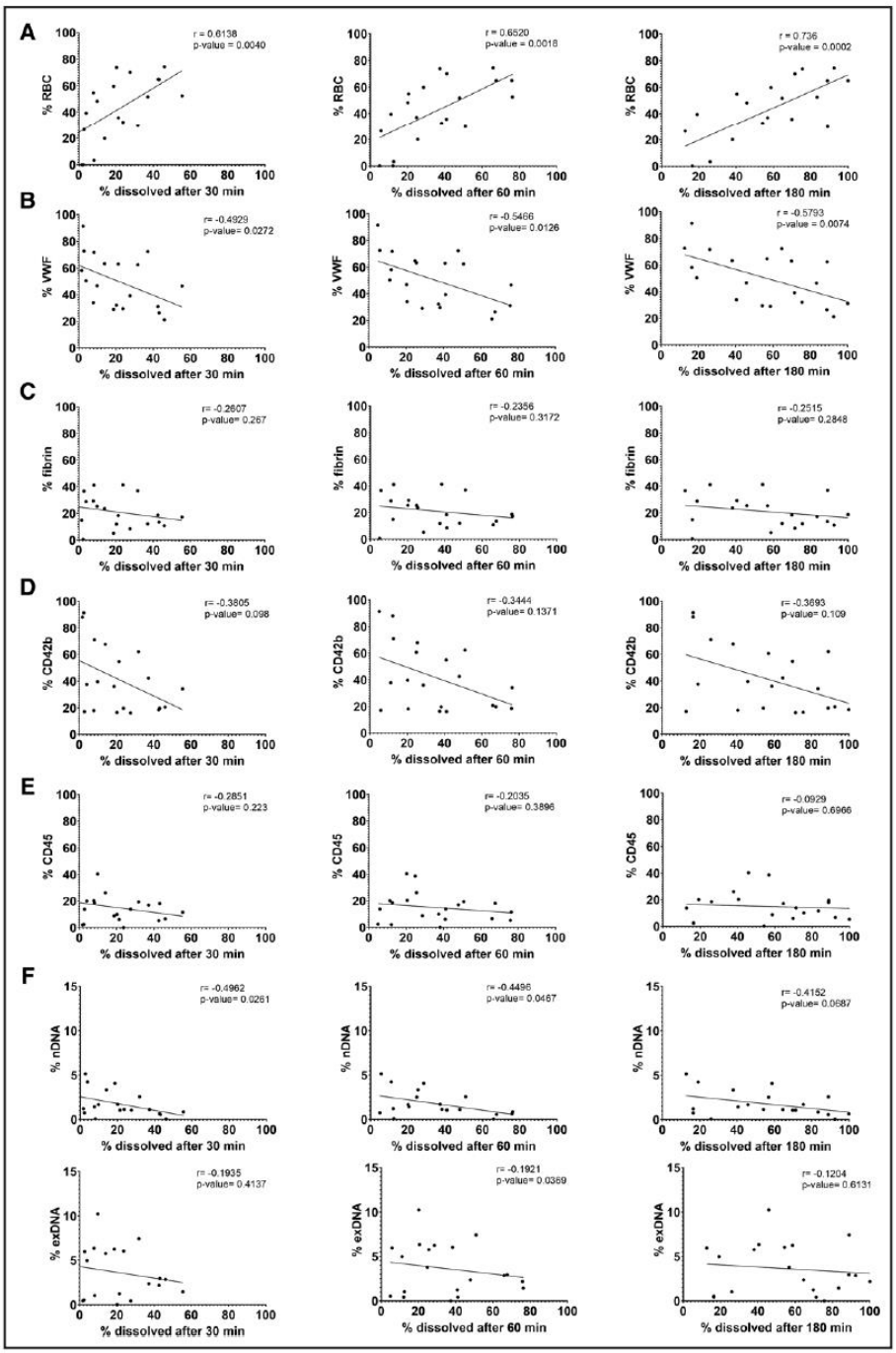

Figure 2. Correlation of thrombus composition and lysis rate.
Correlation between (**A**) red blood cell (RBC) and (**B**) von Willebrand Factor (VWF), (**C**) fibrin, (**D**) CD42b (platelets), (**E**) CD45 (leukocytes), (**F**) DNA (nDNA [nuclear DNA] and exDNA [extracellular DNA]) content of the thrombus and the residual thrombus weight at 30, 60, and 180 min after r-tPA (recombinant tissue-type plasminogen activator)-mediated thrombolysis.

r-tPA depends on the thrombus composition. Thrombi high in RBCs and low in other components such as platelets, VWF and DNA are susceptible to r-tPA mediated thrombolysis. Thrombi low in RBCs but high in other components such as platelets, VWF and DNA are r-tPA resistant.

Downloaded from http://ahajournals.org by on March 26, 2024

ORIGINAL CONTRIBUTION

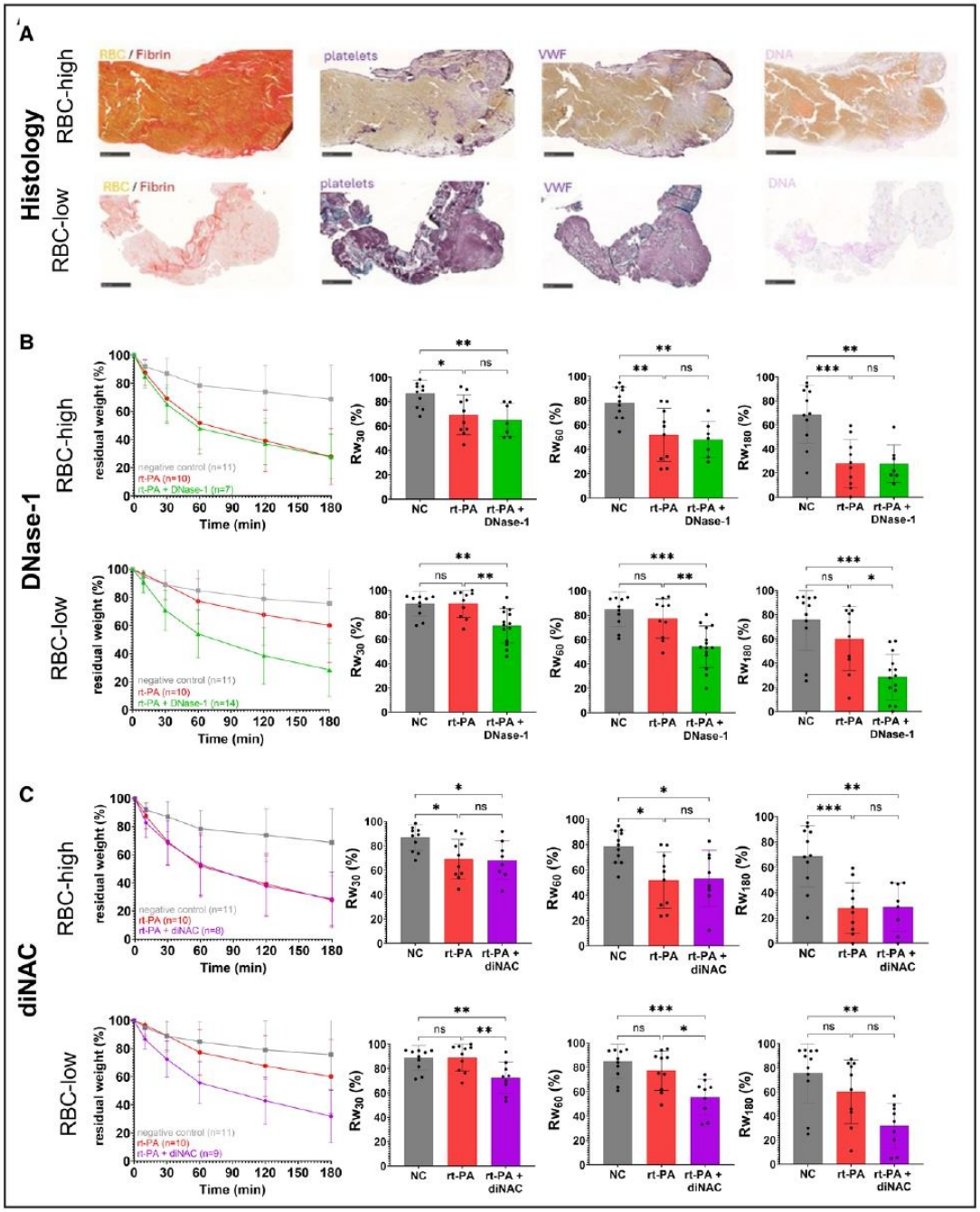

Figure 3. Thrombolysis of red blood cell (RBC)-low and RBC-high ischemic stroke thrombi.
A, Representative images of RBC-high and RBC-low thrombi. Sections were stained with Martius Scarlet Blue to identify RBCs (yellow) and fibrin (dark pink/red). Immunohistochemical stainings were used to identify platelets (CD42b; purple) and von Willebrand Factor ([VWF]; purple). A Feulgen's reaction was used to visualize both intracellular and extracellular DNA. Scale=500 µm (**B**) Ex vivo lysis of human stroke thrombi using r-tPA (recombinant tissue-type plasminogen activator) in combination DNase-1. Thrombi were categorized as RBC high or as RBC low depending on whether their RBC content was higher or lower than 41.6%, respectively (median RBC content of all thrombi). (**C**) Ex vivo lysis of human stroke thrombi using r-tPA in combination with the VWF-reducing agent diNAC. Thrombi were categorized as RBC-high or as RBC-low as described above. Differences between multiple groups at different time points were tested using a 1-way ANOVA test or a Kruskal-Wallis test (based upon normality) with Dunn multiple comparison correction. Two-tailed *P* values ≤0.05 were regarded as significant. All data are represented as mean with SD. ns indicates not significant. **P*≤0.05, ***P*≤0.01, ****P*≤0.001.

Downloaded from http://ahajournals.org by on March 26, 2024

Table 2. Histological Quantification of RBC-High and RBC-Low Thrombi per Thrombolysis Condition

	RBC high					RBC low				
	Negative control (n=11)	r-tPA (n=10)	r-tPA+DNase-1 (n=7)	r-tPA+diNAC (n=8)	Overall (n=36)	Negative control (n=11)	r-tPA (n=10)	r-tPA+DNase-1 (n=14)	r-tPA+ diNAC (n=9)	Overall (n=44)
RBC, mean (±SD)	61.9 (±9.6)	61.6 (±9.5)	60.7 (±11.4)	54.5 (±5.4)	59.9 (±9.3)*	28.4 (±9.4)	22.4 (±15.7)	27.2 (±8.9)	24.0 (±10.1)	25.8 (±11.0)*
Fibrin, mean (±SD)	17.4 (±9.2)	15.3 (±7.5)	16.5 (±7.5)	23.3 (±10.6)	17.9 (±8.9)*	33.8 (±14.4)	26.8 (±13.0)	30.4 (±13.9)	30.9 (±15.1)	30.5 (±13.8)*
Platelets, mean (±SD)	22.1 (±6.9)	26.2 (±10.5)	26.9 (±15.3)	20.5 (±11.3)	23.8 (±10.7)*	42.3 (±14.5)	57.0 (±25.5)	45.7 (±18.4)	32.6 (±10.3)	44.7 (±19.3)*
VWF, mean (±SD)	36.2 (±12.7)	37.9 (±14.6)	35.6 (±17.8)	40.8 (±8.8)	40.2 (±14.2)*	48.0 (±15.7)	62.7 (±15.9)	49.6 (±15.8)	51.4 (±6.3)	50.6 (±16.1)*
CD45, mean (±SD)	13.1 (±8.7)	15.2 (±10.1)	16.7 (±12.3)	10.6 (±6.7)	13.8 (±9.3)	26.8 (±24.9)	14.8 (±12.3)	27.7 (±15.1)	12.5 (±9.0)	21.4 (±17.5)
nDNA, mean (±SD)	1.1 (±0.8)	1.3 (±1.1)	0.9 (±0.7)	0.9 (±0.6)	1.1 (±0.8)*	1.7 (±1.2)	2.2 (±1.6)	3.0 (±3.4)	2.1 (±2.0)	2.3 (±2.3)*
exDNA, mean (±SD)	3.4 (±2.2)	3.5 (±3.2)	3.5 (±4.0)	5.4 .4)	3.8 (±3.5)*	6.3 (±5.1)	3.7 (±1.7)	9.7 (±7.7)	5.6 (±2.8)	6.7 (±5.7)*

Each thrombus was categorized as RBC high or RBC low based on whether its RBC content was respectively higher or lower than the median RBC content of all thrombi used in this study (41.6%). Data are expressed as mean±SD. To statistically analyze the differences in composition between the RBC-high and RBC-low groups, a *t* test or a Mann-Whitney *U* test (based upon normality) was used on the overall data of each group (last column). CD45 indicates cluster of differentiation 45; diNAC, N,N′-diacetyl-l-cystine; exDNA, extracellular DNA; nDNA, nuclear DNA; RBC, red blood cells; r-tPA, recombinant tissue-type plasminogen activator; and VWF, von Willebrand Factor.

*Two-tailed $P \leq 0.05$ were regarded as significant.

DNase-1 Promotes Thrombolysis of r-tPA Resistant Thrombi

Given the ineffectiveness of r-tPA in thrombi with low RBC content, we next investigated whether thrombolysis can be improved by targeting other components that are enriched in these r-tPA resistant thrombi. Considering that DNA is particularly enriched in r-tPA resistant, RBC-low thrombi (Table 2) and that the amount of DNA negatively correlates with r-tPA efficacy (Figure 2F), we tested the combination of r-tPA with the DNA-degrading enzyme DNase-1. A total of 21 consecutive patient thrombi were subjected to ex vivo lysis with r-tPA (1 µg/mL) in combination with DNase-1 (40 U/mL). In line with previous findings, addition of DNase-1 improved overall thrombolysis compared with r-tPA alone resulting in a RW_{30}=68.6%±13.7% RW_{60}=51.4%±15.7% and RW_{180}=28.3%±17.5% (Figure S2). Interestingly, however, classification of these thrombi into RBC-high and RBC-low groups based on the median RBC content, unveiled a striking disparity in the response to DNase-1 treatment between the 2 categories (Figure 3B). In the RBC-high group, the addition of DNase-1 did not result in any further thrombus degradation when compared with the use of r-tPA alone (RW_{30}=65.1%±13.4% versus 69.2%±16.3%, P=0.8131; RW_{60}=48.0%±14.8% versus 51.8%±22.0%, P=0.8916; RW_{180}=27.9%±19.9% versus 27.7%±15.8%, P=0.9998, respectively; Figure 3B). Conversely, use of DNase-1 in the RBC-low thrombi resulted in a substantial enhancement in thrombolysis compared with the administration of r-tPA alone (RW_{30}=70.9%±14.2% versus 89.1%±11.2%, P=0.0031; RW_{60}=54.1%±17.1% versus 77.3%±16.1%, P=0.0036; RW_{180}=28.5%±18.9% versus 60.2%±26.4%, respectively, P=0.05; Figure 3B). These data show that DNase-1 can specifically overcome r-tPA resistance in RBC-low thrombi, whereas it has no effect in RBC-rich thrombi that are r-tPA susceptible.

N,N′-Diacetyl-L-Cystine Promotes Thrombolysis of r-tPA Resistant Thrombi

Similar to DNA, VWF is particularly abundant in RBC-low thrombi and its amount is inversely correlated with the efficacy of r-tPA (Figure 2B). Therefore, we also explored whether targeting VWF could enhance r-tPA-mediated thrombus degradation, especially in RBC-low (r-tPA resistant) thrombi. To this end, 17 thrombi were subjected to ex vivo lysis using 1 µg/mL r-tPA in combination with the VWF-reducing agent diNAC (2 mmol/L). Interestingly, combination of r-tPA with diNAC showed similar results as the combination of r-tPA with DNase-1, leading to an overall improved thrombus degradation (RW_{30}=70.5%±14.0%; RW_{60}=54.5%±18.1%; RW_{180}=30.3%±17.5%; Figure S2). As with DNase-1, the beneficial effect of combining r-tPA with diNAC was specific for the r-tPA-resistant RBC-low thrombi, in which the combination led to a significantly better thrombus degradation than r-tPA alone at early time points (RW_{30}=72.4%±12.8%, P=0.0095; RW_{60}=55.7%±14.8%, P=0.0109; RW_{180}=31.9%±18.7%, P=0.1830; Figure 3C). In RBC-high thrombi, which are r-tPA susceptible, no beneficial effect of adding diNAC to r-tPA was observed

Downloaded from http://ahajournals.org by on March 26, 2024

compared with using r-tPA alone (RW_{30}=68.3%±15.8%, P=0.9899; RW_{60}=53.2%±22.3%, P=0.8803; RW_{180}=28.6%±19.2%; P=0.9973; Figure 3C). These findings demonstrate a composition-specific advantage of targeting VWF in patient thrombi characterized by low RBC content (high-VWF content), which are r-tPA resistant.

DISCUSSION

Thrombolysis is a crucial aspect of AIS treatment. Almost 30 years ago, the introduction of r-tPA marked a significant advancement in stroke treatment. As its introduction, r-tPA-mediated fibrinolysis has remained the only available thrombolytic strategy. However, it has become evident that, despite the advantages of r-tPA, its effective application is limited, particularly due to the low recanalization rates in patients undergoing r-tPA treatment. Consequently, there is a critical need for novel insights and alternative thrombolytic approaches to further advance pharmacological treatment of AIS. In this study, we exploited the accessibility of patient-derived thrombi obtained through thrombectomy, to assess the effectiveness of their dissolution using r-tPA. As one of the main findings, we found that the efficacy with which r-tPA can degrade stroke thrombi is highly dependent on the thrombus composition. Thrombi that contain high amounts of RBCs contain low amounts of VWF, platelets and DNA and are particularly susceptible to r-tPA-mediated lysis. Thrombi containing low amounts of RBCs contain high amounts of VWF, platelets, and DNA and are r-tPA resistant. Mechanistically, these findings fit with our earlier description of the internal architecture of AIS thrombi, where we showed that RBC-rich thrombi have a relatively uncomplicated structure comprising RBCs entangled in a scaffold of relatively thin fibrin strands.[4] In contrast, RBC-poor thrombi were shown to be platelet-rich, having a more complex structure that includes, beside dense fibrin, additional scaffolds of nonfibrin components, such as extracellular DNA and VWF.[4] Most likely, degradation of fibrin through r-tPA-generated plasmin is therefore sufficient to degrade RBC-rich thrombi, whereas fibrinolysis alone is not sufficient to break down more complex RBC-poor thrombi. This study shows for the first time a composition-dependent effect of r-tPA-mediated thrombolysis on AIS thrombi and is in line with clinical observations that early recanalization after intravenous r-tPA has been associated with higher arterial density measured in Hounsfield units on computed tomography scans, a radiological feature that is known to indicate RBC-rich thrombi.[8–12]

The reasons why r-tPA is not always successful in patients remain poorly understood, but our study points toward an important role of the composition of the target occlusion. Our study reveals that r-tPA resistant thrombi exhibit a distinctive composition characterized by low amounts of RBCs and elevated amounts of other nonfibrin components such as VWF and DNA, making the latter attractive targets to enhance thrombolytic therapy.

We and others previously showed the beneficial effect of Dnase-1 on thrombolysis, but its specific effectivity on thrombi with different compositions was not yet known.[13–15] The current study shows that the combined use of r-tPA and Dnase-1 is especially helpful for the lysis RBC-low thrombi, whereas it does not provide an additional benefit for RBC-high thrombi, which are susceptible to fibrinolysis. DNA networks likely impede r-tPA-mediated thrombus lysis because they form a structural nonfibrin scaffold that is resistant to fibrinolysis. Under conditions of shear stress, DNA was shown to be able to directly interact with VWF, which could further enhance the stability of the thrombus, an effect that could be particularly relevant in RBC-low thrombi that contain higher amounts of DNA and VWF.[16] DNA can also alter the structure and thickness of fibrin itself, enhancing the mechanical stability of fibrin and increasing the thrombus stiffness.[15,17,18] In addition, DNA and DNA components were shown to reduce plasminogen activation and plasmin activity, further impeding fibrinolysis.[19] Desilles et al[20] indeed showed that Dnase-1 alongside r-tPA produces a synergistic effect on fibrinolysis itself by effectively mitigating the adverse effects of DNA on plasmin activity.

Besides DNA, VWF also is a structural component that is specifically enriched in platelet-rich AIS thrombi.[4] Together with fibrinogen, VWF acts as a molecular bridge, maintaining platelet-platelet interactions in the thrombus. Furthermore, crosslinking of VWF to fibrin could further contribute to thrombus stabilization and potentially impair fibrinolysis.[21] As a result, VWF has emerged as a novel target to improve thrombolysis, for example, using the VWF-cleaving enzyme ADAMTS13 (a disintegrin-like metalloproteinase with thrombospondin motif type 1 member 13) or the reducing agent NAC.[22,23] NAC, a small, cheap and safe drug that is approved for various clinical indications, has been shown to degrade VWF multimers by reducing the disulfide bonds linking VWF monomers together.[24] In a mouse model, NAC exerted a thrombolytic effect on arterial thrombi.[23] Using an in vitro stenotic coronary artery analog system, Kim et al compared the thrombolytic activity of ADAMTS13, NAC, and diNAC, the dimerized form of NAC.[25] Interestingly, while diNAC was unable to lyse red fibrinous clots, diNAC showed a strong thrombolytic activity toward platelet-rich thrombi, which was superior to NAC and ADAMTS13.[25] The low concentration of ADAMTS13 most likely explains the lack of thrombolytic activity by ADAMTS13 in their study as we indeed previously showed a dose-dependent thrombolytic effect of ADAMTS13 in a mouse stroke model.[22] The reasons for the different effects of NAC and diNAC remain unclear but might be attributed to batch-to-batch variations observed with NAC.[25] In the current study, we

Downloaded from http://ahajournals.org by on March 26, 2024

demonstrated that diNAC, similar to DNase-1, can overcome r-tPA resistance of stroke patient thrombi that are RBC low, further supporting the use of diNAC as a novel adjunct for thrombolysis for platelet-rich thrombi. The exact mechanism of the prothrombolytic effect of diNAC (alone or in combination with r-tPA) needs further study and it would be interesting to compare the efficacy and specificity of different VWF-targeting drugs on patient thrombi in the future. Given the general reducing capacity of NAC, it cannot be excluded that it affects other thrombus molecules besides VWF. Future analysis of the structure and composition of partly lysed thrombi could be insightful in this regard.

Interestingly, we tested the triple therapy combining 1 µg/mL r-tPA, 40 U/mL DNase-1 and 2 mmol/L diNAC on a smaller subset of thrombi (n=8), but no further improvement of thrombolysis was observed in comparison to the combination of r-tPA with either DNase-1 or diNAC (Figure S2). This is an intriguing observation that needs further study. As already discussed, it is plausible that r-tPA, DNase-1, and diNAC do not strictly act on fibrin, DNA, and VWF, respectively, as has been shown for DNase-1, which also increases fibrinolysis.[20] Potentially, combined use of lower concentrations of the 3 drugs could help to better elucidate potential synergistic effects. The limited availability of fresh patient thrombi did not allow us to investigate this in the current study.

Taken together, we demonstrate for the first time a link between r-tPA resistance and the composition of thrombi retrieved from patients with AIS. Platelet-rich thrombi are r-tPA resistant, which may, at least partially, explain current recanalization failure of r-tPA in a large subset of patients. Resistance to r-tPA can be overcome by combining r-tPA with agents that target nonfibrin elements. Most importantly, a thrombolytic strategy based on degrading both fibrin and nonfibrin scaffolds could significantly expand the range of thrombi that can be successfully dissolved in patients, especially in those patients in whom r-tPA is currently ineffective. If proven safe, such a thrombolytic approach could be used regardless of thrombus composition. The exact thrombus composition of the admitted patient with stroke indeed is difficult to predict, although computed tomography and magnetic resonance imaging can reveal RBC-rich thrombi through the presence of a hyperdense artery sign or blooming artefact respectively.[9–11,26]

By using fresh stroke thrombi retrieved from patients, the best possible and most clinically relevant source of thrombus material was used. However, their use also comes with limitations that need to be acknowledged. Only those thrombi that could be successfully retrieved and that were large enough to split into 2 parts could be used. Some patients received r-tPA before thrombectomy, which could influence our results. However, the composition did not differ between thrombi from patients that did or did not receive prior r-tPA (data not shown), indicating that the effect of prior r-tPA on our results was minimal. Due to the ex vivo set-up of our experiments, we were not able to assess potential in vivo side effects of combining r-tPA with DNase or diNAC. Future research, in in vivo settings is needed to address the safety profile, especially in terms of bleeding risk. Currently, the clinical variant of DNase-1, known as Dornase alfa (Pulmozyme), has entered 2 Phase 2 trials (EXTEND-IA DNase, NCT05203224 and NETS-target, NCT04785066) with the objective of assessing its effectiveness in patients with AIS. Similarly, clinical results form a Phase 2 trial using intravenous NAC in patients with stroke need to be awaited (NAC-S, NCT04920448).

ARTICLE INFORMATION

Received November 29, 2023; final revision received January 29, 2024; accepted February 15, 2024.

Presented in part at the International Society on Thrombosis and Haemostasis Congress, Montréal, Canada, June 24–28, 2023, and the European Congress on Thrombosis and Haemostasis, Valencia, Spain, September 13–15, 2023.

Affiliations

Laboratory for Thrombosis Research, KU Leuven Kulak, Kortrijk, Belgium (S.V., L.D., S.S., C.T., K.V., S.F.D.M.). Departments of Medical Imaging (O.F., F.V.G., T.A.) and Neurology (A.V., P.V.), AZ Groeninge, Kortrijk, Belgium. Department of Neurology, University Hospitals Antwerp, Belgium (P.V.). Department of Translational Neuroscience, University of Antwerp, Belgium (P.V.). Department of Neuroradiology, Karolinska University Hospital, and Clinical Neuroscience Karolinska Institutet, Stockholm, Sweden (T.A.).

Acknowledgments

The authors would like to thank the stroke team at AZ Groeninge Hospital (Kortrijk, Belgium) for their support and collaboration in this research. S. Vandelanotte and Dr De Meyer designed the study. S. Vandelanotte performed the experiments. Drs François, Staessens, Vanhoorne, Van Gool, Vanacker, Andersson and L. Desender contributed to data acquisition. S. Vandelanotte analyzed data. S. Vandelanotte, Drs De Meyer, Tersteeg, and Vanhoorelbeke interpreted the results. S. Vandelanotte and Dr De Meyer wrote the article. All authors critically reviewed the article.

Sources of Funding

This work was supported by Fonds voor Wetenschappelijk Onderzoek – Vlaanderen (research grants G.0A86.13, G.0785.17, and 1509216N to Dr De Meyer), by research grants from KU Leuven (OT/14/099 and ISP/14/02L2 to Dr De Meyer), and by a research grant from the Queen Elisabeth Medical Foundation (to Dr De Meyer).

Disclosures

Dr François is a consultant for iVascular. Dr Vanacker received speaker fees from Boehringer-Ingelheim, BMS, Pfizer, Daiichi-Sankyo, and Medtronic. Dr Andersson holds equity for Cereflo Ltd and is a consultant for Anaconda, Cerenovus/Neuravi, Optimize Neurovascular and Rapid medical. The other authors report no conflicts.

Supplemental Material

Supplemental Methods
Table S1
Figures S1–S2

REFERENCES

1. Pan Y, Shi G. Silver jubilee of stroke thrombolysis with alteplase: evolution of the therapeutic window. *Front Neurol.* 2021;12:1–13. doi: 10.3389/fneur.2021.593887
2. Berkhemer OA, Fransen PSS, Beumer D, van den Berg LA, Lingsma HF, Yoo AJ, Schonewille WJ, Vos JA, Nederkoorn PJ, Wermer MJH, et al; MR CLEAN Investigators. A randomized trial of intraarterial

Downloaded from http://ahajournals.org by on March 26, 2024

treatment for acute ischemic stroke. *N Engl J Med*. 2015;372:11–20. doi: 10.1056/NEJMoa1411587
3. Rha JH, Saver JL. The impact of recanalization on ischemic stroke outcome: a meta-analysis. *Stroke*. 2007;38:967–973. doi: 10.1161/01.STR.0000258112.14918.24
4. Staessens S, Denorme F, François O, Desender L, Dewaele T, Vanacker P, Deckmyn H, Vanhoorelbeke K, Andersson T, De Meyer SF. Structural analysis of ischemic stroke thrombi: histological indications for therapy resistance. *Haematologica*. 2020;105:498–507. doi: 10.3324/haematol.2019.219881
5. Di Meglio L, Desilles JP, Ollivier V, Nomenjanahary MS, Di Meglio S, Deschildre C, Loyau S, Olivot JM, Blanc R, Piotin M, et al. Acute ischemic stroke thrombi have an outer shell that impairs fibrinolysis. *Neurology*. 2019;93:e1686–e1698. doi: 10.1212/WNL.0000000000008395
6. Staessens S, De Meyer SF. Thrombus heterogeneity in ischemic stroke. *Platelets*. 2020;32:331–339. doi: 10.1080/09537104.2020.1748586
7. Staessens S, Fitzgerald S, Andersson T, Clarençon F, Denorme F, Gounis MJ, Hacke W, Liebeskind DS, Szikora I, van Es ACGM, et al. Histological stroke clot analysis after thrombectomy: technical aspects and recommendations. *Int J Stroke*. 2020;15:467–476. doi: 10.1177/1747493019884527
8. Ye G, Cao R, Lu J, Qi P, Hu S, Chen K, Tan T, Chen J, Wang D. Histological composition behind CT-based thrombus density and perviousness in acute ischemic stroke. *Clin Neurol Neurosurg*. 2021;207:106804. doi: 10.1016/j.clineuro.2021.106804
9. Puig J, Pedraza S, Demchuk A, Daunis-i-Estadella J, Termes H, Blasco G, Soria G, Boada I, Remollo S, Baños J, et al. Quantification of thrombus Hounsfield units on noncontrast CT predicts stroke subtype and early recanalization after intravenous recombinant tissue plasminogen activator. *Am. J Neuroradiol*. 2012;33:90–96. doi: 10.3174/ajnr.A2878
10. Liebeskind DS, Sanossian N, Yong WH, Starkman S, Tsang MP, Moya AL, Zheng DD, Abolian AM, Kim D, Ali LK, et al. CT and MRI early vessel signs reflect clot composition in acute stroke. *Stroke*. 2011;42:1237–1243. doi: 10.1161/STROKEAHA.110.605576
11. Simons N, Mitchell P, Dowling R, Gonzales M, Yan B. Thrombus composition in acute ischemic stroke: a histopathological study of thrombus extracted by endovascular retrieval. *J Neuroradiol*. 2015;42:86–92. doi: 10.1016/j.neurad.2014.01.124
12. Choi MH, Park GH, Lee JS, Lee SE, Lee SJ, Kim JH, Hong JM. Erythrocyte fraction within retrieved thrombi contributes to thrombolytic response in acute ischemic stroke. *Stroke*. 2018;49:652–659. doi: 10.1161/STROKEAHA.117.019138
13. Ducroux C, Meglio LD, Loyau S, Delbosc S, Boisseau W, Deschildre C, Maacha MB, Blanc R, Redjem H, Ciccio G, et al. Thrombus neutrophil extracellular traps content impair tPA-induced thrombolysis in acute ischemic stroke. *Stroke*. 2018;49:754–757. doi: 10.1161/STROKEAHA.117.019896
14. Laridan E, Denorme F, Desender L, François O, Andersson T, Deckmyn H, Vanhoorelbeke K, De Meyer SF. Neutrophil extracellular traps in ischemic stroke thrombi. *Ann Neurol*. 2017;82:223–232. doi: 10.1002/ana.24993
15. Peña-Martínez C, Durán-Laforet V, García-Culebras A, Ostos F, Hernández-Jiménez M. Pharmacological modulation of neutrophil extracellular traps reverses thrombotic stroke tPA (tissue-type plasminogen activator) resistance. *Stroke*. 2019;50:3228–3237. doi: 10.1161/STROKEAHA.119.026848
16. Grässle S, Huck V, Pappelbaum KI, Gorzelanny C, Aponte-Santamaría C, Baldauf C, Gräter F, Schneppenheim R, Obser T, Schneider SW. Von willebrand factor directly interacts with DNA from neutrophil extracellular traps. *Arterioscler Thromb Vasc Biol*. 2014;34:1382–1389. doi: 10.1161/ATVBAHA.113.303016
17. Varjú I, Longstaff C, Szabó L, Farkas AZ, Varga-Szabó VJ, Tanka-Salamon A, Machovich R, Kolev K. DNA, histones and neutrophil extracellular traps exert anti-fibrinolytic effects in a plasma environment. *Thromb Haemost*. 2015;113:1289–1298. doi: 10.1160/TH14-08-0669
18. Longstaff C, Varjú I, Sótonyi P, Szabó L, Krumrey M, Hoell A, Bóta A, Varga Z, Komorowicz E, Kolev K. Mechanical stability and fibrinolytic resistance of clots containing fibrin, DNA, and histones. *J Biol Chem*. 2013;288:6946–6956. doi: 10.1074/jbc.M112.404301
19. Cruz DB, Helms J, Aquino LR, Stiel L, Cougourdan L, Broussard C, Chafey P, Riès-Kautt M, Meziani F, Toti F, et al. DNA-bound elastase of neutrophil extracellular traps degrades plasminogen, reduces plasmin formation, and decreases fibrinolysis: proof of concept in septic shock plasma. *FASEB J*. 2019;33:14270–14280. doi: 10.1096/fj.201901363RRR
20. Desilles JP, Solo Nomenjanahary M, Consoli A, Ollivier V, Faille D, Bourrienne MC, Hamdani M, Dupont S, Di Meglio L, Escalard S, et al; CompoCLOT Study Group. Impact of COVID-19 on thrombus composition and response to thrombolysis: Insights from a monocentric cohort population of COVID-19 patients with acute ischemic stroke. *J Thromb Haemost*. 2022;20:919–928. doi: 10.1111/jth.15646
21. Hada M, Kaminski M, Bockenstedt P, McDonagh J. Covalent cross-linking of von Willebrand factor to fibrin. *Blood*. 1986;68:95–101. doi: 10.1182/blood.v68.1.95.95
22. Denorme F, Langhauser F, Desender L, Vandenbulcke A, Rottensteiner H, Plaimauer B, François O, Andersson T, Deckmyn H, Scheiflinger F, et al. ADAMTS13-mediated thrombolysis of t-PA-resistant occlusions in ischemic stroke in mice. *Blood*. 2016;127:2337–2345. doi: 10.1182/blood-2015-08-662650
23. De Lizarrondo SM, Gakuba C, Herbig BA, Repessé Y, Ali C, Denis CV, Lenting PJ, Touzé E, Diamond SL, Vivien D, et al. Potent thrombolytic effect of N-acetylcysteine on arterial thrombi. *Circulation*. 2017;136:646–660. doi: 10.1161/CIRCULATIONAHA.117.027290
24. Chen J, Reheman A, Gushiken FC, Nolasco L, Fu X, Moake JL, Ni H, López JA. N-acetylcysteine reduces the size and activity of von Willebrand factor in human plasma and mice. *J Clin Invest*. 2011;121:593–603. doi: 10.1172/JCI41062
25. Kim D, Shea SM, Ku DN. Lysis of arterial thrombi by perfusion of N,N'-Diacetyl-L-cystine (DiNAC). *PLoS One*. 2021;16:e0247496–e0247416. doi: 10.1371/journal.pone.0247496
26. Brinjikji W, Duffy S, Burrows A, Hacke W, Liebeskind D, Majoie CBLM, Dippel DWJ, Siddiqui AH, Khatri P, Baxter B, et al. Correlation of imaging and histopathology of thrombi in acute ischemic stroke with etiology and outcome: a systematic review. *J. Neurointerv. Surg*. 2017;9:529–534. doi: 10.1136/neurintsurg-2016-012391

Downloaded from http://ahajournals.org by on March 26, 2024

SUPPLEMENTAL MATERIAL

RT-PA RESISTANCE IS SPECIFIC FOR PLATELET-RICH STROKE THROMBI AND CAN BE OVERCOME BY TARGETING NON-FIBRIN COMPONENTS

Sarah Vandelanotte, MSc [1], Olivier François, MD[2], Linda Desender, BSc[1], Senna Staessens, PhD[1], Alexander Vanhoorne, MD[3], Fréderick Van Gool, MD[2], Claudia Tersteeg, PhD[1], Karen Vanhoorelbeke, PhD[1], Peter Vanacker, MD[3,4,5], Tommy Andersson, MD[2,6] and Simon F. De Meyer, PhD[1]

SUPPLEMENTAL METHODS

Patient data collection and thrombus processing

Clinical patient data were collected from medical records including demographic features, cardiovascular risk factors, National Institute of Health Stroke Scale (NIHSS) score on admission and at discharge, use of intravenous thrombolysis, occluded target vessel and functional outcome (modified Ranking score (mRS)). Thrombi were retrieved using a stent-retriever or contact aspiration dependent on the preference of the treating physician. After retrieval, the thrombus was delicately detached from the thrombectomy device and stored in saline at 4°C for maximum of 48 hours before starting the experiment.

Histological analysis

Histological analysis was performed on the portion of the thrombus that was not utilized for thrombolysis. Samples were incubated in 4% paraformaldehyde for 24 hours at 4°C and embedded in paraffin blocks. Per thrombus, one 5 µm-thick section, exposing a large cross-sectional area of the entire thrombus, was selected for every staining. We have previously demonstrated that staining one section with a large cross-sectional area is representative for the entire sample.[7] Histological staining procedures were performed as described previously.[4] In brief, thrombus sections were stained with a Martius Scarlet Blue (Crystal Ponceau 6R: sc-214779, Santa Cruz, Dallas, USA; Naphtol Yellow S: sc-215544, Santa Cruz, Dallas, USA; Methyl blue: M6900-50G, Sigma, St. Louis, MO, USA) to identify RBCs (yellow), fibrin (dark pink/red) and collagen (blue), a hematoxylin and eosin staining (H&E, HT110216, Sigma-Aldrich, St. Louis, MO, USA) and a Feulgen's reaction staining (1079070001, Merck Chemicals, MA, USA) to identify DNA (pink). Immunohistochemical (IHC) stainings were performed to examine the presence of platelets (GPIbα, MA5-11642, Invitrogen, Waltham, MA, USA), VWF (A008202-2, Agilent Technologies, Santa Clara, CA, USA) and leukocytes (CD45, 304002, Biolegend, San Diego, CA). In the IHC stainings, nuclei were stained green using a Methyl Green solution (H-3402, Vector Laboratories, Peterborough, UK). Negative controls were obtained by omission of the primary antibody and were negative for all IHC procedures (data not shown).

Quantitative determination of thrombus components

Stained thrombus sections were digitized using a slide scanner (Nanozoomer SQ, Hamamatsu Photonics, Hamamatsu, Japan). Thrombus images were exported in 5X resolution using NDP view2 (Hamamatsu, Japan). Background surrounding the tissue section was removed using Adobe Photoshop CS5 (San José, CA, USA) to prevent false positive signal. Histological stainings were examined by color segmentation and planimetric analysis to calculate the relative amounts for each component using ImageJ software 1.49v (National Institutes of Health, Bethesda, MD, USA; http://imagej.nig.gov/ij/). MSB staining was used to quantify fibrin (dark pink/red) and RBCs (yellow). Quantification of platelets, VWF and CD45 was performed on immunostainings for the respective component. The Feulgen staining was used to quantify all DNA in the whole thrombus section, which appears as a pink color. The H&E staining was used to specifically select the area of all nuclei in the complete thrombus section. To specifically determine the amount of exDNA, the amount of nuclear DNA was subtracted from the total DNA in the thrombus. The quantity of each analyzed thrombus component was presented as the percentage of positive signal relative to the total area of the examined thrombus section.

Major Resources Table

Antibodies

Target antigen	Vendor or Source	Catalog #	Working concentration	Persistent ID / URL
CD42b	Invitrogen	MA5-11642	1µg/ml	https://www.thermofisher.com/antibody/product/CD42b-Antibody-clone-42C01-Monoclonal/MA5-11642
VWF	Agilent Technologies	A008202-2	2µg/ml	https://www.agilent.com/store/en_US/Prod-A008202-2/A008202-2
CD45	Biolegend	304002	1 µg/ml	https://www.biolegend.com/nl-nl/productstab/purified-anti-human-cd45-antibody-710?GroupID=BLG5926
Anti-mouse	Agilent Technologies	E041301-2	3.6 µg/ml	https://www.agilent.com/store/en_US/Prod-E041301-2/E041301-2
Anti-rabbit	Agilent Technologies	E041101-2	1.7 µg/ml	/

Other

Description	Source / Repository	Persistent ID / URL
rt-PA	Actilyse; Boehringer-Ingelheim, Ingelheim am Rhein, Germany	https://www.boehringer-ingelheim.com/products/actilyse
dornase alfa	Pulmozyme; F. Hoffmann-La Roche, Basel, Switzerland	https://www.roche.com/solutions/pharma/productid-1d67247a-0f20-4151-a339-48449bea177c
N,N'-Diacetyl-L-cystine (diNAC)	Cayman Chemical, Michigan, USA	https://www.caymanchem.com/product/17596
human D-dimer ELISA kit	EHDDIMER, Thermo Fisher Scientific, Waltham, MA, USA	https://www.thermofisher.com/elisa/product/D-Dimer-Human-ELISA-Kit/EHDDIMER
Crystal Ponceau 6R	sc-214779, Santa Cruz, Dallas, USA	https://www.scbt.com/p/crystal-ponceau-6r-2766-77-0
Naphtol Yellow S	sc-215544, Santa Cruz, Dallas, USA	https://www.scbt.com/p/naphthol-yellow-s-846-70-8
Methyl blue	M6900-50G, Sigma, St. Louis, MO, USA	https://www.sigmaaldrich.com/BE/en/product/sigma/m6900
Eosin	HT110216, Sigma-Aldrich, St. Louis, MO, USA	https://www.sigmaaldrich.com/BE/en/product/sigma/ht110216
Hematoxylin	51275, Sigma-Aldrich, St. Louis, MO, USA	https://www.sigmaaldrich.com/BE/en/product/sigma/51275
Feulgen	1079070001, Merck Chemicals, MA, USA	
Methyl green	H-3402, Vector Laboratories, Peterborough, UK	https://vectorlabs.com/products/vector-methyl-green-counterstain/

SUPPLEMENTAL FIGURES

Supplemental Figure 1:

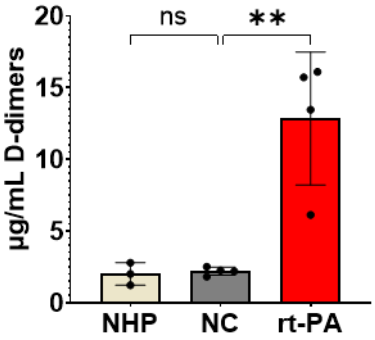

Supplemental Figure 1: D-dimer levels after thrombolysis: Measurement of D-dimer levels in supernatant after thrombolysis of 4 thrombi from negative control group and 4 thrombi from rt-PA group. Normal human plasma D-dimer levels were used as control. Differences between multiple groups was tested using a one-way ANOVA test (normal distribution) with Dunn multiple comparison correction. Two-tailed probability values ≤0.05 were regarded as significant. All data are represented as mean ± standard deviation. **p≤0.01, ns= not significant. NHP, normal human plasma; NC, negative control; rt-PA, recombinant tissue plasminogen activator.

Supplemental Figure 2:

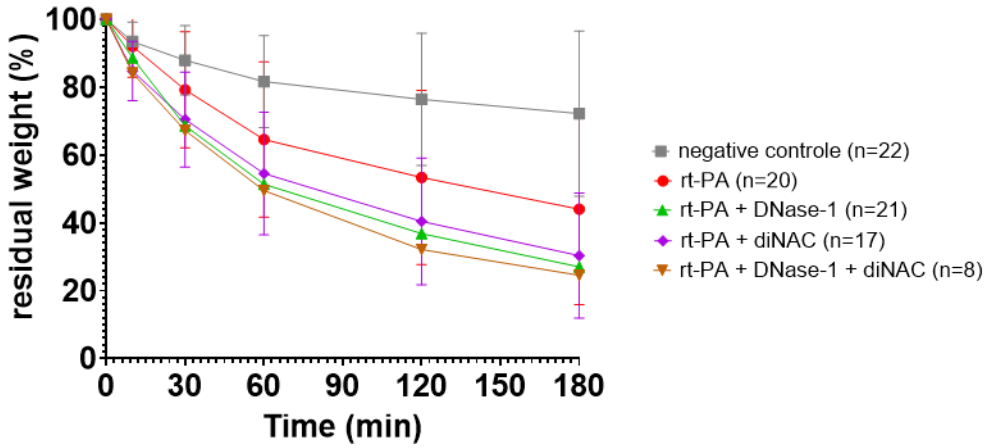

Supplemental Figure 2: Thrombolysis with thrombolytic cocktail: Ex vivo lysis of fresh human stroke thrombi retrieved from ischemic stroke patients with 1 µg/ml recombinant tissue plasminogen activator (rt-PA) in combination with DNase-1 (40 U/ml) and/or diNAC (2mM). Residual thrombus weight (percentage of initial weight) was measured at time points 0, 10, 30, 60, 120 and 180 minutes. Negative control and rt-PA curve retracted from Figure 1. All data are represented as mean ± standard deviation.

CHAPTER 6 - ASSOCIATION BETWEEN THROMBUS COMPOSITION AND FIRST PASS RECANALIZATION AFTER THROMBECTOMY IN ACUTE ISCHEMIC STROKE

Sarah Vandelanotte*[,1], Senna Staessens*[,1], Olivier François[2], Maaike De Wilde[1], Linda Desender[1], Anne-Sophie De Sloovere[2], Tom Dewaele[2], Claudia Tersteeg[1], Karen Vanhoorelbeke[1], Peter Vanacker[3,4,5], Tommy Andersson[6] and Simon F. De Meyer[1]

[1]: Laboratory for Thrombosis Research, KU Leuven Kulak, Kortrijk, Belgium
[2]: Department of Medical Imaging, AZ Groeninge, Kortrijk, Belgium
[3]: Department of Neurology, AZ Groeninge, Kortrijk, Belgium
[4]: Department of Neurology, University Hospitals Antwerp, Antwerp, Belgium
[5]: Department of Translational Neuroscience, University of Antwerp, Antwerp, Belgium
[6]: Departments of Neuroradiology, Karolinska University Hospital, and Clinical Neuroscience, Karolinska Institutet, Stockholm, Sweden

***Contributed equally**

Published article: Journal of Thrombosis and Haemostasis. 2024 Sep;22(9):2555-2561

Contribution for shared first authorship:
S. Staessens performed histological analysis of RBC, fibrin, von Willebrand factor, platelets and CD45 of thrombi. S. Vandelanotte performed histological analysis of DNA and performed data analysis.

Received: 10 April 2024 | Revised: 27 May 2024 | Accepted: 30 May 2024

https://doi.org/10.1016/j.jtha.2024.05.034

ORIGINAL ARTICLE

Association between thrombus composition and first-pass recanalization after thrombectomy in acute ischemic stroke

Sarah Vandelanotte[1] | Senna Staessens[1] | Olivier François[2] | Maaike De Wilde[1] | Linda Desender[1] | Anne-Sophie De Sloovere[2] | Tom Dewaele[2] | Claudia Tersteeg[1] | Karen Vanhoorelbeke[1] | Peter Vanacker[3,4,5] | Tommy Andersson[6,7] | Simon F. De Meyer[1]

[1]Laboratory for Thrombosis Research, KU Leuven Kulak, Kortrijk, Belgium

[2]Department of Medical Imaging, AZ Groeninge, Kortrijk, Belgium

[3]Department of Neurology, AZ Groeninge, Kortrijk, Belgium

[4]Department of Neurology, University Hospitals Antwerp, Antwerp, Belgium

[5]Department of Translational Neuroscience, University of Antwerp, Antwerp, Belgium

[6]Department of Neuroradiology, Karolinska University Hospital, Stockholm, Sweden

[7]Department of Clinical Neuroscience, Karolinska Institutet, Stockholm, Sweden

Correspondence
Simon F. De Meyer, Laboratory for Thrombosis Research, KU Leuven Kulak, E. Sabbelaan 53, 8500 Kortrijk, Belgium.
Email: simon.demeyer@kuleuven.be

Funding information
This work was supported by the Fonds voor Wetenschappelijk Onderzoek – Vlaanderen (research grants G.0A86.13, G.0785.17, and 1509216N to S.F.D.M.), by research grants from KU Leuven (OT/14/099 and ISP/14/02L2 to S.F.D.M.), and by a research grant from the Queen Elisabeth Medical Foundation (to S.F.D.M.).

Abstract

Background: Achieving first-pass recanalization (FPR) has become the primary procedural objective during thrombectomy in acute ischemic stroke patients as it correlates with the best clinical outcome. Understanding factors contributing to FPR failures is essential to enhance FPR success rates. As the central target of thrombectomy, the thrombus itself may be a significant factor influencing FPR.

Objectives: This study aimed to investigate the association between thrombus composition and FPR success rates.

Methods: In total, thrombi from 267 ischemic stroke patients were collected in the AZ Groeninge Hospital (Kortrijk, Belgium). Thrombus composition was determined via detailed histologic analysis of red blood cells (RBCs), fibrin, von Willebrand factor, platelets, leukocytes, citrullinated histone 3 (marker for neutrophil extracellular traps), and intracellular and extracellular DNA. FPR was defined as obtaining a modified thrombolysis in cerebral infarction (mTICI) score of 2c/3 after the first pass.

Results: An mTICI score of 2c/3 was obtained in 180 patients, which was achieved via a successful FPR procedure in 126 cases or after multiple passes in 54 cases. Interestingly, thrombi from FPR cases had a different composition from thrombi that needed multiple passes to obtain an mTICI score of 2c/3. FPR thrombi contained significantly more RBCs (P = .0264), less fibrin (P = .0196), and less extracellular DNA (P = .0457).

Conclusion: Our results indicate that thrombi characterized by lower RBC content, higher fibrin levels, and increased extracellular DNA are less likely to result in an FPR. These results are important to guide future research aiming at improving procedures or technologies to obtain FPR rates in RBC-poor thrombi.

Manuscript handled by: Ton Lisman

Final decision: Ton Lisman, 30 May 2024

Sarah Vandelanotte and Senna Staessens contributed equally to this study.

© 2024 The Author(s). Published by Elsevier Inc. on behalf of International Society on Thrombosis and Haemostasis. This is an open access article under the CC BY license (http://creativecommons.org/licenses/by/4.0/).

KEYWORDS
ischemic stroke, thrombectomy, thrombosis

1 | INTRODUCTION

Mechanical thrombectomy (MT) has become the primary treatment strategy for acute ischemic stroke patients with large vessel occlusion, resulting in significantly improved revascularization rates and clinical outcomes [1–5]. It has become clear that the clinical outcomes of stroke patients treated with MT are better when complete revascularization is achieved with a minimal number of passes [6]. Recently, a new metric called "first-pass recanalization" (FPR) has been introduced, which refers to the achievement of complete or near-complete recanalization (modified thrombolysis in cerebral infarction [mTICI] score 2c-3) in the first pass [7]. Several studies have consistently shown that FPR is indeed associated with improved neurologic outcomes (modified Rankin scale [mRS] score of 0-2 at 90 days) and lower mortality rates [8–17], establishing FPR as a crucial indicator of thrombectomy success. Currently, FPR is achieved in only 25% to 35% of the patients [12], illustrating the need for better insights to increase FPR rates. Various factors influencing FPR have been identified, including age, sex, occlusion site, anesthesia type, and choice of technique [18]. We and others recently showed that ischemic stroke thrombi are highly variable in structure and composition, most likely leading to different treatment responses during thrombectomy [19–21]. Indeed, ongoing research indicates that red blood cell (RBC)–rich thrombi require fewer passes to be retrieved during thrombectomy [22–24]. Additionally, increased levels of leukocytes and the presence of neutrophil extracellular traps (NETs) were shown to be linked to reduced thrombectomy success [25–31]. However, the impact of other factors such as fibrin, von Willebrand factor (VWF), platelets, and extracellular DNA (exDNA) on thrombectomy outcomes remains incompletely understood. The primary objective of this study, therefore, was to explore the relationship between specific thrombus composition and obtaining FPR. Various components were investigated, including RBCs, fibrin, VWF, platelets, leukocytes, NETs, and exDNA.

2 | METHODS

2.1 | Patient thrombi

Thrombi were collected from acute ischemic stroke patients after MT at the AZ Groeninge Hospital in Kortrijk, Belgium (from October 2014 until December 2019). A subset of this thrombus cohort has previously been used in a descriptive analysis [19]. AZ Groeninge patients or their legal representatives provided written consent under the approval of the AZ Groeninge Hospital ethical committee (AZGS2015065). The collection of patient material was performed in agreement with the principles outlined in the Declaration of Helsinki. Clinical data were collected from the Endovascular Treatment of Ischemic Stroke registry, which includes demographic features, cardiovascular risk factors, National Institute of Health Stroke Scale (NIHSS) score on admission and at discharge, use of intravenous thrombolysis, occluded target vessel, final revascularization status (mTICI), the number of passes performed, procedure time (time from groin puncture to final revascularization), and functional outcome (mRS). The most likely stroke etiology was categorized according to the international Trial of Org 10172 in Acute Stroke Treatment (TOAST) classification based upon a full diagnostic workup [32]. Thrombi were retrieved using a stent-retriever or contact aspiration device based on the preference of the treating physician. Thrombus fragments collected in multiple passes from the same patient were pooled and analyzed as 1 thrombus. FPR was defined as obtaining an mTICI score of 2c/3 after the first pass. A non-FRP (NFPR) was defined as obtaining an mTICI score of 2c/3 after multiple passes.

2.2 | Thrombus processing and histologic analysis

Thrombus processing and histologic analysis were performed as described previously [19]. Detailed description of thrombus processing, histologic stainings, and quantifications can be found in the Supplementary Methods.

2.3 | Statistical analysis

Demographic, clinical, and radiological data are summarized as median and IQR or frequencies and percentages. The quantitative data on thrombus components are represented using the median and IQR. Statistical analysis was performed using GraphPad Prism (version 9.0.1; GraphPad Software). A Shapiro–Wilk test was used to analyze normal distribution. Differences in continuous variables between FPR and NFPR were assessed using a *t*-test or Mann–Whitney U-test based on normality. A chi-squared test was used to evaluate the association between categorical patient characteristics across different groups. Two-tailed probability values $<.05$ were regarded as significant.

3 | RESULTS

In total, thrombi from 267 patients were collected during the study period. In this cohort, near-complete/complete recanalization (mTICI score, 2c/3) was obtained in 180 of the 267 patients. FPR was achieved in 126 of the 267 patients, whereas in 54 of the 267 patients,

multiple passes were needed to achieve near-complete/complete recanalization. In 84 patients, near-complete/complete recanalization (mTICI score, 2c/3) could not be achieved. Three patients were excluded from further analysis as the mTICI score or the number of passes was missing. For the scope of this study, 2 patient groups were defined: one comprising individuals in whom near-complete/complete recanalization could be achieved in the first pass (FPR, n = 126) and the other consisting of those for whom near-complete/complete recanalization required multiple attempts (NFPR, n = 54).

Patient demographics and clinical characteristics of our study groups are shown in the Table. There was no difference in age and sex between the 2 groups. The median age was 72.0 (IQR, 60.8-80.3) years in the FPR group and 74.0 (IQR, 62.0-81.3) years in the NFPR group. There was also no difference in risk factors such as smoking, arterial hypertension, atrial fibrillation, diabetes mellitus, or prior stroke/transient ischemic attacks between the 2 groups. In both groups, the majority of the patients had a stroke of cardio-embolic origin according to the TOAST classification system (53.2% [n = 67] in the FPR group and 61.1% [n = 33] in the NFPR group). No differences in stroke etiology according to the TOAST classification system were observed between the groups (P = .4746). Approximately half of the patients received recombinant tissue plasminogen activator (rt-PA) prior to MT, and the presence of prior rt-PA treatment was similar in both groups (P = .1310). The occlusion sites were not different between the 2 groups, with the middle cerebral artery representing the main occlusion site in both groups (68.0% [n = 85] in the FPR group and 61.1% [n = 33] in the NFPR group).

As expected, the median procedure time in the FPR group was significantly shorter compared with the NFPR group (33.0 minutes [IQR, 26.0-42.8 minutes] in the FPR group vs 74.5 minutes [IQR, 44.0-106.3 minutes] in the NFPR group; $P < .0001$). The baseline stroke severity, as assessed by the NIHSS, showed no significant difference (P = .2284) between the 2 groups. However, after 24 hours, the NIHSS score was significantly lower in FPR patients than in the NFPR patients (median [IQR] NIHSS score of 3.0 [1.0-8.0] and 6.0 [2.0-12.5], respectively; P = .0437). Similarly, whereas pre-mRS scores were similar in the 2 groups (P = .1590), the mRS at 90 days was significantly lower in patients in whom FPR was achieved compared with NFPR cases (median [IQR], 1.0 [0.0-3.0] vs 2.0 [1.0-5.0]; P = .0107).

The primary objective of our study was to explore whether FPR thrombi exhibit a distinct molecular and cellular composition compared with thrombi requiring multiple passes to achieve near-complete or complete recanalization. For this purpose, the composition of each thrombus was carefully analyzed via histologic analysis of RBCs, fibrin, VWF, platelets, leukocytes, citrullinated histone H3, nuclear DNA, and exDNA. A summary of these quantifications is presented in the Table. Supplementary Figure S1 provides a graphical overview of the distribution and variation of each compositional parameter. Remarkably, we found significant differences between FPR and NFPR thrombi. Thrombi from FPR patients indeed showed a distinct composition, characterized by significantly more RBCs than thrombi from NFPR patients (median [IQR], 44.9% [29.7%-59.7%] vs 36.6% [24.6%-52.9%]; P = .0264). In addition, FPR thrombi contained significantly less fibrin (median [IQR], 28.0% [20.2%-39.5%] vs 35.8% [22.6%-56.2%]; P = .0196) and less exDNA (median [IQR], 5.4% [2.0%-11.3%] vs 9.1% [2.4%-14.5%]; P = .0457) than thrombi from NFPR patients. No significant difference was found in the other compositional parameters.

4 | DISCUSSION

In this study, we examined the association between thrombus composition and achieving FPR by conducting a comprehensive histologic analysis of a diverse array of thrombus components. Our results revealed that thrombi successfully retrieved in a single pass exhibited significantly higher amounts of RBCs, reduced fibrin content, and lower levels of exDNA compared with thrombi that required multiple passes to achieve near-complete/complete recanalization (mTICI score, 2c/3). These findings underscore the potential influence of thrombus composition on the success rates of MT procedures, particularly in achieving FPR.

Ischemic stroke thrombi demonstrate a broad heterogeneity in their composition, which can have important implications for their susceptibility to treatment [21]. Our group previously reported on the molecular and cellular architecture of ischemic stroke thrombi and described 2 distinct types of thrombus material, referred to as "RBC-rich" and "platelet-rich" thrombus material [19]. RBC-rich thrombus material displays a relatively simple organization, mainly containing RBCs entangled in a matrix of thin fibrin. On the other hand, platelet-rich thrombus material contains almost no RBCs but contains large amounts of platelets, surrounded by dense fibrin structures, interspersed with nonfibrin scaffolds of exDNA and VWF [19]. Our current findings indicate that RBC-rich thrombi are more likely to result in FPR and further support the notion that RBC-poor thrombi, which typically contain higher amounts of exDNA, are more difficult to retrieve [22,23,33]. Our findings are also in line with recent findings showing higher amounts of RBCs or lower amounts of platelets in thrombi from cases that achieved FPR [34,35].

The physical characteristics of a thrombus, such as its stiffness, deformability, and adherence to vessel walls, can be influenced by its composition. Consequently, these properties may affect the susceptibility of the thrombus to mechanical removal. The presence of RBCs can decrease thrombus stiffness and increase deformability, likely enhancing their interaction with the MT devices and contact aspiration catheters [36]. Our study identifies fibrin and in particular exDNA as components that may contribute to thrombectomy resistance. Fibrin is known to increase thrombus stiffness and friction coefficient, most likely hampering efficient retrieval [37,38]. Prior rt-PA treatment could potentially alter the amount or structure of fibrin in the thrombus. Although there were more (though not statistically significant) rt-PA–treated patients in our FPR group, there was no significant difference in fibrin content between patients with or without prior rt-PA treatment.

In a previous study, no association was found between FPR and total thrombus DNA, which included both intra- and exDNA [35].

TABLE Patient demographic, interventional, and clinical characteristics.

Patient characteristics	FPR (*n* = 126)	NFPR (*n* = 54)	*P* value
Age (y), median (IQR)	72.0 (60.8-80.3)	74.0 (62.0-81.3)	.4907
Female, *n* (%)	73 (57.9)	27 (50.0)	.3322
Prior rt-PA treatment, *n* (%)	75 (60.5)[2]	24 (47.1)[3]	.1310
Risk factors, *n* (%)			
Smoking	7 (5.7)[3]	6 (11.3)[1]	.2150
Arterial hypertension	60 (48.0)[1]	22 (41.5)[1]	.5112
Atrial fibrillation	49 (38.9)	21 (39.6)[1]	>.9999
Diabetes mellitus	14 (26.3)	5 (9.4)[1]	>.9999
Prior stroke/TIA	19 (15.2)[1]	8 (15.1)[1]	>.9999
Etiology according to TOAST classification, *n* (%)			.4746
Cardioembolic	67 (53.2)	33 (61.1)	
Large artery atherosclerosis	21 (16.7)	5 (9.3)	
Embolic stroke of unknown source	30 (23.8)	11 (20.4)	
Other	8 (6.3)	5 (9.3)	
Occlusion site, *n* (%)			.7394
ICA or ICA-T	20 (16.0)[1]	9 (16.7)	
MCA	85 (68.0)[1]	33 (61.1)	
BA/ACA/PCA	8 (6.4)[1]	4 (7.4)	
Multisegment occlusion	12 (9.6)[1]	8 (14.8)	
Endovascular treatment			
Procedure time (min), median (IQR)	33.0 (26.0-42.8)[10]	74.5 (44.0-106.3)[1]	**<.0001**
Clinical outcome, median (IQR)			
NIHSS score	18.0 (11.3-21.0)[6]	17.0 (14.5-22.0)[5]	.2284
NIHSS score at 24 h	3.0 (1.0-8.0)[6]	6.0 (2.0-12.5)[5]	**.0437**
NIHSS score difference	11.0 (3.3-16.0)[10]	15.25 (9.0-22.0)[8]	.2527
Pre-mRS score	0.0 (0.0-1.0)[21]	0.0 (0.0-1.0)[5]	.1590
mRS score at 90 d	1.0 (0.0-3.0)[18]	2.0 (1.0-5.0)[7]	**.0107**
Thrombus composition (% of thrombus), median (IQR)			
RBC	44.9 (29.7-59.7)	36.6 (24.6-52.9)	**.0264**
Fibrin	28.0 (20.2-39.5)	35.8 (22.6-56.2)	**.0196**
VWF	24.6 (18.3-40.0)	23.3 (17.1-38.2)	.5918
CD42b	31.3 (20.2-46.6)	33.3 (17.8-48.1)	.9090
CD45	14.1 (7.9-26.2)	13.8 (7.8-24.8)	.7740
H3Cit	3.0 (0.9-6.5)	2.4 (0.7-4.2)	.1499
Nuclear DNA	4.9 (2.8-6.6)	4.6 (3.2-6.3)	.9839
exDNA	5.4 (2.0-11.3)	9.1 (2.4-14.5)	**.0457**

Continuous variables are represented as the median and range, whereas categorical variables are represented using a frequency distribution and the respective percentages compared with the overall population. Differences in continuous variables were assessed using Mann–Whitney U-test. A chi-squared test was used to evaluate the association between categorical patient characteristics across different groups. The superscript numbers represent the number of missing values for the indicated parameter. *P*-values that were signifcant (>.05) are indicated in bold.

ACA, anterior cerebral artery; BA, basilar artery; CD42b, cluster of differentiation 42b; CD45, cluster of differentiation 45; exDNA, extracellular DNA; FPR, first-pass recanalization; H3Cit, citrullinated histone H3; ICA, internal carotid artery; ICA-T, occlusion of the terminal segment of the internal carotid artery; MCA, middle cerebral artery; mRS, modified Rankin scale; NFPR, no first-pass recanalization; NIHSS, National Institute of Health Stroke Scale; PCA, posterior cerebral artery; RBC, red blood cell; rt-PA, recombinant tissue plasminogen activator; TIA, transient ischemic attack; TOAST, Trial of Org 10172 in Acute Stroke Treatment; VWF, von Willebrand factor.

However, based on the hypothesis that specifically exDNA would contribute to MT resistance, we used a combination of different DNA staining methods, enabling the specific measurement of exDNA. Our findings, which establish exDNA as a potential contributor to FPR failure, may be attributed to the ability of DNA to modify the structure and thickness of fibrin, enhancing the mechanical stability of fibrin and increasing thrombus stiffness [39,40]. These findings could explain why NETs, in which exDNA is the primary component, have been linked to an increased number of passes needed for recanalization [30,31]. This is further supported by a case study describing a nearly thrombectomy-resistant thrombus that was characterized by a high amount of exDNA and a low amount of RBCs [29].

While achieving FPR is likely influenced by several factors, including thrombus size, physician experience, and other variables [41], our findings highlight the importance of recognizing the diverse characteristics of thrombi and tailoring thrombectomy approaches accordingly. This highlights the importance of advancing imaging techniques or diagnostic tools for evaluating thrombus composition before determining the optimal treatment strategy, aiming to enhance the success rates of FPR. In computed tomography scans, the identification and intensity of a hyperdense artery sign, quantified in Hounsfield units, at the occlusion site correlate with a higher RBC content, while absence of a hyperdense artery sign is associated with thrombi richer in fibrin and platelets [23,42–47]. In line with our findings, cases showing low Hounsfield unit densities are associated with a reduced likelihood of achieving FPR [48,49]. Emerging technologies designed to detect intravascular thrombus composition prior to thrombectomy are currently in development [50,51]. These advancements have the potential to customize the selection of MT techniques, including the utilization of devices specifically designed for fibrin-rich thrombi [52,53] or retrievers modified with coatings that bind to NETs [54].

This study has several limitations, including the fact that only those thrombi that could successfully be retrieved via thrombectomy were available for study. This impedes assessment of thrombi that were completely thrombectomy-resistant. Furthermore, our study contains data from a single hospital in Belgium. A multicenter approach, preferably across different countries, could increase the strength of the data.

5 | CONCLUSION

Our study shows that thrombi containing fewer RBCs, more fibrin, and more exDNA are associated with a decreased FPR rate. These findings underscore the necessity for future research and technological enhancements aimed at improving FPR rates in thrombi with a low RBC content, enhancing patient outcomes following thrombectomy.

ACKNOWLEDGMENTS

We would like to thank the whole team of the stroke unit at the AZ Groeninge Hospital (Kortrijk, Belgium) for their support and collaboration in this research.

AUTHOR CONTRIBUTIONS

S.V., S.S., and S.F.D.M. designed the study. S.V., S.S., and M.D.W. performed the experiments. O.F., L.D., A.-S.D.S., T.D., P.V., and T.A. contributed to data acquisition. S.V. and S.S. analyzed data. S.V., S.F.D.M., C.T., and K.V. interpreted the results. S.V. and S.F.D.M. wrote the manuscript. All authors critically reviewed the manuscript.

DECLARATION OF COMPETING INTERESTS

P.V. received speaker fees from Boehringer-Ingelheim, BMS, Pfizer, Daiichi-Sankyo, and Medtronic. T.A. holds equity for Cereflo Ltd and is a consultant for Anaconda, Cerenovus/Neuravi, Optimize Neurovascular, and Rapid Medical. O.F. is a consultant for iVascular. All other authors have no conflicting interests.

DATA AVAILABILITY

Data are available upon reasonable written request to the corresponding author.

ORCID

Sarah Vandelanotte https://orcid.org/0000-0003-4249-9025
Simon F. De Meyer https://orcid.org/0000-0002-1807-5882

REFERENCES

[1] Berkhemer OA, Fransen PSS, Beumer D, van den Berg LA, Lingsma HF, Yoo AJ, Schonewille WJ, Vos JA, Nederkoorn PJ, Wermer MJH, van Walderveen MAA, Staals J, Hofmeijer J, van Oostayen JA, Lycklama À, Nijeholt GJ, Boiten J, Brouwer PA, Emmer BJ, de Bruijn SF, van Dijk LC, et al. A randomized trial of intraarterial treatment for acute ischemic stroke. *N Engl J Med*. 2015;372:11–20.

[2] Goyal M, Demchuk AM, Menon BK, Eesa M, Rempel JL, Thornton J, Roy D, Jovin TG, Willinsky RA, Sapkota BL, Dowlatshahi D, Frei DF, Kamal NR, Montanera WJ, Poppe AY, Ryckborst KJ, Silver FL, Shuaib A, Tampieri D, Williams D, et al. Randomized assessment of rapid endovascular treatment of ischemic stroke. *N Engl J Med*. 2015;372:1019–30.

[3] Campbell BCV, Mitchell PJ, Kleinig TJ, Dewey HM, Churilov L, Yassi N, Yan B, Dowling RJ, Parsons MW, Oxley TJ, Wu TY, Brooks M, Simpson MA, Miteff F, Levi CR, Krause M, Harrington TJ, Faulder KC, Steinfort BS, Priglinger M, et al. Endovascular therapy for ischemic stroke with perfusion-imaging selection. *N Engl J Med*. 2015;372:1009–18.

[4] Saver JL, Goyal M, Bonafe A, Diener HC, Levy EI, Pereira VM, Albers GW, Cognard C, Cohen DJ, Hacke W, Jansen O, Jovin TG, Mattle HP, Nogueira RG, Siddiqui AH, Yavagal DR, Baxter BW, Devlin TG, Lopes DK, Reddy VK, et al. Stent-retriever thrombectomy after intravenous t-PA vs. t-PA alone in stroke. *N Engl J Med*. 2015;372:2285–95.

[5] Jovin TG, Chamorro A, Cobo E, de Miquel MA, Molina CA, Rovira A, San Román L, Serena J, Abilleira S, Ribó M, Millán M, Urra X, Cardona P, López-Cancio E, Tomasello A, Castaño C, Blasco J, Aja L, Dorado L, Quesada H, et al. Thrombectomy within 8 hours after symptom onset in ischemic stroke. *N Engl J Med*. 2015;372:2296–306.

[6] Flottmann F, Brekenfeld C, Broocks G, Leischner H, Mcdonough R, Faizy TD, Deb-Chatterji M, Alegiani A, Thomalla G, Mpotsaris A, Nolte CH, Fiehler J, Maros ME, GSR investigators. Good clinical outcome decreases with number of retrieval attempts in stroke thrombectomy: beyond the first-pass effect. *Stroke*. 2021;52:482–90.

[7] Zaidat OO, Castonguay AC, Linfante I, Gupta R, Martin CO, Holloway WE, Mueller-Kronast N, English JD, Dabus G, Malisch TW, Marden FA, Bozorgchami H, Xavier A, Rai AT, Froehler MT, Badruddin A, Nguyen TN, Asif Taqi M, Abraham MG, Yoo AJ, et al. First pass effect: a new measure for stroke thrombectomy devices. *Stroke*. 2018;49:660–6.

[8] Jindal G, De Paula Carvalho H, Wessell A, Le E, Naragum V, Miller TR, Wozniak M, Shivashankar R, Cronin CA, Schrier C, Gandhi D. Beyond the first pass: revascularization remains critical in stroke thrombectomy. *J Neurointerv Surg*. 2019;11:1095–9.

[9] Akpinar CK, Ozdemir AO, Gurkas E, Bilgic AB, Aykac O, Inanc Y, Giray S. Favorable first-pass recanalization rates with NeVa™ thrombectomy device in acute stroke patients: initial clinical experience. *Interv Neuroradiol*. 2021;27:107–13.

[10] Hassan AE, Dibas M, Sarraj A, Ghozy S, El-Qushayri AE, Dmytriw AA, Tekle WG. First pass effect vs multiple passes complete reperfusion: a retrospective study. *Neuroradiol J*. 2022;35:306–12.

[11] Kang DH, Kim BM, Heo JH, Nam HS, Kim YD, Hwang YH, Kim YW, Kim DJ, Kim JW, Baek JH, Kim YS. Effects of first pass recanalization on outcomes of contact aspiration thrombectomy. *J Neurointerv Surg*. 2020;12:466–70.

[12] Abbasi M, Liu Y, Fitzgerald S, Mereuta OM, Arturo Larco JL, Rizvi A, Kadirvel R, Savastano L, Brinjikji W, Kallmes DF. Systematic review and meta-analysis of current rates of first pass effect by thrombectomy technique and associations with clinical outcomes. *J Neurointerv Surg*. 2021;13:212–6.

[13] Abdullayev N, Maus V, Behme D, Barnikol UB, Kutschke S, Stockero A, Goertz L, Celik E, Zaeske C, Borggrefe J, Schlamann M, Liebig T, Kabbasch C, Mpotsaris A. True first-pass effect in basilar artery occlusions: first-pass complete reperfusion improves clinical outcome in stroke thrombectomy patients. *J Clin Neurosci*. 2021;89:33–8.

[14] Bai X, Zhang X, Yang W, Zhang Y, Wang T, Xu R, Wang Y, Li L, Feng Y, Yang K, Wang X, Song H, Ma Q, Jiao L. Influence of first-pass effect on recanalization outcomes in the era of mechanical thrombectomy: a systemic review and meta-analysis. *Neuroradiology*. 2021;63:795–807.

[15] Den Hartog SJ, Roozenbeek B, Boodt N, Bruggeman AAE, Van Es ACGM, Emmer BJ, Majoie CBLM, Van Den Wijngaard IR, Van Doormaal PJ, Van Zwam WH, Lingsma HF, Dippel DWJ. MR CLEAN Registry investigators. Effect of first pass reperfusion on outcome in patients with posterior circulation ischemic stroke. *J Neurointerv Surg*. 2022;14:333–40.

[16] Jadhav AP, Desai SM, Zaidat OO, Nogueira RG, Jovin TG, Haussen DC, Mueller-Kronast N, Liebeskind DS. First pass effect with neurothrombectomy for acute ischemic stroke: analysis of the systematic evaluation of patients treated with stroke devices for acute ischemic stroke registry. *Stroke*. 2022;53:e30–2.

[17] Nikoubashman O, Dekeyzer S, Riabikin A, Keulers A, Reich A, Mpotsaris A, Wiesmann M. True first-pass effect. *Stroke*. 2019;50:2140–6.

[18] den Hartog SJ, Zaidat O, Roozenbeek B, van Es ACGM, Bruggeman AAE, Emmer BJ, Majoie CBLM, van Zwam WH, van den Wijngaard IR, van Doormaal PJ, Lingsma HF, Burke JF, Dippel DWJ, MR CLEAN (Multicenter Randomized Clinical Trial of Endovascular Treatment for Acute Ischemic Stroke in the Netherlands) Registry Investigators. Effect of first-pass reperfusion on outcome after endovascular treatment for ischemic stroke. *J Am Heart Assoc*. 2021;10:e019988.

[19] Staessens S, Denorme F, François O, Desender L, Dewaele T, Vanacker P, Deckmyn H, Vanhoorelbeke K, Andersson T, De Meyer SF. Structural analysis of ischemic stroke thrombi: histological indications for therapy resistance. *Haematologica*. 2020;105:498–507.

[20] Di Meglio L, Desilles JP, Ollivier V, Nomenjanahary MS, Di Meglio S, Deschildre C, Loyau S, Olivot JM, Blanc R, Piotin M, Bouton MC, Michel JB, Jandrot-Perrus M, Ho-Tin-Noé B, Mazighi M. Acute ischemic stroke thrombi have an outer shell that impairs fibrinolysis. *Neurology*. 2019;93:e1686–98.

[21] Staessens S, De Meyer SF. Thrombus heterogeneity in ischemic stroke. *Platelets*. 2021;32:331–9.

[22] Duffy S, Mccarthy R, Farrell M, Thomas S, Brennan P, Power S, O'Hare A, Morris L, Rainsford E, Maccarthy E, Thornton J, Gilvarry M. Per-pass analysis of thrombus composition in patients with acute ischemic stroke undergoing mechanical thrombectomy. *Stroke*. 2019;50:1156–63.

[23] Maekawa K, Shibata M, Nakajima H, Mizutani A, Kitano Y, Seguchi M, Yamasaki M, Kobayashi K, Sano T, Mori G, Yabana T, Naito Y, Shimizu S, Miya F. Erythrocyte-rich thrombus is associated with reduced number of maneuvers and procedure time in patients with acute ischemic stroke undergoing mechanical thrombectomy. *Cerebrovasc Dis Extra*. 2018;8:39–49.

[24] Shin JW, Jeong HS, Kwon HJ, Song KS, Kim J. High red blood cell composition in clots is associated with successful recanalization during intra-arterial thrombectomy. *PLoS One*. 2018;13:e0197492.

[25] Boeckh-Behrens T, Schubert M, Förschler A, Prothmann S, Kreiser K, Zimmer C, Riegger J, Bauer J, Neff F, Kehl V, Pelisek J, Schirmer L, Mehr M, Poppert H. The impact of histological clot composition in embolic stroke. *Clin Neuroradiol*. 2016;26:189–97.

[26] Arturo Larco J, Abbasi M, Liu Y, Madhani SI, Shahid AH, Kadirvel R, Brinjikji W, Savastano LE. Per-pass analysis of recanalization and good neurological outcome in thrombectomy for stroke: systematic review and meta-analysis. *Interv Neuroradiol*. 2022;28:358–63.

[27] Abbasi M, Arturo Larco J, Mereuta MO, Liu Y, Fitzgerald S, Dai D, Kadirvel R, Savastano L, Kallmes DF, Brinjikji W. Diverse thrombus composition in thrombectomy stroke patients with longer time to recanalization. *Thromb Res*. 2022;209:99–104.

[28] Kitano T, Hori Y, Okazaki S, Shimada Y, Iwamoto T, Kanki H, Sugiyama S, Sasaki T, Nakamura H, Oyama N, Hoshi T, Beck G, Takai H, Matsubara S, Mizuno H, Nishimura H, Tamaki R, Iida J, Iba J, Uno M, et al. An older thrombus delays reperfusion after mechanical thrombectomy for ischemic stroke. *Thromb Haemost*. 2022;122:415–26.

[29] Staessens S, François O, Desender L, Vanacker P, Dewaele T, Sciot R, Vanhoorelbeke K, Andersson T, De Meyer SF. Detailed histological analysis of a thrombectomy-resistant ischemic stroke thrombus: a case report. *Thromb J*. 2021;19:11.

[30] Ducroux C, Di Meglio L, Loyau S, Delbosc S, Boisseau W, Deschildre C, Ben Maacha M, Blanc R, Redjem H, Ciccio G, Smajda S, Fahed R, Michel JB, Piotin M, Salomon L, Mazighi M, Ho-Tin-Noe B, Desilles JP. Thrombus neutrophil extracellular traps content impair tPA-induced thrombolysis in acute ischemic stroke. *Stroke*. 2018;49:754–7.

[31] Novotny J, Oberdieck P, Titova A, Pelisek J, Chandraratne S, Nicol P, Hapfelmeier A, Joner M, Maegdefessel L, Poppert H, Pircher J, Massberg S, Friedrich B, Zimmer C, Schulz C, Boeckh-Behrens T. Thrombus NET content is associated with clinical outcome in stroke and myocardial infarction. *Neurology*. 2020;94:e2346–60.

[32] Adams HP, Bendixen BH, Kappelle LJ, Biller J, Love BB, Gordon DL, Marsh EE 3rd. Classification of subtype of acute ischemic stroke. Definitions for use in a multicenter clinical trial. TOAST. Trial of Org 10172 in Acute Stroke Treatment. *Stroke*. 1993;24:35–41.

[33] Liu Y, Brinjikji W, Abbasi M, Dai D, Arturo Larco JL, Madhani SI, Shahid AH, Mereuta OM, Nogueira RG, Kvamme P, Layton KF, Delgado Almandoz JE, Hanel RA, Pereira VM, Almekhlafi MA, Yoo AJ, Jahromi BS, Gounis MJ, Patel B, Fitzgerald S, et al. Quantification of clot spatial heterogeneity and its impact on thrombectomy. *J Neurointerv Surg*. 2022;14:1248–52.

[34] Patel TR, Fricano S, Waqas M, Tso M, Dmytriw AA, Mokin M, Kolega J, Tomaszewski J, Levy EI, Davies JM, Snyder KV, Siddiqui AH, Tutino VM. Increased perviousness on CT for acute ischemic stroke is associated with fibrin/platelet-rich clots. *AJNR Am J Neuroradiol*. 2021;42:57–64.

[35] Delvoye F, Di Meglio L, Consoli A, Nomenjanahary MS, Dupont S, Labreuche J, Maier B, Piotin M, Blanc R, Escalard S, Boursin P, Hamdani M, Redjem H, Smajda S, Hébert S, Sabben C, de Noordhout AM, Jandrot-Perrus M, Lapergue B, Mazighi M, et al. High thrombus platelet content is associated with a lower rate of first pass effect in stroke treated by endovascular therapy. *Eur Stroke J*. 2022;7:376–83.

[36] Sporns PB, Hanning U, Schwindt W, Velasco A, Buerke B, Cnyrim C, Minnerup J, Heindel W, Jeibmann A, Niederstadt T. Ischemic stroke: histological thrombus composition and pre-interventional CT attenuation are associated with intervention time and rate of secondary embolism. *Cerebrovasc Dis*. 2017;44:344–50.

[37] Yuki I, Kan I, Vinters HV, Kim RH, Golshan A, Vinuela FA, Sayre JW, Murayama Y, Vinuela FA. The impact of thromboemboli histology on the performance of a mechanical thrombectomy device. *AJNR Am J Neuroradiol*. 2012;33:643–8.

[38] Gunning GM, McArdle K, Mirza M, Duffy S, Gilvarry M, Brouwer PA. Clot friction variation with fibrin content; implications for resistance to thrombectomy. *J Neurointerv Surg*. 2018;10:34–8.

[39] Varjú I, Longstaff C, Szabó L, Farkas ÁZ, Varga-Szabó VJ, Tanka-Salamon A, Machovich R, Kolev K. DNA, histones and neutrophil extracellular traps exert anti-fibrinolytic effects in a plasma environment. *Thromb Haemost*. 2015;113:1289–98.

[40] Longstaff C, Varjú I, Sótonyi P, Szabó L, Krumrey M, Hoell A, Bóta A, Varga Z, Komorowicz E, Kolev K. Mechanical stability and fibrinolytic resistance of clots containing fibrin, DNA, and histones. *J Biol Chem*. 2013;288:6946–56.

[41] Di Maria F, Kyheng M, Consoli A, Desilles JP, Gory B, Richard S, Rodesch G, Labreuche J, Girot JB, Dargazanli C, Marnat G, Lapergue B, Bourcier R, ETIS investigators. Identifying the predictors of first-pass effect and its influence on clinical outcome in the setting of endovascular thrombectomy for acute ischemic stroke: results from a multicentric prospective registry. *Int J Stroke*. 2021;16:20–8.

[42] Hund H, Boodt N, Arrarte Terreros N, Taha A, Marquering HA, van Es ACGM, Bokkers RPH, Lycklama À, Nijeholt GJ, Majoie CBLM, Dippel DWJ, Lingsma HF, van Beusekom HMM, van der Lugt A, MR CLEAN Registry Investigators. Quantitative thrombus characteristics on thin-slice computed tomography improve prediction of thrombus histopathology: results of the MR CLEAN Registry. *Eur Radiol*. 2022;32:7811–23.

[43] Simons N, Mitchell P, Dowling R, Gonzales M, Yan B. Thrombus composition in acute ischemic stroke: a histopathological study of thrombus extracted by endovascular retrieval. *J Neuroradiol*. 2015;42:86–92.

[44] Liebeskind DS, Sanossian N, Yong WH, Starkman S, Tsang MP, Moya AL, Zheng DD, Abolian AM, Kim D, Ali LK, Shah SH, Towfighi A, Ovbiagele B, Kidwell CS, Tateshima S, Jahan R, Duckwiler GR, Viñuela F, Salamon N, Villablanca JP, et al. CT and MRI early vessel signs reflect clot composition in acute stroke. *Stroke*. 2011;42:1237–43.

[45] Brinjikji W, Duffy S, Burrows A, Hacke W, Liebeskind D, Majoie CBLM, Dippel DWJ, Siddiqui AH, Khatri P, Baxter B, Nogeuira R, Gounis M, Jovin T, Kallmes DF. Correlation of imaging and histopathology of thrombi in acute ischemic stroke with etiology and outcome: a systematic review. *J Neurointerv Surg*. 2017;9:529–34.

[46] Ye G, Cao R, Lu J, Qi P, Hu S, Chen K, Tan T, Chen J, Wang D. Histological composition behind CT-based thrombus density and perviousness in acute ischemic stroke. *Clin Neurol Neurosurg*. 2021;207:106804.

[47] Essig F, Kollikowski AM, Pham M, Solymosi L, Stoll G, Haeusler KG, Kraft P, Schuhmann MK. Immunohistological analysis of neutrophils and neutrophil extracellular traps in human thrombemboli causing acute ischemic stroke. *Int J Mol Sci*. 2020;21:7387.

[48] He G, Deng J, Lu H, Wei L, Zhao Y, Zhu Y, Li Y. Thrombus enhancement sign on CT angiography is associated with the first pass effect of stent retrievers. *J Neurointerv Surg*. 2023;15:146–52.

[49] Waqas M, Li W, Patel TR, Chin F, Tutino VM, Dossani RH, Ren Z, Guerrero WR, Borlongan CV, Pressman E, Snyder K, Davies JM, Ley EI, Ionita CN, Siddiqui AH, Mokin M. Clot imaging characteristics predict first pass effect of aspiration—first approach to thrombectomy. *Interv Neuroradiol*. 2022;28:152–9.

[50] Darcourt J, Brinjikji W, François O, Giraud A, Johnson CR, Patil S, Staessens S, Kadirvel R, Mohammaden MH, Pisani L, Rodrigues GM, Cancelliere NM, Pereira VM, Bozsak F, Doyle K, De Meyer SF, Messina P, Kallmes D, Cognard C, Nogueira RG. Identifying ex vivo acute ischemic stroke thrombus composition using electrochemical impedance spectroscopy. *Interv Neuroradiol*. Published online May 16, 2023. https://doi.org/10.1177/15910199231175377

[51] Skyrman S, Burström G, Aspegren O, Lucassen G, Elmi-Terander A, Edström E, Arnberg F, Ohlsson M, Mueller M, Andersson T. Identifying clot composition using intravascular diffuse reflectance spectroscopy in a porcine model of endovascular thrombectomy. *J Neurointerv Surg*. 2022;14:304–9.

[52] Fennell VS, Setlur Nagesh SV, Meess KM, Gutierrez L, James RH, Springer ME, Siddiqui AH. What to do about fibrin rich "tough clots"? Comparing the Solitaire stent retriever with a novel geometric clot extractor in an in vitro stroke model. *J Neurointerv Surg*. 2018;10:907–10.

[53] Kaneko N, Ghovvati M, Komuro Y, Guo L, Khatibi K, Ponce Mejia LL, Saber H, Annabi N, Tateshima S. A new aspiration device equipped with a hydro-separator for acute ischemic stroke due to challenging soft and stiff clots. *Interv Neuroradiol*. 2022;28:43–9.

[54] Skarbek C, Anagnostakou V, Procopio E, Epshtein M, Raskett CM, Romagnoli R, Iviglia G, Morra M, Antonucci M, Nicoletti A, Caligiuri G, Gounis MJ. Development of a clot-adhesive coating to improve the performance of thrombectomy devices. *J Neurointerv Surg*. 2023;15:1207–11.

SUPPLEMENTARY MATERIAL

The online version contains supplementary material available at https://doi.org/10.1016/j.jtha.2024.05.034

SUPPLEMENTAL MATERIAL

Association between thrombus composition and first pass recanalization after thrombectomy in acute ischemic stroke

Sarah Vandelanotte*[,1], Senna Staessens*[,1], Olivier François[2], Maaike De Wilde[1], Linda Desender[1], Anne-Sophie De Sloovere[2], Tom Dewaele[2], Claudia Tersteeg[1], Karen Vanhoorelbeke[1], Peter Vanacker[3,4,5], Tommy Andersson[6] and Simon F. De Meyer[1]

Supplemental Material

Thrombus processing and histological analysis

After retrieval, thrombi were gently removed from the stent retriever or the aspiration catheter, stored in saline at 4°C for a maximum of 24 hours, followed by incubation in 4% paraformaldehyde for 24 hours at room temperature (RT). When embedding the samples, the thrombus orientation in paraffin blocks was arranged to produce the largest cross-sectional area when cutting 5 µm sections. For each thrombus, a single section was chosen for each staining procedure. We previously demonstrated that one section per thrombus is a good representative for the entire sample.[29] Thrombus sections were stained with a Martius Scarlet Blue (MSB) staining (Crystal Ponceau 6R: sc-214779, Santa Cruz, Dallas, USA; Naphtol Yellow S: sc-215544, Santa Cruz, Dallas, USA; Methyl blue: M6900-50G, Sigma, St. Louis, MO, USA) to identify RBCs (yellow), fibrin (dark pink/red) and collagen (blue), a hematoxylin and eosin staining (H&E, HT110216, Sigma-Aldrich, St. Louis, MO, USA) and a Feulgen's reaction staining (1079070001, Merck Chemicals, MA, USA) to identify DNA (pink). Immunohistochemical (IHC) stainings were performed to examine the presence of platelets (GPIbα, MA5-11642, Invitrogen, Waltham, MA, USA), VWF (A008202-2, Agilent Technologies, Santa Clara, CA, USA), leukocytes (CD45, 304002, Biolegend, San Diego, CA) and citrullinated histone H3 (H3Cit, used as a surrogate marker for NETs, ab5103, Abcam, Cambridge, UK). In the IHC stainings, nuclei were stained green using a Methyl Green solution (H-3402, Vector Laboratories, Peterborough, UK). Negative controls were obtained by omission of the primary antibody and were negative for all IHC procedures (data not shown).

Quantitative determination of thrombus components

Stained slides were digitized using a slide scanner (Nanozoomer SQ, Hamamatsu Photonics, Hamamatsu, Japan) and exported in 5X resolution using NDP view2 Software (Hamamatsu, Japan). Background surrounding the thrombus section (e.g., dust particles, air bubbles) was removed using Adobe Photoshop CS5 (San José, CA, USA) to prevent false positive signal in the quantification. Histological stainings were examined by color segmentation and planimetric analysis to calculate the relative amount of each component using ImageJ software 1.49v (National Institutes of Health, Bethesda, MD, USA; http://imagej.nig.gov/ij/). MSB staining was used to quantify fibrin

and RBCs. Quantification of platelets, VWF, CD45, and H3Cit was performed on immunostainings for the respective component. The Feulgen staining was used to quantify the amount of total DNA in the thrombus section, which includes nuclear DNA and exDNA. To specifically calculate the amount of exDNA, the amount of nuclear DNA (determined via H&E staining) was subtracted from the total DNA in the thrombus. All results are presented as percentage of positive signal relative to the total area of the examined thrombus section.

SUPPLEMENTARY DATA

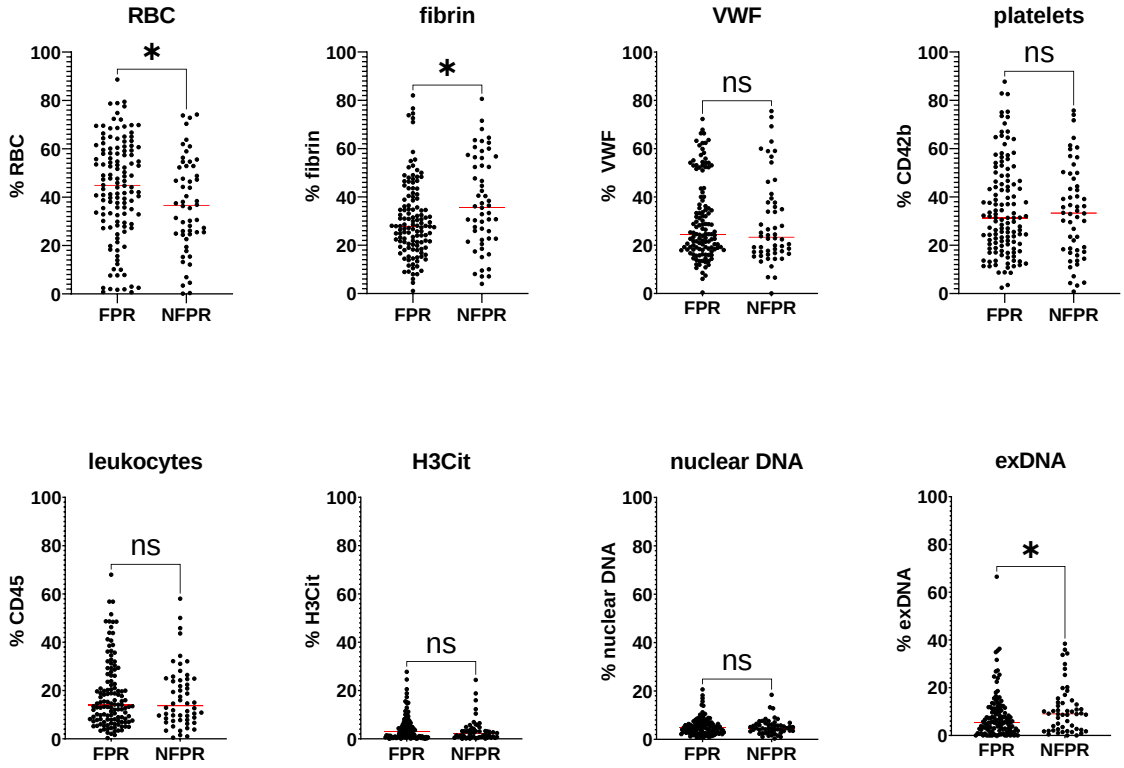

Supplementary Figure S1: Quantification of the different components in ischemic stroke thrombi.

CHAPTER 7 - ULTRASTRUCTURE OF ACUTE ISCHEMIC STROKE THROMBI VIA SCANNING ELECTRON MICROSCOPY: AN OBSERVATIONAL STUDY

Sarah Vandelanotte, MSc [1], Olivier François, MD[2], Alexander Vanhoorne, MD[3], Fréderick Van Gool, MD[2], Claudia Tersteeg, PhD[1], Karen Vanhoorelbeke, PhD[1], Peter Vanacker, MD[3,4,5], Tommy Andersson, MD[2,6] and Simon F. De Meyer, PhD[1]

[1]: Laboratory for Thrombosis Research, KU Leuven Kulak, Kortrijk, Belgium
[2]: Department of Medical Imaging, AZ Groeninge, Kortrijk, Belgium
[3]: Department of Neurology, AZ Groeninge, Kortrijk, Belgium
[4]: Department of Neurology, University Hospitals Antwerp, Antwerp, Belgium
[5]: Department of Translational Neuroscience, University of Antwerp, Antwerp, Belgium
[6]: Departments of Neuroradiology, Karolinska University Hospital, and Clinical Neuroscience Karolinska Institutet, Stockholm, Sweden

Abstract

Background: Acute ischemic stroke (AIS) treatment is based on fast and efficient recanalization of the occluded artery using either pharmacological thrombolysis, mechanical thrombectomy (MT), or a combination of both. However, due to several factors, successful recanalization is often not achieved. The precise mechanisms underlying recanalization failure is not completely understood but it is thought that thrombus composition and structure could play an important role. **Aims:** The aim of this study was to investigate the ultrastructural organization of AIS thrombi using scanning electron microscopy (SEM). **Methods:** Thrombi from AIS patients were retrieved via MT at AZ Groeninge Hospital in Kortrijk. Following fixation, thrombi were halved to allow investigation of the interior and surface of the thrombus and further processed for SEM. **Results:** SEM imaging of AIS thrombi revealed different ultrastructural characteristics of the thrombi. Three main thrombus structures, RBC-rich, platelet-rich and fibrin-rich structures, were observed and described in detail. Typically, AIS thrombi are composed of a combination of the three main thrombus structures, with their relative abundances varying. Furthermore, a distinct thrombus surface was identified that varies within and between thrombi and in which several distinct morphologies can be recognized. **Conclusions:** Our SEM study using patient AIS thrombi, revealed different ultrastructural, architectural features of both the surface and interior of AIS thrombi, improving our understanding of their microstructure

Introduction

Acute ischemic stroke (AIS) occurs when a blood clot obstructs an artery, cutting off blood flow to a part of the brain. Timely removal of the thrombus is crucial to restore circulation and prevent irreversible brain damage. Current treatment options include pharmacological thrombolysis using recombinant tissue plasminogen activator (rt-PA) and mechanical clot removal through mechanical thrombectomy (MT). These approaches, however, sometimes fail to achieve successful recanalization.[1–3] The implementation of MT for the treatment of AIS patients with large vessel occlusion provided researchers the unique opportunity to collect and investigate patient thrombi. Using conventional histological stains and immunohistochemical stainings, we and others previously demonstrated that the composition of acute ischemic stroke (AIS) thrombi is highly variable.[4–6] Using conventional histology, different thrombus regions were previously described, such as red blood cell (RBC)-rich and platelet-rich regions which are both present in different quantities within different thrombi.[4] Recently, we and others showed that the composition of the thrombus can greatly impact its responsiveness to treatment. RBC-rich thrombi tend to be more susceptible to rt-PA mediated lysis, require less passes to be removed via MT and are more likely to generate a first pass recanalization.[7–12] Most research on AIS thrombus composition relies on conventional histology. However, advanced, high resolution imaging techniques such as scanning electron microscopy (SEM) could enhance our understanding of the ultrastructural organization of AIS thrombi. This study aimed to provide a high-resolution, ultra-structural analysis of patient AIS thrombi via SEM.

Methods

Thrombus collection

Fresh thrombi retrieved from AIS patients via thrombectomy were obtained at the AZ Groeninge Hospital (Kortrijk, Belgium). Patients or their legal representative provided written consent under the approval of the AZ Groeninge Hospital ethical committee (AZGS2015065 and AZGS2024042). The collection of patient material was performed in agreement with the principles outlined in the Declaration of Helsinki. Thrombi were retrieved using a stent-retriever or contact aspiration dependent on the preference of the treating physician. After retrieval, the thrombus was delicately detached from the thrombectomy device and stored in saline at 4°C for maximum of 48 hours before further processing. A subset of thrombi was previously collected and fixed in 4%

paraformaldehyde for 24 hours. Following fixation, thrombi were embedded in paraffin blocks and 5 µm sections were made.

Scanning electron microscopy (SEM)

When whole fresh thrombi were used, they were immediately fixed in 2% glutaraldehyde, 0.1 M cacodylate buffer (pH = 7.4) (5169.1, Carl Roth, Karlsruhe, Germany) for 24h at 4°C. After fixation, thrombi were halved using a surgical scalpel blade (Swann-Mortel Number 23, Sheffield, England), allowing for the examination of both the interior and surface of the thrombus. When paraffin embedded thrombus sections were used, thrombus sections were first rehydrated in a series of decreasing ethanol concentration and fixed in 2% glutaraldehyde, 0.1 M cacodylate buffer for 24h at 4°C. After fixation, samples (both whole thrombi and thrombus sections) were rinsed with 0.1 M cacodylate buffer and dehydrated in an increasing concentration of ethanol (50%, 70%, 85%, 96%, 100% ethanol) for 30 minutes each. Finally, samples were incubated in hexamethyldisilazane (3840.2, Carl Roth, Karlsruhe, Germany) for 15 min and air dried. Before imaging, samples were sputter-coated with platinum (3-5 nm). SEM analysis was conducted on the thrombus surface with a JSM-IT200 scanning electron microscope (JEOL, Akishima, Tokyo).

Conventional histology

Conventional histological analysis was performed on paraffin embedded thrombus sections. Histological staining procedures were performed as described previously.[4] In brief, thrombus sections were stained with Martius Scarlet Blue (Crystal Ponceau 6R: sc-214779, Santa Cruz, Dallas, USA; Naphtol Yellow S: sc-215544, Santa Cruz, Dallas, USA; Methyl blue: M6900-50G, Sigma, St. Louis, MO, USA) to identify fibrin (dark pink/red), RBCs (yellow), and collagen (blue). Immunohistochemical staining was performed to assess the presence of platelets (purple) (GPIbα, MA5-11642, Invitrogen, Waltham, MA, USA), while nuclei were stained green using a Methyl Green solution (H-3402, Vector Laboratories, Peterborough, UK).

Immunofluorescent staining

Paraffin embedded thrombus sections were used for immunofluorescent staining procedures, as described previously.[4] Heat-induced antigen retrieval was done using 0.3% sodium citrate (pH 6) at 95°C for 20 min and thrombus sections were then

washed in tris-buffered saline (TBS). Following, thrombus sections were blocked with 1% normal donkey serum, 3% BSA and 0.1% Triton X-100 in TBS for 1h, and incubated overnight at 4°C with primary antibodies: rabbit anti human VWF polyclonal antibody (1:1500; A0082; Dako, Santa Clara, California, USA) and sheep anti-human fibrin(ogen) (1:400; 4440-8004; Biorad, Hercules, California, USA) in 1% normal donkey serum, 3% BSA and 0.1% Triton X-100 in TBS. After washing 3 times for 5 min in TBS, slides were incubated for 1 hour at RT with 1.5 µg/mL of the corresponding antibodies: Alexa Fluor 488 donkey anti-rabbit IgG (A21206; Invitrogen) and Alexa Fluor 647 donkey anti-sheep IgG (A21488, Invitrogen) in 3% BSA and 0.1% Triton X-100 in TBS. Negative controls were obtained by omission of the primary antibody and were negative (data not shown). Images were acquired using an Axio Observer Z1 inverted fluorescent microscope (Zeiss, Carl Zeiss AG, Oberkochen, Germany). To be able to still perform SEM imaging after fluorescent imaging, no mounting medium was used before imaging the thrombus sections.

Results

To improve our understanding of the composition and ultrastructural organization of AIS thrombi, we performed SEM imaging on patient AIS thrombi retrieved via MT. After collection and fixation, patient thrombi were halved, allowing for the examination of both the interior and surface of the thrombus. Nineteen thrombi were investigated, but for 2 thrombi the interior was not examined due to the limited thrombus material available. When examining the interior of patient thrombi, three distinct types of thrombus structures were commonly observed. These included RBC-rich, platelet-rich and fibrin-rich thrombus structures, each of which were studied in more detail.

RBC-rich thrombus structures

More detailed investigation of RBC-rich structures confirmed the presence of high amounts of RBCs. These highly concentrated RBCs are typically interwoven with a thin and branched fibrin network. On average, the fibrin in this network has a thickness of 212.8 nm ± 98.6 nm. Interestingly, our SEM images revealed different RBCs shapes and packing densities, ranging from loosely arranged RBCs with biconcave or rounded shape to densely compacted RBCs that have a polyhedral shape (Figure 1). The loosely arranged RBCs have empty spaces between them, while no gaps are

observed between the densely packed polyhedrocytes, which appear to form an impermeable barrier.

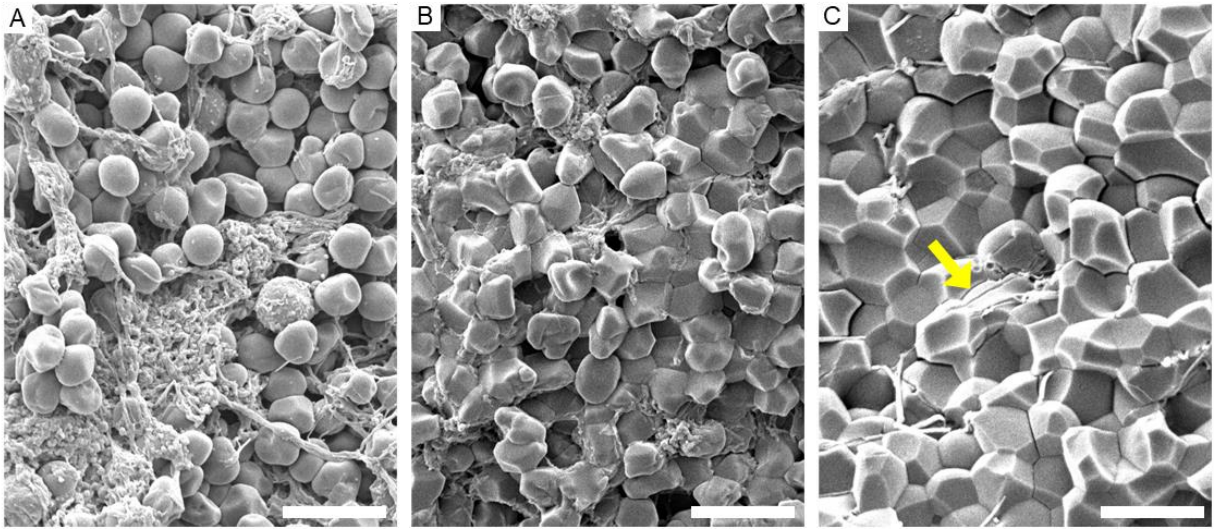

Figure 1: Different densities of red blood cell-rich areas: Range of different densities withing RBC-rich thrombi ranging from loosely arranged RBCs (A), over more densely packed RBCs (B), to tightly packed polyhedrocytes (C). Yellow arrow marks wire-shaped notches attributed to fibrin fibers. scale bar = 10 µM; RBC= red blood cell

These varying densities of packaging likely reflect platelet-mediated clot contraction, which pulls fibrin fibers and compacts red blood cells into densely packed polyhedrocytes.[13,14] Notably, while fibrin fibers are largely absent between polyhedrocytes, wire-shaped notches are visible on the polyhedrocytes. These notches are likely compression marks left by fibrin fibers after clot contraction (indicated by the yellow arrow in Figure 1C; more examples are shown in Supplemental Figure 1). The diameter of these wire-shaped notches averages around 194.8 nm ± 78.7 nm, which roughly matches the size of fibrin fibers typically found in uncontracted RBC-rich areas. While some thrombi showed complete contraction with only polyhedrocytes (n=4), most thrombi had different areas with varying RBC densities (n=11), indicating uneven contraction within the thrombus. Some thrombi lacked highly packed polyhedrocytes (n=7), possibly due to incomplete clot contraction or a limited number of platelets in the thrombus.

Platelet-rich thrombus structures

The ultrastructural appearance of platelet-rich structures greatly differs from RBC-structures. Platelet-rich thrombus material appears as a densely compacted structures of aggregated platelets with low porosity observed in 12 of the 17 thrombi (Figure 2). In five of the investigated thrombi no specific platelet-rich thrombus structures could be defined.

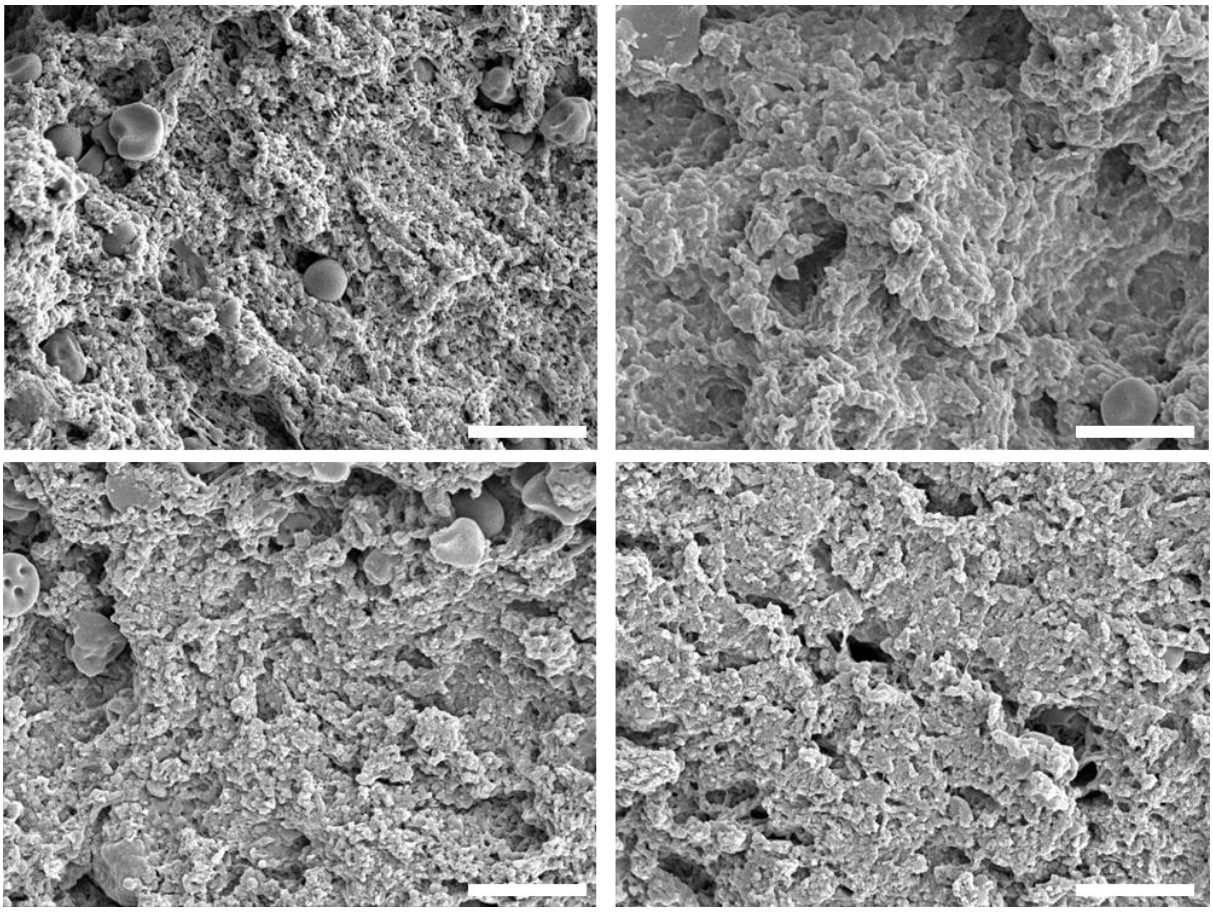

Figure 2: Aggregated platelet-rich area. Regions of densely aggregated platelets in acute ischemic stroke thrombi. Scale bar = 10 µm

Fibrin-rich thrombus structures

Fibrin was a key structural element of all investigated thrombi that typically appears in branched networks of fibers with a diameter of approximately 210-250 nm. Besides its presence in other areas, various specific morphologies of fibrin networks were observed, ranging from compact and densely branched regions with loose ends (spongy fibrin, n=3, Figure 3A) to a more porous network composed of distinct, organized fibrin strands and small fibrin bundles (branched fibrin, n=5, Figure 3B). RBCs can become intertwined within the branched fibrin network, which often forms a layered structure at the transition of different thrombus areas. Occasionally, thick fibrin

bundles are observed, where individual fibrin fibers are aligned into bundles typically around 4 µm in thickness (n=2, Figure 3C), often interspersed with platelet aggregates (Figure 3C, yellow arrows).

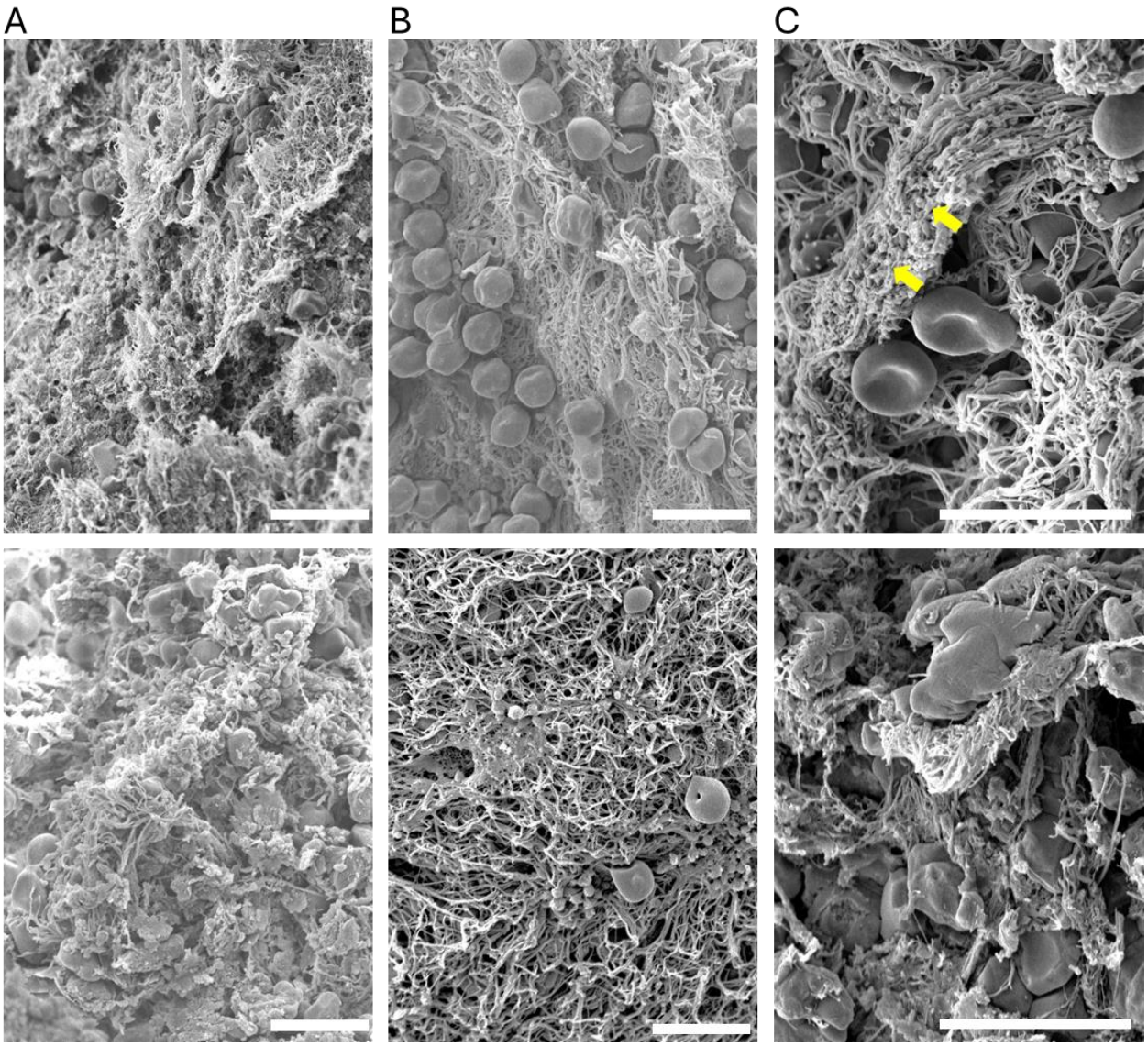

Figure 3: Different morphological fibrin structures. Representative images of the different morphological fibrin structures observed on the inside of AIS thrombi. The different structures can be defined as (A) spongy fibrin containing a compact and densely branched fibrin with loose ends, (B) branched fibrin network consisting of a porous and organized fibrin network, and (C) fibrin bundles interspersed with platelet aggregates (yellow arrow). Scale bar 10 µM

Overall thrombus composition

When studying the overall composition of AIS thrombi, we found that they are generally composed of a combination of RBC-rich, platelet-rich or fibrin-rich structures. Although all three types of structures are typically present in each thrombus, their

relative proportions can vary significantly. Most thrombi have a mixed composition (n=10) of all three thrombus structures, but some thrombi are composed primarily of RBC-rich material (n=5), while others are predominantly made up of platelet-rich material (n=2) as illustrated in Figure 4. A comparison of each thrombus type using conventional histology, confirming the presence of platelets and fibrin within the dense regions, is shown in Supplemental Figure 2. Interestingly, whereas platelet-dominant thrombi are almost completely devoid of RBCs, RBC-rich thrombi consistently contain some platelet and fibrin-rich areas.

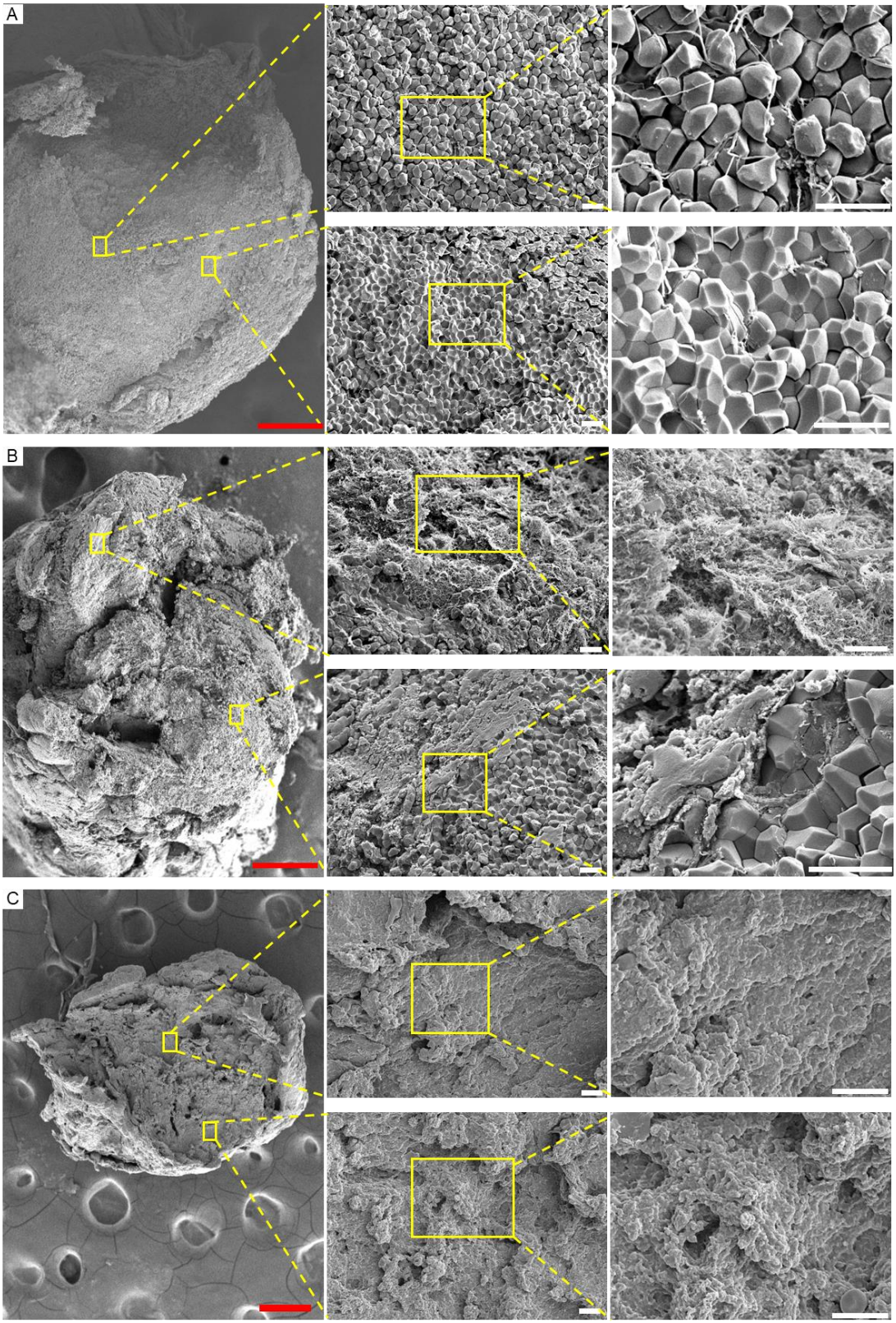

Figure 4: Different thrombus types found acute ischemic stroke patients. Representative images of the three main thrombus types found in AIS patients (A) red blood cell-rich thrombus mainly composed of RBC, (B) mixed-composition thrombus composed of RBC-rich, fibrin-rich and platelet-rich regions and (C) platelet-rich thrombus mainly composed of platelet-rich regions. Three different magnifications of

each thrombus type are shown. The yellow boxed show the regions that are magnified. Red scale bar = 200 µM; white scale bar = 10 µm

Within a thrombus, RBC-rich and platelet-rich structures can sometimes form clearly delineated zones with large, distinct areas of each thrombus material (Figure 5A) or appear as small islands of one within the other (Figure 5B). Other areas may contain unorganized zones with a mix of single RBCs, platelets, and a branched fibrin network (Figure 5C).

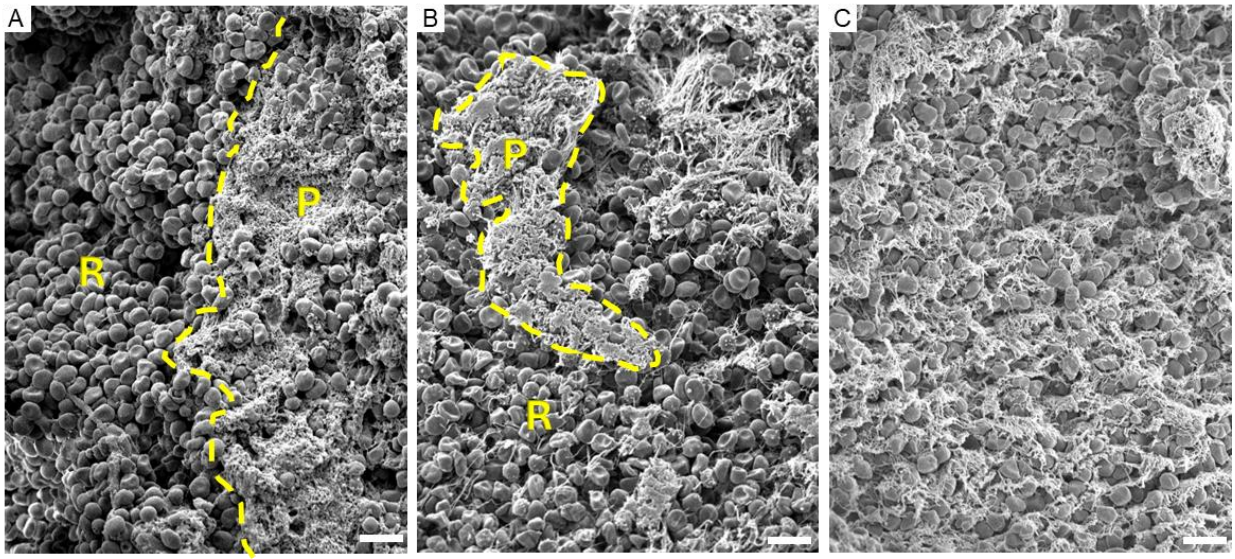

Figure 5: Structural organization of mixed thrombus areas: (A) Delineated zones of RBC-rich material and platelet-rich, (B) small islands of platelets-aggregates within RBCs-rich areas, (C) unorganized zones of RBCs, fibrin and platelets. Scale bar = 10 µM. R= red blood cell rich, P= platelet rich.

Thrombus surface

In addition to examining the interior of AIS thrombi, we also studied the external surface of the thrombi. We found that thrombi typically display a distinct surface that differs from their interior. However, the structure of the surface of one thrombus is not uniform, and various structures can typically be identified. The surface morphologies, shown in Figure 6, include several distinct morphologies: an exterior composed of a porous network of branched fibrin fibers and bundles (Figure 6A); a denser fibrin scaffold covered with aggregated platelets (Figure 6B); a compact surface primarily made up of tightly packed aggregated platelets (Figure 6C), often accompanied by numerous platelet vesicles; and a smooth surface where individual components are indistinguishable, resembling an impermeable seal (Figure 6D). In most thrombi (n=17), the surface of the thrombus contains a mixture of the different morphologies.

Only in 2 thrombi, the surface of the thrombus was completely composed of pack aggregated platelets.

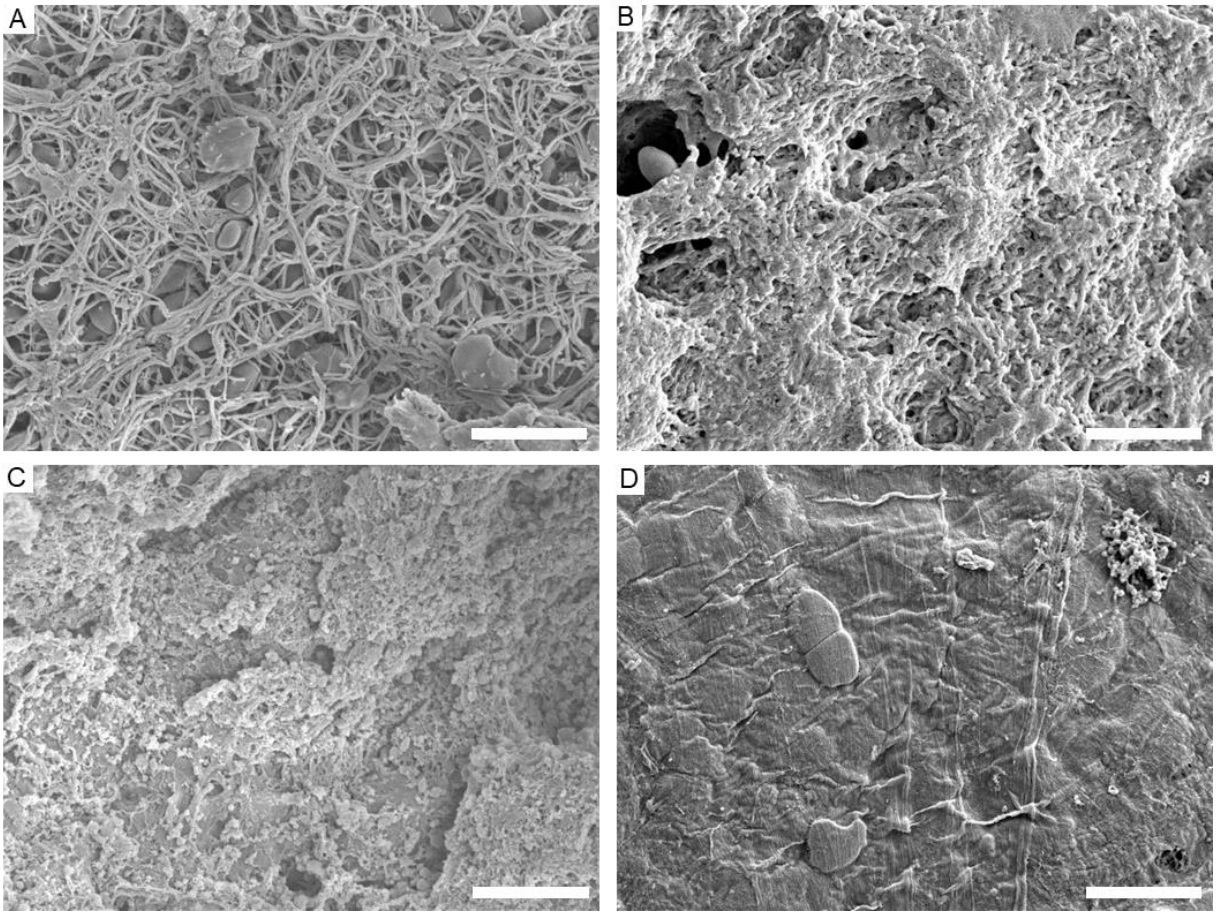

Figure 6: Surface morphologies of AIS thrombi. Different surface morphologies are observed on a thrombus and can vary between different thrombi. Common surface morphologies include: (A) a porous network of branched fibrin fibers and bundles, (B) branched fibrin aligned with aggregated platelet, (C) a compact surface of aggregated platelets, (D) a smooth surface where individual components are indistinguishable. Scale bar = 10 µM.

Interestingly**,** when analyzing the outer layer at the edge of the thrombus, a distinct envelope or shell is occasionally observed, forming a dense barrier around the thrombus (Figure 7). The thickness of this layer can vary throughout the thrombus, typically ranging from approximately 1 µm to 10 µm.

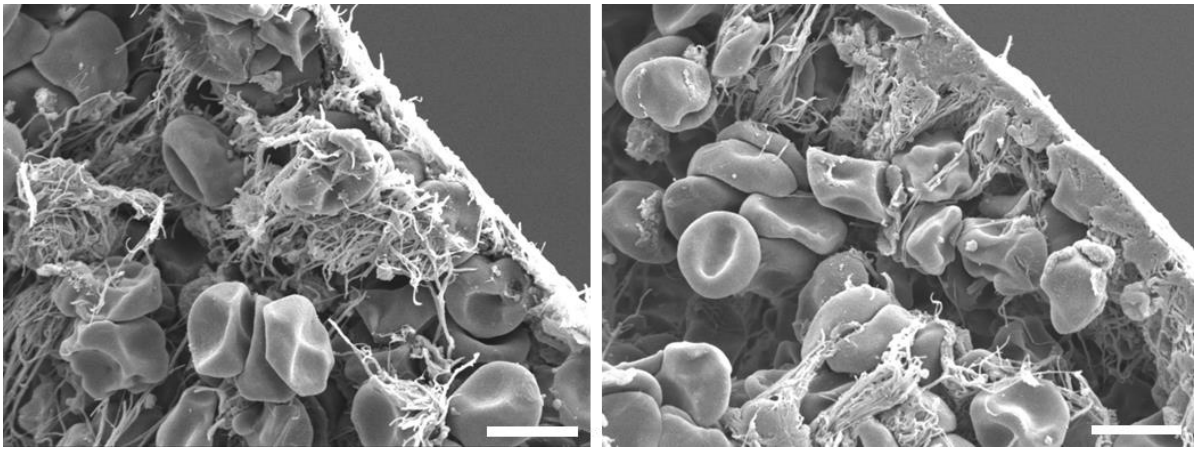

Figure 7: Thrombus envelope. Example of the cross-section of an acute ischemic stroke thrombus at two different regions, indication a varying thickness of the thrombus envelope within the same thrombus. Scale bar = 5 µm

Discussion

In this study, we used SEM to study the ultrastructural organization of patient AIS thrombi. Since the occluding thrombus is the primary target of recanalization therapy in AIS patients, a detailed understanding of the composition of the thrombus can aid in improving recanalization strategies. In recent years, conventional histological analysis has been mainly used to investigate AIS thrombus composition, revealing a heterogeneous composition of stroke thrombi.[4–6,15] Consistent with previous studies, our SEM analyses identified common structural features in these thrombi, including RBC-rich and platelet-rich regions, along with fibrin networks or bundles that extend throughout or in between these areas. Compared to conventional histology, SEM allows for higher-resolution imaging and visualizing 3D surface topography, giving a more accurate representation of the spatial organization of different elements in AIS thrombi. In line with earlier reports[16–20], our SEM imaging of RBC-rich regions revealed differences in the packing density within the thrombus, ranging from areas with loosely organized RBCs to regions containing tightly packed polyhedrocytic RBCs. The compression and deformation of RBC into polyhedrocytes are a morphological sign of clot contraction mediated by the contractile forces of activated platelets on fibrin.[13,14] Interestingly, polyhedrocytes frequently exhibited wire-shaped notches corresponding to the size of individual fibrin fibers. These indentations are likely caused by the strong forces of fibrin on RBCs during clot contraction. The extend of clot contraction varied across the thrombi studied. Some were predominantly composed of tightly packed polyhedrocytes, with occasional intermediate-density RBC regions, while others

lacked well-defined polyhedrocytic RBCs. Several factors may influence clot contraction, likely causing the variation in contraction densities observed both between different thrombi and within individual thrombi. Since platelets are key mediators, both platelet count and functionality can influence the rate and extent of clot contraction.[21] Additionally, high RBC content in thrombi can impede clot contraction.[21]

Using conventional histology, platelet-rich thrombus regions were shown to have a complex structure of besides platelets also dense fibrin, VWF and extracellular DNA.[4] Via SEM, platelet-rich regions consistently appeared as dense structures, in which individual components seem to be fused together, making it difficult to identify separate elements. It is specifically difficult to distinguish fibrin, VWF and NETs, as all three have fiber-like structures and colocalize within platelet-rich regions.[4,22] We conducted a first pilot experiment in which we first performed immunofluorescent VWF and fibrin staining on 5 µm thick sections immediately followed by SEM, confirming the previous findings of VWF colocalization with dense fibrin/platelet-rich regions (Supplemental Figure 3).[4] Further enhancements of antigen-specific methods, such as gold-labeling combined with electron microscopy, or a combination of electron microscopy and fluorescence microscopy could be useful to further unravel the complex structure of these platelet-rich formations.[23,24]

Besides RBCs and platelets, fibrin forms a major component of AIS thrombi that can be organized in different manners. Within RBC-rich regions a thin branched fibrin network was observed as previously described using conventional histology.[4] In some regions, a highly branched and thin spongy fibrin network was observed, which was first described by Khismatullin et al.[16] The differences in organization and thickness of fibrin could arise from variations in factors involved in coagulation and hemostasis.[25–27] Alternatively, the differences observed could be caused by different exposure to rt-PA as was suggested by Mereuta et al. and Khismatullin et. al.[16,19] In our study, we did not observe a clearly defined difference between patients who received intravenous rt-PA treatment or not (data not shown). However, a systematic detection method could be beneficial in investigating this issue.

Recanalization therapy is not always successful, as several structural factors of the thrombus can influence its susceptibility to thrombolysis or mechanical removal. Previously, we and others showed that platelet-rich thrombi show resistance to rt-PA.[8,10] Using SEM images, we identified these platelet-rich regions and noticed the fusion of various components within the dense areas, which may reduce the

accessibility of fibrin and its susceptibility to rt-PA. Similarly, the presence of thick fibrin bundles as shown in this study, could reduce thrombolysis response. Furthermore, the presence of dense polyhedrocytic regions as marker of clot contraction was shown to reduce the rate of external fibrinolysis, due to the reduced porosity, increased fibrin density and reduced surface area accessible to rt-PA.[14,28] The outer layer of AIS thrombi has attracted particular interest because it has been described as a fibrinolytic-resistant shell that encapsulates the thrombus.[9,29] Via classical histology and SEM, this shell was shown to be mainly composed of dense fibrin, VWF, platelets and extracellular DNA.[9,30] Interestingly, we found a distinct outer layer in some but not all thrombi. The organization of the thrombus surface varied between different thrombi and also differed within a single thrombus, ranging from loosely arranged fibrin to much denser and seemingly impermeable platelet aggregates. It is currently unclear what caused the variations observed between patient thrombi and within the thrombus surface of a single patient and its impact on thrombolysis success.

Various thrombus components were also shown to impact MT success. Indeed, recent research indicates that RBC-rich thrombi require less passes to be retrieved during thrombectomy and are more likely to result in a first pass recanalization[7,11,31,32] whereas the presence of dense platelet rich regions including the presence of platelets, dense fibrin, VWF and exDNA, negatively affects recanalization success following MT.[7,11,31–34] RBCs within a thrombus result in a decreases thrombus stiffness and increase deformability, likely enhancing the interaction with the MT devices.[35] However, it is currently not know how the differences in packing of RBCs further influence MT success, but dense polyhedrocytic regions may not interact well with the MT device due to the limited deformability.[18] Furthermore, in venous thromboembolism, it was shown that less contracted clots are more likely to embolize.[36] Further studies are needed to specifically investigate how the structural organization of specific thrombus components can influence MT success.

While SEM allows for increased resolution of thrombus imaging, it does have some limitations. During thrombus retrieval, it is difficult to preserve the initial orientation (distal versus proximal) of the thrombus. Furthermore, we cannot exclude the formation of new thrombus material during occlusion or removal, which could not completely reflect the composition of the initial embolus. In our study, thrombi were sectioned allowing for the examination of both the interior and surface of the thrombus. However, this meant that we could only examine one cross-section of the interior of

the clot. Nevertheless, we have previously demonstrated that examining one section per thrombus, using conventional histology, provides a reliable representation of the entire thrombus.[37] Although not systematically performed, SEM can be used to specifically quantify different thrombus components.[16,17] However, methodological differences in quantification methods between SEM and conventional histology lead to discrepancies in the quantitative results. Large-scale quantitative analyses of AIS thrombi using SEM are challenging due to its labor-intensive nature, though such studies would be helpful for linking structural features with clinical data like etiology, stroke severity, and outcomes. In our study, we did not quantify thrombus components, however it was noted that only a small number of single leukocytes could be visualized, which were not consistently visible across all thrombi (data not shown). This contrasts with the high leukocyte numbers often reported by conventional histology.[4,38,39] Future studies and standardized methods to perform a quantitative analysis of AIS thrombi via SEM could help clarify these variations.

In conclusion, our SEM study reveals various ultrastructural details of both the exterior and interior of AIS thrombi, offering a detailed assessment of their microstructure. This information is essential for better understanding of the heterogeneity of AIS thrombus architecture and could help elucidate the reasons for recanalization failure.

Acknowledgements

We would like to thank the stroke team at AZ Groeninge Hospital (Kortrijk, Belgium) for their support and collaboration in this research.

Sources of funding

This work was supported by Fonds voor Wetenschappelijk Onderzoek - Vlaanderen (research grants G.0A86.13, G.0785.17, and 1509216N to S.F.D.M), by research grants from KU Leuven (OT/14/099 and ISP/14/02L2 to S.F.D.M), and by a research grant from the Queen Elisabeth Medical Foundation (to S.F.D.M).

Authorship Contributions

S.V. and S.F.D.M. designed the study. S.V. performed the experiments. O.F, A.V., F.V.G., P.V., T.A. contributed to data acquisition. SV analyzed data. S.V., S.F.D.M., C.T. and K.V. interpreted the results. S.V. and S.F.D.M. wrote the manuscript. All authors critically reviewed the manuscript.

Disclosure of Conflicts of Interest

The author(s) declared following potential conflicts of interest with respect to the research, authorship, and/or publication to this article: S.V., A.V., F.V.G., C.T., K.V., S.F.D.M. have no relevant conflicts of interest to declare. O.F. is a consultant for iVascular. P.V. received speaker fees from Boehringer-Ingelheim, BMS, Pfizer, Daiichi-Sankyo, and Medtronic. T.A. holds equity for Cereflo Ltd and is a consultant for Anaconda, Cerenovus/Neuravi, Optimize Neurovascular and Rapid medical.

References

1. Menon BK, Al-Ajlan FS, Najm M, Puig J, Castellanos M, Dowlatshahi D, Calleja A, Sohn S Il, Ahn SH, Poppe A, et al. Association of clinical, imaging, and thrombus characteristics with recanalization of visible intracranial occlusion in patients with acute ischemic stroke. *JAMA - J. Am. Med. Assoc.* 2018;320:1017–1026.
2. Zeinhom MG, Khalil MFE, Kamel IFM, Kohail AM, Ahmed SR, Elbassiouny A, Shuaib A, Al-Nozha OM. Predictors of the unfavorable outcomes in acute ischemic stroke patients treated with alteplase, a multi-center randomized trial. *Sci. Rep.* 2024;14:1–9.
3. Yoo AJ, Andersson T. Thrombectomy in acute ischemic stroke: Challenges to procedural success. *J. Stroke*. 2017;19:121–130.
4. Staessens S, Denorme F, François O, Desender L, Dewaele T, Vanacker P, Deckmyn H, Vanhoorelbeke K, Andersson T, De Meyer SF. Structural analysis of ischemic stroke thrombi: Histological indications for therapy resistance. *Haematologica*. 2020;105:498–507.
5. Staessens S, De Meyer SF. Thrombus heterogeneity in ischemic stroke. *Platelets*. 2020;32:331–339.
6. Vandelanotte S, De Meyer SF. Acute Ischemic Stroke Thrombus Composition. *Neuroscience*. 2024;550:11–20.
7. Vandelanotte S, Staessens S, François O, De Wilde M, Desender L, De Sloovere AS, Dewaele T, Tersteeg C, Vanhoorelbeke K, Vanacker P, et al. Association between thrombus composition and first-pass recanalization after thrombectomy in acute ischemic stroke. *J. Thromb. Haemost.* 2024;1–7.
8. Vandelanotte S, François O, Desender L, Staessens S, Vanhoorne A, Van Gool F, Tersteeg C, Vanhoorelbeke K, Vanacker P, Andersson T, et al. Rt-PA resistance is specific for platelet-rich stroke thrombi and can be overcome by targeting non-fibrin components. *Stroke*. 2024;1–10.
9. Di Meglio L, Desilles J-PP, Ollivier V, Nomenjanahary MS, Di Meglio S, Deschildre C, Loyau S, Olivot J-MM, Blanc R, Piotin M, et al. Acute ischemic stroke thrombi have an outer shell that impairs fibrinolysis. *Neurology*. 2019;93:E1686–E1698.
10. Choi MH, Park GH, Lee JS, Lee SE, Lee SJ, Kim JH, Hong JM. Erythrocyte fraction within retrieved thrombi contributes to thrombolytic response in acute ischemic stroke. *Stroke*. 2018;49:652–659.
11. Maekawa K, Shibata M, Nakajima H, Mizutani A, Kitano Y, Seguchi M, Yamasaki M, Kobayashi K, Sano T, Mori G, et al. Erythrocyte-rich thrombus is associated with reduced number of maneuvers and procedure time in patients with acute ischemic stroke undergoing mechanical thrombectomy. *Cerebrovasc. Dis. Extra*. 2018;8:39–49.
12. Boeckh-Behrens T, Schubert M, Förschler A, Prothmann S, Kreiser K, Zimmer C, Riegger J, Bauer J, Neff F, Kehl V, et al. The Impact of Histological Clot Composition in Embolic Stroke. *Clin. Neuroradiol.* 2016;26:189–197.
13. Tutwiler V, Mukhitov AR, Peshkova AD, Le Minh G, Khismatullin RR, Vicksman J, Nagaswami C, Litvinov RI, Weisel JW. Shape changes of erythrocytes during blood clot contraction and the structure of polyhedrocytes. *Sci. Rep.* 2018;8:1–14.
14. Cines DB, Lebedeva T, Nagaswami C, Hayes V, Massefski W, Litvinov RI, Rauova L, Lowery TJ, Weisel JW. Clot contraction: Compression of erythrocytes into tightly packed polyhedra and redistribution of platelets and

fibrin. *Blood*. 2014;123:1596–1603.
15. Staessens S, François O, Brinjikji W, Doyle KM, Vanacker P, Andersson T, De Meyer SF. Stroke Studying Stroke Thrombus Composition After Thrombectomy What Can We Learn? *Stroke*. 2021;52:3718–3727.
16. Khismatullin RR, Nagaswami C, Shakirova AZ, Vrtková A, Procházka V, Gumulec J, MačÁk J, Litvinov RI, Weisel JW. Quantitative Morphology of Cerebral Thrombi Related to Intravital Contraction and Clinical Features of Ischemic Stroke. *Stroke*. 2020;51:3640–3650.
17. Chernysh IN, Nagaswami C, Kosolapova S, Peshkova AD, Cuker A, Cines DB, Cambor CL, Litvinov RI, Weisel JW. The distinctive structure and composition of arterial and venous thrombi and pulmonary emboli. *Sci. Rep.* 2020;10:1–12.
18. Dumitriu LaGrange D, Bernava G, Reymond P, Wanke I, Vargas MI, Machi P, Lövblad KO. A high resolution scanning electron microscopy analysis of intracranial thrombi embedded along the stent retrievers. *Sci. Rep.* 2022;12:1–11.
19. Mereuta OM, Fitzgerald S, Christensen TA, Jaspersen AL, Dai D, Abbasi M, Puttappa T, Kadirvel R, Kallmes DF, Doyle KM, et al. High-resolution scanning electron microscopy for the analysis of three-dimensional ultrastructure of clots in acute ischemic stroke. *J. Neurointerv. Surg.* 2021;13:906–911.
20. Swanepoel AC, Pretorius E. Scanning electron microscopy analysis of erythrocytes in thromboembolic ischemic stroke. *Int. J. Lab. Hematol.* 2012;34:185–191.
21. Tutwiler V, Litvinov RI, Lozhkin AP, Peshkova AD, Lebedeva T, Ataullakhanov FI, Spiller K, Cines DB, Weisel JW. Kinetics and mechanics of clot contraction are governed by themolecular and cellular composition of the blood.pdf. *Blood*. 2016;127:149–159.
22. Krautgartner WD, Klappacher M, Hannig M, Obermayer A, Hartl D, Marcos V, Vitkov L. Fibrin mimics neutrophil extracellular traps in SEM. *Ultrastruct. Pathol.* 2010;34:226–231.
23. Goldberg MW, Fišerová J. Immunogold labeling for scanning electron microscopy. *Methods Mol. Biol.* 2016;1474:309–325.
24. Hayashi S, Ohno N, Knott G, Molnár Z. Correlative light and volume electron microscopy to study brain development. *Microscopy*. 2023;72:279–286.
25. Alisa S. Wolberg, Campbell RA. Thrombin Generation, Fibrin Clot Formation and Hemostasis. *Transfus Apher Sci.* 2008;38:15_23.
26. Pretorius E, Swanepoel AC, Oberholzer HM, Van Der Spuy WJ, Duim W, Wessels PF. A descriptive investigation of the ultrastructure of fibrin networks in thrombo-embolic ischemic stroke. *J. Thromb. Thrombolysis*. 2011;31:507–513.
27. Pretorius E, Steyn H, Engelbrecht M, Swanepoel AC, Oberholzer HM. Differences in fibrin fiber diameters in healthy individuals and thromboembolic ischemic stroke patients. *Blood Coagul. Fibrinolysis*. 2011;22:696–700.
28. Tutwiler V, Peshkova AD, Le Minh G, Zaitsev S, Litvinov RI, Cines DB, Weisel JW. Blood clot contraction differentially modulates internal and external fibrinolysis. *J. Thromb. Haemost.* 2019;17:361–370.
29. Di Meglio L, Philippe Desilles J, Mazighi M, Ho-Tin-Noé B. Thrombolysis-resistant intracranial clot. *Neurology*. 2018;90:1075.
30. Ahn SH, Hong R, Choo IS, Heo JH, Nam HS, Kang HG, Kim HW, Kim JH. Histologic features of acute thrombi retrieved from stroke patients during mechanical reperfusion therapy. *Int. J. Stroke*. 2016;11:1036–1044.

31. Duffy S, Mccarthy R, Farrell M, Thomas S, Brennan P, Power S, O'Hare A, Morris L, Rainsford E, Maccarthy E, et al. Per-Pass Analysis of Thrombus Composition in Patients With Acute Ischemic Stroke Undergoing Mechanical Thrombectomy. *Stroke*. 2019;50:1156–1163.
32. Shin JW, Jeong HS, Kwon HJ, Song KS, Kim J. High red blood cell composition in clots is associated with successful recanalization during intra-arterial thrombectomy. *PLoS One*. 2018;13:1–13.
33. Liu Y, Brinjikji W, Abbasi M, Dai D, Arturo Larco JL, Madhani SI, Shahid AH, Mereuta OM, Nogueira RG, Kvamme P, et al. Quantification of clot spatial heterogeneity and its impact on thrombectomy. *J. Neurointerv. Surg.* 2021;14:neurintsurg-2021-018183.
34. Patel TR, Fricano S, Waqas M, Tso M, Dmytriw AA, Mokin M, Kolega J, Tomaszewski J, Levy EI, Davies JM, et al. Increased perviousness on CT for acute ischemic stroke is associated with fibrin/platelet-rich clots. *Am. J. Neuroradiol.* 2021;42:57–64.
35. Sporns PB, Hanning U, Schwindt W, Velasco A, Buerke B, Cnyrim C, Minnerup J, Heindel W, Jeibmann A, Niederstadt T. Ischemic Stroke: Histological Thrombus Composition and Pre-Interventional CT Attenuation Are Associated with Intervention Time and Rate of Secondary Embolism. *Cerebrovasc. Dis.* 2017;44:344–350.
36. Peshkova AD, Malyasyov D V, Bredikhin RA, Le Minh G, Andrianova IA, Tutwiler V, Nagaswami C, Weisel JW, Litvinov RI, Litvinov I. Reduced Contraction of Blood Clots in Venous Thromboembolism Is a Potential Thrombogenic and Embologenic Mechanism. 2018;2:104–115.
37. Staessens S, Fitzgerald S, Andersson T, Clarençon F, Denorme F, Gounis MJ, Hacke W, Liebeskind DS, Szikora I, van Es ACGM, et al. Histological stroke clot analysis after thrombectomy: Technical aspects and recommendations. *Int. J. Stroke*. 2020;15:467–476.
38. Laridan E, Denorme F, Desender L, François O, Andersson T, Deckmyn H, Vanhoorelbeke K, De Meyer SF. Neutrophil extracellular traps in ischemic stroke thrombi. *Ann. Neurol.* 2017;82:223–232.
39. Staessens S, François O, Desender L, Vanacker P, Dewaele T, Sciot R, Vanhoorelbeke K, Andersson T, De Meyer SF. Detailed histological analysis of a thrombectomy-resistant ischemic stroke thrombus: a case report. *Thromb. J.* 2021;19:1–7.

SUPPLEMENTAL MATERIAL

CHAPTER 7 – ULTRASTRUCTURE OF ACUTE ISCHEMIC STROKE THROMBI VIA SCANNING ELECTRON MICROSCOPY: AN OBSERVATIONAL STUDY

Sarah Vandelanotte, MSc [1], Olivier François, MD[2], Alexander Vanhoorne, MD[3], Fréderick Van Gool, MD[2], Claudia Tersteeg, PhD[1], Karen Vanhoorelbeke, PhD[1], Peter Vanacker, MD[3,4,5], Tommy Andersson, MD[2,6] and Simon F. De Meyer, PhD[1]

SUPPLEMENTAL FIGURES

Supplemental Figure 1

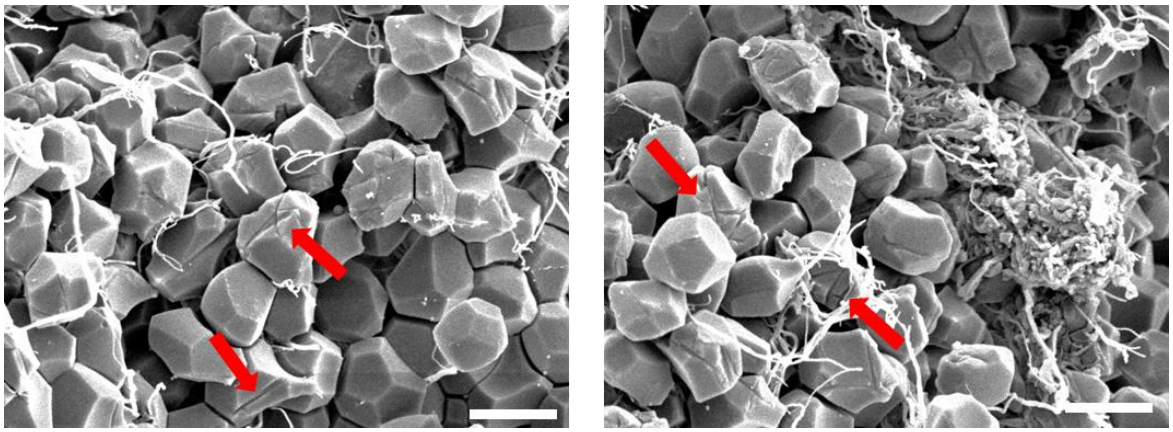

Supplemental Figure 1: Wire-shaped notches in polyhedrocytes. High magnification of dense RBC-rich region with polyhedrocytes. Wire-shaped notches (red arrows) likely originating from compression marks left by fibrin fibers after clot contraction. Scale bar = 5µM

Supplemental Figure 2

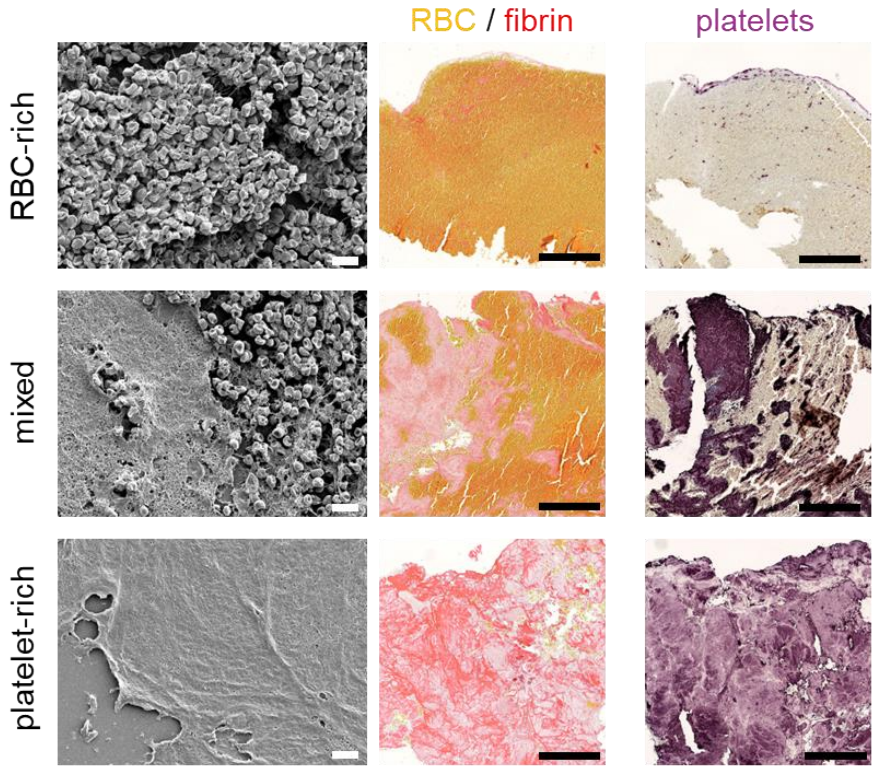

Supplemental Figure 2: Different thrombus types via SEM and conventional histology. Representative images of the three main thrombus types analyzed using SEM and conventional histological stains. Thrombus sections were stained with Martius Scarlet Blue to visualize RBCs (yellow) and fibrin (dark pink/red). Immunohistochemical stainings was used to identify platelets (CD42b; purple). White scale bar = 10 µM; Black scale bar = 100 µM

Supplemental Figure 3

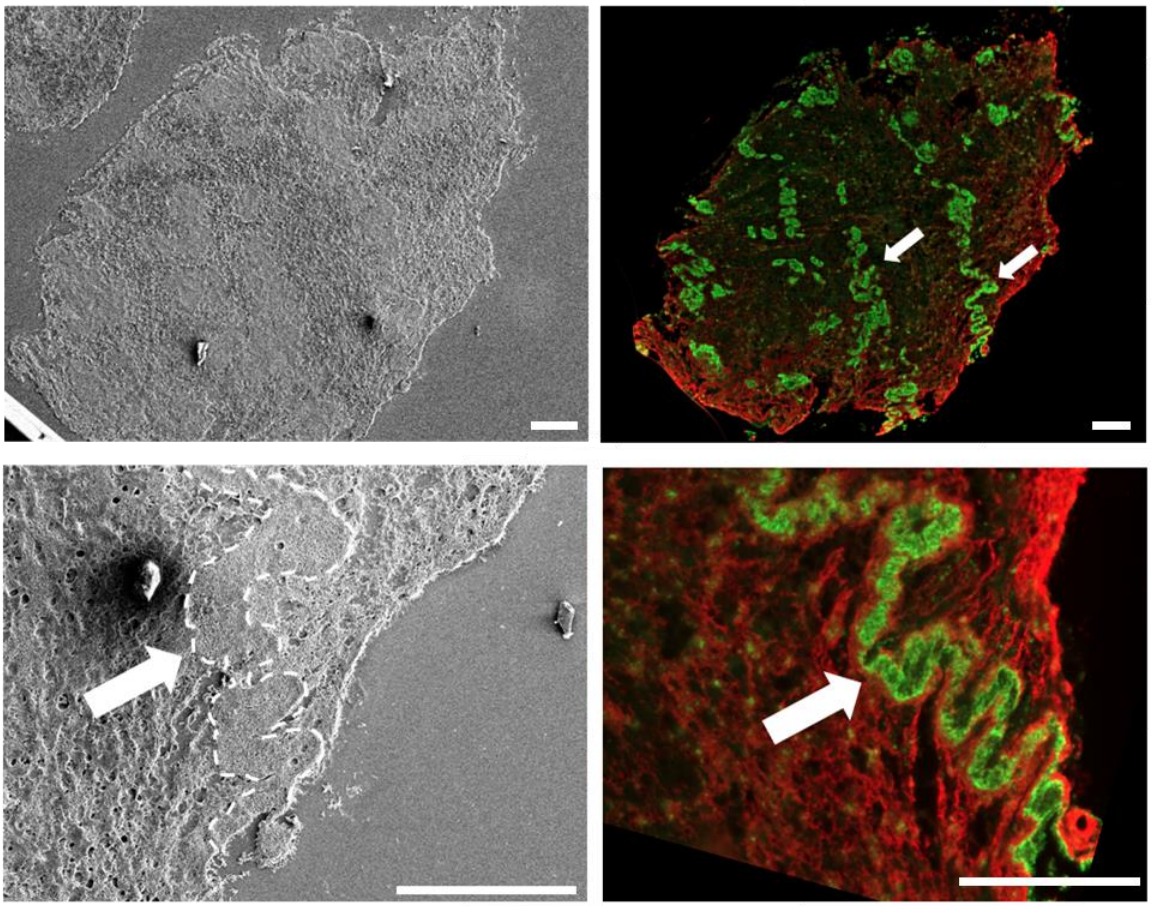

Supplemental Figure 3: Colocalization of dense platelet-rich areas and von Willebrand Factor. Immunofluorescent VWF (green) and Fibrin (Red) staining of 5 µm thrombus section followed by SEM. Colocalization (white arrows) of VWF areas and dense platelets rich regions. Scale bar = 100 µm

CHAPTER 8 - DISCUSSION AND FUTURE PERSPECTIVES

Acute ischemic stroke (AIS) arises when a blood clot obstructs the blood flow to a specific region of the brain, leading to rapid and often irreversible neurological damage. It is one of the leading causes of death and sustained disability worldwide, affecting over 12.2 million new patients a year.[1,2] Current therapy aims at a fast and complete recanalization through pharmacological thrombolysis using recombinant tissue plasminogen activator (rt-PA) or via mechanical removal of the obstructing clot via mechanical thrombectomy (MT), or a combination of both. Unfortunately, current recanalization therapies are often unsuccessful or not applicable, leading to poor patient outcomes.[3–5] Since the obstructing thrombus is the main target of both recanalization strategies, its characteristics and composition likely impact recanalization success. This PhD thesis aimed to better understand how thrombus composition affects the effectiveness of pharmacological and mechanical recanalization. In recent years, our understanding on the composition of stroke thrombi has greatly improved thanks to the availability to human AIS thrombi obtained through MT. AIS thrombi are highly heterogeneous and have a complex composition involving red blood cells (RBC), platelets, von Willebrand factor (VWF), and fibrin, alongside inflammatory components such as leukocytes and neutrophil extracellular traps (NETs).[6–9] Staessens et al. described the presence of two distinct thrombus materials: RBC-rich and platelet-rich thrombus areas.[6] RBC-rich thrombus areas have a rather simple structure of densely packed RBCs in a thin meshwork of fibrin. This is in contrast to the complex platelet rich areas consisting of platelets, dense fibrin, VWF, leukocytes and extracellular DNA.[6]

AIS thrombus composition: a determinator of recanalization success

This PhD thesis revealed the importance of the thrombus composition as a determinator of recanalization success following pharmacological thrombolysis or MT. Indeed, using freshly retrieved patient AIS thrombi, we showed that the rt-PA mediated thrombolysis efficacy is directly linked to the thrombus composition.[10] Thrombi with a high RBCs content contain low amounts of VWF, platelets and DNA and were particularly susceptible to rt-PA-mediated lysis. Conversely, thrombi with a low RBC content have elevated amounts of VWF, platelets, and DNA and showed resistance to rt-PA.[10] Our results are in line with clinical observations that patients with early recanalization show diagnostic imaging signs linked to RBC-rich thrombi and provide

an intriguing starting point for developing new thrombolytic strategies focusing on the platelet-rich, rt-PA resistant thrombi.[11,12]

We further demonstrated the importance of thrombus composition as determinator of recanalization success following MT. Nowadays, interventional radiologists do not only strive towards complete recanalization but towards complete recanalization in the first pass (first pass recanalization (FPR), since it has been linked to improved neurological outcome and decreased mortality rates.[13–22] Investigation of over 260 patient AIS thrombi revealed that thrombi successfully retrieved in a single pass contain significantly higher amounts of RBCs, lower fibrin levels, and a reduced exDNA level compared with thrombi that required multiple passes to achieve near-complete/complete recanalization.[23] Our findings are also in line with recent findings showing higher amounts of RBCs or lower amounts of platelets in thrombi from cases that achieved FPR.[24,25]

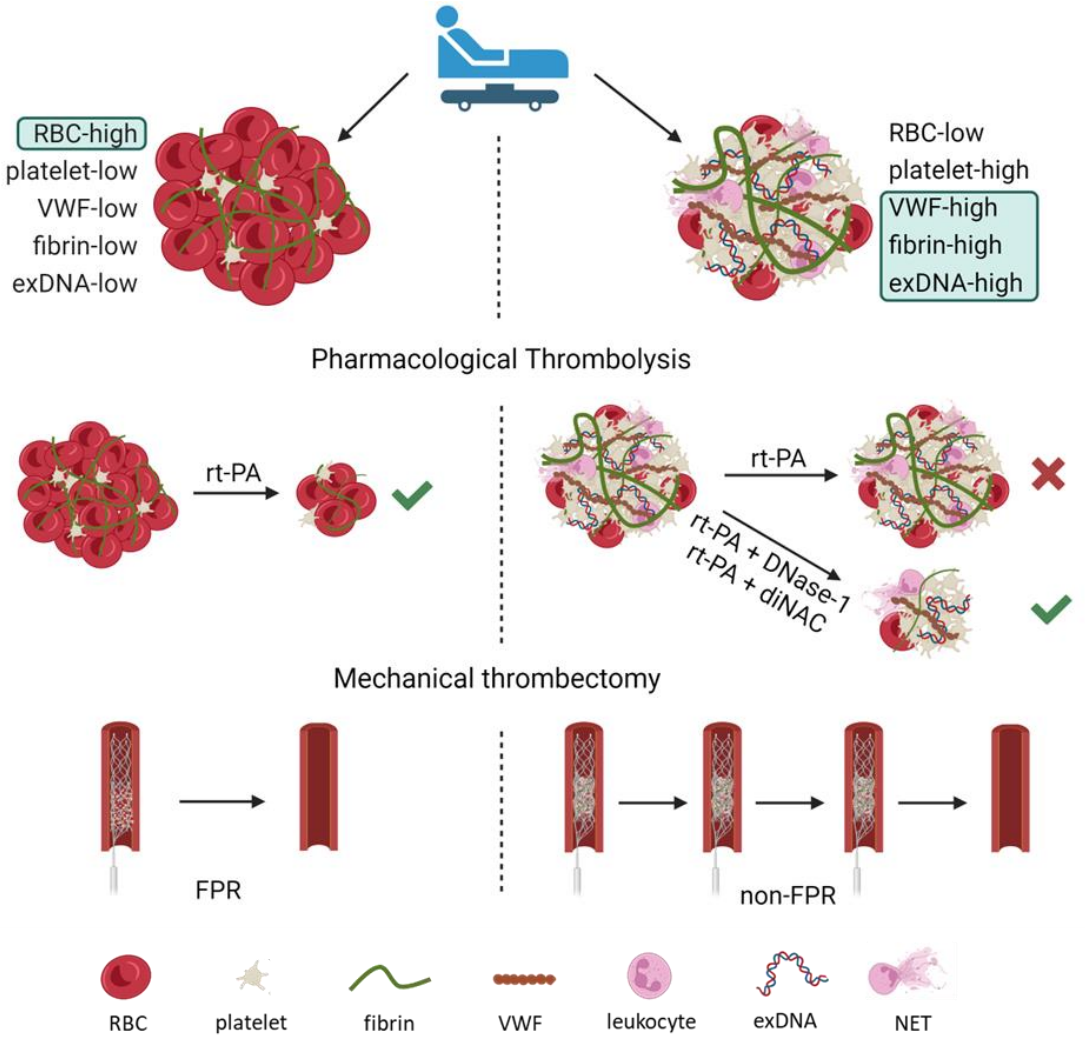

Figure 1: Thrombus composition a determinator of recanalization success. Patient AIS thrombi typically contain elevated levels of RBCs combined with low

platelet, fibrin, VWF and exDNA levels or low RBCs levels combined with high platelet, fibrin, VWF and exDNA levels. In this thesis, we demonstrated that RBC-high thrombi are more susceptible to rt-PA mediated thrombolysis and are linked with FPR. RBC-low thrombi and especially due to the high VWF, exDNA and fibrin levels, show resistance to rt-PA and are less likely to obtain a FPR. Additionally, the observed rt-PA resistance in RBC-low thrombi can be overcome by targeting other structural factors such as DNA using DNase-1 or VWF using diNAC.

Taken together, our results further highlight the importance of thrombus composition as a determinator of recanalization success, with thrombi that are rich in RBC and low in platelet, VWF, dense fibrin and exDNA being linked to fast and efficient recanalization either via pharmacological thrombolysis or MT, as schematically illustrated in Figure 1.

Towards improved recanalization strategies

Interestingly, in this PhD project we discovered that targeting non-fibrin components of rt-PA resistant thrombi such as VWF and exDNA, can specifically improve thrombolysis in rt-PA resistant thrombi. We demonstrated the beneficial effect of the DNA-degrading enzyme DNase-1, consistent with earlier research indicating its prothrombolytic properties.[26–28] Interestingly, we showed for the first time that this beneficial effect is specific to RBC-low, rt-PA resistant thrombi and that no additional effect was obtained in thrombi rich in RBCs.[10] Similarly, we explored the potential of targeting VWF within the thrombus. Previous studies demonstrated the thrombolytic effect of the reducing agent NAC in an experimental stroke mouse model.[29] Kim et al. further highlighted the superior efficacy of the dimerized form of NAC in the lysis of platelet-rich thrombi in an in vitro stenosis model.[30] In our study, we observed enhanced thrombolysis with diNAC combined with rt-PA, particularly in rt-PA resistant thrombi.[10] Interestingly, when combining rt-PA, DNase-1 and diNAC no additional improvement of thrombolysis was observed.[10] The exact reason requires further investigation. However, from both clinical and economic perspectives, it is noteworthy that achieving the same maximal thrombolytic effect with a combination of two pharmacological agents instead of three could offer advantages in terms of cost and safety. However, the safety aspects still need thorough evaluation in patients.

Our results warrant further investigation of other, potentially more potent thrombolytic approaches targeting VWF or DNA. The VWF-cleaving enzyme, ADAMTS13, previously emerged as an intriguing and promising enzyme to target VWF in the

context of ischemic stroke.[31,32] Our lab showed the effectiveness of ADAMTS13 in an experimental stroke mouse model with rt-PA resistant thrombi.[31] The effect of ADAMTS13 is highly dose dependent, as demonstrated in an in vitro arterial stenosis model where a low dose of ADAMTS13 had no impact on the lysis of occlusions.[30,33] Notably, the use of a constitutively active ADAMTS13 variant, referred to as caADAMTS13, yielded efficient restoration of blood flow even at lower concentrations.[32] Ongoing research currently further investigates the effect of ADAMTS13 in the lysis of different types of human AIS thrombi.

The observed improved thrombolytic effect of DNase-1 or diNAC in combination with rt-PA may hold the potential to increase the therapeutic use of rt-PA. Currently the use of rt-PA in clinical settings comes with the risk of intracerebral hemorrhage and its use is therefore restricted by multiple contra-indications and the limited time-window.[34] Since no thrombolytic effect was observed when using DNase-1 or diNAC treatment without rt-PA (preliminary unpublished data and Ducroux et.al.[26]), a possible synergistic effect between rt-PA and DNase-1 or diNAC could be suggested. This synergetic effect could potentially allow for the use of lower concentrations of t-PA, in both rt-PA resistant and rt-PA susceptible thrombi, potentially reducing the risk of hemorrhage and extending the therapeutic window. Interestingly, we are currently investigating the use of DNase-1 or diNAC in combination with lower rt-PA dosages. Preliminary results in our in vitro model using patient thrombi, show indeed similar results as standard rt-PA dose in combination with DNase-1 or diNAC. However, further investigation is needed to translate these lower in vitro concentrations to lower in vivo or in human concentrations.

Our thrombus specific treatment responses raise the question whether a patient-personalized protocol for thrombolysis based on thrombus composition would be needed. Due to the emerging nature of ischemic stroke, it is crucial to initiate treatment as soon as possible. We believe that, if proven safe, a cocktail of thrombolytic agents targeting both fibrin components using rt-PA and non-fibrin components using either DNase-1 or diNAC, could offer a potential ‘one size fits all’ approach to thrombolysis, regardless of the specific thrombus composition.

New insights of thrombus composition beyond traditional histology

In addition to conventional histology, advanced microscopy techniques have the potential to reveal more detailed and comprehensive aspects of thrombus architecture. Scanning electron microscopy (SEM) provides high-resolution imaging and enables visualization of 3D surface topography, giving a more accurate representation of the spatial organization of different elements in AIS thrombi. We and others described various structural thrombus components identified via SEM such as polyhedrocytes, different fibrin organizations and the presence of an outer shell.[35–41] Di Meglio et al found that this outer shell shows resistance to fibrinolysis.[41] Interestingly, we found that the organization of the thrombus surface varied between different thrombi and also differed within a single thrombus, ranging from loosely arranged fibrin to much denser and seemingly impermeable platelet aggregates. Future studies should focus on further evaluating the role of different structural organizations in therapy response. Since SEM cannot specifically differentiate fibrin, VWF, and NETs, due to their similar fiber-like structures, future studies should emphasize on using antigen-specific techniques such as CLEM (Correlative Light and Electron Microscopy), which combines the strengths of fluorescence microscopy (FM) and SEM, or employing gold-labeling techniques with SEM.[42–45] Development of standardized or automated methods to analyze SEM images of AIS thrombi could increase the possibility to perform large scale analysis to link structural features with patient clinical data. A novel approach recently adapted to stroke thrombi is the use of spatial transcriptomics.[46] Spatial transcriptomics allows to analyze spatial distribution of various gene expression pathways involved in inflammation, embolization, thrombolysis response.[46,47] The high cost, labor intensiveness and complex data analysis of spatial transcriptomics could limit the large scale use of spatial transcriptomics in the context of stroke thrombus composition.

In addition to high-resolution imaging and detailed spatial transcriptomics, obtaining a 3D image of the thrombus using light-sheet fluorescent microscopy, may also be important for understanding its internal structural organizations. Full 3D visualization of an entire thrombus could for example improve our understanding of the thrombus shell or the distribution of platelet-rich thrombus regions. Currently, we are

investigating the potential of visualizing whole AIS thrombi using light-sheet microscopy. Some challenges include (1) achieving complete thrombus clearance to minimize light scattering and absorption and (2) ensuring the efficient penetration of specific antibodies deep within the thrombus. Figure 2 shows a first 3D image, obtained with the ZEISS 7 lightsheet microscope of a small thrombus that was stained for fibrin (green), VWF (pink) and platelet (red) and in which various previously described structural elements can be recognized. We are currently further optimizing the imaging protocols to yield better 3D images with increased resolution.

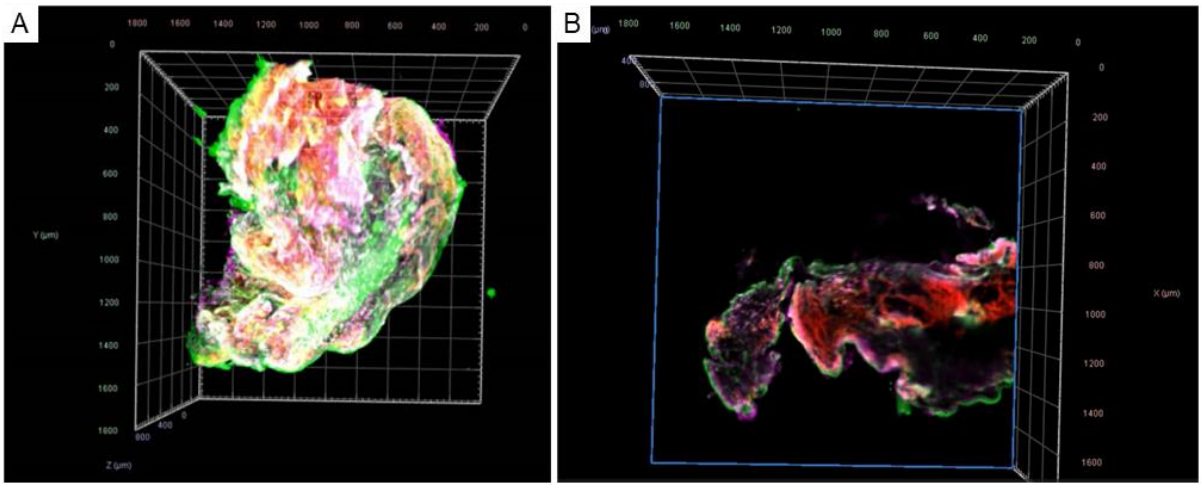

Figure 2: Three-dimensional image of human AIS thrombus. Three-dimensional image of AIS thrombus visualizing fibrin (green), VWF (pink) and platelet (red) within the thrombus. (A) general overview of the thrombus. (B) cross-section at a random position within the thrombus. Images taken with ZEISS Lightsheet 7 microscope, 5x objective.

In vitro AIS clot analogs as model to study therapy resistance

Patient AIS thrombi are crucial for studying therapy responses but are often limited by their unpredictable availability and composition, leading to increased interest in using in vitro clot analogs. Various protocols have been described to generate clot analogs each with their specific advantages and limitations.[7,48–55] Based on previous protocols and our increased understanding of the composition of human AIS thrombi, we developed a standardized model to generate AIS clot analogs with diverse compositions, closely mimicking patient AIS clots. Using our method, three AIS clot analogs were developed that mirror three common clot types observed in patients: RBC-rich, platelet-rich, or mixed composition clots. Conventional histology as well as SEM revealed key features of patient AIS thrombi in our in vitro clot analogs, including

the colocalization of VWF in platelet-rich areas[6], deformed and polyhedral RBCs[56,57] and the presence of an distinct outer surface[41,58].

While the use of AIS analogs may have its limitations, the specific characteristics of our in vitro clot analogs make them an ideal model for advancing the field in several ways. Indeed, we demonstrated that RBC-rich clot analogs show an increased susceptibility to rt-PA mediated thrombolysis compared to mixed or platelet-rich clots analogs. This is in line with our results on patient thrombi and clinical observations that linked early recanalization after rt-PA treatment with higher arterial density measured in Hounsfield units on computed tomography (CT) scans, a radiological indicator of RBC-rich thrombi.[11,59–62] Furthermore, our AIS clot analogs are highly suitable to investigate susceptibility of newly developed thrombolytic strategies. For example, in the future we will use our clot analogs to investigate the potential of specifically targeted rt-PA-loaded vesicles in the lysis of thrombi with different compositions. Additionally, our AIS clot analogs with varying compositions can aid in the understanding of thrombectomy related characteristics such as thrombus stiffness, deformability and fragmentation. Finaly, specific characteristics of the thrombi using clinical imaging protocols, could assist in predicting thrombus composition in patients.

Future perspectives: From Laboratory Testing to Clinically Relevant Applications

The findings from this PhD research could be highly relevant for clinical applications. The new insights into the composition of stroke thrombi and their effect on recanalization strategies are no longer merely a subject of basic research but have been finding their way into translational and clinical research. For example, clinical trials are being set up to investigate the beneficial effect of targeting DNA or VWF in AIS patients. Indeed, the use of the clinically available form of DNase-1, Dornase alfa (Pulmozyme; F. Hoffmann-La Roche, Basel, Switzerland) is presently being investigated as adjuvant therapy for AIS in several clinical trials. The EXTEND-IA DNase trial (NCT05203224) is a phase 2 clinical trial assessing the intravenous administration of Dornase Alfa as adjuvant thrombolytic alongside rt-PA to hopefully improve recanalization. In the NETS-Target (NCT04785066) and ReSCInD (NCT05880524) phase 2 clinical trials, Dornase alfa will be administered after recanalization to target distal occlusions or reduce systemic inflammation after AIS, respectively. Furthermore, a phase 2 clinical trial investigating the safety of

intravenous NAC treatment in combination with alteplase is ongoing (NCT04920448). It will be interesting to see the outcomes of these clinical trials, hopefully showing improved outcomes in AIS patients.

Further advancements to improve the effectiveness of DNase-1 are currently being investigated. Indeed, besides DNase-1, DNase-1L3 is an endogenous enzyme that clears DNA and NETs from circulation. DNase-1 mainly targets double-stranded DNA, while DNase-1L3 digests various forms, including chromatin-bound DNA. Efficient NET degradation likely requires both enzymes.[63,64] Recently a recombinant human DNase1/DNase1L3 variant was developed, combining key functions of both enzymes.[65] Similarly, the company Neutrolis developed NTR-441, an enhanced DNase1L3 analog designed for systemic activity after intravenous injection, now in phase-1 clinical trials for COVID (NCT04941183). Future studies could explore the use of DNase-1L3 variants in AIS and this could be the focus of future follow-up clinical trials.

Novel insights into thrombus composition are also shaping the future of MT techniques. These insights drive technical advances in the development of new devices and approaches, enabling more effective, safer, and personalized treatments. The NIMBUS Geometric Clot Extractor® (NIMBUS, Cerenovus, Irvine, CA) for example has a specific architecture consisting of a proximal spiral portion followed by a distal regular mesh to facilitate the removal of tough fibrin-rich thrombi,[66] and was proven to increase MT effectiveness in the removal of challenging thrombi.[67–69] Another example is the development of a new aspiration catheter with a hydro-separator technology, showing improved efficacy in removing challenging experimental large soft, fragile clots, and stiff clots in tortuous anatomy (Irvine Neurovascular, CA, USA).[70] Given our findings that exDNA is particularly abundant in thrombi that are challenging to retrieve, the application of adhesive coatings designed to specifically bind to DNA could be highly beneficial for enhancing thrombus attachment to mechanical thrombectomy. Interestingly, Skarbek et. al. indeed developed a chemical surface modification using a DNA-binding compound, which can be applied to all commercially available MT devices, leading to a reduction of distal embolization.[71]

Unlike the general one-size-fits-all approach we propose for thrombolysis treatment, we believe that patient-personalized protocols could be beneficial in the context of MT.

This thrombus-specific recanalization strategy depend on the prior identification of thrombus composition, a capability currently being developed through emerging technologies. Advancements in imaging techniques and interpretation resulted in the identification of various signs that can be linked with thrombus composition. The presence of a hyperdense artery sign on CT scan, or susceptibility vessel sign on magnetic resonance imaging at the site of occlusion is associated with a higher RBC content, while its absence is associated with thrombi richer in fibrin and platelets.[12,59,61,72–77] Furthermore, new technologies such as electrochemical impedance spectroscopy combined with machine learning, have the potential to improve the accuracy and reliability of predicting thrombus composition in MT procedures.[78–80] Tailoring treatment based on the composition could especially be helpful in aiding the choice of MT device to improve FPR rate.

General Conclusion

In conclusion, this PhD thesis provides valuable new insights into how specific thrombus components impact the success of recanalization through rt-PA-mediated thrombolysis and MT. Moreover, these insights were used to demonstrate the effectiveness of novel thrombolytic agents in the lysis of stroke thrombi that are resistant to the currently used rt-PA. Additionally, SEM imaging allowed for detailed ultrastructural analysis of AIS thrombi, deepening our understanding of thrombus composition. These findings have the potential to significantly influence the future of AIS therapy, and it will be exciting to see how they contribute to its evolution in the coming years.

References

1. GBD 2019 Stroke Collaborators. Global, regional, and national burden of stroke and its risk factors, 1990-2019: A systematic analysis for the Global Burden of Disease Study 2019. Lancet Neurol. 2021;20(10):1–26.
2. Feigin VL, Brainin M, Norrving B, Martins S, Sacco RL, Hacke W, et al. World Stroke Organization (WSO): Global Stroke Fact Sheet 2022. International Journal of Stroke. 2022;17(1):18–29.
3. Menon BK, Al-Ajlan FS, Najm M, Puig J, Castellanos M, Dowlatshahi D, et al. Association of clinical, imaging, and thrombus characteristics with recanalization of visible intracranial occlusion in patients with acute ischemic stroke. JAMA - Journal of the American Medical Association. 2018;320(10):1017–26.
4. Zeinhom MG, Khalil MFE, Kamel IFM, Kohail AM, Ahmed SR, Elbassiouny A, et al. Predictors of the unfavorable outcomes in acute ischemic stroke patients treated with alteplase, a multi-center randomized trial. Sci Rep. 2024;14(1):1–9.
5. Yoo AJ, Andersson T. Thrombectomy in acute ischemic stroke: Challenges to procedural success. J Stroke. 2017;19(2):121–30.
6. Staessens S, Denorme F, François O, Desender L, Dewaele T, Vanacker P, et al. Structural analysis of ischemic stroke thrombi: Histological indications for therapy resistance. Haematologica. 2020;105(2):498–507.
7. Staessens S, De Meyer SF. Thrombus heterogeneity in ischemic stroke. Platelets. 2020;32(3):331–9.
8. Ho-Tin-Noé B, Desilles JP, Mazighi M. Thrombus composition and thrombolysis resistance in stroke. Res Pract Thromb Haemost. 2023;7(4):100178.
9. Vandelanotte S, De Meyer SF. Acute Ischemic Stroke Thrombus Composition. Neuroscience. 2024;550(December 2023):11–20.
10. Vandelanotte S, François O, Desender L, Staessens S, Vanhoorne A, Van Gool F, et al. Rt-PA resistance is specific for platelet-rich stroke thrombi and can be overcome by targeting non-fibrin components. Stroke. 2024;(May):1–10.
11. Puig J, Pedraza S, Demchuk A, Daunis-i-Estadella J, Termes H, Blasco G, et al. Quantification of thrombus Hounsfield units on noncontrast CT predicts stroke subtype and early recanalization after intravenous recombinant tissue plasminogen activator. American Journal of Neuroradiology. 2012;33(1):90–6.
12. Tang SZ, Sen J, Goh YG, Anil G. Susceptibility vessel sign as a predictor for recanalization and clinical outcome in acute ischaemic stroke: A systematic review and meta-analysis. Journal of Clinical Neuroscience. 2021;94:159–65.
13. Jindal G, Carvalho HDP, Wessell A, Le E, Naragum V, Miller TR, et al. Beyond the first pass: Revascularization remains critical in stroke thrombectomy. J Neurointerv Surg. 2019;11(11):1095–9.
14. Akpinar CK, Ozdemir AO, Gurkas E, Bilgic AB, Aykac O, Inanc Y, et al. Favorable first-pass recanalization rates with NeVa^{TM} thrombectomy device in acute stroke patients: Initial clinical experience. Interventional Neuroradiology. 2021;27(1):107–13.
15. Hassan AE, Dibas M, Sarraj A, Ghozy S, El-Qushayri AE, Dmytriw AA, et al. First pass effect vs multiple passes complete reperfusion: A retrospective study. Neuroradiology Journal. 2021 Jun 1;0(0):1–7.
16. Kang DH, Kim BM, Heo JH, Nam HS, Kim YD, Hwang YH, et al. Effects of first pass recanalization on outcomes of contact aspiration thrombectomy. J Neurointerv Surg. 2020;12(5):466–70.

17. Abbasi M, Liu Y, Fitzgerald S, Mereuta OM, Arturo Larco JL, Rizvi A, et al. Systematic review and meta-analysis of current rates of first pass effect by thrombectomy technique and associations with clinical outcomes. J Neurointerv Surg. 2021;13(3):212–6.
18. Abdullayev N, Maus V, Behme D, Barnikol UB, Kutschke S, Stockero A, et al. True first-pass effect in basilar artery occlusions: First-pass complete reperfusion improves clinical outcome in stroke thrombectomy patients. Journal of Clinical Neuroscience. 2021;89:33–8.
19. Bai X, Zhang X, Yang W, Zhang Y, Wang T, Xu R, et al. Influence of first-pass effect on recanalization outcomes in the era of mechanical thrombectomy: a systemic review and meta-analysis. Neuroradiology. 2021;63(5):795–807.
20. Den Hartog SJ, Roozenbeek B, Boodt N, Bruggeman AAE, Van Es ACGM, Emmer BJ, et al. Effect of first pass reperfusion on outcome in patients with posterior circulation ischemic stroke. J Neurointerv Surg. 2022;14(4):333–40.
21. Jadhav AP, Desai SM, Zaidat OO, Nogueira RG, Jovin TG, Haussen DC, et al. First Pass Effect with Neurothrombectomy for Acute Ischemic Stroke: Analysis of the Systematic Evaluation of Patients Treated with Stroke Devices for Acute Ischemic Stroke Registry. Stroke. 2022 Feb 1;53(2):E30–2.
22. Nikoubashman O, Dekeyzer S, Riabikin A, Keulers A, Reich A, Mpotsaris A, et al. True First-Pass Effect: First-Pass Complete Reperfusion Improves Clinical Outcome in Thrombectomy Stroke Patients. Stroke. 2019;50(8):2140–6.
23. Vandelanotte S, Staessens S, François O, De Wilde M, Desender L, De Sloovere AS, et al. Association between thrombus composition and first-pass recanalization after thrombectomy in acute ischemic stroke. Journal of Thrombosis and Haemostasis. 2024;(April):1–7.
24. Patel TR, Fricano S, Waqas M, Tso M, Dmytriw AA, Mokin M, et al. Increased perviousness on CT for acute ischemic stroke is associated with fibrin/platelet-rich clots. American Journal of Neuroradiology. 2021;42(1):57–64.
25. Delvoye F, Di Meglio L, Consoli A, Nomenjanahary MS, Dupont S, Labreuche J, et al. High thrombus platelet content is associated with a lower rate of first pass effect in stroke treated by endovascular therapy. Eur Stroke J. 2022 Dec 1;7(4):376–83.
26. Ducroux C, Meglio L Di, Loyau S, Delbosc S, Boisseau W, Deschildre C, et al. Thrombus Neutrophil Extracellular Traps Content Impair tPA-Induced Thrombolysis in Acute Ischemic Stroke. Stroke. 2018;49(3):754–7.
27. Laridan E, Denorme F, Desender L, François O, Andersson T, Deckmyn H, et al. Neutrophil extracellular traps in ischemic stroke thrombi. Ann Neurol. 2017;82(2):223–32.
28. Peña-Martínez, Carolina Durán-Laforet, Violeta García-Culebras, Alicia Ostos, Fernando Hernández-Jiménez M. Pharmacological Modulation of Neutrophil Extracellular Traps Reverses Thrombotic Stroke tPA (Tissue-Type Plasminogen Activator) Resistance. Stroke. 2019;50(11):3228–37.
29. De Lizarrondo SM, Gakuba C, Herbig BA, Repessé Y, Ali C, Denis C V., et al. Potent thrombolytic effect of N-acetylcysteine on arterial thrombi. Circulation. 2017;136(7):646–60.
30. Kim D, Shea SM, Ku DN. Lysis of arterial thrombi by perfusion of N,N'- Diacetyl-L-cystine (DiNAC). PLoS One. 2021;16(2 February):1–16.
31. Denorme F, Langhauser F, Desender L, Vandenbulcke A, Rottensteiner H, Plaimauer B, et al. ADAMTS13-mediated thrombolysis of t-PA-resistant occlusions in ischemic stroke in mice. Blood. 2016;127(19):2337–45.

32. South K, Saleh O, Lemarchand E, Coutts G, Smith CJ, Schiessl I, et al. Robust thrombolytic and anti-inflammatory action of a constitutively active ADAMTS13 variant in murine stroke models. Blood. 2022;139(10):1575–87.
33. Denorme F, Langhauser F, Desender L, Vandenbulcke A, Rottensteiner H, Plaimauer B, et al. ADAMTS13-mediated thrombolysis of t-PA–resistant occlusions in ischemic stroke in mice. Blood. 2016 May;127(19):2337–45.
34. Aguiar de Sousa D, von Martial R, Abilleira S, Gattringer T, Kobayashi A, Gallofré M, et al. Access to and delivery of acute ischaemic stroke treatments: A survey of national scientific societies and stroke experts in 44 European countries. Eur Stroke J. 2019;4(1):13–28.
35. Khismatullin RR, Nagaswami C, Shakirova AZ, Vrtková A, Procházka V, Gumulec J, et al. Quantitative Morphology of Cerebral Thrombi Related to Intravital Contraction and Clinical Features of Ischemic Stroke. Stroke. 2020;51(12):3640–50.
36. Chernysh IN, Nagaswami C, Kosolapova S, Peshkova AD, Cuker A, Cines DB, et al. The distinctive structure and composition of arterial and venous thrombi and pulmonary emboli. Sci Rep. 2020;10(1):1–12.
37. Dumitriu LaGrange D, Bernava G, Reymond P, Wanke I, Vargas MI, Machi P, et al. A high resolution scanning electron microscopy analysis of intracranial thrombi embedded along the stent retrievers. Sci Rep. 2022;12(1):1–11.
38. Mereuta OM, Fitzgerald S, Christensen TA, Jaspersen AL, Dai D, Abbasi M, et al. High-resolution scanning electron microscopy for the analysis of three-dimensional ultrastructure of clots in acute ischemic stroke. J Neurointerv Surg. 2021;13(10):906–11.
39. Swanepoel AC, Pretorius E. Scanning electron microscopy analysis of erythrocytes in thromboembolic ischemic stroke. Int J Lab Hematol. 2012;34(2):185–91.
40. Ahn SH, Hong R, Choo IS, Heo JH, Nam HS, Kang HG, et al. Histologic features of acute thrombi retrieved from stroke patients during mechanical reperfusion therapy. International Journal of Stroke. 2016;11(9):1036–44.
41. Di Meglio L, Desilles JPP, Ollivier V, Nomenjanahary MS, Di Meglio S, Deschildre C, et al. Acute ischemic stroke thrombi have an outer shell that impairs fibrinolysis. Neurology. 2019;93(18):E1686–98.
42. Krautgartner WD, Klappacher M, Hannig M, Obermayer A, Hartl D, Marcos V, et al. Fibrin mimics neutrophil extracellular traps in SEM. Ultrastruct Pathol. 2010;34(4):226–31.
43. Goldberg MW, Fišerová J. Immunogold labeling for scanning electron microscopy. Methods in Molecular Biology. 2016;1474:309–25.
44. van Rijnsoever C, Oorschot V, Klumperman J. Correlative light-electron microscopy (CLEM) combining live-cell imaging and immunolabeling of ultrathin cryosections. Nat Methods. 2008;5(11):973–80.
45. Hayashi S, Ohno N, Knott G, Molnár Z. Correlative light and volume electron microscopy to study brain development. Microscopy. 2023;72(4):279–86.
46. Walker M, Federico E, Espinoza JL, Dupont CL. Unveiling Molecular Diversity in Cerebral Thrombi via Spatial Transcriptomics. Stroke. 2024 Oct 1;
47. Mai H, Zhang T, Zhang T, Lu A, Wu Z, Yang B, et al. Spatial Proteomics Analysis of Soft and Stiff Regions in Human Acute Arterial Thrombus. Stroke. 2023 Jun 1;54(6):1636–44.
48. Yuki I, Kan I, Vinters H V., Kim RH, Golshan A, Vinuela FA, et al. The impact of thromboemboli histology on the performance of a mechanical thrombectomy device. American Journal of Neuroradiology. 2012 Apr;33(4):643–8.

49. Gralla J, Schroth G, Remonda L, Fleischmann A, Fandino J, Slotboom J, et al. A dedicated animal model for mechanical thrombectomy in acute stroke. American Journal of Neuroradiology. 2006;27(6):1357–61.
50. Kan I, Yuki I, Murayama Y, Viñuela FA, Kim RH, Vinters H V, et al. A novel method of thrombus preparation for use in a swine model for evaluation of thrombectomy devices. American Journal of Neuroradiology. 2010;31(9):1741–3.
51. Chueh JY, Wakhloo AK, Hendricks GH, Silva CF, Weaver JP, Gounis MJ. Mechanical characterization of thromboemboli in acute ischemic stroke and laboratory embolus analogs. American Journal of Neuroradiology. 2011;32(7):1237–44.
52. Roth C, Junk D, Papanagiotou P, Keuler A, Körner H, Schumacher M, et al. A comparison of 2 stroke devices: The new aperio clot-removal device and the solitaire AB/FR. American Journal of Neuroradiology. 2012;33(7):1317–20.
53. Duffy S, Farrell M, McArdle K, Thornton J, Vale D, Rainsford E, et al. Novel methodology to replicate clot analogs with diverse composition in acute ischemic stroke. J Neurointerv Surg. 2017;9(5):486–91.
54. Fitzgerald STT, Liu Y, Dai D, Mereuta OMM, Abbasi M, Larco JLALA, et al. Novel human acute ischemic stroke blood clot analogs for in vitro thrombectomy testing. American Journal of Neuroradiology. 2021;42(7):1250–7.
55. Berndt M, Prothmann S, Maegerlein C, Oberdieck P, Zimmer C, Hegge B, et al. Artificial Stroke Clots: How Wide is the Gap to the Real World? World Neurosurg. 2018;110:e90–9.
56. Cines DB, Lebedeva T, Nagaswami C, Hayes V, Massefski W, Litvinov RI, et al. Clot contraction: Compression of erythrocytes into tightly packed polyhedra and redistribution of platelets and fibrin. Blood. 2014;123(10):1596–603.
57. Tutwiler V, Mukhitov AR, Peshkova AD, Le Minh G, Khismatullin RR, Vicksman J, et al. Shape changes of erythrocytes during blood clot contraction and the structure of polyhedrocytes. Sci Rep. 2018;8(1):1–14.
58. Mereuta OM, Agarwal T, Ghozy S, Dai D, Arul S, Brinjikji W, et al. Shell Versus Core Architecture and Biology of Thrombi in Acute Ischemic Stroke: A Systematic Review. Clinical and Applied Thrombosis/Hemostasis. 2023 Jan 1;29.
59. Ye G, Cao R, Lu J, Qi P, Hu S, Chen K, et al. Histological composition behind CT-based thrombus density and perviousness in acute ischemic stroke. Clin Neurol Neurosurg. 2021;207(July):106804.
60. Choi MH, Park GH, Lee JS, Lee SE, Lee SJ, Kim JH, et al. Erythrocyte fraction within retrieved thrombi contributes to thrombolytic response in acute ischemic stroke. Stroke. 2018;49(3):652–9.
61. Liebeskind DS, Sanossian N, Yong WH, Starkman S, Tsang MP, Moya AL, et al. CT and MRI early vessel signs reflect clot composition in acute stroke. Stroke. 2011;42(5):1237–43.
62. Simons N, Mitchell P, Dowling R, Gonzales M, Yan B. Thrombus composition in acute ischemic stroke: A histopathological study of thrombus extracted by endovascular retrieval. Journal of Neuroradiology. 2015;42(2):86–92.
63. Sisirak V, Sally B, D'Agati V, Martinez-Ortiz W, Özçakar ZB, David J, et al. Digestion of Chromatin in Apoptotic Cell Microparticles Prevents Autoimmunity. Cell. 2016;166(1):88–101.
64. Napirei M, Ludwig S, Mezrhab J, Klöckl T, Mannherz HG. Murine serum nucleases - Contrasting effects of plasmin and heparin on the activities of DNase1 and DNase1-like 3 (DNase1l3). FEBS Journal. 2009 Feb;276(4):1059–73.

65. Englert H, Göbel J, Khong D, Omidi M, Wolska N, Konrath S, et al. Targeting NETs using dual-active DNase1 variants. Front Immunol. 2023;14(May):1–12.
66. Fennell VS, Setlur Nagesh SV, Meess KM, Gutierrez L, James RH, Springer ME, et al. What to do about fibrin rich “tough clots”? Comparing the Solitaire stent retriever with a novel geometric clot extractor in an in vitro stroke model. J Neurointerv Surg. 2018;10(9):907–10.
67. Nordmeyer H, Belachew NF, Phung TH, Gralla J, Molina Gil S, Douglas A, et al. NIMBUS geometric clot extractor for challenging clots: Real-world clinical experience and clot composition. Interventional Neuroradiology. 2023;1–7.
68. Lehnen NC, Paech D, Zülow S, Bode FJ, Petzold GC, Radbruch A, et al. First Experience with the Nimbus Stentretriever: A Novel Device to Handle Fibrin-rich Clots. Clin Neuroradiol. 2023;33(2):491–7.
69. Boriesosdick J, Michael AE, Kröger JR, Niehoff JH, Saeed S, Pflug M, et al. Mechanical thrombectomy using the Nimbus stent-retriever – initial experiences in a single-center observational study. Interventional Neuroradiology. 2024;30(3):380–8.
70. Kaneko N, Ghovvati M, Komuro Y, Guo L, Khatibi K, Ponce Mejia LL, et al. A new aspiration device equipped with a hydro-separator for acute ischemic stroke due to challenging soft and stiff clots. Interventional Neuroradiology. 2021 Feb 1;0(0):1–7.
71. Skarbek C, Anagnostakou V, Procopio E, Epshtein M, Raskett CM, Romagnoli R, et al. Development of a clot-adhesive coating to improve the performance of thrombectomy devices. J Neurointerv Surg. 2023;15(12):1207–11.
72. Maekawa K, Shibata M, Nakajima H, Mizutani A, Kitano Y, Seguchi M, et al. Erythrocyte-rich thrombus is associated with reduced number of maneuvers and procedure time in patients with acute ischemic stroke undergoing mechanical thrombectomy. Cerebrovasc Dis Extra. 2018;8(1):39–49.
73. Hund H, Boodt N, Arrarte Terreros N, Taha A, Marquering HA, van Es ACGM, et al. Quantitative thrombus characteristics on thin-slice computed tomography improve prediction of thrombus histopathology: results of the MR CLEAN Registry. Eur Radiol. 2022;32(11):7811–23.
74. Simons N, Mitchell P, Dowling R, Gonzales M, Yan B. Thrombus composition in acute ischemic stroke: A histopathological study of thrombus extracted by endovascular retrieval. Journal of Neuroradiology. 2015;42(2):86–92.
75. Brinjikji W, Duffy S, Burrows A, Hacke W, Liebeskind D, Majoie CBLM, et al. Correlation of imaging and histopathology of thrombi in acute ischemic stroke with etiology and outcome: A systematic review. J Neurointerv Surg. 2017;9(6):529–34.
76. Essig F, Kollikowski AM, Pham M, Solymosi L, Stoll G, Haeusler KG, et al. Immunohistological analysis of neutrophils and neutrophil extracellular traps in human thrombemboli causing acute ischemic stroke. Int J Mol Sci. 2020;21(19):1–13.
77. Kim SK, Yoon W, Kim TS, Kim HS, Heo TW, Park MS. Histologic analysis of retrieved clots in acute ischemic stroke: Correlation with stroke etiology and gradient-echo MRI. American Journal of Neuroradiology. 2015;36(9):1756–62.
78. Patil S, Darcourt J, Messina P, Bozsak F, Cognard C, Doyle K. Characterising acute ischaemic stroke thrombi: insights from histology, imaging and emerging impedance-based technologies. Stroke Vasc Neurol. 2022 Aug 1;7(4):353–63.
79. Darcourt J, Brinjikji W, François O, Giraud A, Johnson CR, Patil S, et al. Identifying ex vivo acute ischemic stroke thrombus composition using electrochemical impedance spectroscopy. Interventional Neuroradiology. 2023;0:0.

80. Messina P, Garcia C, Rambeau J, Darcourt J, Balland R, Carreel B, et al. Impedance-based sensors discriminate among different types of blood thrombi with very high specificity and sensitivity. J Neurointerv Surg. 2023 Jun 1;15(6):526–31.

SUMMARY – SAMENVATTING

Summary

Acute ischemic stroke (AIS) occurs when a blood clot obstructs the blood flow to the brain. The aim of therapy is fast recanalization of the occluded artery, either through mechanical thrombectomy (MT) or pharmacological thrombolysis using recombinant tissue plasminogen activator (rt-PA), or a combination of both. Recanalization is however not always successful, often resulting in poor patient outcomes. Indeed, rt-PA leads to successful recanalization only in less than half of the patients that receive it and MT fails to successfully recanalize in approximately 30% of treated patients, leading to poor clinical outcome. Since the occluding thrombus is the central target for both recanalization strategies, it is likely that the thrombus itself influences recanalization success. The general aim of this thesis was to gain better insights in how thrombus composition affects pharmacological and mechanical recanalization.

In this thesis, **Chapter 1** presents a brief introduction to the most relevant aspects of this research, followed by **Chapter 2**, which provides a review discussing the state-of-the-art on the composition of AIS thrombi. The aims of this doctoral work are outlined in **Chapter 3**.

When investigating AIS thrombus composition and its potential link with recanalization, one of the most important aspects is the availability of AIS thrombi. Due to the widespread use of MT, the occluding thrombus became available providing the opportunity to investigate its composition and response to treatment. However, the use of patient AIS thrombi is frequently limited by the unpredictable daily availability and highly variable composition of the thrombi. Our first sub-aim, addressed in **Chapter 4**, was therefore to develop a standardized model of AIS clot analogs prepared from human blood that represent the range of thrombi typically found in patients. Using a modified Chandler loop system, three AIS clot analogs (red blood cell (RBC)-rich clots, platelet-rich clots, and mixed composition clots) were generated. Comprehensive histological analysis showed strong similarities between the AIS clot analogs and patient-derived AIS cots. When subjecting the AIS clot analogs to pharmacological thrombolysis using rt-PA, we found that clot composition had a significant impact on successful lysis by rt-PA, with RBC-rich clot analogs showing enhanced lysis compared to mixed and platelet-rich analogs.

In C**hapter 5**, we further investigated and confirmed the distinct response of thrombi with a different composition to rt-PA-mediated thrombolysis. Freshly retrieved patient AIS thrombi were split into two parts. One part was subjected to rt-PA mediated

thrombolysis while the other part was used for detailed histological analysis to be able to link the degree of lysis to the thrombus composition. In line with our findings in AIS clot analogs, we found that the efficacy of rt-PA-mediated thrombolysis is strongly correlated with thrombus composition. Especially, platelet-rich thrombi containing low amounts of RBCs and higher amounts of DNA and von Willebrand Factor (VWF) showed resistant to rt-PA. Most importantly, we also investigated the possibility to overcome the rt-PA resistance by directly targeting DNA and VWF instead of solely fibrin. Interestingly, we showed that combined use of the DNA-degrading enzyme DNase-1 or the reducing agent diNAC with rt-PA resulted in efficient thrombolysis of platelet-rich thrombi that are rt-PA resistant.

While enhancing pharmacological lysis options for treating AIS is crucial due to their practical ease of application compared to MT, it is equally important to focus on improving patient outcomes following MT. Recently, it became clear that first pass recanalization (FPR), in which successful recanalization is obtained in the first MT attempt, is linked to the best clinical outcome. In **Chapter 6**, we therefore analyzed compositional data from over 250 AIS thrombi to investigate a potential link between thrombus composition and achieving FPR. Similar to our observations on pharmacological thrombolysis, we found that those thrombi characterized by low RBC content and high levels of fibrin and extracellular DNA tend to be more resistant to MT as these were associated with a reduced likelihood of achieving FPR.

During this PhD project, it became clear that the composition of AIS thrombi highly influences the response to both pharmacological thrombolysis and MT. Although conventional histopathological investigation of AIS thrombi significantly improved our understanding of the composition of stroke thrombi, its resolution is rather limited. Therefore, in **Chapter 7**, we used high resolution scanning electron microscopy to investigate the ultrastructural organization of AIS thrombi. These studies revealed that the interior of AIS thrombi has a varying composition of mainly RBCs, fibrin and platelets that can be organized in different manners. The surface of the AIS thrombus is composed of a combination of branched fibrin, branched fibrin aligned with aggregated platelet, aggregated platelets and a sealed layer.

Finally, **Chapter 8** (general discussion), discuss the broader impact, clinical implications and future perspectives of this doctoral work.

Samenvatting

Een acute ischemische beroerte (AIS) treedt op wanneer een bloedklonter de bloedstroom naar de hersenen blokkeert. Het doel van therapie is om het afgesloten bloedvat snel te recanaliseren, hetzij door middel van mechanische trombectomie (MT) of farmacologische trombolyse met behulp van recombinant weefsel-plasminogeenactivator (rt-PA), of een combinatie van beide. Recanalisatie is echter niet altijd succesvol, wat vaak leidt tot slecht herstel van de patiënt. Rt-PA leidt inderdaad slechts bij minder dan de helft van de patiënten die het ontvangen tot succesvolle recanalisatie, en MT slaagt bij ongeveer 30% van de behandelde patiënten er niet in om succesvol te recanaliseren, wat verder leidt tot een slechte klinische uitkomst. Aangezien de bloedklonter het centrale doelwit is voor beide recanalisatie strategieën, is de kans bestaand dat de bloedklonter een invloed heeft op het succes van de recanalisatie. Het algemene doel van deze thesis was om meer inzicht te krijgen in hoe de samenstelling van de bloedklonter de farmacologische en mechanische recanalisatie beïnvloedt.

Hoofdstuk 1 van deze thesis omvat een korte inleiding over de meest relevante aspecten van dit onderzoek, gevolgd door **Hoofdstuk 2**, wat een overzicht biedt van de huidige stand van zaken met betrekking tot de samenstelling van AIS bloedklonters. De doelstellingen van dit doctoraatsproject worden beschreven in **Hoofdstuk 3**.

Wanneer we de samenstelling van AIS bloedklonters willen onderzoeken en zijn mogelijke link met recanalisatie, is een van de meest belangrijke aspecten de beschikbaarheid van AIS bloedklonters. Door het algemene gebruik van MT werd de bloedklonter beschikbaar voor onderzoek naar de samenstellen en reactie op behandelingen. Het gebruik van patiënten bloedklonters is echter vaak gehinderd door de onvoorspelbare dagelijkse beschikbaarheid en variabele samenstelling van de klonters. Ons eerste subdoel, aangekaart in **Hoofdstuk 4**, was daarom om een gestandaardiseerd model voor AIS klonter analogen te ontwikkelen die gemaakt zijn van menselijk bloed en die de verschillende samenstellingen van patiënten klonters nabootsen. Door gebruik te maken van een gemodificeerd Chandler-loop systeem werden drie AIS klonter analogen (rode bloed cel (RBC)-rijke klonter, plaatjes-rijke klonter en gemengde-compositie klonter) ontwikkeld. Een uitgebreide histologische analyse toonde de sterke overeenkomsten tussen de AIS klonteranalogen en de patiënten klonters aan. Wanneer de AIS klonteranalogen onderworpen werden aan

farmacologische trombolyse met behulp van rt-PA, bleek de samenstelling van de klonter een aanzienlijke invloed te hebben op het succes van rt-PA. Hierbij toonden RBC-rijke AIS klonteranalogen een significant verbeterde afbraak ten opzichte van gemengde en plaatjes-rijke analogen.

In **Hoofstuk 5** onderzochten en bevestigden we verder de verschillende reactie op rt-PA door klonters met een verschillende samenstelling. Verse klonters die verwijderd waren bij AIS patiënten werden in twee delen gesplitst. Het ene deel werd onderworpen aan rt-PA-gemedieerde trombolyse, terwijl het andere deel werd gebruikt voor gedetailleerde histologische analyse om de mate van afbraak te kunnen koppelen aan de samenstelling van de klonter. In lijn met onze bevindingen bij de AIS klonteranalogen, vonden we dat de effectiviteit van rt-PA-gemedieerde trombolyse sterk gecorreleerd is met de samenstelling van de klonter. Vooral plaatjes-rijke klonters met lage hoeveelheden RBC's en hogere hoeveelheden DNA en von Willebrand Factor (VWF) bleken resistent tegen rt-PA. Verder onderzochten we ook de mogelijkheid om de rt-PA-resistentie te overwinnen door direct DNA en VWF aan te pakken in plaats van uitsluitend fibrine. Interessant genoeg hebben we aangetoond dat het gecombineerde gebruik van het DNA-afbrekende enzym DNase-1 of het reducerende middel diNAC met rt-PA resulteerde in een efficiënte trombolyse van plaatjes-rijke, rt-PA resistent klonters.

Hoewel het verbeteren van farmacologische trombolyse mogelijkheden voor de behandeling van AIS cruciaal zijn vanwege hun praktische eenvoud in vergelijking met MT, is het minstens even belangrijk om te focussen op het verbeteren van het resultaat na MT. Recent werd duidelijk dat eerste-passage recanalisatie (FPR), waarbij succesvolle recanalisatie wordt verkregen bij de eerste MT-poging, verband houdt met de beste klinische uitkomst. In **Hoofdstuk 6** hebben we daarom compositiegegevens van meer dan 250 AIS-klonters geanalyseerd om een mogelijk verband te onderzoeken tussen de samenstelling van de klonter en het bereiken van FPR. Net zoals bij onze observaties over farmacologische trombolyse, vonden we dat die klonters die gekenmerkt worden door een laag RBC-gehalte en hoge niveaus van fibrine en extracellulair DNA, meer resistent zijn tegen MT, omdat deze klonters geassocieerd waren met een verminderde kans om een FPR te bereiken.

Tijdens dit doctoraatsproject werd duidelijk dat de samenstelling van AIS klonters de reactie op zowel farmacologische trombolyse als MT sterk beïnvloedt. Hoewel conventioneel histopathologisch onderzoek van AIS-klonters onze kennis over hun

samenstelling aanzienlijk heeft verbeterd, is de resolutie ervan vrij beperkt. Daarom hebben we in **Hoofdstuk 7** hoge-resolutie scanning elektronenmicroscopie gebruikt om de ultra-structurele organisatie van AIS klonters te onderzoeken. Deze studie toonde aan dat dat de binnenkant van AIS klonters een variërende samenstelling heeft van voornamelijk RBC's, fibrine en plaatjes die op verschillende manieren georganiseerd kunnen zijn. Het oppervlak van het AIS klonters bestaat uit een combinatie van vertakte fibrine, vertakte fibrine uitgelijnd met geaggregeerde plaatjes, geaggregeerde plaatjes en een afgesloten laag.

Tot slot bespreekt **Hoofdstuk 9** (algemene discussie) de bredere impact, klinische implicaties en toekomstperspectieven van dit doctoraatsonderzoek.

ACKNOWLEDGEMENTS, PERSONAL CONTRIBUTION AND CONFLICT OF INTEREST

ACKNOWLEDGEMENTS

My great appreciation and gratitude goes to our close collaborators of the AZ Groeninge hospital (Dr. Olivier François, Dr. Frédrick Van Gool, Dr. Alexander Van Hoorne, Prof. Dr. Tommy Andersson, Prof. Dr. Peter Vanacker) for collecting the stroke thrombi, providing us with the clinical data related to the stroke thrombi and for their critical input in the analysis of the data. Additionally, I would like to thank the whole staff of the stroke unit and especially all nurses for the fruitful collaboration.

PERSONAL CONTRIBUTION

Sarah Vandelanotte, first author of the thesis chapters, contributed to study design, data acquisition, analysis and interpretation of the data and wrote the research articles and thesis manuscript.

Contribution for shared first authorship of chapter 6: S. Staessens performed histological analysis of RBC, fibrin, von Willebrand factor, platelets and CD45 of thrombi. S. Vandelanotte performed histological analysis of DNA, performed data analysis and wrote the manuscript.

FUNDING

Part of this research was funded by:

- Research Foundation Flanders (Fonds voor Wetenschappelijk onderzoek) to Simon F. De Meyer
    - FWO G.0A86.13
    - FWO G.0785.17
    - FWO 1509216N
- Research Fund of KU Leuven to Simon F. De Meyer
    - OT/14/099
    - ISP/14/02L2
- Queen Elisabeth Medical Foundation for Neuroscience to Simon F. De Meyer

- European Union’s Horizon 2020 Research and Innovation Program to Simon F. De Meyer
    - INSIST under agreement Number 777072

CONFLICT OF INTEREST

The following authors declared a conflict of interest:

- Prof. Dr. Tommy Andersson declares consultancy for Anaconda, Cerenovus, Neuravi and Rapid Medical and holds equity for Cereflo Ltd
- Dr. Olivier François is a consultant for iVascular
- Prof. Dr. Peter Vanacker received speaker fees from Boehringer-Ingelheim, BMS, Pfizer, Daiichi-Sankyo, and Medtronic.

CURRICULUM VITAE

Personal

Name	Sarah Vandelanotte
Date of birth	23/09/1997
Place of birth	Bruges, Belgium
E-mail	Sarah.vandelanotte@hotmail.com
Name of Institution	KU Leuven
Department	Cardiovascular Sciences – Laboratory for Thrombosis Research
Address	Etienne Sabbelaan 53 8500 Kortrijk

Education

2020 – present **PhD student in Biomedical sciences; laboratory for thrombosis research – KU Leuven Kulak**
PhD project: Towards improved thrombolysis in ischemic stroke exploring novel therapeutic targets
Supervisor: Prof. Dr. Simon De Meyer (KU Leuven, Belgium)

2018 – 2020 **Master in Biomedical Sciences; KU Leuven, Leuven**
Specialization: Communication and management
Thesis: De invloed van gemeenschapsacties op de alcoholnorm, attitude en
consumptie in Leuven en het effect op screening en korte interventie in de huisartsenpraktijk: Basismeting en ontwikkeling
Supervisor: Prof. Dr. Bert Aertgeerts
Grade: Magna Cum Laude

2015 – 2018 **Bachelor in Biomedical Sciences; KU Leuven Kulak**
Grade: Cum Laude

Skills/certificates

Language skills	Dutch – Native speaker English – Advanced level proficiency French – Basic level proficiency
Computer skills	MS Office (Word, Excel, Powerpoint), Graphpad Prism, SPSS statistics, ImageJ, Zen software
Certificates	Laboratory animal science (FELASA B), Academic writing for junior researchers
Skill trainings	Creating effective scientific posters, Infographics, Networking, Masterclass Powerpoint, Masterclass excel, academic writing for junior researchers, presentation skills, Tick@lab

Publication list

Yogendrakumar V, **Vandelanotte S**, Mistry EA, Hill MD, Coutts SB, Nogueira RG, Nguyen TN, Medcalf RL, Broderick JP, Meyer SF De, Campbell BC V. Emerging Adjuvant Thrombolytic Therapies for Acute Ischemic Stroke Reperfusion. 2024;(October).

Vandelanotte S, Staessens S, François O, De Wilde M, Desender L, De Sloovere AS, Dewaele T, Tersteeg C, Vanhoorelbeke K, Vanacker P, Andersson T, De Meyer SF. Association between thrombus composition and first-pass recanalization after thrombectomy in acute ischemic stroke. J Thromb Haemost. 2024;(April):1–7.

Vandelanotte S, François O, Desender L, Staessens S, Vanhoorne A, Van Gool F, Tersteeg C, Vanhoorelbeke K, Vanacker P, Andersson T, De Meyer SF. Rt-PA resistance is specific for platelet-rich stroke thrombi and can be overcome by targeting non-fibrin components. Stroke. 2024;(May):1–10.

Vandelanotte S, De Meyer SF. Acute Ischemic Stroke Thrombus Composition. Neuroscience. 2024;550(December 2023):11–20.

Vandelanotte S, Calcoen B, Tersteeg C, Vanhoorelbeke K, de Meyer S. Gene Therapy for Von Willebrand Disease. Belgian J Hematol. 2023;14.

Aspegren O, Staessens S, **Vandelanotte S**, Desender L, Andersson T, Arnberg F. Unusual Histopathological Findings in Mechanically Removed Stroke Thrombi – A Multicenter Experience. Front Neurol. 2022;13(May):1–16.

Pussig B, Van Nuland M, Pas L, **Vandelanotte S**, Matheï C, Aertgeerts B, Vermandere M. Community involvement to facilitate the discussion of alcohol use in primary care: a nominal group study". The European Journal of General Practice. 2021; 27 (1), 130-139.

Pussig B, **Vandelanotte S**, Matheï C, Pas L, Aertgeerts B. Mapping key components of community-oriented strategies to facilitate alcohol-related early identification and brief intervention in general practice: a scoping review. Family Practice. 2021 Sep 7

Awards

1. Helaers Research Prize for Stroke, 2021 (EUR 3000)
2. CSL Behring Encouragement Award in haemostasis and thrombosis, 2022 (EUR 10 000)
3. Paul Capel prize for best oral communication in the category ‘fundamental research’ at the annual meeting of the BSTH, 2022 (EUR 750)
4. Paul Capel prize for best oral communication in the category ‘fundamental research’ at the annual meeting of the BSTH, 2023 (EUR 750)

Grants

1. Travel grant 2022 - Belgian Society on Thrombosis and Haemostasis BSTH: ‘Association between thromboembolus composition and first pass recanalization after thrombectomy in ischemic stroke’. 30th Congress of the International Society on Thrombosis and Haemostasis (ISTH), London, England, U.K., July 9-13, 2022 (EUR 500)

Participation in national and international congresses

1. Belgian stroke workshop, September 2021, Brussel, Belgium, **‘**Towards improved thrombolysis in ischemic stroke exploring novel therapeutic targets’ (Oral presentation)
2. 20th Belgian Stroke Council Scientific Symposium, December 2021, Belgium, **‘**Towards improved thrombolysis in ischemic stroke exploring novel therapeutic targets’ (Oral presentation)
3. 8th European Stroke Organisation Conference, Lyon, France, May 4-6, 2022 ‘Association between thromboembolus composition and first pass recanalization after thrombectomy in ischemic stroke’. (Oral poster-presentation)
4. 30th Congress of the International Society on Thrombosis and Haemostasis (ISTH), London, England, U.K., July 9-13, 2022, “‘Association between thromboembolus composition and first pass recanalization after thrombectomy in ischemic stroke”. (poster)
5. Belgian stroke workshop, September 2022, Charleroi, Belgium, **‘**DNase-1 overcomes rt-PA resistance in platelet-rich ischemic stroke thrombi’ (Oral presentation)
6. Belgian Society on Thrombosis and Haemostasis - Annual Meeting, November 2022, Mechelen; Belgium, ‘DNase-1 overcomes rt-PA resistance in platelet-rich ischemic stroke thrombi’ (Oral presentation)
7. Belgian Society on Thrombosis and Haemostasis - Annual Meeting, November 2022, Mechelen; Belgium, ‘Association between thromboembolus composition and first pass recanalization after thrombectomy in ischemic stroke’. (poster)
8. 31th Congress of the International Society on Thrombosis and Haemostasis (ISTH), Montreal, Canada, June 24-28, 2023, ‘DNase-1 overcomes rt-PA resistance in platelet-rich ischemic stroke thrombi’ (poster)
9. 5th European Congress on Thrombosis and Haemostasis (ECTH2023), Valencia, Spain, September 13-15, 2023, ‘DNase-1 overcomes rt-PA resistance in platelet-rich ischemic stroke thrombi’ (oral presentation)
10. Belgian Society on Thrombosis and Haemostasis - Annual Meeting, November 2023, Mechelen; Belgium, ‘Analysis of the ultrastructural architecture of ischemic stroke thrombi using scanning electron microscopy: an observational study’. (Oral presentation)

Co-Author in national and international congresses

1. L. M. Klein, M. Solanki, I. Portier, **S. Vandelanotte**, W. Zhang, E. Ehrke-Schulz, K. Vanhoorelbeke, S. F. De Meyer and A. Ehrhardt. Molecular design of high-capacity adenoviral vectors as large transgene carriers exemplified by von Willebrand factor. Abstract for 30th European society of gene & cell therapy congress
2. C. A. Bresette, **S. Vandelanotte**, S. F. De Meyer, D. N. Ku. Heterogenous Growth of Platelet Thrombi. Abstract for 32nd Congress of the International Society on Thrombosis and Haemostasis (ISTH),

Teaching Experience

Courses:

- U04C9a Bloedsomloop: practicum: 2021-present
- U03E3a Initiatie tot het medisch wetenschappelijk onderzoek: 2021-present
- U04D3a Bachelorproef (practical course): 2021 – 2022
- Extra-curricular: Junior college: 2021 - present

Bachelor dissertations

- 2021-2022: Elias Deslovere. KU Leuven Kulak. Bachelor of medicine. 'Vergelijking van DNase 1 + recombinant tissue plasminogen activator (rt-PA) als combinatietherapie versus rt-PA alleen voor de behandeling van ischemische beroertes' – bachelor dissertation
- 2022-2023: Morgan Cordy. VIVES Campus Roeselare. Bachelor Agro- and biotechnology. 'Onderzoek naar de efficiëntie van endotheel-specifieke promotoren voor de ontwikkeling van adenovirale vectoren voor de ziekte van Von Willebrand' – bachelor internship and dissertation

Summer internships

- 2020-2021: Elias Deslovere. KU Leuven Kulak

Other

- AAP/BAP representative at IRF (2022-present)
- AAP/BAP representative group biomedical science (2022-2024)
- AAP/ABAP representative KULAK Academic Council (2022-present)